Depostional environments, diagenesis and reservoir modelling of concession NC115, Murzuq Basin, SW Libya.

Nuri Mohamed Fello

DEPOSITIONAL ENVIRONMENTS, DIAGENESIS AND RESERVOIR MODELLING OF CONCESSION NC115, MURZUQ BASIN, SW LIBYA

NURI MOHAMED FELLO

DEPARTMENT OF GEOLOGICAL SCIENCES

UNIVERSITY OF DURHAM

Ph.D. THESIS **2001**

Depositional Environments, Diagenesis and Reservoir Modelling of Concession NC115, Murzuq Basin, SW Libya

Nuri Mohamed Fello

Department of Geological Sciences
University of Durham

A thesis submitted to the University of Durham in fulfilment of the degree of Doctor of Philosophy.

Repsol Oil Operations

University of Durham

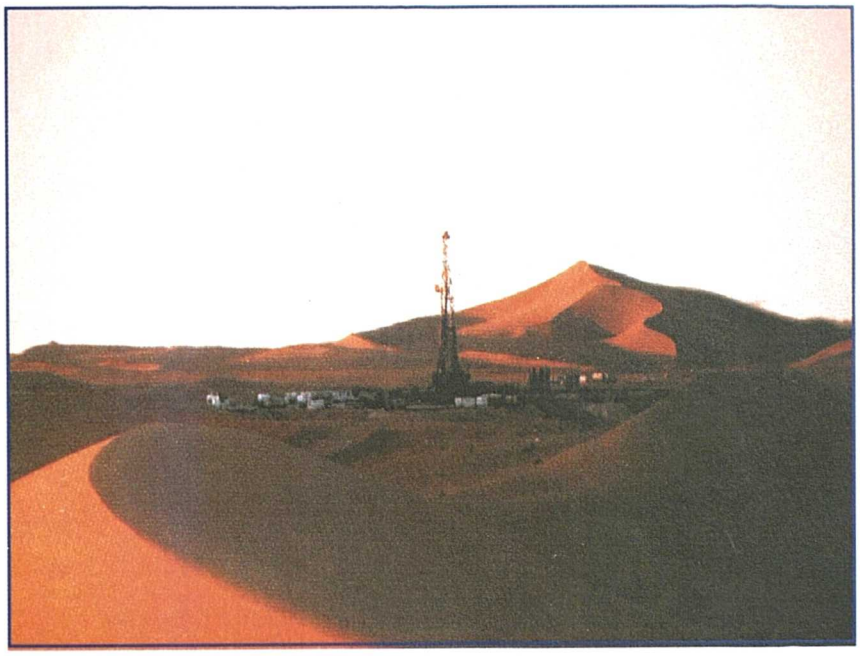

General View of the Drilling Rig within NC115 Concession.

DECLARATION

No part of this thesis has been submitted previously for a degree in this or any other university. The work described in this thesis is entirely that of the author, except where reference is made to previous published or unpublished work.

Nuri Mohamed Fello

Department of Geological Sciences,

University of Durham

October, 2001

ABSTRACT

The Murzuq Basin, SW Libya, is one of a series of Palaeozoic intracratonic sag basins on the North African Saharan Platform. The structural fabric of the basin was developed during the Late Proterozoic Pan-African orogenic event, which has strongly influenced the stratigraphy and depositional patterns within the predominantly Palaeozoic clastic basin-fill. The Upper Ordovician (Ashgillian) Mamuniyat Formation is the primary reservoir target in three oilfields: A, B and H within Repsol Oil Operations Concession area NC115, which lies on the northwestern flank of the Murzuq Basin.

The present study is based on slabbed cores, photographs, core samples, wireline log data and conventional core analysis of the Mamuniyat siliciclastic sediments, which attain a total thickness of about 170 m. The petrology, textural properties, lithology, sedimentary structures, sequence stratigraphy, lithofacies and depositional environments of these sediments have been studied in detail.

Lithostratigraphically the Mamuniyat Formation has been divided into a Lower, Middle and Upper Member according to grain-size, wireline log response and the proportion of sandstone to siltstone and shale. The three members have been assigned informal status within the Mamuniyat Formation and are the basis for facies analysis of the Mamuniyat sandstones throughout the El-Sharara Field. Throughout the Mamuniyat Formation ten facies have been recognized, based on particular associations of rock types and their lithological, sedimentological and biological characteristics. These facies have been grouped into three different facies associations.

The Lower Member of the Mamuniyat Formation is characterized by the presence of a sandstone dominated coarsening-upward sequence accompanied by increased bioturbation, towards the northeast. The sandstone is internally structured by small-scale trough cross-bedding, hummocky cross-stratification and ripple cross-lamination. The Middle Member of the Mamuniyat Formation is dominated by heterolithic-claystone sediments. It is mainly composed of black shales (Radioactive Shale) with subordinate fine- to medium-grained sandstone and occasional coarse-grained siltstone. The black shales are intercalated with wavy, rippled reddish-brown fine-grained sandstone and coarse-grained-siltstone beds. The entire Middle Member shows a general fining-upward trend and passes sharply upwards into fine-grained sandstone, siltstone and shale. The Upper Member of the Mamuniyat Formation also consists of sandstone, showing a coarsening-upward sequence from coarse- to very coarse-grained, which becomes more poorly sorted upwards, accompanied by an increase in bed thickness and the scale of cross-bedding.

A major problem with the Mamuniyat is the location of the sediment provenance, due to the lack of adequate subsurface and outcrop data, and the relationship and controls on sediment flux, and the depositional systems. Petrographic data derived from sandstone samples from cored intervals through the Mamuniyat Formation show that they are mainly sublitharenites, with some quartz arenites and litharenites. Compositional data for the three oilfields indicates that they were derived from a similar parent rock, but with differences in modal composition, textural attributes and porosity of the Lower, Middle and Upper Members of the Mamuniyat. These are attributed to temporal variations in source area uplift, base level change, sediment flux and accommodation space.

Sequence stratigraphic analysis of the Mamuniyat Formation emphasizes the role of unconformity-bounded sediment packages. These are interpreted in terms of regional tectonic events, especially the Taconic orogenic event, and changes in shelf physiography in response to relative fluctuations in sea-level, which in turn affected stream equilibrium profiles. Transgressive, highstand and lowstand systems tracts have been identified within the biostratigraphically, poorly constrained Mamuniyat Formation, thereby allowing for a more accurate correlation between the three oilfields. Stratigraphically the Mamuniyat has been divided into a Lower, Middle and Upper part, each assigned informal member status. In terms of this subdivision the Lower Mamuniyat corresponds to a transgressive systems tract when sediment was deposited concomitant with a relative rise in sea-level, flooding the entire shelf. During the final stage of this transgression a radioactive shale unit, recording a maximum flooding surface, was deposited in the lower part of the Middle Mamuniyat. The upper part of the Middle Mamuniyat corresponds to a highstand systems tract, and the Upper Mamuniyat, which is confined to the B-Field, records lowstand conditions. The Tanezzuft Shale, above the Mamuniyat Formation, records a major transgressive event of regional and economic significance.

Sediment composition, regional facies patterns and sequence stratigraphic analysis suggest that the Mamuniyat sandstones were derived from a nearby, tectonically active, granitic basement source terrain, which was most probably the uplifted Ghat/Tikiumit Arch, which is only 150 km to the southwest of the Concession area NC115. Periodic uplift of the basin margin in the SW, and associated base level changes led to the basinward progradation of braided fluvial systems followed by marine transgressive events emanating from Palaeotethys in the northeast. Both the braided fluvial and shallow water marine sandstones of the Mamuniyat Formation are primary hydrocarbon reservoir targets, with the main source and seal being the eustatically controlled Lower Silurian Tanezzuft Shale (Hot Shale). These same tectonic events influenced facies patterns, sediment deposition and interaction between a variety of shallow water marine and fluvial depositional environments across a NW-SE oriented storm-influenced coastline. The NC115 Concession is unlike most other Palaeozoic basins in Libya, in that there is no direct evidence of a glacial influence on deposition during Upper Ordovician (Ashgillian) times.

ACKNOWLEDGEMENTS

This project was set up and supervised by Dr. Brian R. Turner. The completion of this thesis would not have been possible without the help and support of a large number of people. I gratefully acknowledge all those who have in any way been involved in this project. I would like to take this opportunity to thank Brian for all his help over the course of this project and especially for spending many hours critically reading the manuscript and making valuable comments. I should also like to take this opportunity to thank Brian for his help in improving my understanding of the English language, both written and spoken English.

This project has been supported by Mr. Ibrahim K. Sherif, Chairman of Repsol Management Committee, by Mr. Mohamed M. Wail, Superintendent, Personnel Services and Mr. Bashir B. Garea, Exploration Co-ordinator of Repsol Oil Operations who gave me the opportunity to study again, after fifteen years, as well as providing me with all the data I needed for this project. Many thanks are due to all the staff of Repsol Oil Operations, particularly the Exploration Department for their support and encouragement throughout this study, and to all my friends for their continued encouragement and assistance.

In the department at Durham, I would like to thank Professor Maurice E. Tucker, Dr. Moyra Wilson, Dr. Stuart Jones, Dr. Dougal Jerram and Dave Schofield for helping with the occasional question. Dave Asbery, Carole Blair, Karen Atkinson and Janice Oakes are thanked for their general helpfulness and friendliness and Dave Stevenson, and Gary Wilkinson for their help in trying to keep my computer on the rails. The postgraduate students in Durham are thanked for making the past three years enjoyable ones. I would also like to thank Dr. Issa Makhlouf, Hashemite University, Zarka, Jordan and Dr. Keith Adamson, University of Wales, Aberystwyth for their general interest in my project and providing publications needed for my work. Above all I would like to thank all my Arab friends in Durham for making my study years enjoyable.

Last, but by no means least, I especially owe thanks to my mother (Fatma) during her visit to Durham and for her prayers and encouragement during my study. Finally my deepest grateful appreciation is also due to my family, particularly to my wife and my children, Mahmoud, Muatasem-Bellah and Monderr for their patience and support during my study at Durham. Meanwhile, this thesis is dedicated to all my family, relatives and friends particularly my mother, my wife and my children.

TABLE OF CONTENTS

CHAPTER 2 SEDIMENTOLOGY.....40

CHAPTER 3 PETROLOGY AND DIAGENESIS.....115

LIST OF FIGURES

CHAPTER 1

CHAPTER 2

CHAPTER 3

CHAPTER 4

CHAPTER 5

CHAPTER 6

CHAPTER 7

LIST OF TABLES

CHAPTER 1

CHAPTER 2

CHAPTER 3

CHAPTER 4

CHAPTER 7

LIST OF PLATES

CHAPTER 3

CHAPTER 1

INTRODUCTION

INTRODUCTION

1.1 Previous geological research

The earliest geographical records about southern Libya are those of Herodotus who visited the Fazzan during the Roman occupation of North Africa. Until the early 19th century maps including the Fazzan were based largely on his observation. In the late 18th century and during the 19th century the natural history notes of early North African explorers included the first scientific and geological work undertaken in the Fazzan. In 1797 two Germans, Frederick Horneman, a student of natural sciences and an explorer, and Joseph Freudenberg, visited Murzuq on a scientific mission of the African Association of London, the aim of which was to reach the River Niger from the Mediterranean coast and to record natural historical and cultural observation.

In 1799 Horneman succeeded in reaching the River Niger via Bornu, but died in 1800 at 28 years of age. In 1822, members of Captain Dixon Denham's expedition, including H. Clapperton, were the first Europeans to visit and draw up maps of the Ghat–Al Awaynat district. In 1849 a scientific expedition led by a cleric, J. Richardson, and including a German naturalist and geologist, A. Overweg, and an archaeologist, H. Barth, made detailed reports on the oases of the Fazzan, including Ghat and Awaynat Wanin. Before Overweg died in 1851 he made detailed observations of many of the Palaeozoic rocks of the Murzuq Basin (Pesce, 1969).

During the Italian administration work was carried out by Desio, Borghi, Chesa and others (Desio *et al.*, 1939-1953) who provided the first fairly comprehensive topographic documentation of southern Libya, and the first geological framework of the Murzuq Basin. The establishment by Desio of the Natural History Museum in Tripoli in the late 1930's facilitated detailed recording of stratigraphic data. During the French administration of the Fazzan (1942-1951) accurate geological mapping and surveying was continued on a systematic basis and much of it was published by the Institute de Recherches Sahariennes at the University of Algiers (*e.g.* Dalloni, 1948).

This work resulted in the publication of a 1:2,000,000-scale map of the Central Sahara for the International Geological Congress of 1952. Geological mapping and field work was continued by the French after 1951, the key work on Southwest Libya being that of Freulon (1964) and that published by Beuf *et al.* (1971).

Lelubre (1952) and Furon (1955) provide full reviews of the geological exploration of the Fazzan. Freulon (1964) undertook a study of the Palaeozoic succession of the Central Sahara based upon field mapping in the Tassel N'Ajjer of Algeria and in the Fazzan. During five field seasons, of six to eight months duration each, he surveyed these areas topographically and undertook primary geological mapping. The work was done between 1950 and 1955 on foot, on camel and in the later years with jeeps. The Jabal Akakus and Tadrart of the Ghat and Al Awaynat lay at the centre of his field study area, and he was responsible for its first geological surveying, the resulting map being published as the Forth Charlet map on a scale of 1:5,000,000. Despite the central position of the Ghat–Al Awaynat area the majority of Freulon's stratigraphic research was undertaken in southern Algeria in the Qarqaf region.

The excellent exposure of these undeformed sediments makes the outcrops surrounding the Hoggar and Reguibat massifs (**Fig. 1.1**) ideal areas for such a study within North Africa and Arabia (Clark-Lowes, 1985). The research recorded in the compilation of Beuf *et al.* (1971) is largely that of French Saharan geologists who had been working in the area since 1958. In the late 1950's and early 1960's petroleum exploration programmes in southwest Libya, in the Murzuq Basin, and on the shoulder between the Murzuq and Ghadames Basins, were undertaken by a number of companies after oil had been discovered in the Polignac Basin.

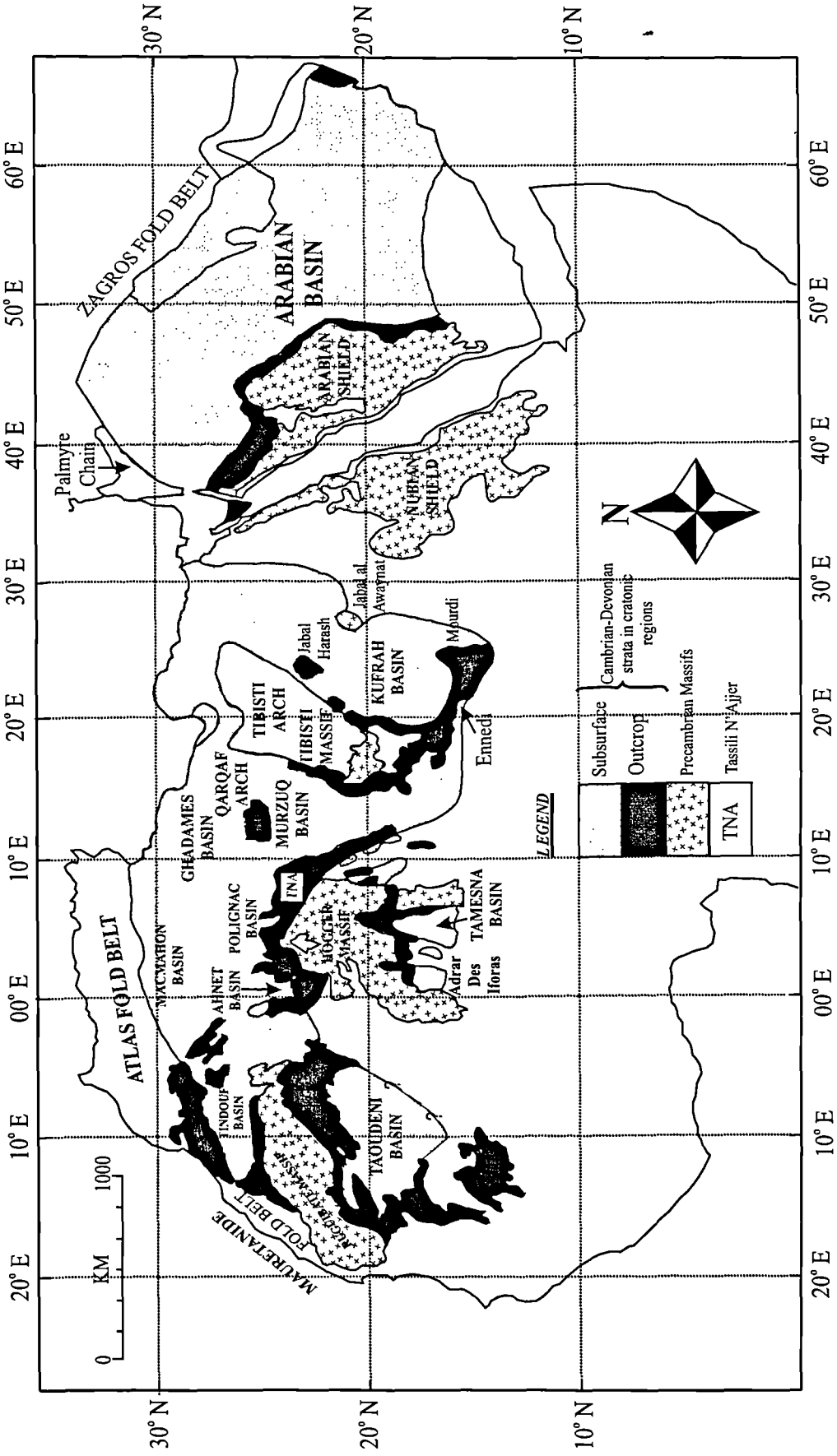

Fig. 1.1 Subsurface and Outcrop occurrence of Cambrian to Devonian strata in North Africa and Arabia (After Clark-Lowes, 1985).

Ten boreholes were drilled in several concessions in the Murzuq Basin, SW Libya (**Fig. 1.2**), and geological field parties studied the outcropping Palaeozoic strata on the margins of the basin (*e.g.* Collomb, 1962; Furst and Klitzsch, 1963; Collomb *et al.*, 1960, 1961; Craig *et al.*, 1958; Collomb and Heller, 1958). The need for an accepted stratigraphic nomenclature become clear and in 1960 the Lexique Stratigraphique International (Libya) was published through the efforts of A. Desio and the Names and the Nomenclature Committee of the Petroleum Exploration Society of Libya. In 1969, Klitzsch, as part of a revision of the Palaeozoic part of the Lexicon under his chairmanship, published details of sections which he measured in the Silurian to lower Devonian succession on the west of the Murzuq Basin, and of associated palaeontological work, and proposed the adoption of these as type sections.

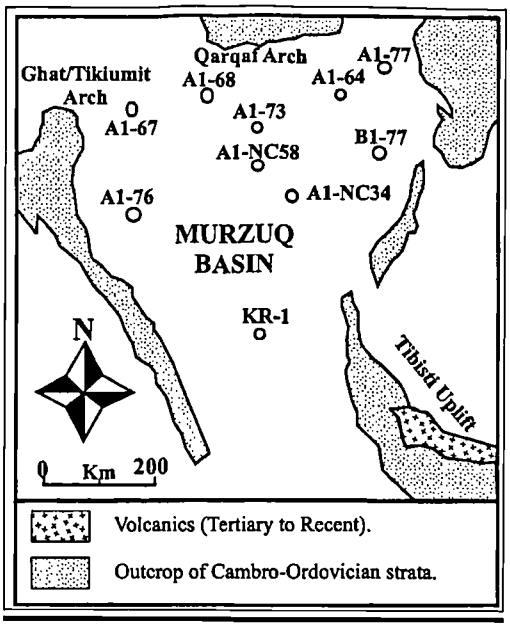

Fig. 1.2 Geological map illustrating the location of the first ten oil exploration wells drilled in the Murzuq Basin, SW Libya.

The most recent reviews of the geology of southwest Libya are those of Bellini and Massa (1980), who drew together a large a mount of previously published and unpublished academic and oil company data in a major review of the Palaeozoic of the southern sedimentary basins of Libya. Klitzsch (1981) provided a valuable review of the extensive research he and his co-workers have undertaken in the Murzuq Basin.

A more comprehensive picture of regional stratigraphic relations in the Murzuq Basin, based on surface and subsurface data is given by Pierobon (1991). Other work on the Ghadames and Murzuq Basins include Hammuda (1980), Vos (1981a, b), Van Houten and Karasek (1981), Whitbread and Kelling (1982), Clark-Lowes (1985), Castro *et al.* (1991), Bracaccia *et al.* (1991) and Adamson *et al.* (1997) amongst others.

In 1996 Repsol Oil Operations (ROO) organized the first geological field trip to southwestern Libya, which covered the classic areas around Ghat-Al Awaynat and the Qarqaf High (synonyms: Jabal Hasawnah, Jabal Fazzan). These outcrops are located some 100 to 200 kms to the southwest and northeast of the oilfield held by Repsol, and potentially provide much information essential for the subsurface geological work in NC115 Concession.

The Mamuniyat Formation and Melaz Shuqran Formation are genetically related units. Soft sediment deformation is ubiquitous at their lower contact, which locally shows considerable relief. Slumping, de-watering structures and up to boulder size conglomerates indicate a rapid and in parts chaotic sedimentation of the lowermost Mamuniyat Formation. They are followed or intercalated by greenish to reddish sandstones with some sandstone layers.

The upper section of the Mamuniyat Formation shows a more uniform grain-size than lower section, various types of cross-bedding and is very porous. The equivalent of the southwest part of the study area, in the El-Sharara Field, has not been found in outcrop. The Melaz Shuqran Formation shales separate the Mamuniyat Formation sandstones from the Cambro-Ordovician aquifer and cause different salinity and pressure heads in the B-Field. Silicification and fracturing are widespread and will also affect the NC115 reservoir rocks (Geological Field Trip, 1996).

1.2 The present study

1.2.1 Introduction

This study investigates the petrography, sedimentology and sequence stratigraphy of the Cambro-Ordovician "Ashgillian" Mamuniyat reservoir interval drilled by Repsol Oil Operations, NC115 Concession on the northwestern flank of the Murzuq Basin, Great Socialist People's Libyan Arab Jamahiriya.

The study presented in this thesis was undertaken on the Mamuniyat Formation, and represents the results of a Concession-wide study, which includes data from three oilfields (A, B and H-Fields), and a number of the exploration wells within NC115 Concession (**Table 1.1**). Some facies studies had been undertaken previously particularly in A-Field, for some 30-50 m of core cut through the main part of the Mamuniyat Formation in well A28-NC115 located in the depocenter of A-Field within El-Sharara Field (Fello, 1996).

The main focus of this study is the Upper Ordovician (Ashgillian) Mamuniyat Formation, which is the primary reservoir target in three oilfields: A, B and H within Repsol Concession area NC115. A problem with the Mamuniyat Formation is the location of the sediment provenance, and the relationship and controls on sediment flux and the depositional systems, due to the lack of adequate subsurface and outcrop data.

WELL NAME	*CORE NO.*	*CORE INTERVAL (m)*		*CORE THICKNESS (m)*	*GEOLOGICAL FORMATION*
		TOP	*BOTTOM*		
A1-NC115	8-17	1434.4	1526.7	92.3	Mamuniyat
A2-NC115	2-5	1516.4	1588.4	72.0	Mamuniyat
A4-NC115	2-5	1531.4	1584.4	53.0	Mamuniyat
A8-NC115	1-9	1409.5	1541.5	132.0	Mamuniyat
Total core recovered from the Mamuniyat Formation in A-Field: 349.3 m.					
B2-NC115	2-9	1416.3	1528.4	112.1	Mamuniyat
B3-NC115	1-11	1416.3	1550.4	134.1	Mamuniyat
B8-NC115	1-13	1414.3	1510.4	96.1	Mamuniyat
B27-NC115	1-2	1453.4	1479.9	26.5	Mamuniyat
Total core recovered from the Mamuniyat Formation in B-Field: 368.8 m.					
H2-NC115	2-7	1484.4	1563.4	79.0	Mamuniyat
H3-NC115	3-14	1435.3	1576.4	141.1	Mamuniyat
H4-NC115	1-9	1479.6	1529.6	50.0	Mamuniyat
H5-NC115	9-17	1469.5	1530.5	61.0	Mamuniyat
Total core recovered from the Mamuniyat Formation in H-Field: 331.1 m.					

Table. 1.1. Available conventional core data from the 12 oil wells used in this study within A, B and H-Fields, NC115 Concession.

1.2.2 Aims of the study

The main aims of the study are as follows:

1) To examine the petrographic characteristics of the sandstones in the Mamuniyat Formation, in order to identify texture, mineral composition, diagenetic features and porosity with a view to assessing the reservoir potential of the sandstones;
2) To integrate the petrographic data with conventional core analysis data in order to gain an understanding of controls in reservoir quality, in addition to comparing results from different facies in surface and subsurface formations;

3) To attempt to produced a new stratigraphic subdivision of the Cambro-Ordovician reservoir interval;
4) To provide a detailed sedimentological description of over 310 mets (1016 ft) of the core from three oilfields and a number of additional exploration wells;
5) To established for each field and the concession as a whole a sedimentary facies scheme for the Mamuniyat reservoir formation;
6) To integrate the sedimentological and wireline log data in order to derive depositional models which adequately account for all observed characteristics of the Mamuniyat Formation in the study area;
7) To review the use of wireline logs in sequence stratigraphy and define various characteristics log patterns, especially gamma-ray patterns and integrate them with the core; and
8) Apply sequence stratigraphic methods of analysis to the Mamuniyat Formation, using the variation in facies tracts and stacking patterns in relation to changes in base level.

1.3 Location of NC115 Concession

The Murzuq Basin also called the Djado Basin in SW Libya is sub-circular in shape and clearly visible on satellite images. The Murzuq Basin, covers an area of some 350,000 km^2, extending southwards into Niger (Thomas, 1995). Early Palaeozoic tectonism created a series of NNW trending arches and sub-basins across North Africa, filled with siliciclastic continental and shallow-marine deposits. This Early Palaeozoic tectonism effectively controlled the distribution of Upper Ordovician hydrocarbon reservoirs and the distribution of Silurian "Hot Shale" source and seal rocks which onlap early-formed fault blocks (Selley, 1997).

Repsol NC115 Concession lies on the northwesthern flank of the Murzuq Basin, about 807 miles (1,330 km) southwest of Tripoli. It covers an area of 9,969 $miles^2$ (25,850 km^2) (**Fig. 1.3**).

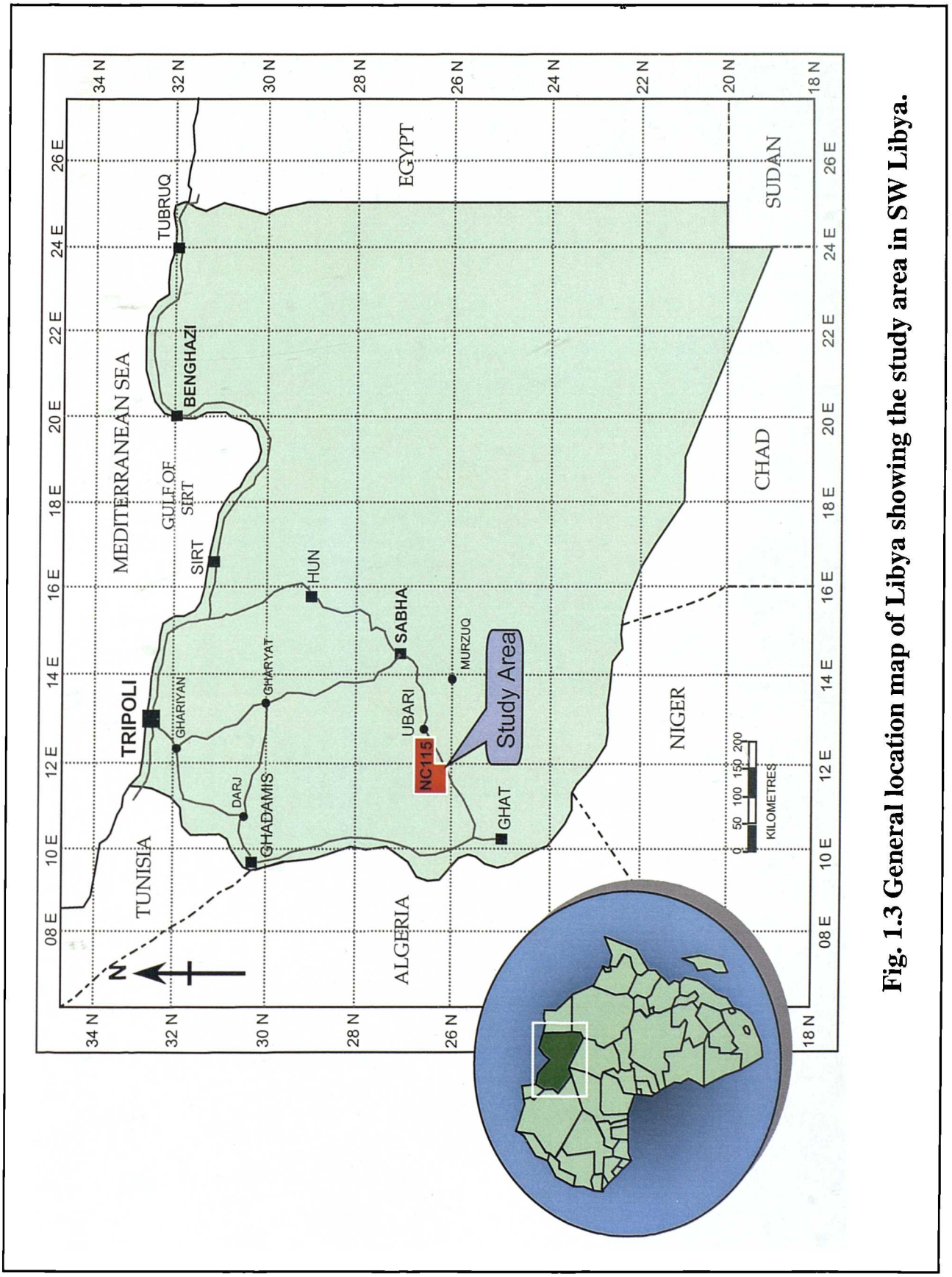

Fig. 1.3 General location map of Libya showing the study area in SW Libya.

1.4 Methodology and available material

A large amount of material was available for this study, including slabbed cores photographs, samples for petrographic analysis (thin sections), wireline data (electrical logs) and conventional core analysis data from 12 oil wells throughout the three main oilfields (**Fig. 1.4**). The data set is outlined below.

1.4.1 Conventional core data

Limited core plug samples of two wells A17 and B21-NC115, and thin section samples (**Table 1.2**):

WELL NAME	FORMATION	CORES NO.	NET LOGGED (m)	THIN SECTIONS NO.
A1-NC115	Mamuniyat	8-17	92.3	12
A2-NC115	Mamuniyat	2-5	72.0	7
A4-NC115	Mamuniyat	2-5	53.0	4
A8-NC115	Mamuniyat	1-9	132.0	17
B2-NC115	Mamuniyat	2-9	112.1	6
B3-NC115	Mamuniyat	1-11	134.1	11
B8-NC115	Mamuniyat	1-13	96.1	11
B27-NC115	Mamuniyat	1-2	26.5	2
H2-NC115	Mamuniyat	2-7	79.0	6
H3-NC115	Mamuniyat	3-14	141.1	9
H4-NC115	Mamuniyat	1-9	50.0	9
H5-NC115	Mamuniyat	9-17	61.0	11
Total of the net logged and number of thin sections within A, B and H-Fields.			**1049.2**	**105**

Table. 1.2. Available cores and thin sections from Upper Ordovician "Ashgillian" strata from the 12 oil wells used from A, B and H-Fields, NC115 Concession (After calibration with electrical logs), used in this study.

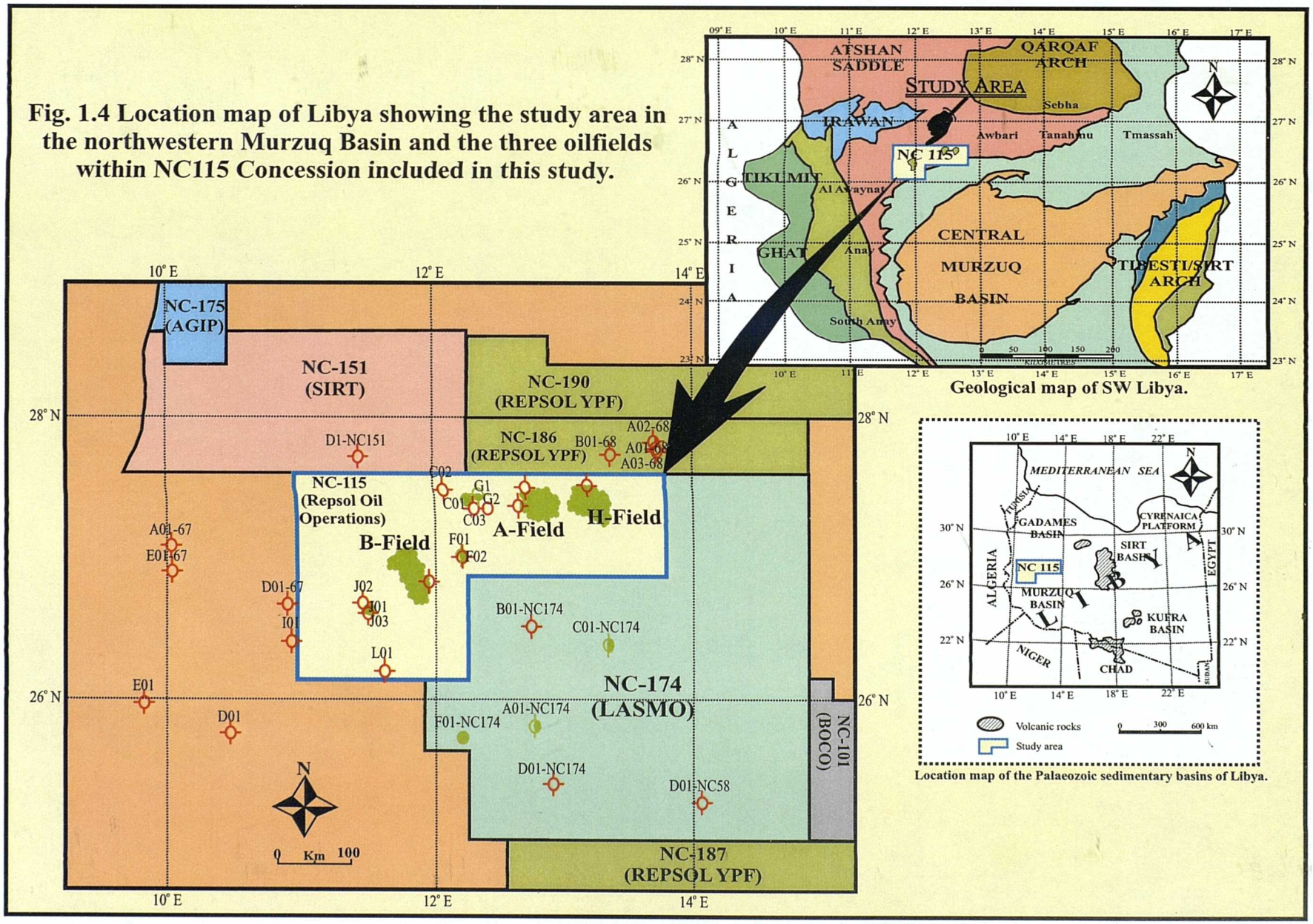

Fig. 1.4 Location map of Libya showing the study area in the northwestern Murzuq Basin and the three oilfields within NC115 Concession included in this study.

A total of 105 thin sections were examined from 12 oil wells within A, B and H-Fields. Each sample was vacuum impregnated with blue resin to facilitate the recognition of porosity and stained with a mixed Alizarin Reds and potassium ferricyanide solution to aid in the identification of carbonate minerals. In addition samples were stained with a sodium cobaltini solution to aid the recognition of alkali feldspar. Each thin section was point counted (300 points) with the summary petrographic data presented in chapter two.

1.4.2 Wireline log data

Electrical wireline logs used in this study here provided by Repsol Oil Operations "Exploration Department" in an ASCII format:

The electrical wireline log data for the 12 wells, include Gamma-ray (GR), Spontaneous potential (SP), Neutron porosity (NPHI) and Resistivity log (RT). These were used for facies correlation, determining the position of marker beds, and the thickness of facies units and systems tracts sequence boundaries. However, the gamma-ray log was the most useful for delineating facies geometries and depositional relationships. Depth of the core, wireline logs and thickness of internal structures is given in both imperial and metric scales.

Wells A8, B2 and H4-NC115 are considered the type section wells for the three oilfields A, B and H (**Figs. 1.5, 1.6 and 1.7**), based on the core coverage of over 133 m in A8-NC115, 126 m in B2-NC115 and 54 m in H4-NC115.

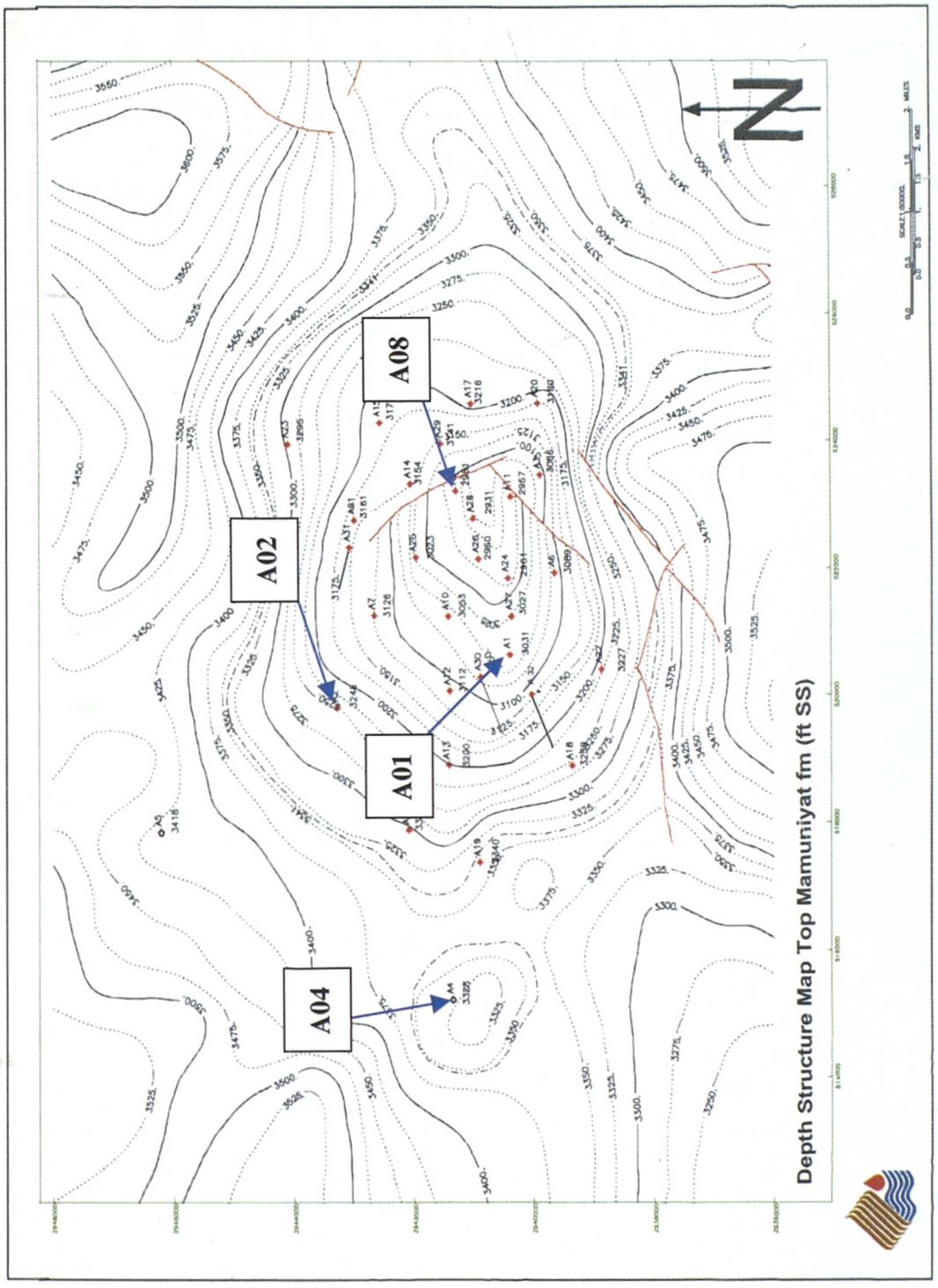

Fig. 1.5 Repsol location map of A-Field showing the wells included in this study.

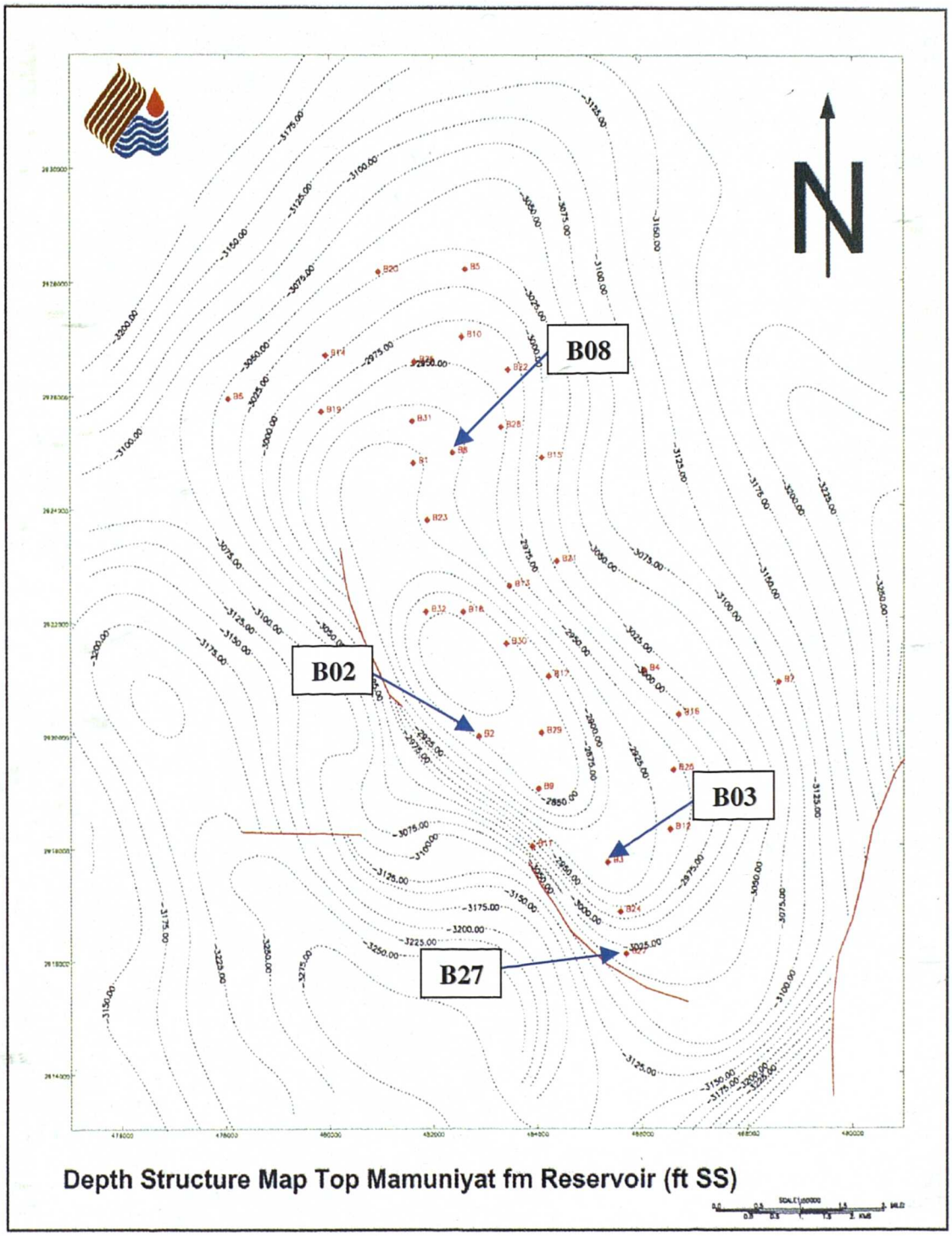

Fig. 1.6 Repsol location map of B-Field showing the wells included in this study.

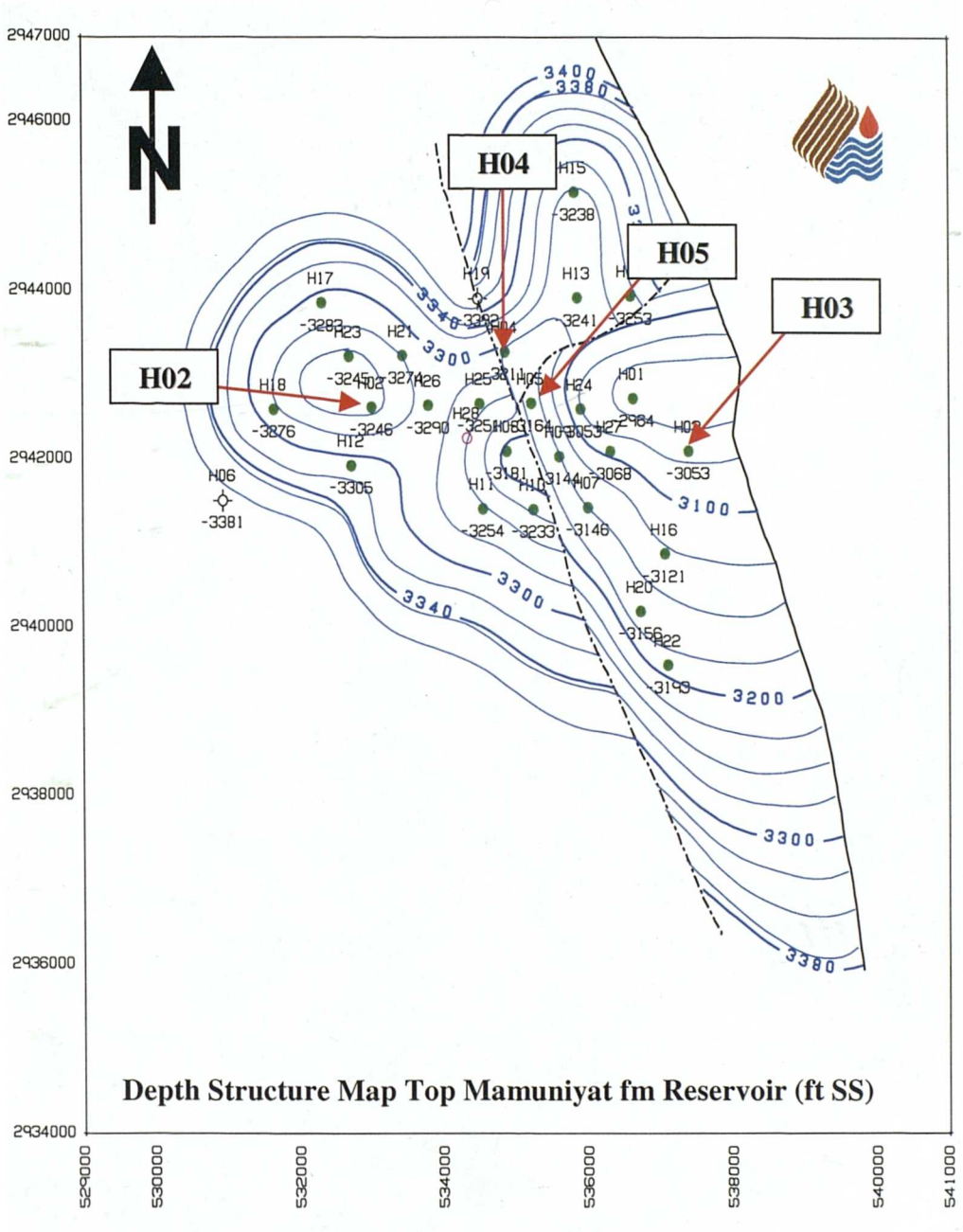

Fig. 1.7 Repsol location map of H-Field showing the wells included in this study.

1.5 Regional setting of the Murzuq Basin

1.5.1 Stratigraphic and tectonic framework

Libya is situated on the Mediterranean coast of North Africa, and has an area of about 1,775,500 km^2 (685,524 miles^2); the country extends about 1,525 km (950 miles) east and west and as much as 1,450 km (900 miles) north and south. This makes it slightly larger than Alaska (**Fig. 1.3**). Except for the northernmost parts, the country lies entirely within the Sahara. Difficulties of travel and survival have long caused the country to remain unmapped, and geological information has been acquired slowly. Libya has been the site of deposition of vast blankets of continental debris and of several incursions of the sea with consequent accumulations of a wide variety of sedimentary rocks. The country is divided into four Palaeozoic and one Mesozoic Basins (**Fig. 1.8**).

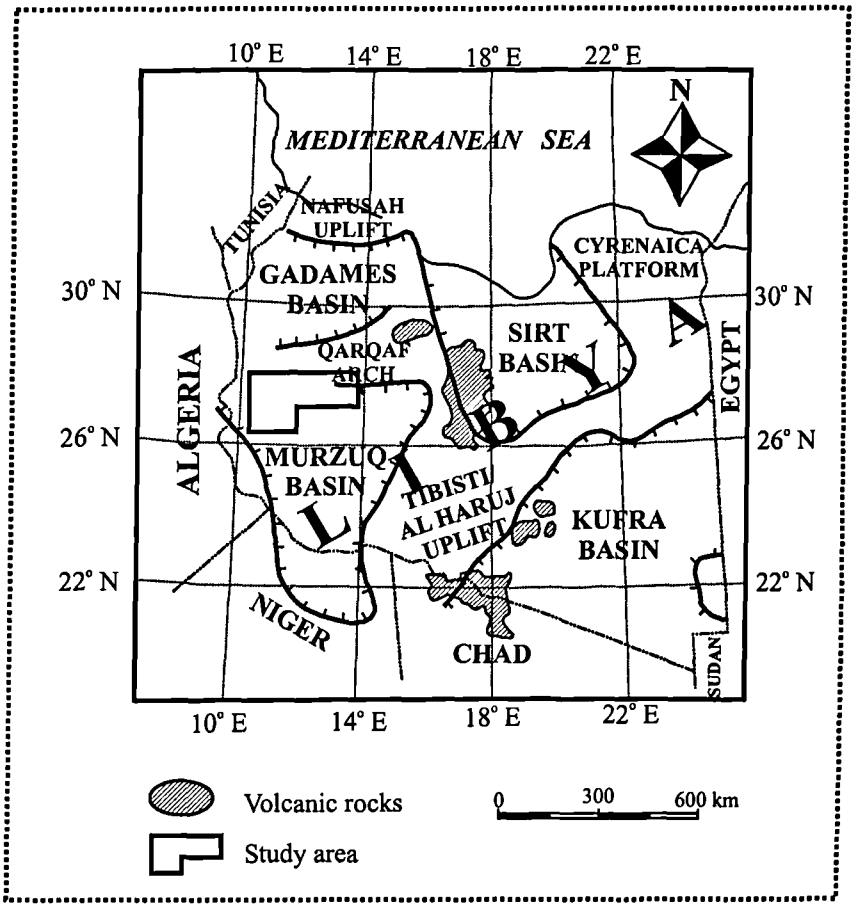

Fig. 1.8 Location map of the sedimentary basins of Libya.

The Taconic, Caledonian, Hercynian and Alpine tectonic events affected Murzuq Basin development, specially Caledonian and Hercynian orogenies (Bellini and Massa, 1980). The Caledonian orogeny started in the Middle Silurian and persisted through to the lower part of the Lower Devonian, which is for some 25 million years. This has been proved in several localities in the south of the Ghadames Basin, in the Murzuq Basin and also in the Kufra Basin (**Fig. 1.8**).

The Hercynian orogeny is the second major tectonic phase to affect the Palaeozoic. Its initial phase can be dated as Middle to Upper Carboniferous and it persisted through to the Permian. The Hercynian orogeny caused folding, faulting and strong subsidence in Tripolitania (Bellini and Massa, 1980). Tectonically, Libya is affected by two sets of faults, which are thought to parallel the rift system in the Gulf of Suez and east African areas (**Fig. 1.9**) (Conant and Goudarzi, 1967).

The erosional unconformity surfaces produced by these events are clearly recognised in the rock record. The thickest sedimentary section is located northwest of NC115 Concession, with a secondary thickening to the southeast. The thick sedimentary section to the northwest has been completely removed leaving the thick section of the sediment to the southeast modified by erosion, as the present day centre of the basin (Geological Field Trip, 1996).

The reconstruction of the tectonic history of the Murzuq Basin formed part of a recent study undertaken by Repsol Oil Operations and an external Apatite Fission Track Analysis (AFTA) study undertaken in 1998 for Repsol by Robertson Research (Report in preparation).

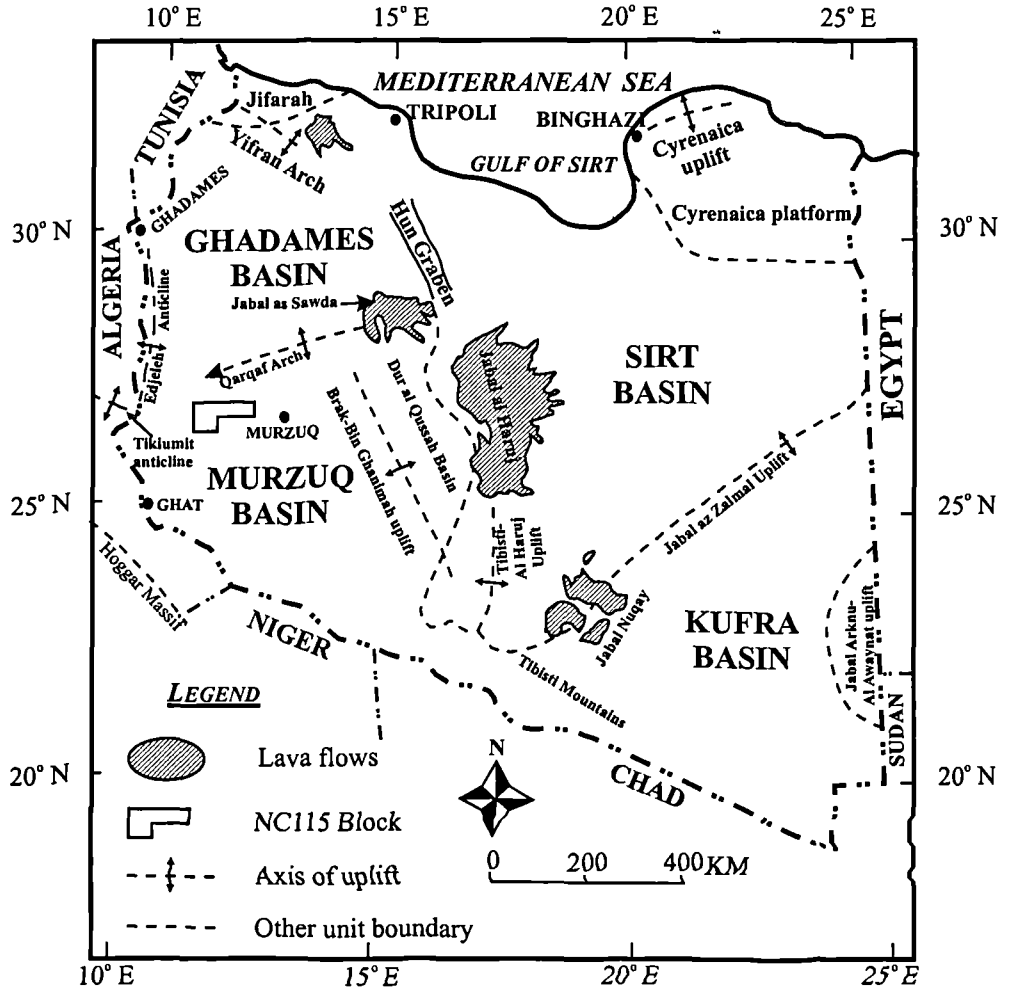

Fig. 1.9 Map showing the general tectonic framework of Libya.

1.5.2 Murzuq Basin

The Murzuq Basin of SW Libya forms one of a series of Palaeozoic intracratonic sag basins on the Saharan Platform. The structural fabric imparted to the North African continental lithosphere during the late Proterozoic, Pan-African event has played an important role in controlling the subsequent structural and stratigraphic evolution of the basin. Early Palaeozoic tectonism created a series of NNW trending arches and sub-basins across North Africa, which filled with siliciclastic continental and shallow marine deposits and transgressive open marine facies. Early Palaeozoic tectonism effectively controlled the distribution of late Ordovician reservoirs and the distribution of Silurian "Hot Shale" which onlap early-formed fault blocks (Klitzsch, 1995).

The Murzuq Basin, an intra-cratonic sag basin, is a huge ladle-shaped structural basin covering more than 350,000 km^2 and has a roughly triangular shape, narrowing towards the south from Libya into Niger. The sedimentary fill is predominately marine and continental Palaeozoic, with some Mesozoic and Cenozoic sediments overlying Precambrian crystalline basement. In the central part of the basin the total sedimentary thickness exceeds 3500 m (Thomas, 1995). The Murzuq Basin is separated from the Illizi Basin, Algeria, to the west by the north-south ridge of the Ghat/Tikiumit Arch (Conant and Goudarzi, 1967; Bennacef *et al.*, 1971). It is located between three tectonic elements: the Qarqaf uplift in the north, the Tibesti/Haruj uplift in the east and the Precambrian Hogger on the south which extends into Algeria and Niger (**Fig. 1.8**).

The whole sedimentary succession is well exposed along much of the edge of the basin, as well as on the southern flank of the Qarqaf Arch. The full sedimentary succession is present in only a few outcrop areas due to regional erosion connected with the Caledonian and Hercynian orogenies, and other lesser unconformities affecting all formations. In the core of the Qarqaf arch the crystalline basement outcrops in relatively small areas (Selley, 1976). The structure of the Murzuq Basin is quite simple. The sub-horizontal or gently dipping strata is faulted and the faults are most frequently parallel to the axis. Tectonic movements affected the basin to a greater or lesser degree from early Palaeozoic (Caledonian) to Post-Eocene (Alpine) times (Bellini and Massa, 1980).

Uplift of the northern flank of the basin, the east trending Qarqaf Arch, was initiated during "Hercynian" epeirogenesis, which promoted trap formation through localised transpressional fault reactivation of subsurface fault systems. Although local Triassic transtensional movements along the Qarqaf Arch modified the northern margin of the basin, the Mesozoic interval was characterized by relative tectonic quiescence and deposition of a southerly derived siliciclastic wedge of Triassic, Jurassic and Cretaceous age. Apatite Fission Track Analysis (AFTA) indicates the maximum burial of the Silurian source was achieved during the Cretaceous. No Tertiary sediments are recorded in the basin although Tertiary basaltic provinces are developed along the basin margins (Selley, 1997).

1.5.3 Exploration history

Although geographically remote, the basin has had an exploration history since the late 1950s. Gulf Oil, Amoseas, British Petroleum, and Wintershell drilled exploration wells during the 1960s with very limited success. This was in the main a response to the ESSO standard discovery made in 1957 in the Atshan area, which was the first Libyan oil discovery (**Fig. 1.2**). In Atshan Field, 2 wells tested oil from Devonian and Carboniferous sandstones, and the play was a continuation of the Palaeozoic trend found productive in the neighbouring Edjeleh region of the Illizi Basin in adjacent eastern Algeria.

As exploration moved to the Sirt Basin of north central Libya, the Murzuq Basin was virtually forgotten. In the mid-1970s Occidental acquired Concession NC34, and drilled A1-NC34 in 1977, which encountered oil indications in Cambro-Ordovician sandstones. The interval was not tested. Meanwhile, Braspetro had Concession NC58. This was a relatively large permit, which encompasses most of the west-central Murzuq Basin. Braspetro acquired some 3000 km lines of seismic and drilled seven wells with one A1-NC58, a minor, sub-commercial oil discovery in Cambro-Ordovician sandstone reservoirs. Permit NC58 was relinquished in the early 1980s (Thomas, 1995).

Rompetrol, the state oil company of Romania (NC115), and BOCO, the state oil company of Bulgaria (NC101), were subsequently awarded exploration permits on the northwestern and north central flanks of the basin, respectively. Oil discoveries were made on both in the Upper Ordovician Mamuniyat Formation. In late 1994, a group led by Repsol as operator was formally awarded the ex-Rompetrol Murzuq field complex permit. Plans are for field development and oil pipeline construction to the El Hamra terminus in the southeast Ghadames Basin, where a pipeline system to the coast is already in place. BOCO, holder of permit NC101, acquired approximately 4300 km lines of seismic and drilled 18 exploration and appraisal wells since 1981. Sixteen prospects have been drilled, resulting in the discovery of five oil accumulations in Cambro-Ordovician and minor oil accumulations in the Devonian.

Lasmo was awarded open acreage (NC174) between the Repsol and BOCO permits in 1990. Approximately 2700 km lines of seismic were acquired, and in 1992-1993 four wildcats were drilled. Results are confidential, but two were reported as Ordovician oil discoveries, with one well flowing 450 bbl/d of oil. In October 1997 the discovery well F1-NC174, encountered a gross oil column of 113 m, and was tested at a cumulative rate of 7500 bbl/d of 38 degree API crude.

In November 2000 Repsol YPF (Madrid) announced an oil discovery in well A-1 in the exploration block NC186 of the Murzuq Basin. The well A1-NC186, the first one drilled by Repsol YPF in Block NC186, has found a significant oil column in the sandstone of the Hawaz Formation. Repsol YPF is the operator for the exploration blocks NC186, NC187 and NC190 of the Murzuq Basin, on behalf of a group of four European companies including: Repsol (Spain), OMV (Austria), Total Fina Elf (France) and Saga Petroleum Mabruk (Norsk Hydro, Norway).

1.6 Stratigraphic succession of the Murzuq Basin

The stratigraphic nomenclature of the Murzuq Basin is that used by Repsol Oil Operations (**Fig. 1.10**) (Fello and Herzog, 1996), although reference is made to the stratigraphic summary in Pierobon (1991). Most sedimentary units forming the stratigraphic column of the basin are widespread and have good correlation in the subsurface and outcrop. The Murzuq Basin has a relatively structure and simple stratigraphy, and it contains sedimentary rocks ranging in age from Cambrian to Tertiary-Quaternary. Maximum thickness in the basin centre (Awbari Trough) is about 3950 m (13,000 ft.).

The sedimentary fill of the Murzuq Basin is typical of cratonic Palaeozoic basins in other parts of the world. The depositional history is relatively uncomplicated with some conspicuous characteristic facies patterns. During the whole of the Palaeozoic period, the marine incursions came from the northwest. The major sedimentary deposits defined in the Ghadames Basin in subsurface areas and on the outcrops are also found more to the south in the Murzuq Basin (Pierobon, 1991).

The reservoir study within NC115 Concession focuses on the Mamuniyat Formation, which has an Upper Ordovician (Ashgillian) age. The Cambro-Ordovician system of Libya was first defined in the area of the Qarqaf Arch and is widespread over large portions of the North Africa craton (Pierobon, 1991). Five formations, four of them formally defined by Massa and Collomb (1960), represent this system in Libya. These are the Hasawnah, Ash Shabiyat, Hawaz, Melaz Shuqran and Mamuniyat Formations, which have been grouped into the Qarqaf Group by Burollet (1960).

In the Murzuq Basin the application of depositional models (McDougall and Martin, 1998) generated from outcrop studies supports the interpretation of the subsurface geology. The lateral and vertical extent of the Cambro-Ordovician sandstones is remarkable. Field studies indicate that the Upper Cambrian section (Hasawnah Formation) is of continental origin, the remaining part of the Palaeozoic succession being predominantly fluvial to marine deposits in the Upper Ordovician (Pierobon, 1991).

Typical deltaic sediments do not seem to occur in the Palaeozoic section of the basin. The occurrence of storm-wave deposits (tempestites) characterizes, most of the Silurian, Devonian and Carboniferous rocks (Pierobon, 1991). The Silurian system of the Murzuq Basin represents a classic example of a transgressive-regressive depositional cycle.

Rhythmic alternation of shales, siltstones and very fine-grained sandstones which occur in the Tanezzuft and Lower Akakus Formations show characteristics of turbidity current deposition over a broad marine platform. The constant influx of terrigenous material could have diluted the organic matter accumulated in the bottom sediment, thus precluding good quality source rock from being formed over large portions of the basin during the Silurian.

ERA	PERIOD / SUBPERIOD		EPOCH	AGE My	Uncon-formity	New ROO Terminology (IRC - based)
CENOZ.	*Quaternary or Pleistocene*		Holocene	0.01	15	Quaternary
			Pleistocene	*1.64*	14	Al Mahruqah Fm.
	Tertiary	Neogene	Pliocene	5.2		
		22	Miocene	23,3	13	& basalts
		Paleogene	Oligocene	35.4		Mazul Ninah Fm.
			Eocene	56,5		Bishima Fm.
65	*63*	42	Palaeocene	*65,0*		Surfah Fm.
MESOZOIC	*Cretaceous*		Upper Cretaceous	97.0	12	Zmam Formation
	81		Early Cretaceous	*145.6*	11	Messak Formation
	Jurassic		Malm	157.1		Taouratine Fm.
			Dogger	178.0		
	62		Lias	*208.0*	10	
	Triassic		Late	235.0		Zarzaitine Fm.
			Mid	241.1		
180	*37*		Lower	*245.0*		
PALAEOZOIC	*Permian*		Zechstein	256.1	9	
	45		Rot-liegendes	*290.0*		Tiguentourine Formation
	Carbon-iferous	Upper	Stephanian	303.0	8	
			Westphalian	318.0		Dembaba Fm.
		43	Namurian	332.9	7	Assedjefar Fm.
		Lower	Visean	349.5		Marar Fm.
	73	30	Tournaisian	*362.5*		"Lwr. Marar Fm."
	Devonian		Late	377.4	6a 6	Awaynat Wanin BDS
			Middle	386.0		Fm.
			Early			Ouan Kasa/
	46			*408.5*	5	Tadrart Fms.
	Silurian		Wenlock-Prid.	430.4		Akakus Fm.
			Llandove-rian		4	Tanezzuft Fm. Hot sh.mbr
	Ordo-vician	Upper	Ashgillian	443.1		Mamuniyat Fm.
			Caradocian	463.9	3	Tashgart / Melaz Shuqran Formations
		Middle	Llanv./ Lland.	476.1		Ash Shabiyat / Hawaz Formations
		Lower	Arenig	493.0		
	71		Tremadoc	*510.0*	2	
	Cambrian		Upper	517.0		Hasawnah Fm.
			Middle	536.0	1	
325	*60*		Lower	570.0		
	INFRACAMBRIAN		Algonkian	2500.0		Mourizdie Fm.
4330	*PRECAMBRIAN*		Archean	4000.0		Basement

Legend

Not Present in NC 115 | Study Formation | Present in NC115

Fig. 1.10 Stratigraphic column of the Palaeozoic, Mesozoic and Cenozoic successions in NC115 Concession, Murzuq Basin, SW Libya.

1.6.1 Mourizidie Formation: *Precambrian (Algonkian)*

The oldest sedimentary rocks, which and known as the Mourizidie Formation or the Infracambrian sequence have not yet been recognized in the area under study; it has been reported in the Dor Al Qussa area, along the eastern flank of the Murzuq Basin (Burollet, 1960). The basement in the Murzuq Basin is exposed in cores in the Tibisti and Hoggar uplifts, and in some erosional windows in the Jabal Qarqaf. Basement rocks can be roughly divided into two main groups, a high-grade metamorphic series and a semi-metamorphic series (Desio, 1939, 1953), which includes the Mourizidie Formation.

In NC115 Concession, the Mourizidie Formation is disconformably overlain by the basal conglomerate of the more or less horizontal strata of the Cambrian Hasawnah Formation. In the El Sharara Field, only a few wells have penetrated this sequence so far; A1, A28, B31 and H27-NC115 (Fello and Herzog, 1996). Type well A1-NC115 penetrated about 75 m of extrusive acidic to intermediate rocks (rhyolite to rhyodacite) which were equivalent to the Mourizidie Formation (Pierobon, 1991; Fello and Herzog, 1996).

1.6.2 Hasawnah Formation: *Upper Cambrian*

Massa and Collomb (1960) introduced the Hasawnah Formation after Jabal Hasawnah. Cepek (1980) studied it in more detail. It represents an extensive, blanket-type, medium- to coarse-grained, highly cross-bedded sandstone, forming a 160-500 m thick, uniform sandy complex spread over vast portions of the Saharan platform (Pierobon, 1991). The Hasawnah Formation is unconformably overlain by the fine-grained Ordovician clastics of the Ash Shabiyat Formation (Collmob, 1962); in the subsurface they are difficult to distinguish from each other (Pierobon, 1991; Fello and Herzog, 1996).

In west Al Qarqaf and Dur Al Qussah, this formation occurs as a thick sequence of coarsening-upward fluvial-continental deposits. The depositional setting of the Hasawnah Formation has been interpreted as braided-stream deposits due to their high sandstone/shale ratio (Pierobon, 1991). An increasing marine influence upwards can be correlated with a broad transgressive phase, as inferred from the global coastal onlap chart (Millepied, 1984). Massa and Collomb (1960) separated the overlying Hawaz Formation from the Hasawnah Formation based upon *Tigillites*, having assigned an Upper Cambrian age to the Hasawnah.

1.6.3 Ash Shabiyat Formation: *Lower Ordovician (Tremadocian)*

The Ash Shabiyat Formation was defined by Havlicek and Massa (1973). It is 65 m thick, and characterized by medium- to coarse-grained sandstone, with abundant *Tigillites* zones, and common trace fossils such as *Cruziana* and *Harlania* (Bellini and Massa, 1980). Ash Shabiyat and Hasawnah Formations are very similar (Pierobon, 1991)

This formation is probably equivalent to the Hawaz Formation, which was defined on the Qarqaf Arch. Good exposures of the Ash Shabiyat Formation are accessible, and can be easily examined close to the Ghat region, although the contact with the underlying Hasawnah Formation is not exposed. A conformable contact with the overlying Hawaz Formation was reported by Havlicek and Massa (1973). The Ash Shabiyat Formation has not been accepted by some authors, who prefer to include the corresponding interval in the lower part of the Hawaz Formation (Pierobon, 1991).

The geological setting of the Ash Shabiyat Formation is interpreted as a possible transition from a fluvial to a marine setting. Pierobon (1991) stressed its predominantly lobate depositional geometry. Palynological studies of the Ash Shabiyat Formation strongly indicate a Lower Ordovician (Tremadocian) age (Havlicek and Massa, 1973; Bellini and Massa, 1980).

1.6.4 Hawaz Formation: *Middle Ordovician (Llandeilian / Llanvirnian)*

The Hawaz Formation was named by Massa and Collomb (1960) after Jabal Hawaz (West of Jabal Qarqaf). It has been described by Pierobon (1991) as "typically consisting of cross-bedded, quartzitic sandstones in part kaolinitic, with thin shaley intercalations. *Tigillites*-bioturbated levels and ripple marks are conspicuous".

The Hawaz Formation is conformably overlain by Melaz Shuqran Formation. Clark-Lowes (1985) describes a similar type section in the Ghat region. The formation thickness ranges from 50 m (Dor Al Qussah) to 280 m (Al Qarqaf) in outcrops, and 30 m to 170 m in the subsurface. Pierobon (1991) suggested a probable transition to a shallow marine (foreshore to shoreface) depositional setting, with the offshore tidal sands (shoal massifs) of the continental shelves of northern Brazil, the North Sea and China's Yellow Sea as possible modern depositional analogues. Palynological studies of the Hawaz Formation strongly indicate a Middle Ordovician (Llanvirnian - Llandeilian) age for the whole of the Hawaz Formation, based on palynological data from Braspetro type well C1-NC58 (Millepied, 1984; Pierobon, 1991).

1.6.5 Tashgart Formation: *Upper Ordovician (Caradocian / Ashgillian)*

Radulovic (1985) observed the Tashgart Formation for the first time in the Wadi Anlalin locality. The Tashgart Formation type locality in Wadi Anlalin covers the Tashgart region from where its name originated (Grubic *et al.*, 1991). The Tashgart Formation has a generally uniform thickness of up to 70 m, throughout the whole area (Wadi Tanezzuft, Wadi Anlalin and Tikiumit area).

The Tashgart Formation is characterized by coarse-grained sandstone, with subordinate siltstone. This formation also contains various sedimentary structures such as flute casts and slumping. Further upward in the formation are alternations of silty and fine-grained to medium-grained sandstones. The formation ends with medium-grained ferruginous sandstone.

According to its structural and textural features, lithological characteristics and spatial position, the Tashgart Formation can be considered as a transitional unit between the Melaz Shuqran and Mamuniyat Formations (Grubic *et al.*, 1991). The deposits of the Tashgart Formation develop gradually from the Melaz Shuqran Formation. The turbiditic character of the Tashgart Formation is linked to an event connected with the opening of a rather large depression in the generally shallow epicontinental sea. No fossils were found in this formation. The age of this formation, however, has been estimated in relation to its superposition. As the Tashgart Formation gradually develops from the Caradocian Melaz Shuqran Formation, and shows an upward gradual transition into the Ashgillian Mamuniyat Formation, it should be ascribed to the Caradocian – Ashgillian in age (Grubic *et al.*, 1991).

1.6.6 Melaz Shuqran Formation: *Upper Ordovician (Caradocian)*

The Melaz Shuqran Formation was introduced by Massa and Collomb (1960) after the Melaz Shuqran mountains in west Al Qarqaf. The sediments of this formation are mainly argillaceous, consisting of greenish-grey claystone, intercalated with lenses of medium to fine-grained sandstone, "exhibiting micro-hummocks, wave ripples and bioturbation which attest to a shallow marine facies" (Pierobon, 1991). In the type locality, the Melaz Shuqran Formation is between 10-45 m thick in outcrop. In the subsurface significant facies changes seem to occur, because only thin, highly radioactive shales are present within siltstones and fine sandstones. The formation's thickness ranges between 15-75 m thick in the subsurface, and exceptionally, reaches 120 m thick in well A1-NC34 (Pierobon, 1991; Blanpied *et al.*, 2000).

The sediments were deposited in a quite marine setting, reflecting a widespread transgressive system. Marine fossils (*Brachiopods*, *Bryozoans*, *Crynoids*, *Pelecypods*, *Trilobites* and *Graptolites*) are commonly found in this formation (Pierobon, 1991). Palynological studies of the Melaz Shuqran Formation strongly indicate an Upper Ordovician (Caradocian) age (Millepied, 1979, 1984; Uesugui, 1984; Pierobon, 1991).

1.6.7 Mamuniyat Formation: *Upper Ordovician (Ashgillian)*

The Mamuniyat Formation was defined by Massa and Collomb (1960) after Jabal Al Mamuniyat (West of Al Qarqaf). It has been described by Grubic *et al.* (1991) and Pierobon (1991). This formation is composed entirely of sandstones, which makes it very prominent and easy to recognize throughout the area. The composition of the Mamuniyat Formation is relatively simple and monotonous. It consists mainly of medium- to coarse-grained and conglomeratic sandstones locally showing high percentages of kaolinitic matrix, with thick-bedded to massive, and less frequently thin-bedded quartz sandstones, characterized by a regressive cross-bedded, sandstone unit.

The upper part of the Mamuniyat comprises medium- to coarse-grained sandstone with well developed wavy cross-bedding (Grubic *et al.*, 1991). The subsurface occurrence of the Mamuniyat Formation is widespread, with thicknesses between 20-170 m; a regional thickening towards Al Qarqaf high was noted by Pierobon (1991). The top part of the Mamuniyat Formation is normally transitional with the transgressive Silurian shales (Klitzsch, 1966). On the geological map of Libya (Conant and Goudarzi, 1964) this formation is included in the "Cambrian and Ordovician rocks". In the Murzuq Basin, the main producing reservoir lies in the Mamuniyat quartzitic sandstones. The overall Ordovician sandstone reservoir quality of the Mamuniyat Formation varies greatly. However, porosity as high as 20% has been noted. The clastic deposits of this formation provide the best reservoirs in the northwestern flank of the Murzuq Basin (Boote *et al.*, 1998).

The sandstones of the Mamuniyat Formation were deposited in a shallow sublittoral environment in the lower part of the Mamuniyat column and later agitated (Grubic *et al.*, 1991). Meanwhile, outcrops of the Melaz Shuqran Formation represent the first glacial-marine and the Mamuniyat Formation represent the second glacial-marine cycle of the Palaeozoic period in the Murzuq Basin; a periglacial depositional setting is interpreted based on ecological grounds, sediment texture and structure. Wave ripples and *Skolithos* tracks attest to a shallow-water marine deposition (Pierobon, 1991).

An Upper Ordovician age was established by Collomb (1962) on palynological ground for the western basin; an Ashgillian age was suggested on the basis of brachiopods by Havlicek and Massa (1973). In the Wadi Tanezzuft area palynological investigation revealed the following: from the Acritarcha group *Veryhachium* sp., *Leiosphaeridia* sp., and Leiofuse sp., from the Chitinozoa group *Cymatiosphaera* sp., *Chitinozoa* gen. et sp. indet., *Sporites* sp. and algae *Tortunehma* sp., All theses point to an Upper Ordovician age (Grubic *et al.*, 1991; Pierobon, 1991).

1.6.8 Tanezzuft Formation: *Lower Silurian (Llandoverian)*

The Tanezzuft Formation was introduced by Desio (1936a) after Wadi Tanezzuft, about 65 km northeast of Ghat. It is easily recognized in the field because of its typical relief, with rounded and heavily dissected hills and predominantly dark greyish to black colour, graptolitic shales with intercalation of siltstones and very fine-grained sandstones, often forming rhythmic alternations (Pierobon, 1991). From the south to the north the Tanezzuft Formation varies in thickness. In the Ghat area it is 480 m thick, in the Wadi Tanezzuft area (Kaf Al Junun) the thickness decreases to 360 m and in the eastern part of the Tikiumit area up to 100 m is present (Grubic, *et al.*, 1991). In the Murzuq Basin, the average subsurface thickness of the Tanezzuft Formation ranges from 45-320 m (Pierobon, 1991).

The Silurian system records the first major marine transgression in western Libya; one that lasted through much of that period and extended into Chad and Niger. On the flanks of the Murzuq basin, about 300 m of graptolitic shale is exposed, overlain by a thick regressive sandstone. On the western flank of the Murzuq Basin about 300 m of shale and several hundred met of the sandstone are exposed in a high escarpment (Conant and Goudarzi, 1967).

In the Tanezzuft Formation, combined gamma-ray log and geochemical data show that high mounts of hydrocarbon-prone organic matter were locally concentrated in the sediment. The radioactive shale (Hot Shale Mb.) marker of the basal Tanezzuft has a wide subsurface occurrence in the Murzuq Basin. All the sediments of the Tanezzuft Formation point to a sharp change in environment after the deposition of the huge Cambro-Ordovician sandstones blanket. It was deposited in restricted to open marine conditions associated with an early Silurian marine transgression over a Taconic erosional surface. The Hot Shale Member is the primary source rock for the basin. It is restricted to Taconic unconformity palaeotopographic lows and therefore is only present in certain areas of the basin (Grubic *et al.*, 1991).

Graptolitic and palynology studies of drill cutting samples in the Tanezzuft Formation, indicate an Early Llandoverian age (Pierobon, 1991). Graptolitic shale indicates a broad, relatively shallow epicontinental sea. The bottom position over the wave base is indicated by frequent symmetrical ripple marks and the remoteness of the shore by the absence of *Tigillites* and stromatolites. The upper boundary with the Akakus Formation is conformable, and is placed at the base of a conspicuous sandstone marker bed. The sediments of the Tanezzuft Formation are rich in graptolites, especially the first 100 m. The fauna is rich in individual forms but poor in species.

1.6.9 Akakus Formation: *Upper Silurian (Wenlockian / Pridolian)*

The Akakus Formation was introduced by Desio (1936a) after Jabal Akakus in the Ghat area. This rock unit is essentially sandstone with thin beds of shale and siltstone interbedded with dark-grey graptolitic shales in the lower and middle parts of the Akakus Formation (Klitzsch, 1969). The distinction between this formation and the underlying Tanezzuft Formation is not clear due to the gradational contact between them (Bellini and Massa, 1980).

The type section of the Akakus Formation is 340 m thick. It forms a narrow but morphologically outstanding belt from South Anay in the south, over Jabal Akakus to domains east of Ghat and northwest of Al Awaynat (Pierobon, 1991).

Sandstones of the Akakus Formation are interpreted as representing the regressive phase of the Silurian sedimentary cycle. Deposition of regressive clastics began after the transgression acme was reached in the Middle Silurian. Deposition is characterized by numerous oscillatory changes of regressions (intertidal with *Tigillites* and *Corophioides* in the fine- to medium-grained sandstones) and transgressions (subtidal with *Harlania* and *Cruziana* in the fine-grained sandstones and siltstones, offshore bars with cross-bedded medium-grained sandstones). Ferruginous and convolute intercalation point to high supratidal and land condition (Grubic, *et al.*, 1991). The lowermost part of the Akakus shales were dated by Klitzsch (1965; 1969) as middle Llandoverian on the basis of graptolites (*Climacograptus* and *Monograptus*). The formation overlies the Llandoverian Tanezzuft Formation, and is overlain by the Siegenian Tadrart Formation, which places the Akakus Formation in the Wenlockian-Ludlovian (Grubic *et al.*, 1991).

Palynological data from two Braspetro wells in NC58 Concession, northwestern Murzuq Basin, indicate a Ludlovian to Wenlockian age for the whole Akakus Formation (Pierobon, 1991). Recent palynological analysis, indicates a Wenlockian to Pridolian age for the Akakus Formation.

1.6.10 Tadrart Formation: *Early Devonian (Siegenian)*

The Tadrart Formation was separated by Burollet (1960) in the Jabal Tadrart area and named after it. The formation has the shape of a thick lens deposited south of the Al Qarqaf Arch. The lower boundary of this formation is disconformable. The Tadrart Formation crops out conspicuously in Al Qarqaf, Jabal Akakus and Dur Al Qussah, showing a marked wedge-out toward the north. Klitzsch (1965, 1969) described its type section at Takharkhouri pass along the eastern margin of Wadi Wan Kasa. In Klitzsch's type section the Tadrart Formation is 310 m thick. The formation is thickest and best developed in the Al Awaynat area where it is 350 m thick (Grubic *et al.*, 1991).

The lower and middle parts (> 100 m thick) are composed of alternations of medium- to coarse-grained, cross-bedded sandstones, and very coarse-grained to microconglomeratic sandstones with frequently recumbently deformed cross-bedding, and brown cross-bedded microconglomerates. The upper part of the formation consists of medium- to fine-grained sandstone and subordinate siltstones, with rare plant remains (*Lepidodendron*) in the lower part; the upper part displays thin-bedded marine sandstones with abundant *Tigillites* (Pierobon, 1991). The Tadrart Formation is usually poorly cemented; in well logs it shows very good reservoir characteristics. The basal part of the formation is marked by a ferruginous sandstone resting unconformably on Silurian rocks, and conformably overlain by the Ouan Kasa Formation. Burollet (1960), by analogy with a similar sequence found in the Illizi Basin (Algeria), suggested Siegenian as the age for whole of the Tadrart Formation.

1.6.11 Ouan Kasa Formation: *Early Devonian (Emsian)*

The Ouan Kasa Formation was introduced by Borghi and Chiesa (1940) in Wadi Wan Kasa in the Murzuq Basin. It is thought to lie conformably above the Tadrart Formation. It is 43 m thick, and comprises shale with intercalation of argillaceous siltstone and fine-grained sandstone (Klitzsch, 1969).

Three lithologies are present in the Ouan Kasa Formation all of which are bioturbated: grey shales with gypsum beds and some silty-horizons; light grey to grey siltstones with thin shale intercalations, and thinly-bedded fine-grained sandstones. These are arranged in a coarsening-upward sequence, and characterized by the brachiopods, *Styliolines* and *Tentaculitids* (Klitzsch, in Clark-Lowes, 1985).

The separation of the Ouan Kasa from the Tadrart Formation in the subsurface is not evident. Electrical logs from wells A1-76 and H1-NC58 suggest a rapid transitional passage of the estuarine upper Tadrart to the shallow marine-neritic Ouan Kasa sandstone and siltstones (tidal bar facies) (Pierobon, 1991). Subsurface data from the Murzuq and Ghadames Basins reveals a rich assemblage of palynomorphs indicative of an Emsian age (Massa and Moreau-Benoit, 1976; Pierobon, 1991). The upper contact of the Ouan Kasa Formation is conformable with the overlying Awaynat Wanin Formation.

1.6.12 Awaynat Wanin Formation: *Middle-Late Devonian (Couvinian / Strunian)*

The Awaynat Wanin Formation was introduced by Lelubre (1946) after a well in western Jabal Al Qarqaf. Massa and Moreau-Benoit (1976) raised the formation to the rank of a group, splitting it into four informal units (I to IV). This same subdivision in not feasible for the subsurface of the Murzuq Basin (Pierobon, 1991). Bellini and Massa (1980) described a type section reaching 225 m thick, in the western Al Qarqaf area, with a subsurface thickness from 20-210 m thick.

Pierobon (1991) suggested the geological setting of the Awaynat Wanin Formation as predominantly marine with fluvial-deltaic deposits in the middle and upper parts. In outcrops of this formation, two types of deltaic facies are recognised: fine-grained suspension deposits (delta front) and coarse-grained traction sediments (fluvial-distributary channels), all of them intensely reworked by tide and storm waves (Castro *et al.*, 1985). Palynological analysis of samples from the Braspetro well, within NC58 Concession, confirms the ages as Couvinian to Strunian (Pierobon, 1991).

1.6.13 Tahara Formation: *Late Devonian (Famennian / Strunian)*

The Tahara Formation was introduced by Massa and Moreau-Benoit, (1976) in the Ghadames Basin. It is defined in well B1-49 located in Wadi Tahara. This formation is placed within the Devonian, but its basal contact cannot easily be picked out in the subsurface because of the extreme lithological similarities with the underlying Awaynat Wanin Formation. The formation crops out in the Murzuq Basin, primarily in the west Al Qarqaf area. Its contact with the transgressive Marar Formation is conformable, and it is difficult to distinguish between them (Bellini and Massa, 1980).

The thickness of the Tahara Formation reaches 50 m in outcrops, and 20-60 m in the subsurface. Its consists of sandstone and shales in which the sandstones are generally fine- to very fine-grained, feldspathic and commonly ferruginous and hematitic (Bellini and Massa 1980). The geological setting of the Tahara Formation suggests that suspension deposits, carried into the marine basin by fluvial channels were reworked and re-deposited as offshore shales rich in marine fauna. Famennian to Strunian is the most probable age (Uesugui, 1984; Pierobon, 1991).

1.6.14 Marar Formation: *Lower Carboniferous (Tournaisian / Visean)*

The Marar Formation was established by Lelubre (1946) in the Al Qarqaf area. In the subsurface the thick section ranges between 180-240 m thick, and is characterised by interbedded marine shale and sandstones. In the geological column of the Marar Formation can be recognized; a lower part of fine- to locally coarse-grained, kaolinitic sandstones of cyclic appearance, interbedded with dark grey to black, finely laminated, carbonaceous shale and siltstones, which become predominant in the upper and middle parts (Whitbread and Kelling, 1982).

The Marar Collenia Beds was introduced by Freulon (1953) for stromatolitic limestone in the Zegher area, southwest Dembaba and north of the Tihemboka structure, as well as in boreholes drilled in the north-northwest. However, these are missing in the eastern, central and southern portions of the basin. The Collenia beds are mostly regarded as the upper member of the Marar Formation (Grubic *et al.*, 1991). The thickness of the Collenia bed is between 1-10 m, separated by silty clay, fine-grained sandstone and gypsiferous siltstone. Original carbonates are partly replaced by SiO_2 (Whitbread and Kelling, 1982). The amount of preserved carbonate increases towards the northwest, where it represents a brief-regressive intertidal interval deposited at the end of the Marar sequence (Grubic *et al.*, 1991).

The depositional setting of the Marar Formation comprises deltaic deposits developed on relatively stable cratonic areas. These deposits contain 15 dominantly coarsening-upward depositional cycles. Palynological analysis on samples from some Braspetro wells in NC58 Concession give a Tournaisian to Visean age (Pierobon, 1991).

1.6.15 Assedjefar Formation: *Upper Carboniferous (Namurian)*

In the western part of the Murzuq Basin the Assedjefar Formation was first mentioned by Collomb and Heller (1958). It forms a regional layer, which thickens northwards from 5-30 m in the Anay area to 140 m in the Hasi Anjiwal area. The Assedjefar Formation is characterized by dark grey to black shales interbedded with siltstones and fine- to very fine-grained, argillaceous sandstones forming thin lenses and beds up to tens of meters thick (Pierobon, 1991).

Sediments of the Assedjefar Formation were deposited under variable shallow marine conditions. Siltstone and claystone with gypsum indicate a lagoonal environment. Cross-laminated sandstones record an offshore environment, while the limestones were deposited in a sublittoral high energy zone (Grubic *et al.*, 1991).

According to fossil assemblages and palynological analysis this formation is assigned to a Namurian age. The upper boundary of the Assedjefar Formation is gradational and conformable with the Dembaba Formation, and is marked by stromatolitic structures (Pierobon, 1991).

1.6.16 Dembaba Formation: *Upper Carboniferous (Westphalian)*

The presence of the Dembaba Formation in the western part of the Murzuq Basin, was first reported by Collomb and Heller (1958). The lower boundary of this formation is conformable and marked by the first bed of stromatolitic limestone. It is a marine to transitional sequence of argillaceous limestones and dolomite calcilutites, interbedded with marly claystone which grade downwards into shale. Thin beds of very fine- to fine-grained sandstones are intercalated with the other lithologies (Pierobon, 1991).

The thickness of the formation in the subsurface ranges from 35-55 m thick. Burollet (1960) divided the Dembaba Formation into three informal subunits: an upper limestone unit with a rich fauna of productids and gastropods; a middle shale unit with occasional sandy/dolomitic beds and rare gypsum; and a lower limestone unit with some intercalations of dolomite and green shale. Palynological data analysis and seismic data gathered by the Braspetro company within NC58 Concession, assigned the Dembaba Formation to a Westphalian age (Banerjee, 1980).

1.6.17 Tiguentourine Formation: *Upper Carboniferous – Early Permian (Stephanian / Rotliegendes)*

The Tiguentourine Formation was introduced by Lapparent and Lelubre (1948) north of Edjeleh area, on the Algerian/Libyan border. It was defined by Burollet (1960) as consisting of reddish-brown to mauve clays and shale, often slightly dolomitic with characteristic gypsum beds near the base, and thin intercalations of very fine- to medium-grained, calcareous sandstones.

The thickness of the Tiguentourine Formation ranges between 130-520 m in the subsurface (Pierobon, 1991). The formation is conformable with the Middle Carboniferous Dembaba Formation, and is unconformably overlain by the Triassic Zarzaitine Formation, which was deposited after a long hiatus. The geological setting of this rock unit represents the last regressive phase of the Carboniferous transgression. Its sediments are most likely of lagoonal origin (Grubic *et al.*, 1991).

The Tiguentourine Formation does not contain fossils and its age could be not be determined by biostratigraphic means. The formation is thus regarded as Upper Carboniferous, as suggested by Lapparent and Lelubre (1948) and established by Hoen (1968) in the type locality in Algeria. However, the upper transitional to continental section has a poor microfossil record, although some of the spore assemblages obtained suggest an Upper Carboniferous to Early Permian age (Uesugui, 1984).

1.7 Stratigraphy succession of the Mamuniyat Formation within NC115 Concession area, NW Murzuq Basin

In the Murzuq Basin, SW Libya the formations making up the stratigraphic column range from Precambrian to Quaternary in age and they mostly have a widespread distribution and good lateral correlation between the subsurface and outcrop. The stratigraphy has been related to tectonic phases and major cyclic sea-level changes documented world wide (Bellini and Massa, 1980). The main tectonic orogenies affecting the study area are the Caledonian, Hercynian and Alpine.

In this study the Mamuniyat Formation has been divided into: Lower, Middle and Upper members according to geometry, lithology, sedimentary structures, fossil content and electrical wireline log data, each member corresponding to a specific facies association as shown in **Table 2.3.** Each facies association is in turn composed of a number of component facies.

The Lower Member is the thickest. It consists of up to 4 complete coarsening-upward sandstone dominated units that show a progradational stacking pattern; each unit shows evidence of having been deposited on a marine shelf subjected to frequent storms. The Middle Member comprises offshore shales and siltstones showing a fining-upward trend, overlain by nearshore wavy and hummocky cross-stratified shoreface sandstones. The Upper Member consists of coarse to very coarse, cross-bedded and massive sandstone organised into two coarsening-upward packages; these show an overall coarsening-upward trend which is attributed to proximal and distal parts of a braided stream system draining an alluvial plain with the palaeoslope towards the NE **(Figs 2.2, 2.3 and 2.4).**

1.8 Summary

The Murzuq Basin, SW Libya, is one of a series of Palaeozoic intracratonic sag basins on the North African Saharan Platform. The structural fabric of the basin was developed during the Late Proterozoic Pan-African orogenic event, which has strongly influenced the stratigraphy and depositional patterns within the predominantly Palaeozoic clastic basin-fill. The main focus of this study is the Upper Ordovician (Ashgillian) Mamuniyat Formation, which is the primary reservoir target in three oilfields A, B and H within Repsol Oil Operations Concession area NC115, on the northwest flank of the Murzuq Basin. A major problem with the Mamuniyat is the location of the sediment provenance, due to the lack of adequate subsurface and outcrop data, and the relationship and controls on sediment flux and the depositional systems.

CHAPTER 2

SEDIMENTOLOGY

SEDIMENTOLOGY

2.1 Introduction

2.1.1 Facies

The term "Facies" was introduced into geology by Gressly (1838). It meant the entire aspect of a part of the earth's surface during a certain interval of geological time (Teichert, 1958). The word itself is derived from the latin *facia* or *facies*, implying the external appearance, or look of something. The modern usage was introduced by Jamieson (1860), who used the term to imply the sum total of the lithological and palaeontological aspects of a stratigraphic unit.

Translations of Gressly's extended definition are given by Teichert (1958) and Middleton (1978). The term facies can also be extended to other non-observable aspects (Reading, 1986) such as seismic facies, which is based on seismic reflection, configuration, amplitude and velocity, and log facies which is dependant on electric, acoustic and radioactive properties.

Middleton (1978), Reading (1978) and De Raaf *et al.* (1965) used the more common and modern definition of facies based on "Lithological, structural and organic aspects detectable in the field". This definition of the term facies can be extended. For example, when characteristic biological material is present, then the facies is called a biofacies. When fossils are not present, the term lithofacies is used. Finally the facies definition is the total lithologic and biologic characteristics of a sedimentary deposit resulting from accumulation in a depositional environment (Richard and Davis, 1983).

2.1.2 Facies correlation

Probably the most important single concept that must be thoroughly understood and applied by the sedimentologist and stratigrapher was formulated by Johannes Walther in 1894. He stated that "only those facies and facies-areas can be superimposed primarily which can be observed beside each other at the present time" (Walther, 1894).

Also called the law of correlation (or succession) of facies, this fundamental principle of geology is used universally, but without knowledge of its origin (Middleton, 1973), and is frequently mis-stated. However, this law can only be applied to facies without any break between them (Blatt *et al.*, 1972). This principle has been used to explain the fining-upward sequence of fluvial point bar sandbodies deposited in meandering river channels (Allen, 1965) and the progradation of deltas leading to coarsening-upward sequences (Reading, 1986).

2.1.3 Facies models

The construction and use of facies models continues to be one of the most active areas in the general field of stratigraphy, as is demonstrated by several new books in the field. This emphasis is not new, many of the ideas were embodied in Dunbar and Rodger's principles of stratigraphy in 1957, and were based on studies dating back to Gressly and Walther in the 19th century (Middleton, 1973).

A facies model could thus be defined as a general summary of a specific sedimentary environment. Our aim, as geologists, is partly to identify different environments in ancient rocks, and also to understand the range of processes that can operate within these environments (Walker, 1984).

2.1.4 Facies analysis

Facies analysis has been greatly stimulated over the past few years by rapid conceptual advances in "sequence stratigraphy". The term facies analysis has been, and remains an important subject for many authors in order to describe, correlate and interpret the depositional environment. Important references include Allen (1970), Middleton (1973), Reading (1978), Miall (1977, 1978) and Walker (1984).

2.2 Sedimentological characteristics of the Upper Ordovician, Mamuniyat Formation, NC115 Concession

2.2.1 Introduction

This section attempts to integrate data derived from the Upper Ordovician reservoir interval of the Mamuniyat Formation in the three oilfields, together with data gained from various wells within NC115 Concession, in order to assess its sedimentological development on a concession-wide scale. The study describes and interprets the facies and facies associations in three type wells NC115-A8, B2 and H4 from the three oilfields, A, B and H **(Fig. 1.4)**. The facies reflect deposition by a variety of different depositional processes within different depositional environments. It is based on the detailed description and analysis of both the colour photographs of the slabbed core and wireline logs of the three type wells, augmented by information from the other wells used in this study **(Table 2.1)**.

Facies are defined from slabbed core on the basis of lithology, grain-size, sedimentary structures and wireline log response. Moreover, this section also includes a discussion on the probable environments of deposition and the sedimentary sequences identified within the study sections of these wells. Sedimentological evaluation of cores from A8, B2 and H4 wells reveal a sequence dominated by graded-bedded, internally structureless sandstones, interbedded with local shale and/or claystone.

Well Name	*Core No.*	*Top ft (kb)*	*Base ft (kb)*	*Recovery ft*	*Recovery %*	*Geological Formation*
A8-NC115	1	4623	4652	29	100%	Mamuniyat
	2	4652	4682	27	90%	Mamuniyat
	3	4682	4725	38.7	90%	Mamuniyat
	4	4725	4784	59	100%	Mamuniyat
	5	4784	4844	60	100%	Mamuniyat
	6	4844	4905	61	100%	Mamuniyat
	7	4905	4941	36	100%	Mamuniyat
	8	4941	5000	59	100%	Mamuniyat
	9	5000	5056	56	100%	Mamuniyat
Total core recovered 425.7 ft.				*Total core Mamuniyat 425.7 ft.*		
B2-NC115	1	4537.3	4563.6	6.6	25%	Tanezzuft
	2	4645.6	4675.1	26.2	89%	Mamuniyat
	3	4675.1	4698.1	18	78%	Mamuniyat
	4	4707.9	4737.5	27.9	94%	Mamuniyat
	5	4776.8	4806.4	29.5	100%	Mamuniyat
	6	4806.4	4835.9	29.5	100%	Mamuniyat
	7	4835.9	4865.4	29.5	100%	Mamuniyat
	8	4931	4960.6	29.5	100%	Mamuniyat
	9	5003.2	5013.1	9.8	99%	Mamuniyat
Total core recovered 206.5 ft.				*Total core Mamuniyat 127.8 ft.*		
H4-NC115	1	4853	4869	16	100%	Mamuniyat
	2	4869	4902	6.6	20%	Mamuniyat
	3	4902	4918	16	100%	Mamuniyat
	4	4918	4935	13.6	80%	Mamuniyat
	5	4935	4951	16	100%	Mamuniyat
	6	4951	4967	1.6	10%	Mamuniyat
	7	4967	4984	10.2	60%	Mamuniyat
	8	4984	5000	13.6	85%	Mamuniyat
	9	5000	5017	17	100%	Mamuniyat
Total core recovered 110.6 ft.				*Total core Mamuniyat 110.6 ft.*		

Table. 2.1 Core data for type wells A8, B2 and H4 within the NC115 Concession study area.

These sediments are assigned to the Upper Ordovician "Ashgillian" Mamuniyat Sandstone Formation, which is transgressively overlain by the Early Silurian "Llandovery" Tanezzuft Shale Formation **(Fig. 2.1)** (Pierobon, 1991; Fello and Herzog, 1996). The lithological characteristics of the facies types for the Mamuniyat Formation are discussed in turn below, with special emphasis on the Mamuniyat reservoir sequence.

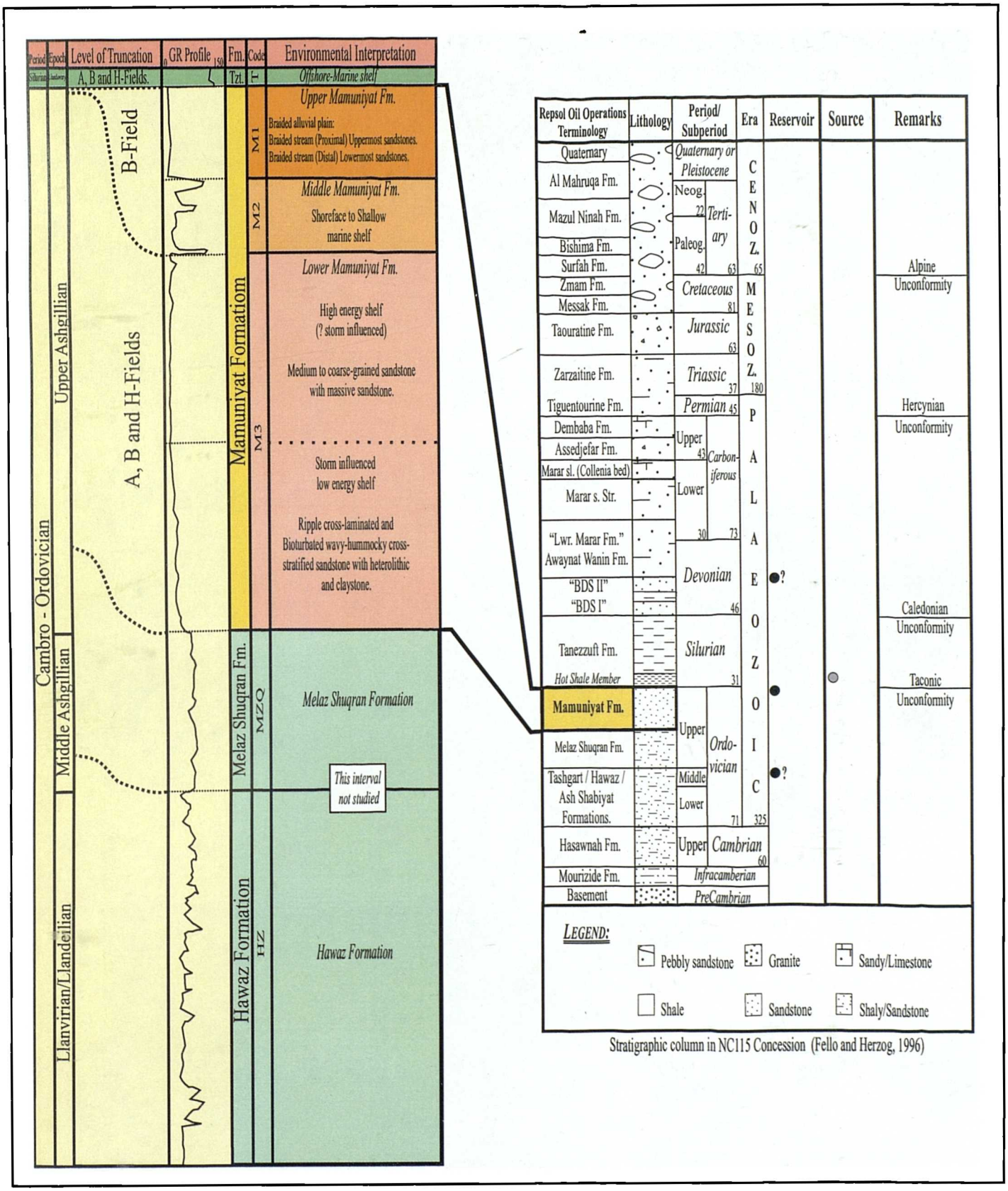

Stratigraphic column in NC115 Concession (Fello and Herzog, 1996)

Fig. 2.1 General stratigraphic columnar section of NC115 Concession, and sedimentological characteristic of the Mamuniyat Formation, on the northwest flank of the Murzuq Basin, SW Libya.

2.2.2 Objectives

The main objectives of the sedimentological study of the Mamuniyat Reservoir Formation are:

1) To provide a detailed sedimentological description of more than 310 met (1016 ft) of slabbed core from three type wells A8, B2 and H4 from the three oilfields A, B and H (**Fig. 1.4**);
2) To integrate the sedimentological, biostratigraphical and wireline log data in order to derive depositional models, which adequately account for all observed characteristics of the studied Mamuniyat Reservoir Formation;
3) To establish for each field, and the concession as a whole, a sedimentary facies scheme for the lower Palaeozoic Reservoir Formation (Mamuniyat);
4) To attempt to produce a reservoir zonation for the Upper Ordovician Reservoir interval; and
5) To integrate the petrographic data with conventional core analysis data in order to gain an understanding of the controls on reservoir quality, in addition to comparing results from different facies and formations.

2.2.3 Available material and methods

A large amount of material was made available as detailed below.

1) Colour photographs of the slabbed cores (**Table 2.2**), and thin sections were prepared by Corex Services Ltd. Aberdeen, UK;
2) Wireline logs for 12 exploration and development wells throughout A, B and H-Fields, have been analysed by sonic, and gamma-ray amplitudes. Thickness and depth intervals for the Mamuniyat Formation, and the total Cambro-Ordovician sandstone, were recorded;
3) Two core plug samples of the two oil wells, A17-NC115 at 4900 ft. and B21-NC115 at 4794 ft. (Mamuniyat Formation); and

4) A review of all relevant literature and accessible unpublished reports known to the author concerning the Upper Ordovician "Ashgillian" Mamuniyat Formation, including outcrop and subsurface information;

Well Name	*Core No.*	*Core Interval ft (kb)*	*Core Thickness (ft)*	*Geological Formation*
A1-NC115	8 – 17	4704.7 – 5007.5	302.8	Mamuniyat
A2-NC115	2 – 5	4973.7 – 5209.9	236.2	Mamuniyat
A4-NC115	2 – 5	5022.9 – 5196.8	173.9	Mamuniyat
A8-NC115	1 – 9	4623.0 – 5056.0	433.0	Mamuniyat
B2-NC115	6 – 9	4623.5 – 4796.5	173.0	Mamuniyat
B3-NC115	1 – 11	4645.6 – 5085.2	439.6	Mamuniyat
B8-NC115	1 – 13	4639.0 – 4954.0	315.0	Mamuniyat
B27-NC115	1 – 2	4767.0 – 4854.0	87.0	Mamuniyat
H2-NC115	2 – 7	4868.7 – 5127.9	259.2	Mamuniyat
H3-NC115	3 – 14	4707.9 – 5170.5	462.6	Mamuniyat
H4-NC115	1 – 9	4853.0 – 5017.0	164.0	Mamuniyat
H5-NC115	9 – 17	4820.0 – 5020.0	200.0	Mamuniyat

Table. 2.2 Showing the exploration and development wells in the three oilfields within the Mamuniyat study interval, NC115 Concession.

2.3 Sedimentary facies associations and facies of the Mamuniyat Formation

The maximum vertical succession is approximately 133 m (437 ft), 126 m (415 ft) and 54 m (178 ft) in the three type wells A8, B2 and H4-NC115 respectively (**Figs. 2.2, 2.3 and 2.4**). Initially, the Mamuniyat Formation in the El-Sharara Field was subdivided into three members characterized by differing log responses. The log responses are strongly tied to lithology. Thus, well-to-well correlation of the three members imposes a lithostratigraphic framework on the Mamuniyat Formation.

These three members have been assigned informal status within the Mamuniyat Formation and are the basis for facies analysis of the Mamuniyat sandstones throughout the NC115 Concession (Fello and Turner, 2001a). Throughout the Mamuniyat Formation ten facies have been recognized, based on particular associations of rock types and their lithological, sedimentological and biological characteristics (Miall, 1977, 1978, 1996). These facies have been grouped into three different Facies Associations as summarised in **Table 2.3**. The attributes of these facies and their environmental interpretation are described below.

2.3.1 Facies Association (A): Alluvial Plain

This facies association is restricted to the uppermost part of the succession in most of the reservoir interval in B-Field, particularly type well B2-NC115 **(Fig. 2.3)**. It only occurs in the upper part of the Mamuniyat Formation (M1) in the southwest part of NC115 Concession. This facies association (A) is represented by the cored interval from 1402 m (4598 ft) to 1430 m (4690 ft) in the type well.

This facies association (A) comprises two distinctive facies; each facies type is defined on the basis of lithology, grain size, sedimentary structures and log response. These facies are described and interpreted below.

2.3.1.1 Facies (A1): Coarse to very coarse grained sandstone

Description

This facies occurs in the subsurface in the uppermost part of the Mamuniyat Formation. It has been found only in the southwestern part of the study area in the B-Field of the El-Sharara Field, Block NC115. It makes up the bulk of the uppermost Mamuniyat sandstones and is represented by the cored interval from 1402 m to 1419 m in type well B2-NC115 **(Fig. 2.3)**. It consists of sandstone with occasional siltstone interbeds, and pebbly sandstones with minor shaley lenses.

Formation	Member		Facies Associations	Sedimentary Facies Type	Sedimentary Environment	
Tanezzuft	–		–	Laminated Claystone with Shale	Offshore - Marine Shelf	
Mamuniyat Formation	Upper	M1	Alluvial Plain	Coarse-Very Coarse Sandstone (A1)	Braided alluvial plain	Braided stream "Proximal"
				Massive Sandstone (A2)		Braided stream "Distal"
	Middle	M2	Shoreface to Shallow Marine Shelf	Wavy-Hummocky Cross Stratified Sandstone (B1)	Shoreface	
				Heterolithic-Claystone Facies (B2)	Offshore	
	Lower	M3	Shallow Marine Shelf	Medium-Coarse Grained Sandstone (C1)	High Energy Shelf (? Storm Influenced)	
				Massive (? Bedded) Sandstone (C2)		
				Ripple Cross-laminated Sandstone (C3)	Storm Influenced Low Energy Shelf	
				Bioturbated Wavy-Hummocky Cross-stratified Sandstone (C4)		
				Heterolithic Facies (C5)		
				Claystone Facies (C6)		

Table. 2.3 General characteristics of the Facies Associations and component facies types in the Mamuniyat Formation, based on A, B and H wells in NC115 Concession, on the NW flank of the Murzuq Basin, SW Libya.

Legend

M1 M2 *Present in B-Field* M3 *Present in A, B and H-Fields*

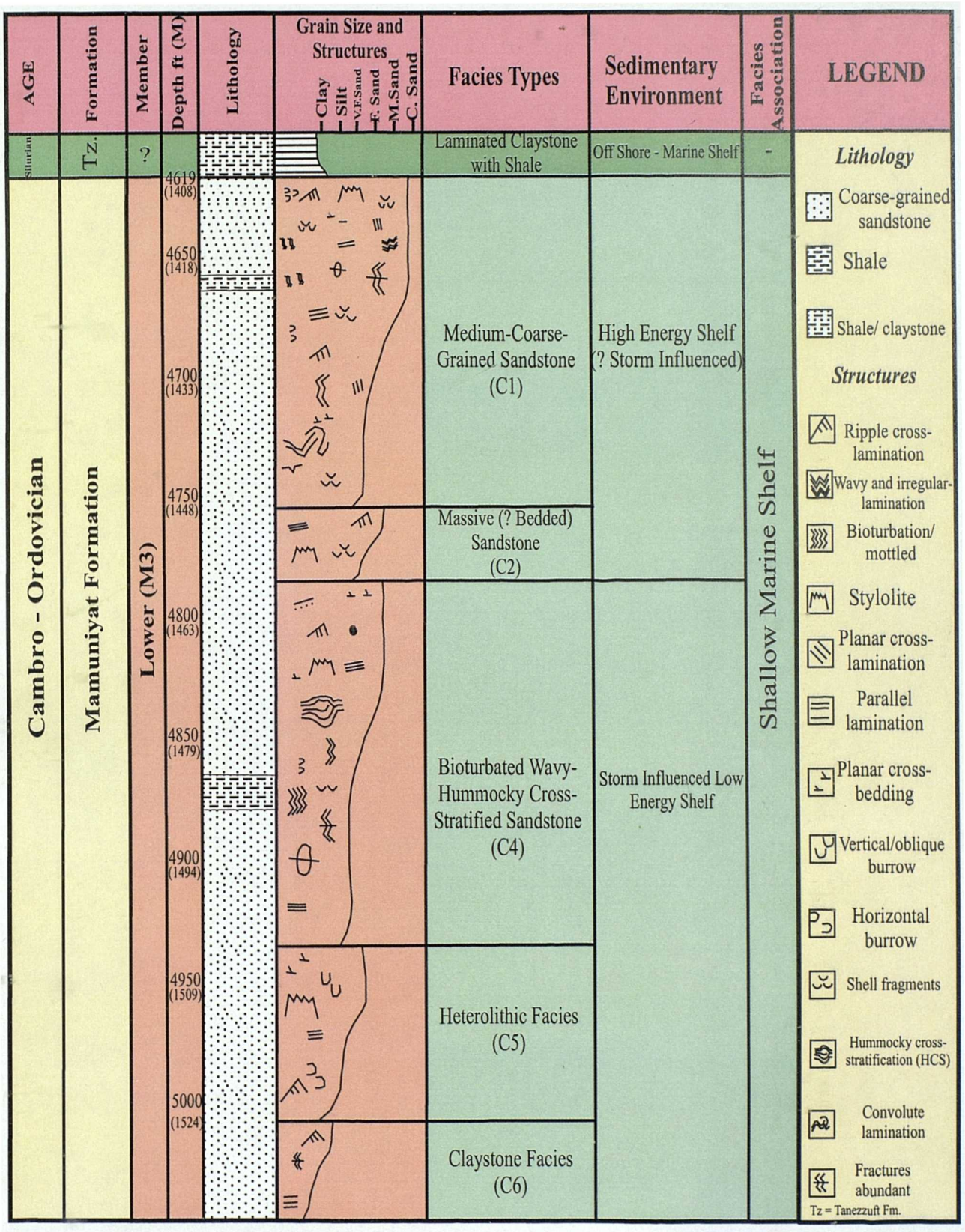

Fig. 2.2 Lithology and sedimentary environments for the cored interval between 5056 ft (1542 m) and 4619 ft (1408 m) in type well A8 - NC115 (A - Field).

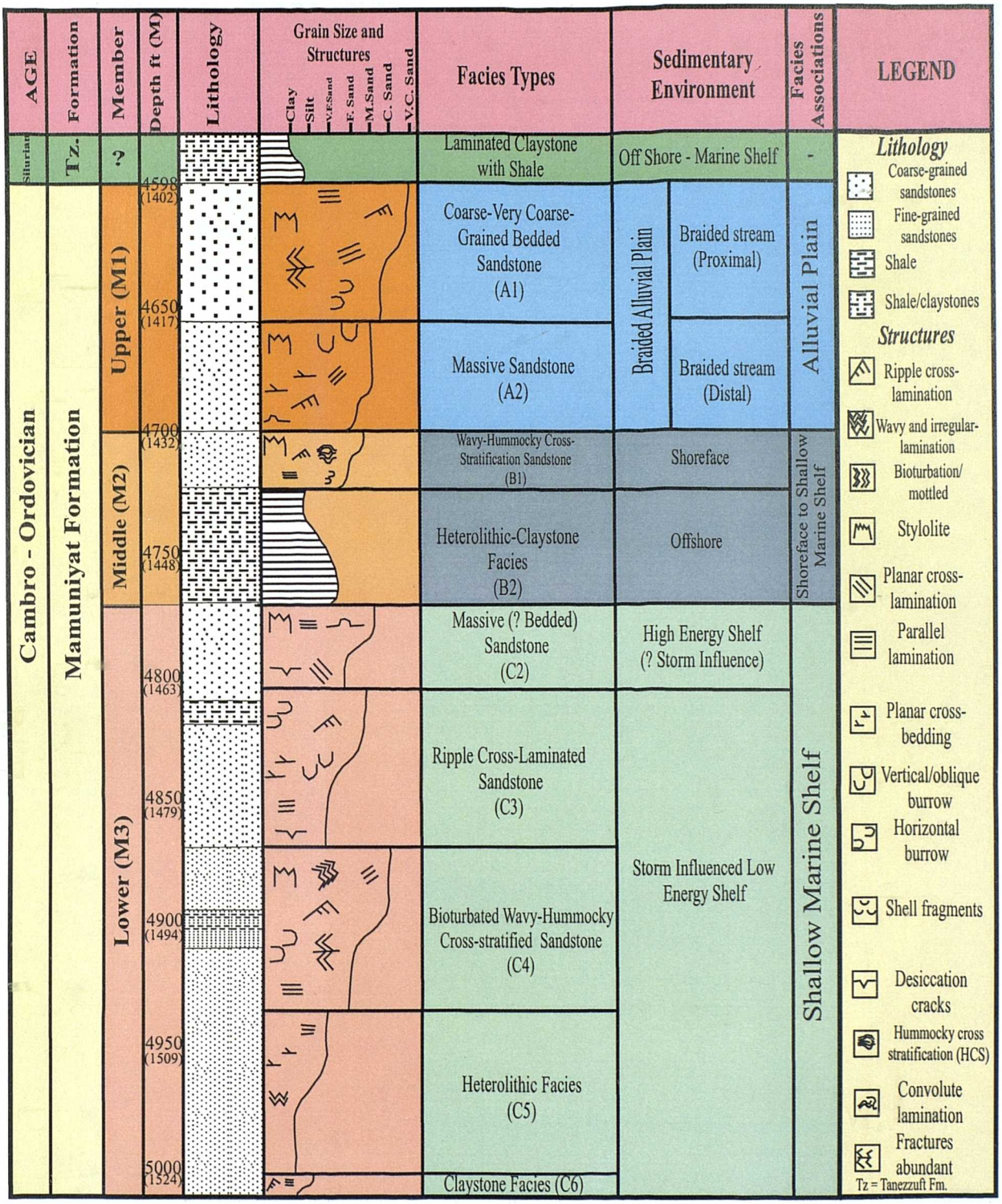

Fig. 2.3 Lithology and sedimentary environments for the cored interval between 5013ft (1528 m) and 4598 ft (1402 m) in type well B2 - NC115 (B - Field).

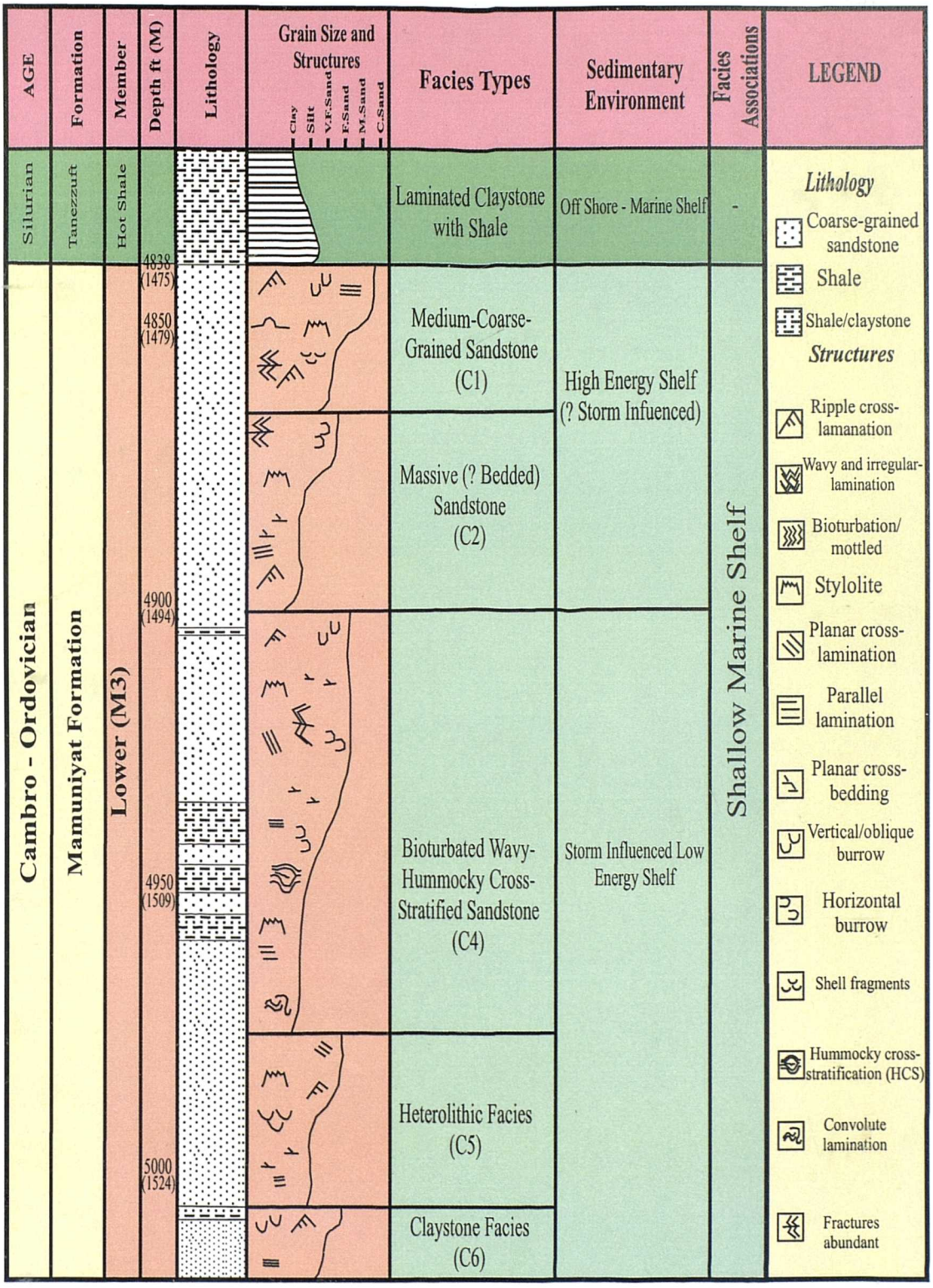

Fig. 2.4 Lithology and sedimentary environments for the cored interval between 5016 ft (1529 m) and 4838 ft (1475 m) in type well H4 - NC115 (H - Field).

The dominant sandstones are up to 5 cm thick; and individual beds can be traced throughout all the wells in B-Field (32 wells). Thus, they are laterally traceable over a distance of up to 10 km. The sandstones are poorly sorted, and the grains are angular to subangular. Detailed study of the sandstone is confined to two type wells B2 and B8 within B-Field. The facies can be divided into two sections (upper and lower), according to geometry, lithology, sedimentary structures and fossil content.

Lower section: The lower section is about 12 m thick. It comprises interbedded, locally laminated, medium to coarse-grained sandstone with minor siltstone. The sandstones are up to 10 cm thick, and they are much better sorted than the sandstone in the upper section. The sandstones also show a high degree of grain angularity. Sedimentary structures in the sandstones in the lower section include horizontal laminae, ripple cross-lamination, planar bedding, planar and trough cross-bedding and low angle massive beds.

The siltstones in this section range from 1 cm to 5 cm in thickness, and are mainly confined to the lower part of this section. The lower section shows a general coarsening-upward trend with individual sandstone beds, characterized by lenses and layers of medium-grained sandstones, which occur between the coarse-grained sandstone. The medium-grained sandstones are truncated laterally at the very coarse base of the overlying coarse units.

Upper section: The upper section is about 5 m thick and composed mainly of coarse- to very coarse-grained sandstones with minor pebbly sandstones. Intraformational clasts consist of angular to subangular sandstone and they are extremely poorly sorted to unsorted, occasionally massive, unfossiliferous, and argillaceous in character. In the uppermost part of this upper section some siltstone and claystone occurs, both of which significantly lower sediment permeability. Some sandstone beds in the upper section show a fining-upward trend from very coarse to coarse-grained sandstone (*e.g.* 1415 m in type well B8-NC115) **(Fig. 2.5)**.

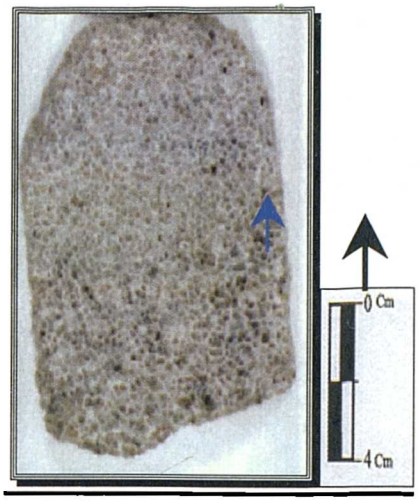

Fig. 2.5 Slabbed core sample from well B8-NC115, at 1415 m, showing the grain-size variation and general fining-upward trend (arrowed).

The sedimentary structures in the upper section are dominated throughout by medium-scale, trough cross-bedding from 10 to 25 cm thick. The troughs occur in cosets that become smaller in scale towards the top. The middle part of the upper section consists of medium-grained sandstones containing large-scale, solitary planar sets and cosets. Individual sets range from 0.25 m to 0.45 m in thickness. The sandstone beds show an upward increase in thickness with a concomitant decrease in the abundance of pebbles, horizontal lamination and ripple cross-lamination, which is confined to the upper part of the sandstone beds.

In addition to shale intraclasts, small pebble and minor pebble conglomerate lenses are scattered throughout the sandstone together with more extensive, irregular lenses of finer sandstone and silty-shale; many of which are associated with internal scoured surfaces. Siltstone and mudstone units within the facies are relatively rare compared with their abundance in the Middle Member of the Mamuniyat Formation. The general characteristics of the siltstone and mudstone include colour variation between very light grey and dark grey. The siltstones and mudstones are either laminated or massive and are observed in two forms. They occur either as thin lenses between sandstone beds and range in thickness from 25 mm up to 75 mm, or they form the upper parts of the above-mentioned upward-fining sequences.

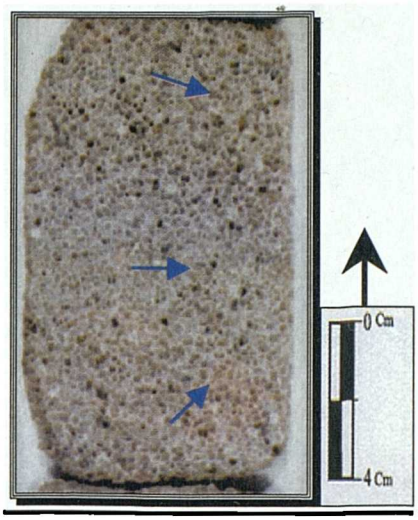

Fig. 2.6 Slabbed core sample from well B8-NC115, at 1417 m, showing the relationship between coarse-grained (lower portion) to very coarse-grained sandstone (upper portion).

A feature of this entire facies in type well B8-NC115 is the presence of alternations of thick sequences of very coarse and medium-grained sandstones. Data from the southwest part of NC115 Concession indicates that these alternations form part of coarsening-upward sequences (*e.g.* 1417 m in type well B8-NC115) **(Fig. 2.6)**, up to 4 m thick. These coarsening-upward sequences occur together with locally developed fining-upward sequences giving an overall coarsening-upward trend to the entire facies (*e.g.* type well B8-NC115) **(Fig. 2.7)**.

Two locally developed types of fining-upward sequences occur in this facies as described below: 1) Scoured, intraclast-strewn surface, overlain by coarse to very coarse-grained, medium- to small-scale trough cross-bedded sandstone and fine-grained ripple cross-laminated and horizontally-laminated sandstone with some siltstone; and 2) medium to fine-grained, large-scale planar cross-bedded sandstone in which individual sets decrease in scale upwards, overlain by fine-grained sandstone containing small-scale trough cross-bedding.

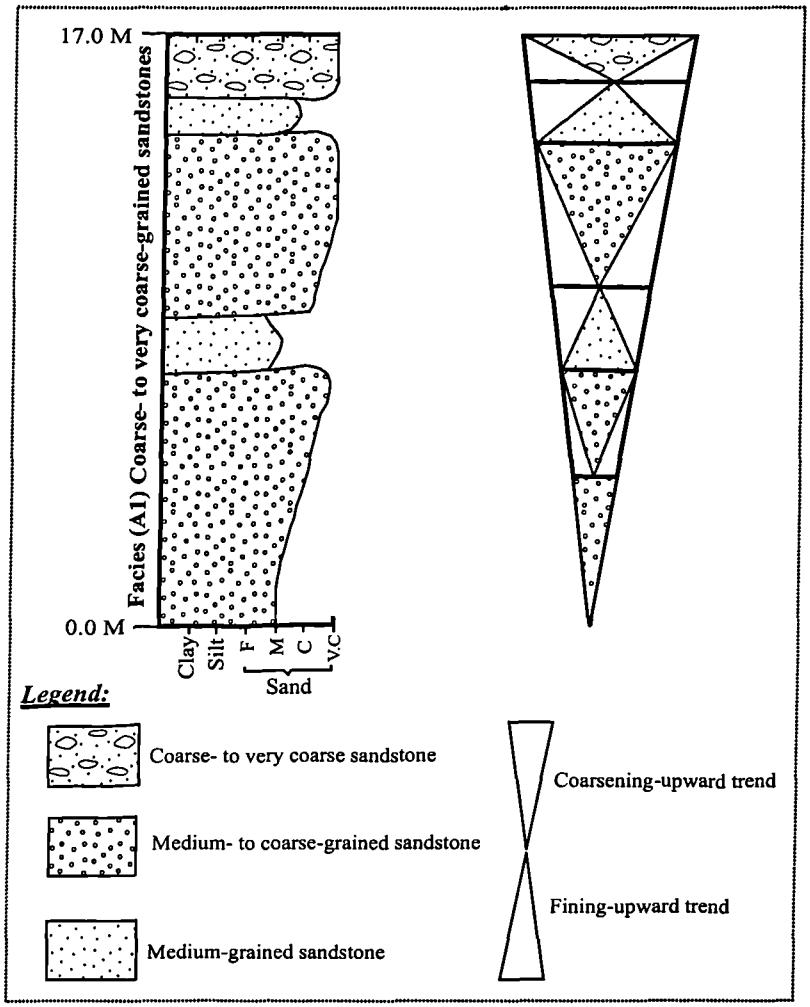

Fig. 2.7 Generalized measured section for Facies A1 showing the coarsening-upward trend with locally developed fining-upward units.

Interpretation

The coarse grain-size, solitary planar cross-beds sets, small fining-upward and coarsening-upward sequences within multistoried, laterally erosively-based, truncated packages is most consistent with a braided fluvial depositional environment for this facies (Miall, 1977). Direct analogous outcrops of this facies have not been found in the SW Murzuq Basin (Herzog, 1997), therefore the internal architecture of the sandstones is unknown, apart from the core in the B-Field (facies A1) and by e-logs from A and H-Fields. The upward increase in bed thickness, grain-size, and the scale of cross-bedding indicates increasing proximity to detrital clastic influx and the source area.

Thus, the lower fine-grained section is considered to be a distal environmental equivalent of the upper section. This interpretation of this facies is consistent with the abrupt transition from very coarse-grained to medium-grained sandstone in the succession, the low ratio of shale and siltstone to sandstone, and lack of fossils. The shales record deposition by vertical accretion from overbank floods, interrupted periodically by influxes of coarse sediment during more severe floods, giving rise to the interbedded fine sandstones and siltstones. Locally, low-angle stratification occurs which is typical of the bars developed in many braided streams (Miall, 1977).

The occurrence of trough cross-bedding, planar cross-bedding and flat-bedding above an erosive surface and basal pebble lag suggests deposition within a channel (Cant and Walker, 1976). In coarse sandy braided streams neither longitudinal bars nor transverse bars contain abundant large-scale trough cross-beds (Smith, 1970). Most large-scale troughs in sandy braided streams result from megaripple migration within the channels and are unrelated to bar formation (Miall, 1997). The planar laminated interbeds are considered to be upper flow regime, bar top sands (Eriksson, 1978) formed during diminishing flood stage. Planar cross-beds probably represent lower flow regime, linguoid sandbars (Reineck and Singh, 1973), or the simple bars of Allen (1984).

Intimate interbedding of pebbly sandstone and coarse- to very coarse sandstone, plus the occasional presence of thin shales and siltstones within facies A1, indicates that the changes in flow conditions were both frequent and extreme. Grain-size variations within lenticular beds indicate lateral as well as vertical changes in current velocities. The variation in thickness of sets is probably a function of temporal fluctuation in flow regime and flow depth during deposition (Vos, 1977). The overall lithological characteristic pattern of sedimentation and lack of evidence of subaerial exposure, are consistent with a year round rainfall and relatively high runoff, hence perennial braided streams.

2.3.1.2 Facies (A2): Massive sandstone

Description

This facies occurs immediately beneath facies A1 in type well B2-NC115, between cored interval 1419 m to 1430 m, where it forms the lower part of the Upper Mamuniyat Formation (M1) **(Fig. 2.3)**. It consists mainly of light brownish grey, brownish grey and dark brownish grey (colour reflecting degree of oil staining) sandstone with occasional siltstone interbeds.

Facies A2 is about 11 m thick. Sedimentary structures are rarely preserved. In some places thin lamination of slightly coarse siltstone are seen, and elsewhere the rock is indistinctly mottled. This facies includes ungraded to poorly inversely graded sandstones which are distinguished by their poor sorting, and abundant red-brown mud matrix, compared with facies A1 which are better sorted sandstones, and which have a light grey coloured matrix.

Coarse-grained sandstones are more prevalent in the upper portion of the facies. However, in most cases individual beds lack any grain-size trend and range from 0.5 cm to 15 cm in thickness. The rare sedimentary structures in facies A2 are characterized by planar and trough cross-bedding, flat bedding and ripple cross-lamination (0.02 m to 0.5 m thick). Some units of the facies (0.03 m to 0.8 m thick) are characterized by cross and horizontal laminated strata. Superficially, massive beds are common within facies A2, but it is probable that there are many subtle hidden features which would only be revealed by a detailed study of the rocks, including X-Ray analysis.

The sandstones of facies A2 also contain a few stylolites with the orientation of some of the sutured seams generally parallel to bedding (*e.g.* 1426 m in type well B2-NC115) **(Fig. 2.8)**. Thus, the stylolite axes are perpendicular to the primary bedding surface (Bauerle *et al.*, 2000).

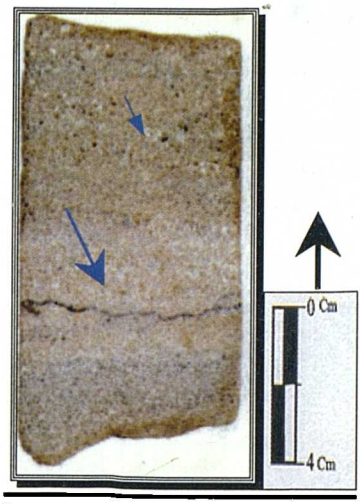

Fig. 2.8 Slabbed core sample from well B2-NC115, at 1426 m, of the massive sandstone facies. The arrows show the horizontal stylolites (large arrow) and coarsening-upward trend (small arrow).

Flame structures are also evident and rare subvertical fractures, possibly enhanced by coring, which were open to silica and silica cement. However, the sandstones beds are generally massive (structureless) to horizontally laminated and they have subplanar, nonerosional or slightly erosional boundaries. Massively bedded (structureless) sandstones are preserved within facies A2. Normal grading is occasionally developed as are primary sedimentary structures in the lower portion of facies A2 (e.g. 1430 m in type well B2-NC115) **(Fig. 2.9)**.

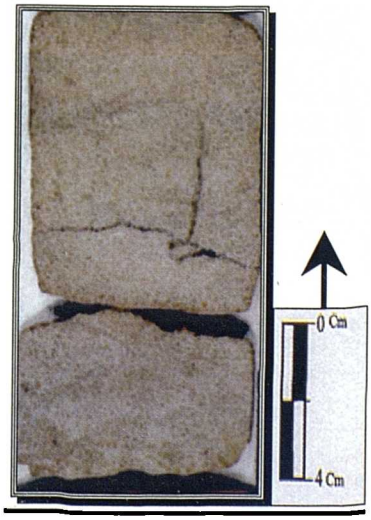

Fig. 2.9 Slabbed core sample from well B2-NC115, at 1430 m, in the lower portion of the massive sandstone facies, showing indistinct mottling.

The sedimentation units within facies A2, particularly in type well B2-NC115, mainly show a fining-upward trend. Multilateral and multistoried channelling results in laterally impersistent channel-fill geometries (Wadman *et al.*, 1979; Boggs, 1995). Individual fining-upward units range from decimetre to 1.5 m thick, and extend laterally for tens of meters, showing a sheet like geometry throughout the B-Field.

The entire facies shows a general coarsening-upward trend due to the fact that the upper portion of facies A2 is thicker than the lower portion and comprises medium-grained sandstones that become coarser-grained upward.

Interpretation

The characteristics of this facies are similar to sandy braided-stream deposits (Miall, 1977). The vertical succession of textures and primary sedimentary structures within this facies including channel scouring, and low-stage accretion, resemble the deposits of shallow streams on the lower reaches of braided alluvial plains (Williams and Rust, 1969; Cant and Walker, 1976; Miall, 1977, 1978; Rust, 1978).

Furthermore, the generally poorly sorted and mud-rich, medium to coarse-grained sandstones, possibly indicate braided stream sedimentation in a zone of decreased gradient and stream power with increased entrapment of fine-grained detritus (Vos, 1981a). The shallow sandy braided streams were characterized by an abundance of linguoid sand bars and intervening shallow channels containing in-channel dunes, as evidenced by the trough cross-bedding.

The apparent lack of well-developed cyclicity may be attributed to a lack of topographic differentiation in the stream channel (Miall, 1977). The characteristic sedimentary structures of facies A2 sediments are interpreted as products of a braided stream environment. Furthermore, the predominantly fine-grained nature of the sandstones and the absence of lithic clasts indicate that deposition took place in a low-relief environment (Haycock *et al.*, 1997).

Multilateral and multistoried channelling is characteristic of modern braided stream environments (Allen, 1965; Williams and Rust, 1969). The sediment of this facies, particularly in type well B2-NC115, consists predominantly of fine- to medium-grained sandstone, which indicate that they were deposited further away from the source area than facies A1. Such features characterise a homogeneous distal braided system. However, the uniformity and medium grain-size of the clastic material could be related to the nature of sediment-available from the main source area (Ghat/Tikiumit Arch) located to the southwest of NC115 Concession (Fello and Turner, 2001b).

Vertical sequence analyses of facies A2, reveals the presence of small-scale, coarsening-upward and fining-upward sequences within the Upper Mamuniyat Member. Considered as a whole, facies A2, deposited within the B-Field, southwest NC115 Block, shows an overall upward increase in grain-size and mineralogical maturity. The fine to medium grain-size, better sorting and limited thickness of the sandstone of facies A2 compared to deposits of facies A1, suggests that facies A2 is a distal braided stream deposit laid down on a distal plain braid.

The close association of facies A2 with some coarse siltstone, and their deposition under upper flow regime conditions suggests that they may represent distal braided streams at the toes of a braided alluvial plain (Tunbridge, 1981; Hubert and Hyde, 1983).

Facies A2 is volumetrically the most important of the braided alluvial plain sediments encountered in cores from the Murzuq Basin sector of southwest NC115. The interconnection of sandstones has been shown by Leeder (1978) to depend upon the rate of sediment accumulation on the floodplain and the rate of channel avulsion. The observed interconnectedness of facies A2 sandstones, in the core, is very low in the distal part of the braided stream system but it increases upward in proximal part of the facies A1 within the Upper Mamuniyat Formation.

2.3.2 Facies Association (B): Shoreface to Shallow Marine Shelf

This facies association can be recognised in the middle part of the sandstone cores, and their presence inferred from wireline log interpretation of uncored wells. It only occurs in the middle section of the Mamuniyat Formation (M2), in the reservoir interval of the B-Field, southwest part of NC115 Concession, particularly in type well B2-NC115 **(Fig. 2.3)**.

This facies association is represented by the cored interval from 1430 m (4690 ft) to 1456 m (4776 ft), in type well B2-NC115. It comprises two distinctive facies; each facies type is defined on the basis of lithology, grain size, sedimentary structures and log response. These facies are described and interpreted below.

2.3.2.1 Facies (B1): Wavy-hummocky cross-stratified (HCS) sandstone

Description

This facies makes up the bulk of the upper part of the Middle Mamuniyat Formation (M2). It is represented by the cored interval from 1430 m to 1440 m in type well B2, southwest part of NC115 Concession **(Fig. 2.3)**. Facies B1 is about 10 m thick. Furthermore, it is a very large sheet-like body of sandstone throughout B-Field, in the study area, and characterized by light brownish grey, fine-to medium-grained sandstones with local coarse-grained siltstones, and some glauconitic sandstones (Fello, 1996).

Glauconite is an important constituent of the fine-grained sandstone and interestingly, it is found to be associated dominantly with the hummocky cross-stratified sequence (Ghosh, 1991). The sandstones are well indurated, and moderately well sorted, with indurated grains mostly subangular to subrounded. The sandstone beds of facies B1, range in thickness from 0.20 m to 1.20 m, and are characterized by HCS small- to large-scale planar-tabular or trough cross-stratification, graded bedding, symmetrical to asymmetrical wave ripples, and current ripples, as well as wavy ripple lamination and parallel laminations.

Hummocky cross-stratification (HCS) is the dominated sedimentary structure in this facies. Description of HCS follows the terminology of Dott and Bourgeois (1982). Commonly, sets are 0.30 m thick, with spoon-shaped bases. The amplitude and wavelength of the preserved bed forms vary between 0.20 m to 0.30 m and 0.60 m to 0.70 m, respectively. The foresets of sets are concave upward with a tangential lower contact. Individual set boundaries are marked by discontinuous siltstone partings. The coarser fractions are commonly present along the bottom as well as the top of the set or cosets. Within the HCS sandstones tabular cross-bedsets occur, which is usually 0.30 m to 0.40 m thick. The foresets of the tabular sets are slightly asymptotic (Ghosh, 1991). Discontinuities in the foresets of tabular cross-stratified sets are presented locally in facies B1. No small-scale cross-stratification was observed within the foresets.

Fine-to medium-grained quartzose sandstones of facies B1 are generally overlain by concordant laminae, with interbedded cross-bedding and ripple-cross laminated sandstone, low-angle scours overlain by low-contrast laminated, high-contrast laminated and rippled, very fine- to fine-grained, micaceous sandstones. Grain-size in facies B1 is most commonly medium-grained but extremes occur, particularly in type wells B2 and B8-NC115. Coarsening-upward and fining-upward trends are not developed over the entire thickness of facies B1 sandstones, but both are noted as minor trends over intervals, near the upper or lower contacts. Internally this facies displays flat, low-angle and coarse-grained siltstone layers up to 15 cm thick, laterally continuous for hundreds of meters (Herzog, 1997; McDougall and Martin, 1998).

In facies B1 the association of basal lags with HCS is rarely observed. The sandstone bodies contain successive internal erosional surfaces with or without wave-winnowed pebble lags (Levell, 1980) and wave ripples mantle them (Johnson, 1977). Internal divisions may include a basal zone with hummocky or micro-hummocky cross-stratification (described by Dott and Bourgeois, 1982; p. 678), a wave-and/or current-rippled zone (*e.g.* 1435 m and 1436 m in type well B2-NC115) (**Fig. 2.10**), and an upper laminated very fine-grained sandstone with a minor coarse-grained siltstone zone.

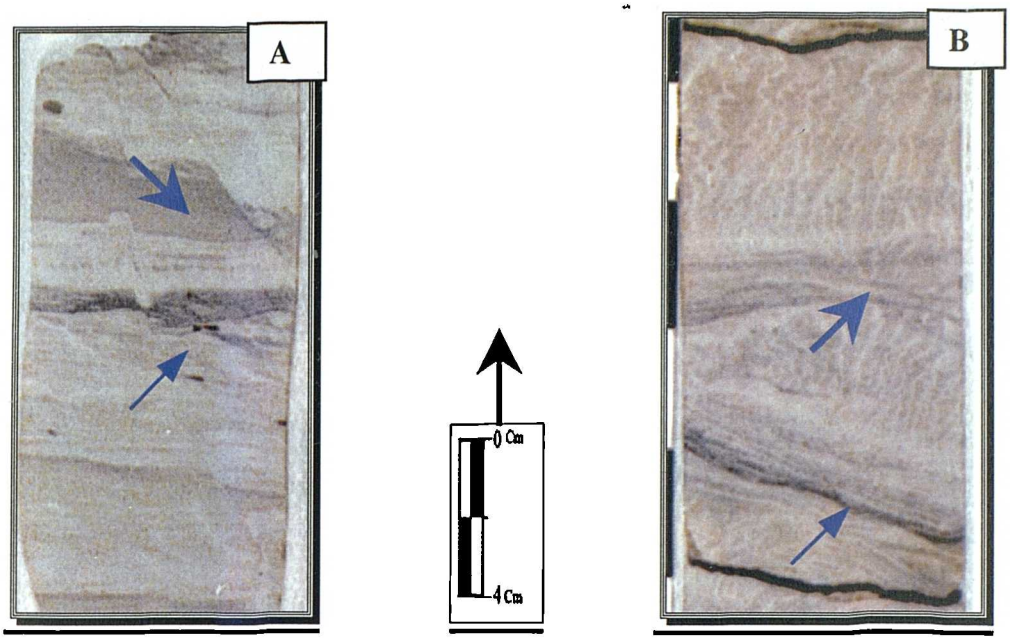

Fig. 2.10 A and B) Slabbed core sample from well B2-NC115 at 1435 m and 1436 m, respectively showing the wavy hummocky cross-stratification (large arrow) and micro-hummocky cross-stratification.

Vertical sequences of sedimentary structures of facies B1 are present within each bed. This pattern compares with the idealized succession of Dott and Bourgeois (1982) and is analogous to the Bouma succession. The sandstone beds are usually sharp based, sometimes with small-scale scours and erosion into the underlying sandstone. The position of the hummocks above erosional depressions is similar to the stratification described by Surlyk and Noe-Nygaard (1991) from Jurassic sandstones in Denmark.

This facies contains sparse C*ruziana*. Bioturbation is restricted to rare, moderately preserved vertical burrows (? *Skolithos*). These burrows occur mostly as narrow tubes up to 3 cm long and up to 2 mm wide, and the most characteristic type of burrow is known in the Sahara as *Tigillites*, and elsewhere in the world as *Skolithos* or *Monocraterion* (Selley, 1996). The average diameter of the vertical burrows is a few mm's in this facies, (*e.g.* 1437 m and 1438 m in type well B2-NC115) **(Fig. 2.11)**.

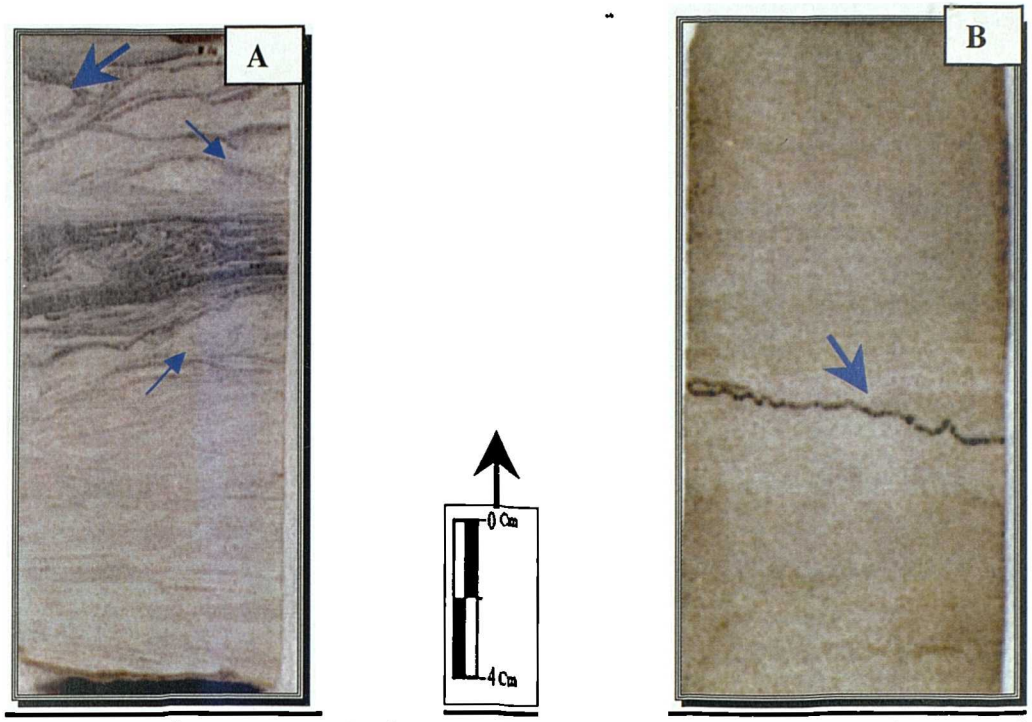

Fig. 2.11 A) Slabbed core sample from well B2-NC115, at 1437 m, showing the vertical burrows (Cruziana, large arrow) in the middle part of facies B1 and shell fragments (small arrows). B) Slabbed core sample from B2-NC115, at 1438 m, showing the stylolites (arrow) with structureless sandstones in facies B1.

Interpretation

During the last 15 years there have been important contributions from geologists and oceanographers on a distinctive type of low-angle cross-stratification, named hummocky cross-stratification (HCS) (Harms *et al.*, 1975). This is considered to be diagnostic of shoreface to shallow marine shelf (*e.g.* Greenwood and Sherman, 1986). The hummocky cross-stratification is thought to form in the area between fairweather wave-base and storm wave-base (Tucker, 1991).

The wavy-hummocky cross-stratified sandstone is interpreted as representative of the middle/intermediate shoreface of a nearshore zone, evidencing two alternate hydraulic regimes (traction and suspension) (Ghosh, 1991). Bose *et al.* (1988) considered that during the calmer phase the sediment influx was relatively less and only wave activity prevailed, reworking the earlier-deposited sediments.

Throughout facies B1, the presence of subordinate proportions of fine-grained sandstone/siltstone may infer the possibility of random and/or periodic fluctuations of the hydraulic regime at the depositional site. The bed configuration of facies B1 may have been initiated as a shallow, concave-upward scour, with a wavelength for the hummocky erosion surface of the order of 0.60 m to 0.70 m. This is below the lower end of the scale originally defined by Harms *et al.* (1975).

Symmetrical bedforms that generate HCS may be as much a consequence of sediment-charged unidirectional flow, as bi-directional, oscillatory flows in stormy shallow marine environments above storm wave base, which are traditionally deduced from HCS (Cotter and Graham, 1991). Hummocky cross-stratification (HCS) (Harms *et al.*, 1975) has been recognized in many ancient shelf deposits (Byers and Dott, 1981; Dott and Bourgeois, 1982). The most distinctive features are the low angle of the cross-bedding (less than the angle of repose), the presence of both convex-up and concave-up curvature to the sets, and the presence of low-angle internal bed truncations **(Fig. 2.12)**.

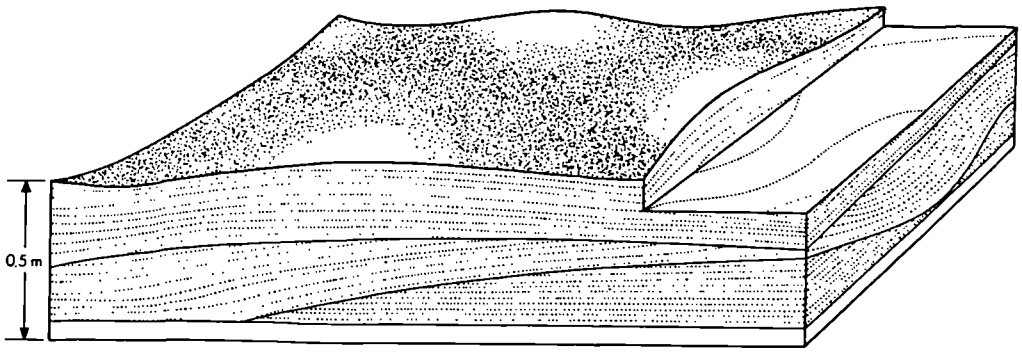

Fig. 2.12 Block diagram of hummocky cross-stratification. It is common in coarse siltstone or very fine sandstone within the lower shoreface and offshore facies (After Harms *et al.*, 1975).

High suspended loads and finer sand may also be responsible for a variety of sedimentary structures that resemble hummocky cross-stratification (Harms *et al.*, 1982).

Hummocky cross-stratification (HCS) is a three-dimensional structure with an undulatory lower erosion surface with domes and basins overlain by accretion lamina that thicken into the domes or hummocks. Swaley cross-stratification is characterized by thickening into the basins or swales (Todd, 1996).

The HCS is thought to result from episodic storm wave activity and wave-generated surges (*e.g.* Bourgeois, 1980; Dott and Bourgeois, 1982; Brenchley, 1985; Walker and Plint, 1992). Variations of the HCS beds described herein can be explained in terms of amalgamated HCS, constructed under the influences of fluvial outflow, waves and tides. In type well B2-NC115 the preservation of HCS in a middle/intermediate shoreface setting may be promoted by a relatively sudden decrease in wave energy, at the end of a given storm, to a level that is insufficient to rework deposits in less than a few meters of water (Walker and Plint, 1992).

The various features of the HCS in facies B1 were produced by both oscillatory and combined oscillatory/unidirectional flows that prevailed during various stages of individual storms (Cheel and Leckie, 1992). The abundance and orientation of cross-bedding in facies B1 points to deposition from lower flow regime traction currents. The fine grain-size, however, shows these currents to have had significantly lower velocities than those, which deposited the braided alluvial plain sandstones above (Facies A1 and Facies A2). The occurrence of tabular planar cross-beds, and the absence of channelling indicates that these were open flow currents that were not confined by channel banks.

In type well B2-NC115, the associated rippled very fine sandstones show that gentle traction currents sometimes occurred, while the absence of cross-laminated cosets and the presence of a few clay drapes on ripples crests suggests that these currents pulsated gently. Both *Skolithos* and *Cruziana* are characteristic of shallow-marine deposits, and the *Tigillites* ichnofacies, which is diagnostic of shallow marine conditions, is sometimes so abundant that locally it has destroyed any original sedimentary structures that may have once existed (Selley, 1996).

The HCS sandstone has been reported from ancient marine environments on shoreface and shelves (Duke, 1985; Cheel and Leckie, 1992). Moreover, the waves were characteristically short and steep, and subject to continuous forcing by wind at the shoreline; wave approach angles seldom exceed 10° (Greenwood and Sherman, 1986). The weight of the evidence suggests that the wavy-hummocky cross stratification sandstones of facies B1 in type well B2-NC115, B-Field, southwest NC115 Block, originated in middle/intermediate shoreface environments.

The mixed medium-grained sandstone with occasional coarse-grained siltstones and some glauconitic sandstone within facies B1 is interpreted as storm- and wave dominated shelf sediments deposited near fair-weather wave base. The scarcity of wave-produced features suggests relatively minor wave influence between storm events (Selley, 1996). Glauconite in the sandstones of facies B1 is more abundant than kaolinite (Fello, 1996). This is a characteristic of marine sediments (Visher, 1969).

Nottvedt and Kreisa (1987) interpret low-angle cross-bedding in isolated fine-to medium-grained sandstones as forming under combined flow storm conditions like those forming wavy-hummocky cross-stratification in fine- to medium-grained sandstones and coarse-grained siltstone of this facies.

2.3.2.2 Facies (B2): Heterolithic-claystone facies

Description

This facies occurs in the lower part of the Middle Mamuniyat Formation (M2). It has been found only in the southwestern part of the study area in the B-Field. It occurs immediately subjacent to facies B1, and is characterized by abundant black shale (Radioactive Shale), particularly in type wells B2 and B8-NC115.

Facies B2 is represented by the cored interval from 1440 m to 1456 m in type well B2-NC115 (**Fig. 2.3**). It extends over 16 m of the cored thickness and is composed of silty shale, mudstone and fine-grained sandstone.

The entire facies shows a general coarsening-ûpward trend and passes sharply upwards into shales, siltstones and fine-grained sandstones. Greyish black, well compacted/indurated, carbonaceous, micaceous, fissile, commonly pyritic shales, form laminae-sets 0.5 cm to 3 cm thick (*e.g.* 1442 m in type well B2-NC115) **(Fig. 2.13)**.

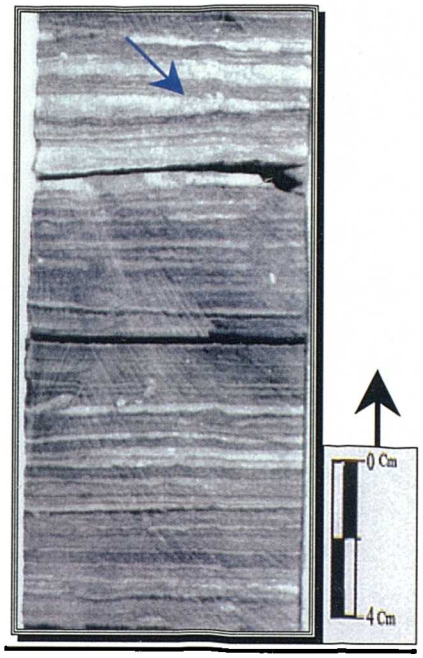

Fig. 2.13 Slabbed core sample from well B2-NC115, at 1442 m, showing the heterolithic facies B2. Core shows fine sandstones (arrow) and dark grey claystone with mudstone forming lamina-sets in the lower part of facies B2.

The heterolithic-claystone facies contains organic material, preserved on lamination planes parallel to fissility, and pyrite in the form of streaks and lenses. Some of the plant material is large (up to 5 cm long), and occurs mainly as compressed stems, some of them being replaced by pyrite. The fine-grained sandstone is characterized by a scoured basal surface with local relief of up to 2.5 cm, containing rounded to subrounded poorly sorted fine rip-up mud clasts.

The sandstones contain laminated shale flasers and minor soft-sediment deformation structures, and local vertical burrows < 2.5 cm long passing upward into highly bioturbated shale. The facies forms beds ranging between 5 cm to 10 cm thick. Beds are tabular and sharp based, with small-scale rippled and/or parallel-lamination.

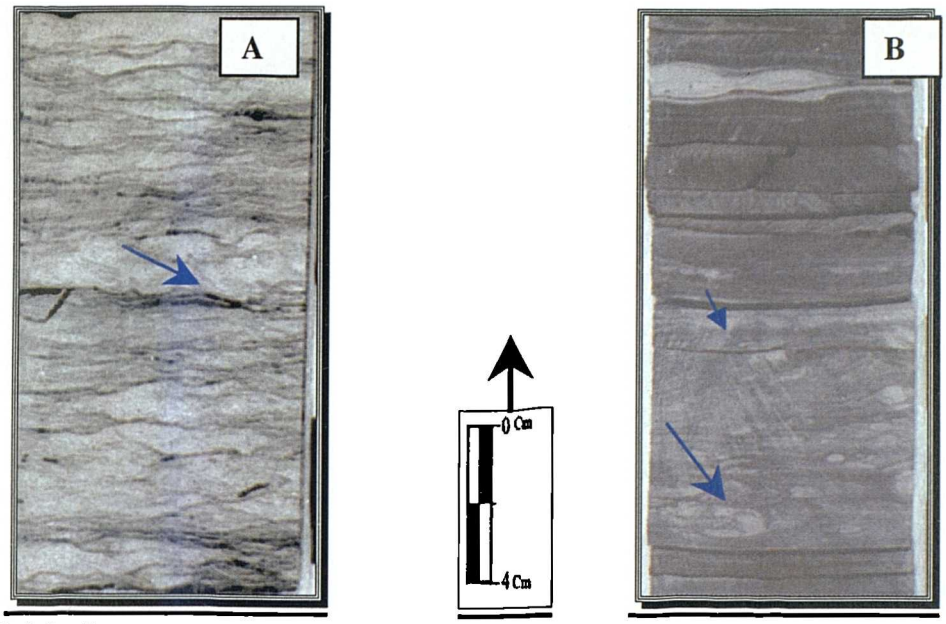

Fig. 2.14 Slabbed core samples from heterolithic-claystone facies: A) Well B2-NC115, at 1440 m, showing the intensity bioturbated to mottled nature with horizontal burrows (arrow). B) Well B8-NC115, at 1455 m, showing trace fossil (small arrow) and dispersed horizontal burrows mixed with heterolithic claystone with ferruginous concretions, which occur as single nodules (large arrow).

In the type well, the effect of biogenic reworking can be seen in the light grey coloured mottling of shale and sand, with some coarse-grained siltstones (*e.g.* 1440 m in type well B2-NC115) **(Fig. 2.14A)**. Fine shell hash and whole shells are present in the middle part of facies B2 (*e.g.* 1455 m in type well B8-NC115) **(Fig. 2.14B)**, either scattered or in local concentrations. Bioturbation has destroyed the primary structures and homogenised the sediment.

Colour mottling may be produced by the oxidation of original small pyritic concentrations around organic remains, and stirring by burrowing. The burrows are dispersed, but decrease in abundance upward throughout the facies B2. Most of the vertical and horizontal burrows occur within the silty shale units of this facies (*e.g.* 1456 m in type well B8-NC115) **(Fig. 2.15)**. Local abundant ooids, < 2 mm in diameter occur, especially near the bottom of the facies (base of the core) (*e.g.* 1450 m in type well B8-NC115) **(Fig. 2.16)**. It is well to moderately sorted and locally pyritic.

Traces fossils are common, especially horizontal burrows (few mm's in diameter), as well as ferruginous concretions, which occur as single nodules ranging from 1.0 cm to 2.5 cm in diameter. The most organic-rich part of the Middle Mamuniyat Formation is the radioactive shale at the base, which is present over the whole of the southwestern part of the El-Sharara Field.

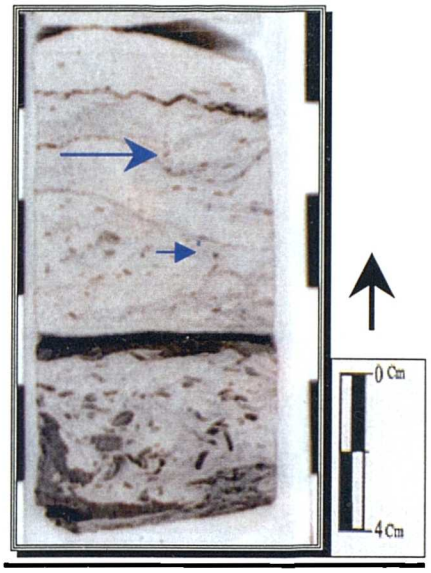

Fig. 2.15 Slabbed core sample from heterolithic-claystone facies, of the type well B2-NC115, at 1456 m, showing the mudstone, silty shale and sandstone. Note the horizontal burrows (large arrow) and dispersed vertical burrows (small arrow).

Iron-rich lamina makes up about 10% of the total facies. They alternate irregularly with silty shale (black shale) and mudstone; the contact between them being sharp. The iron-rich laminaes are ranging from 0.3 cm to 1.0 cm thick (*e.g.* 1450 m in type well B8-NC115) **(Fig. 2.16)**. Iron-rich laminaes (? *Siderite*) are characterized by bioturbated to massive iron-rich nodules 5 mm to 1 cm long dispersed in the mudstone.

Irregular sandstone laminae with sharp scoured bases occur within the silty shale and locally within the iron-rich sediment. Some laminae show well-preserved small-scale ripple profiles 1 cm to 2 cm thick. Closely spaced poorly oriented desiccation cracks 5 mm to 1.0 cm deep, filled with kaolinite and ooids occur within the iron-rich unit.

The ooids are up to 2 mm in diameter, ovoid to flattened in shape and well sorted (*e.g.* 1450 m in type well B8-NC115) **(Fig. 2.16)**. Ooids are replaced by kaolinite, which contains some unaltered detrital feldspar (discussed in Chapter Three). These may have acted as a nucleus for the formation of the ooids and as a precursor to the formation of kaolinite. Other ooids preserve concentric laminae (Van Houten and Karasek, 1981).

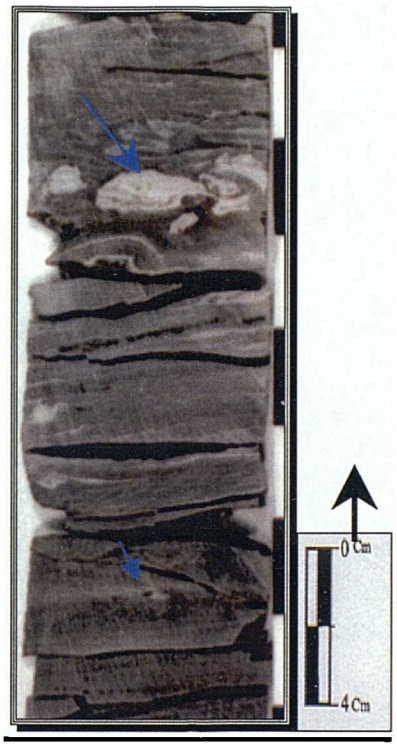

Fig. 2.16 Slabbed core sample from well B8-NC115, at 1450 m, showing bioturbated mudstone, silty shale and sandstone. Note the disseminated oolites (large arrow) at the top, and the ironstone bed with sharp contact, containing streaky sandstone laminae and closely spaced desiccation cracks (filled with calcite, small arrow) at the bottom.

The micrite contains angular to subangular, fine-grained quartz, feldspar and remnant detrital fine muscovite. Analysis of the spectral gamma-ray response of the lower part of the Middle Mamuniyat Formation (M2), particularly within B-Field, shows that the strongly radioactive shale results from an increasing content of uranium, peaking at 70 ppm compared to 2-4 ppm in the overlying lean shales. Some underlying Ordovician shales also show high gamma-ray values. However, this increase is due to an increase in thorium and potassium, with the concentration of uranium remaining at normal background levels of about 4-5 ppm. (Luning *et al.*, 1999).

The elevated gamma-ray levels in the Ordovician shales may simply indicate an increased amount of Th and K into the ocean, possibly associated with the increased erosional rate of Gondwanan basement areas during the late Ordovician period (Luning *et al.*, 1999). In facies B2 the chlorite, illite, kaolinite and illite-smectite mixed-layer are the clay minerals occurring in the radioactive shale fractions, only the kaolinite and chlorite display remarkable variation in their relative abundance (discussed in Chapter Three). Relative concentrations of kaolinite are higher in the radioactive shale; possibly indicating that deposition took place under humid climatic condition (Rodrigues *et al.*, 1995).

The radioactive shale zone within facies B2 has been found only in a very limited number of wells in the El-Sharara Field. This suggests that the lateral continuity of this facies was curtailed either at the time of deposition, or subsequently, as a result of erosion. The apparently discontinuous occurrence of facies B2 (the radioactive shale zone) across the NC115 Concession cannot be definitively explained.

Facies B2 can be seen only in B-Field, southwestern part of NC115 Block. Similarly, radioactive shales are absent in A and H-Fields, northeastern part of the El-Sharara Field, but the strong seismic reflector occurs only in the B-Field, the structure on which the wells were drilled. This relationship suggests that the present day structural high in A and H-Fields, may have already existed in the earliest Ordovician, with radioactive shale deposition in the southwestern part of NC115 Concession, but not across the palaeo-high in the northeastern part of the El-Sharara Field, NC115 Block (Hadley, 1992).

Interpretation

The facies B2 deposits underlie and overlie shelf beds and indicate an offshore shelf receiving fine-grained detritus (Vos, 1977). A similar fine-grained deposit overlies shelf beds of the Mississippi delta (Coleman and Gagliano, 1964). In the distal or offshore shelf, reworking is mainly by biological activity, resulting in a sequence of bioturbated siltstone-silty shale.

The offshore shallow marine environment is sedimentologically complex because of the number of different processes, which operate within it. Relative to other sediment, the products of these processes are poorly known because of the physical difficulties involved in studying them and because of the present disequilibrium of continental shelves. Thus, although the interpretation of ancient shallow marine sediments must be approached with considerable caution, it provides a fascinating challenge to sedimentologists (Banks, 1973).

The silty shale and mudstone imply an offshore shelf environment where iron-rich lamina typically accumulates under shallow, high-energy conditions (Ekdale *et al.*, 1984). Sandstone was deposited during high-energy storms. The sharp bases between iron-rich lamina, silty shale and mudstone represent rapid deposition by storm events. Oolitic iron-rich have been described from the Devonian Shatti Formation in west central Libya (Van Houten and Karasek, 1981) which is very close to the Mamuniyat Formation of NC115 Concession. Oolitic iron deposits occur within marine beds, but they may form pedogenically in certain types of soil such as laterites (Kimberley, 1978).

In facies B2, the horizontal lamination probably indicates a depositional environment near to or below wave base. The most likely setting is an offshore shelf on which chemical and suspension sedimentation predominated (Vos, 1981b). Suspension settling of clay and rare silts occurred on the more proximal reaches of the offshore shelf whereas in deep waters beyond clastic input chemical precipitation of iron and silica was enhanced. The rhythmic interlayering of siliceous and ferruginous layers reflects fluctuating Eh and pH conditions which may have been seasonal (Eugster, 1970) or diurnal due to photosynthesis (Johnson, 1977).

Hadley (1992) suggested that muddy sediment with burrows was deposited in a calm, protected environment, whereas the abundance of iron-rich sediment suggests proximity to a river. Ooids, concentrated in burrows, suggest moderate agitation along a sediment surface penetrated by burrows (Van Houten, 1981).

The ooids are typical of those developed in other iron-rich formation in many parts of the world. The black shale of facies B2 has an organic carbon content. It also is enriched with respect to a number of heavy metals (Eugster, 1970). The relatively high uranium content of the black shale allows this facies of the Middle Mamuniyat Formation to be readily traced on gamma-ray well logs among oilfields and scattered boreholes throughout the B-Field (*e.g.* Hobday and Horne, 1977).

The presence of red to brown colours indicates deposition in an oxidising environment, whereas grey colours suggest deposition under more reducing condition (Reineck and Singh, 1973). The red colour is due to the presence of iron minerals, which are typical of humid tropical climates (Reineck and Singh, 1973) where the source material was sufficiently deeply weathered to supply free ferric-oxide. This facies represents the lowest energy facies, in which two hydraulic regimes were present. Low energy periods are represented by deposition of silt and clay layers from suspension, whilst high energy conditions were marked by the introduction of sand layers (Johnson, 1977). Kaolinite is the constituent of the ooids. It is a common primary and secondary clay mineral formed by weathering or hydrothermal alteration of aluminium silicates, particularly feldspar (in B-Field). It is found in soil and can be transported by water and mixed with quartz and other minerals (Eugster, 1970).

In the Murzuq Basin, particularly in the B-field, southwest of the study area, the highly radioactive shales of facies B2, are mainly confined to localized palaeotopographic lows (valleys, erosional or structural depressions) or to broad areas flanking highs such as the A and H structures of Concession NC115 (From Teknica Canada Report, 1996).

Figure 2.17 shows a depositional model for the Upper and Middle Mamuniyat Formation, throughout the B-Field, in the southwestern part of the study area. These deposits are interpreted to have eroded from the rising mountain chain (Ghat/Tikiumit Arch) source area to the SW of NC115 Concession (Fello and Turner, 2001a).

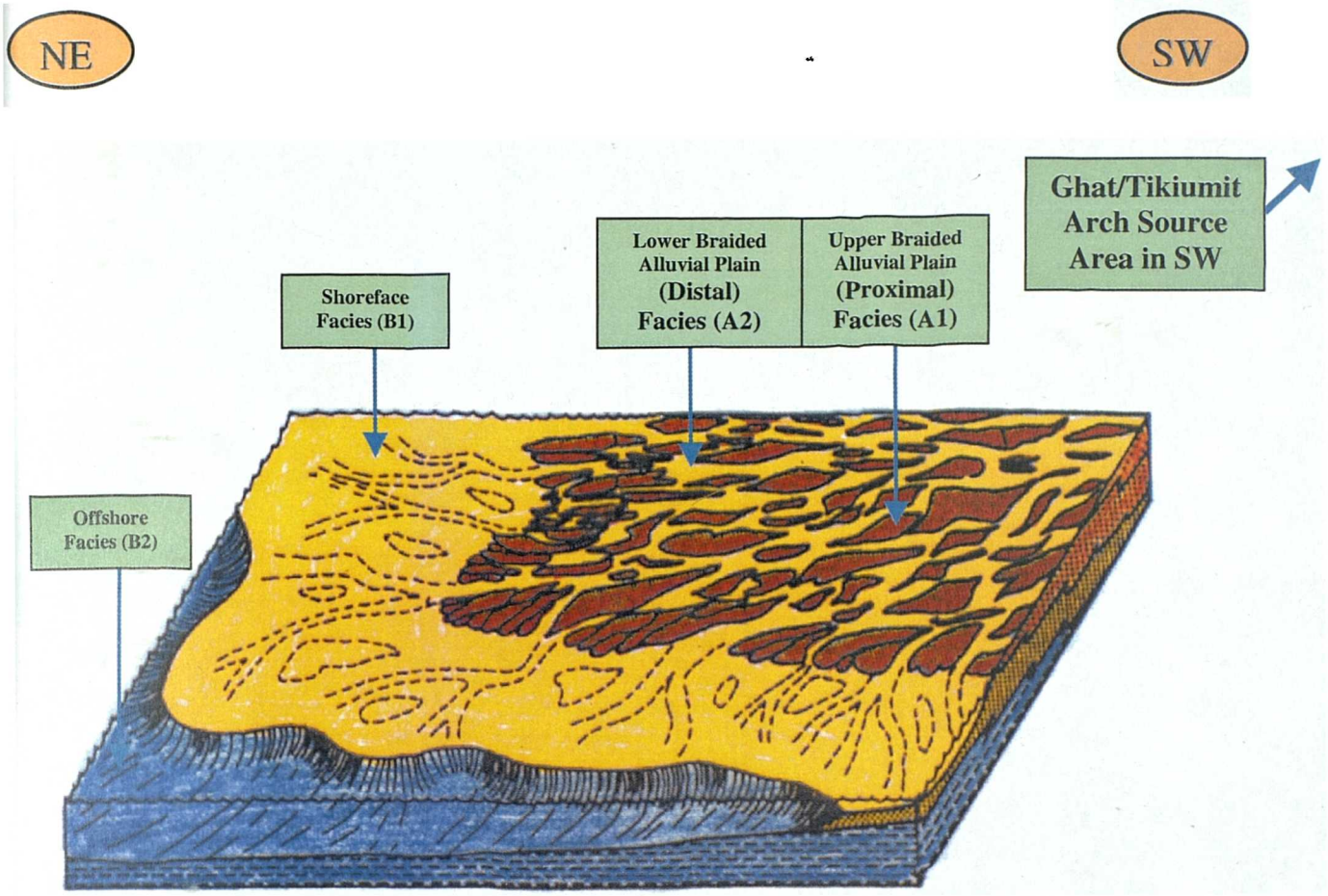

Fig. 2.17 Generalised depositional model for the Upper and Middle Mamuniyat Formation, SW of NC115 Concession, on the northwest flank of the Murzuq Basin, SW Libya.

2.3.3 Facies Association (C): Shallow Marine Shelf

This facies association (C) occurs in the type wells of the study area (A, B and H-Fields). It is included in the lowermost part of the Mamuniyat Formation (M3), that is, the Lower Quartzitic sandstone Member (M3) of the Mamuniyat Formation **(Figs. 2.2, 2.3 and 2.4)**, which is generally represented by a series of coarsening-upward sandstone sequences, throughout the El-Sharara Field, NC115 Concession **(Table 2.3)**.

Facies association (C) represented by the cored interval from 1408 m (4619 ft) to 1541 m (5056 ft) in type well A8-NC115, the cored interval from 1456 m (4776 ft) to 1528 m (5013 ft) in type well B2-NC115 and the cored interval from 1475 m (4838 ft) to 1529 m (5016 ft) in type well H4-NC115.

Sedimentological analysis of the shallow marine shelf facies association shows it to be almost totally dominated by sandy component facies types, though an interval of interbedded muddy and sandy facies occurs towards the top of the Mamuniyat reservoir level. This facies association comprises six facies, defined on the basis of lithology, grain-size, sedimentary structure and log response. These facies are described below.

2.3.3.1 Facies (C1): Medium-coarse grained sandstone

Description

This facies is restricted to the uppermost part of the Lower Mamuniyat Formation (M3). It has been found only in the northeast part of the El-Sharara Field, NC115 Concession, particularly in A and H-Fields. It gradationally underlies the laminated claystone and shale facies of the Tanezzuft Formation (Seal Rock) **(Table 2.3)**.

This facies is represented by the cored interval from 1408 m to 1450 m in type well A8-NC115 and the cored interval from 1475 m to 1484 m in type well H4-NC115 **(Figs. 2.2 and 2.4)**. This facies makes up the majority of the uppermost portion of the Lower Mamuniyat Member (M3) in the northeast NC115 Concession (A and H-Fields). The top and bottom of the facies are irregularly layered (*e.g.* 1419 m in type well A8-NC115) **(Fig. 2.18A)**.

The facies comprises mainly medium- to coarse-grained sandstones, with associated grey mudstones and fine-grained muddy sandstones. Variegated mudstone beds are intercalated locally. It can be traced laterally for tens of kilometres within NC115 Concession. This facies can be divided into four subfacies, each of which is described separately.

Subfacies (C1a): Trough cross-bedded sandstone

Description: This subfacies occurs in the uppermost portion of facies C1, between the cored interval 1408 m to 1420 m, throughout the lower Mamuniyat Formation (M3), particularly in type well A8-NC115. It consists of medium- to coarse-grained, yellowish grey to medium light brownish grey, locally dark brownish grey, moderately well-sorted sandstone. The subfacies C1a occasionally consists of muddy sandstone beds, which frequently overlie the variegated mudstone beds.

The thickness of individual medium- to coarse-grained sandstone beds generally ranges from 1 m to 5 m, and some beds attain thicknesses of 10 m in type well A8-NC115. The mudstone beds are thinner and less abundant than those in the Upper and Middle Mamuniyat Members. The subfacies C1a consists of thinly bedded, medium- to coarse- grained sandstone, generally represented by a series of coarsening-upward (*e.g.* 1419 m in type well A8-NC115) (**Fig. 2.18A**), well-sorted sandstones dominated by trough cross-bedding with subordinate tabular cross-bedding and minor low angle parallel lamination in the lower portion.

Body fossils are rare within this subfacies and are limited to fragmented, unidentifiable molluscan shells. The bioturbation in the subfacies is relatively rare, but the amount of bioturbation increases upward and well preserved trace fossils including the *Cruziana* ichnofacies occur at the contact between interbeds. There are horizontal burrows near the top of the coarsening-upward sequence (*e.g.* 1410 m in type well A8-NC115) (**Fig. 2.18B**). Horizontal stylolites are rare, especially in the upper two-thirds of the coarsening-upward sequence.

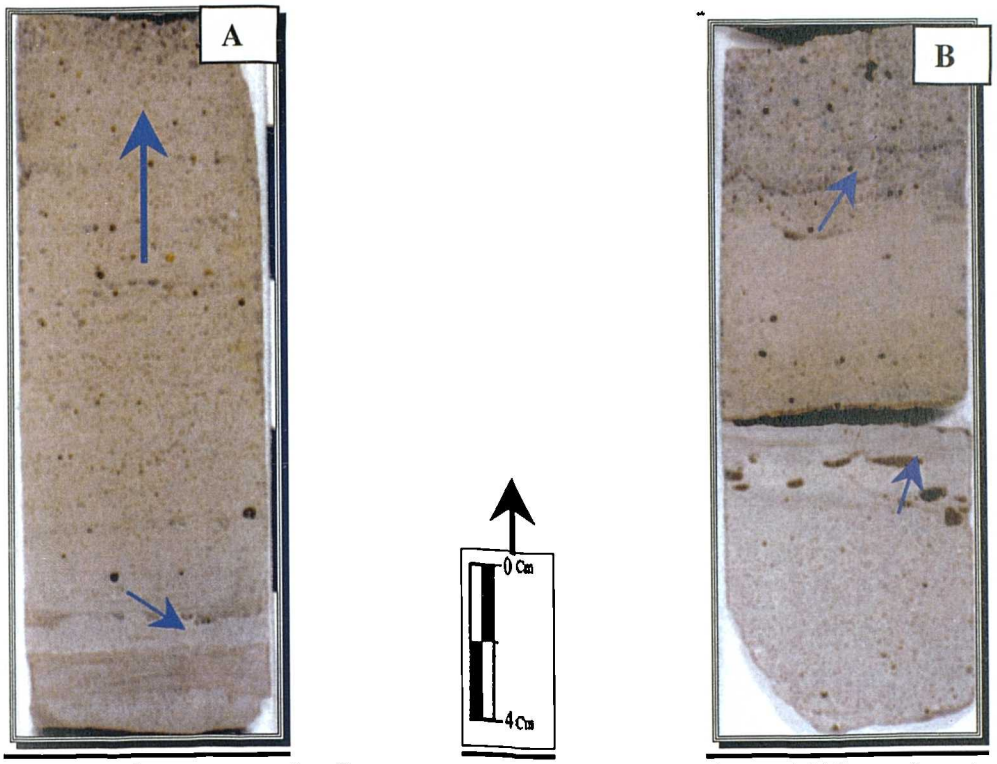

Fig. 2.18 Slabbed core samples from type well A8-NC115: A) at 1419 m, showing the coarsening-upward trend, with cross-bedding and minor low angle parallel lamination in lower portion (small arrow). B) at 1410 m, showing the horizontal burrows near the top of the coarsening-upward trend (arrows).

Subfacies (C1b): Ripple cross-laminated sandstone

Description: This subfacies occurs immediately subjacent to the subfacies C1a within the northeast part of NC115 Concession, particularly in type well A8-NC115. It is represented by the cored interval from 1420 m to 1424 m. The subfacies consists mainly of medium- to coarse-grained light brownish grey, locally dark brownish grey sandstone with rare fine-grained sandstone in the bottom portion. Sorting is usually poor to moderate and the quartz grains are well to moderately rounded.

The sandstones are highly quartzose and locally contain small amounts of glauconite; low amplitude symmetrical ripples are ubiquitous in the fine- to medium-grained sandstone (Fello, 1996). Occasional thicker sandstone units contain trough cross-bedding and contemporaneous deformation structures within the subhorizontal lamination.

The sandstones of this subfacies are characterized by a coarsening-upward trend from fine-grained sandstone at the base to medium and coarse-grained sandstone at the top. It is marked by alternations of medium- to coarse-grained sandstone and minor very coarse-grained sandstone ranging from a few centimetres to several decimetres in thickness (*e.g.* 1421 m in type well A8-NC115) **(Fig. 2.19)**. Core samples of the subfacies C1b are not adequate to show cross-bedding length and shape, although these sedimentary structures may well be similar to those of the trough cross-bedding in C1a in their shape and mode of preservation. They show some similarities with the thick sets described by Allen and Banks (1972).

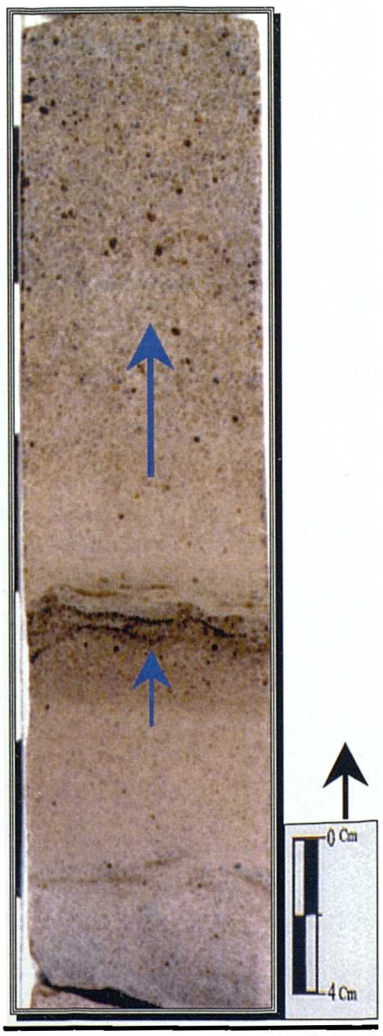

Fig. 2.19 Slabbed core sample from type well A8-NC115 at 1421 m, showing the coarsening-upward trend (large arrow), with occasional siltstone lenticles in the middle portion of the subfacies C1b (small arrow).

Subfacies (C1c): Low angle cross-bedded sandstone

Description: This subfacies occurs between the cored interval 1424 m to 1442 m in type well A8-NC115. It is characterized by light brownish grey/yellowish grey, medium-grained locally coarse-grained sandstone. These occasionally alternate with very thin layers of claystone (1 cm to 3 cm thick), with very thin subhorizontal stylolites and silty, mud laminae (*e.g.* 1441 m in type well A8-NC115) **(Fig. 2.20)**.

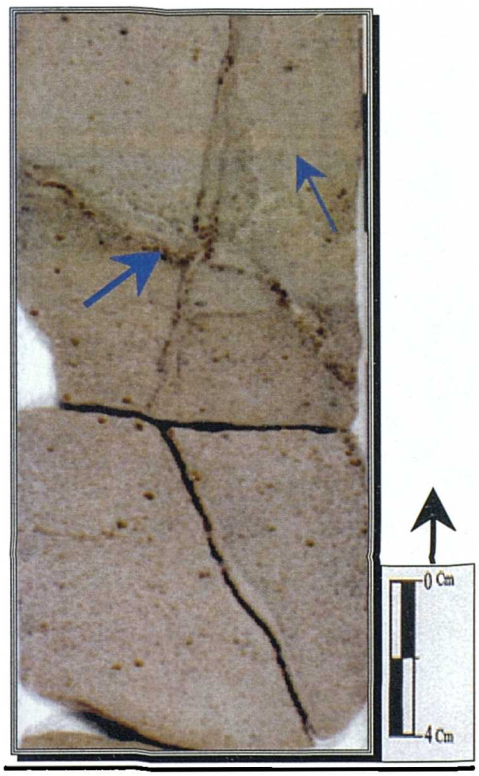

Fig. 2.20 Slabbed core sample from well A8-NC115, at 1441 m, showing the parallel laminated sandstone (small arrow) with very thin subhorizontal stylolites and silty mud laminae (large arrow).

The sandstone beds (3 cm to 7 cm thick) exhibit a clear normal grading from coarse- to medium- or fine-grained sandstones. Boundaries are sharp, with strongly erosional and irregular bases. Bed thicknesses show local lateral variation within the northeast part of NC115 Concession (Particularly in A and H-Fields), as a result of the abundant scours. Two or three graded beds may be stacked forming a sandstone package, or they may be separated by thin mudstone beds, showing a thinning-upward pattern.

The internal sedimentary structure of this subfacies is predominately cross-bedding with low angle and parallel lamination. Ripple cross-lamination is present in the middle part of the subfacies, and typically forms semi-continuous layers where sets of ripples are partly separated by fine-grained drapes. There are also cosets comprising two or three sets of cross-bedded fine- to medium-grained sandstone **(Fig. 2.21A)** (*e.g.* A8-NC115) some of which show small angles of climb **(Fig. 2.21C)**. The inclination of the sets ranges from 7° to 12°, with a thickness of less than 10 cm.

The boundary between subfacies C1c and other subfacies is gradational. Subfacies C1c is also characterized by numerous fractures, from 10 cm to 13 cm in length, with widths up to 0.5 cm. These fractures are partially to completely occluded by siliceous material. Where parallel lamination with parting lineation is found in the same bed as cross-lamination, it almost always occurs below it.

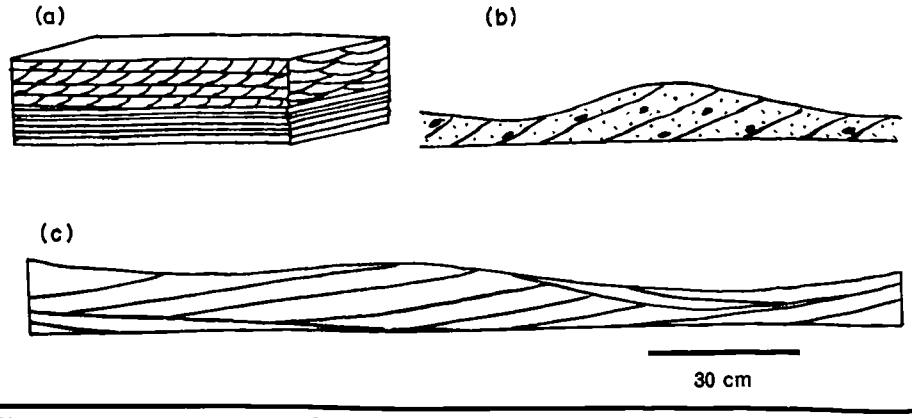

Fig. 2.21 Sedimentary structures of subfacies C1c in type wells A8 and H4-NC115. (A) Parallel lamination overlain by cross-lamination in fine sandstones. (B) Cross-bedded, coarse sandstone. (C) Low angle cross-bedding. Very low angle beds often show parting lineation.

Occasional coarse-grained sandstone beds are present, particularly within two type wells A8 and H4-NC115. These are mainly coarse with occasionally very coarse-grained sandstones. Beds less than 5 cm thick show grading, with some beds up to 15 cm thick in the upper section **(Fig. 2.21B)**.

Subfacies (C1d): Siltstone

Description: The siltstone subfacies occurs at the base of most sequences of facies C1 within the Lower Mamuniyat Formation, in type well A8-NC115, between the cored interval from 1442 m to 1450 m. It consists either of horizontally interbedded siltstone and sandstone, with some claystone, represented by upward thinning, light grey, occasionally brown, poor to moderately sorted siltstone. The entire subfacies shows a general fining-upward trend from medium- to fine-grained sandstone at the base to the very fine-grained siltstone at the top (*e.g.* 1442 m and 1448 m in type well A8-NC115) **(Fig. 2.22)**.

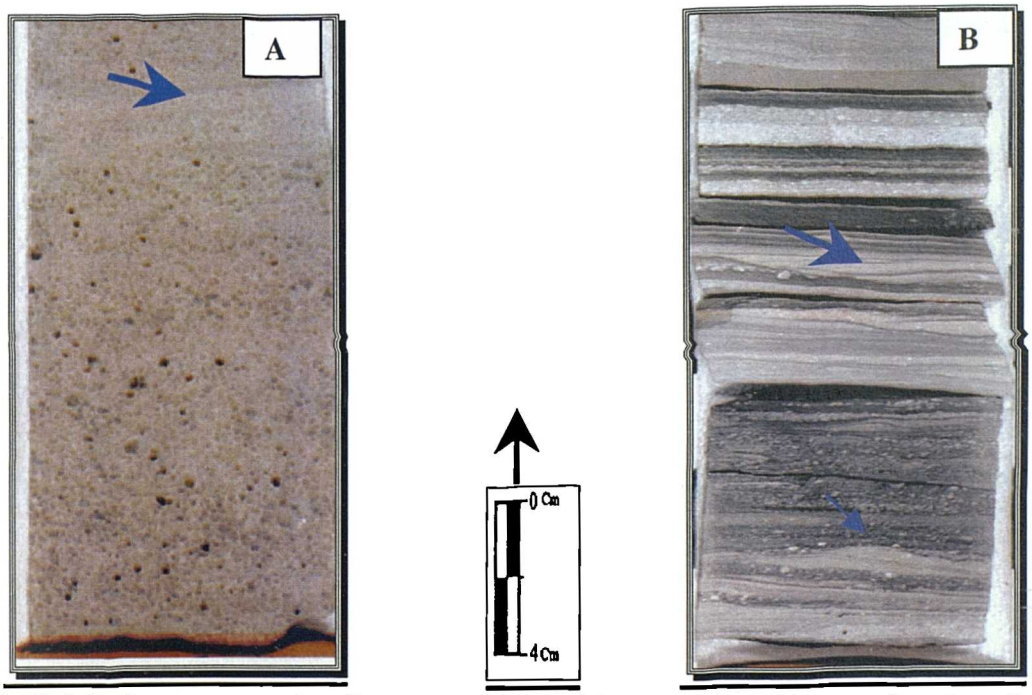

Fig. 2.22 Slabbed core samples from well A8-NC115: A) at 1442 m, showing the fining-upward trend, with lenticles of siltstone (arrow). B) at 1448 m, showing the cross-bedding with minor low angle and parallel lamination (large arrow) with internal ripple cross-lamination and lenses of claystone (small arrow).

Sedimentary structures include wave-ripples, cross-stratification and flaser-rippled fine-grained sandstone. Other internal structures include rare, small-scale planar tabular cross-bedding. Moreover, this subfacies contains small-scale trough cross-bedded sets from 5 cm to 15 cm thick. This subfacies is also characterized by the *Cruziana* and *Skolithos* ichnofacies.

In most cases, erosion of the siltstone blanket has preceded deposition of the overlying sediments, so that although persistent siltstone layers do occur, the silt is usually in the form of a discontinuous horizon of lenses (*e.g.* 1444 m in type well A8-NC115) **(Fig. 2.23)**. Siltstone pebbles have occasionally been found in the overlying unit.

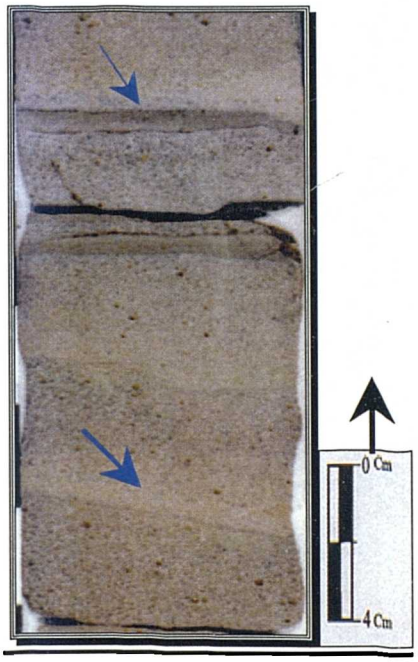

Fig. 2.23 Slabbed core sample from well A8-NC115, at 1444 m, showing the siltstone layers (large arrow) with discontinuous horizon of siltstone lenses (small arrow), and medium-grained sandstone in subfacies C1d.

Interpretation

The alternation of sandstones and finer sediments throughout the facies shows that the environment was one of fluctuating current strengths. Mud, silt, and probably some of the thinnest sand laminae were deposited directly from suspension, but in the thicker sandstones bed load transport resulted in the development of bedforms, and primary sedimentary structures. The parallel lamination with parting lineation is considered to have formed under the "plane bed with sediment movement" conditions Simon *et al.* (1965) and the cross-lamination formed from the migration of small-scale ripples. The low angle cross-bedding possibly formed in the "washed out dune" phase of Simons *et al.* (1965) and Saunderson and Lockett (1983).

The absence of high angle cross-stratification in the fine-grained sandstones may be due to the narrow range of flow power, especially under condition of decreasing current strength (Allen, 1970). Facies C1 shows a range of storm-generated wave and current features, which indicate that the normal, quieter background sedimentation was overprinted by episodic storm conditions. Vertical changes in sedimentary structures and grain-size within this facies indicate changes in wave and current energy (Anderton, 1976).

In facies C1 the well sorted, highly quartzose, glauconite-bearing sandstone suggests deposition in a shallow marine environment (Fello, 1996). The upward coarsening pattern within each sequence, accompanied by an increase in the proportion of cross-bedded to rippled sandstones, implies periodic or episodic shallowing (Hobday and Reading, 1972). The energy factors responsible for sedimentation on an open shelf which is unaffected by river currents are waves, semi-permanent currents and tides (Swift, 1969). The siltstone subfacies was less affected by these currents, and during fair weather was accumulating in deeper water, primarily by fallout of finer sediment from suspension.

This facies is interpreted as representing an offshore-to-shoreface transition zone. It occurs between strata bearing an open-marine fauna and those formed in a variety of strandline environments (Kreisa, 1981). The facies is similar to offshore-to-shoreface transition zone sediments described from cores taken in recent sediments in the North Sea (Reineck and Wunderlich, 1968). In facies C1 the trace fossil assemblage belongs to the *Skolithos* and *Cruziana* ichnofacies and is very similar to ichnofacies described in similar rocks of the Cretaceous Interior Seaway of North America **(Fig. 2.24)** (Frey and Pemberton, 1984; Pemberton *et al.*, 1992). The presence of symmetrical ripples within subfacies C1b shows that deposition occurred within the zone of effective wave action which fits with Seilacher's (1967) interpretation of *Cruziana* facies traces fossils representing an environment that was sub-tidal, but above wave base (Banks, 1973). Although burrows are relatively common in facies C1 physical reworking of the sediment was the dominant process.

Furthermore, bioturbation increases away from the shore as water depths increase and sediment becomes finer-grained. Similar patterns of bioturbation are characteristic of typical nearshore shelf sequence (Pemberton *et al.*, 1992).

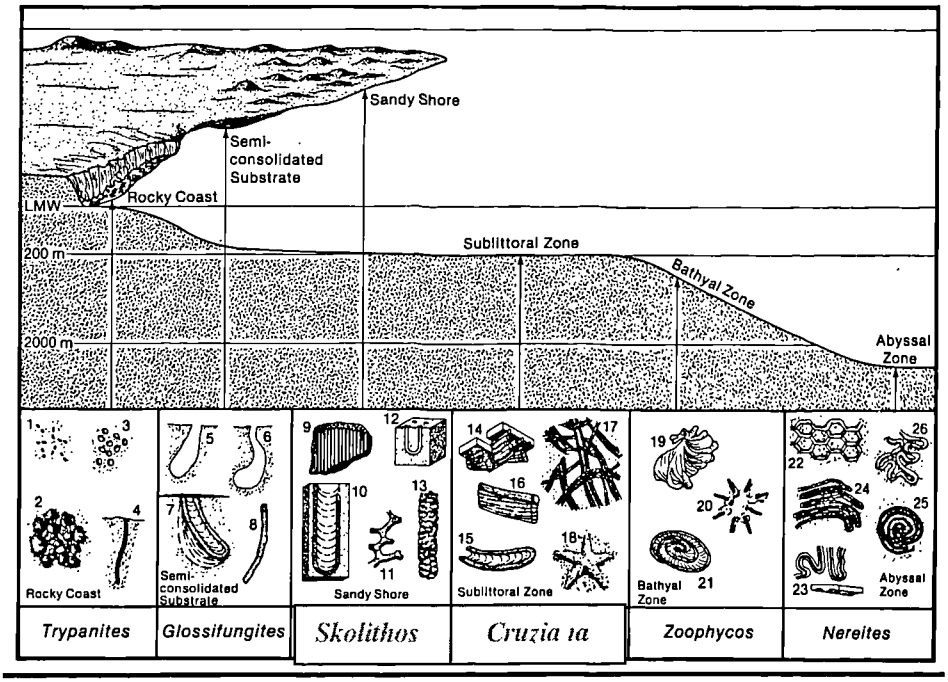

Fig. 2.24 Trace fossil associations in marine ichnofacies sets. The shaded area represents the mixed *Skolithos* and *Cruziana* ichnofacies found in the Mamuniyat Formation in the study area, NC115 Concession SW Libya (From Pemberton *et al.*, 1992). Not to scale.

In facies C1 the coarse/fine-grained sandstone alternations show diagnostic marine storm sedimentation features and the fine subfacies can also be interpreted as storm sediments. Storm processes had a decisive effect on sedimentation, not only producing characteristic storm layer deposits but also controlling the preservation of "fair-weather" tidal bedforms (Galloway and Hobday, 1983).

The evidence recounted in facies C1 suggests that for the sandstone, accretion is mainly a fair weather process and destruction a storm process. Possibly fair weather accretion by coastal currents combined with destruction by storms are also responsible for some patterns (Hobday and Reading, 1972).

Moreover, the variability of storm-generated C1 facies sequence can be related to changes in water depth. Thus, storm deposits may be useful in basin analysis to estimate relative water depth and trace transgressive and regressive events (Kreisa, 1981). This facies was also characterized by two hydraulic regimes (Johnson, 1977). Moderate energy conditions resulted in deposition of the wavy laminated sandstone layers, which were as accompanied by frequent wave agitation. Evidence of unidirectional bedload transport is relatively uncommon, where the larger size of the wave ripples and increased sand deposition indicate that wave action was more intense than in areas accumulating Upper and Middle Mamuniyat Members.

The thicker, interbedded sandstones within facies C1 represent deposition during the highest energy periods. The internal stratification closely resemble offshore, sheet sandstone beds believed to result mainly from the deposition of sand from suspension during storms (Gadow and Reineck, 1969; Goldring and Bridges, 1973; Banks, 1973; Anderton, 1976). Each sandstone bed represents deposition during a single storm event; its wave rippled top reflecting wave oscillations during the waning stage of the storm (Johnson, 1977).

2.3.3.2 Facies (C2): Massive (? Bedded) sandstone

Description

This facies is dominantly present in the Lower Mamuniyat Formation (M3), throughout the El-Sharara Field (**Table 2.3**). It occurs in both type wells of the study area (A, B and H-Fields). Facies C2 is represented by the cored interval from 1450 m to 1458 m in type well A8-NC115, the cored interval from 1456 m to 1465 m in type well B2-NC115 and the cored interval from 1484 m to 1494 m in type well H4-NC115 (**Figs. 2.2, 2.3 and 2.4**).

In general the beds of this facies C2 are more laterally persistent than those of facies C1 and can usually be traced for at least 50 Km within NC115 Concession. Facies C2 characterized by light grey, locally brownish quartz rich sandstones.

The sandstone shows a wide range of grain-size from fine- to coarse-grained, although most are medium- to coarse-grained sandstone. Coarse-grained sandstones of facies C2 are more prevalent in the A-Field, particularly in A8-NC115 (*e.g.* 1455 m in type well A8-NC115) **(Fig. 2.25)**.

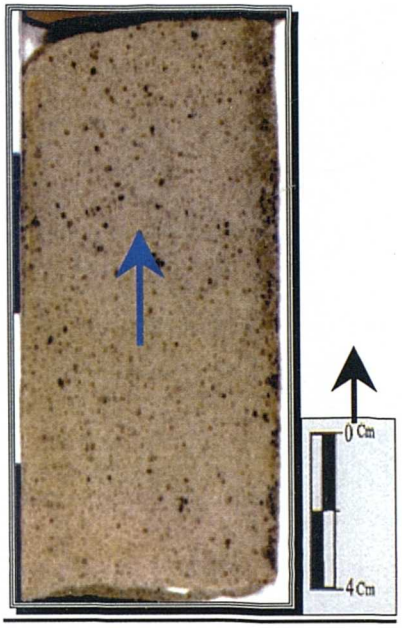

Fig. 2.25 Slabbed core sample from well A8-NC115, at 1455 m, showing the coarsening-upward trend (arrow) in the lower portion of facies C2, within the A-Field.

The entire facies shows a general coarsening-upward trend from fine-grained sandstone at the base to medium and coarse-grained sandstone at the top (*e.g.* 1455 m in type well A8-NC115) **(Fig. 2.25)**. The majority of the sandstones within facies C2 are poorly sorted and contain some granules and small pebbles of quartz as well as mudstone intraclasts. Quartz grains are subrounded to rounded and cemented by silica overgrowths. The sandstone has moderate visible porosity.

Massive sandstone beds generally occur within a thicker succession of associated coarse and fine-grained sandstone. This whole succession may be referred to as a massive sandstone *complex* (Stow and Johansson, 2000). In some cases, such a complex may be equivalent to a named geological Member or even Formation.

In facies C2, the laminae are generally visible as slightly higher concentrations of coarser-grains along particular horizons, but in some cases they can be discerned only by alignment of platy mudclasts (*e.g.* 1456 m in type well A8-NC115). Facies C2 in type well A8-NC115, is characterized by massive beds (thickness greater than 8 m). The beds are often structureless in appearance, and generally homogeneous, occasionally exhibiting pebbly-stringers.

Locally the sandstone may coarsen towards the base, and fine towards the top (*e.g.* 1454 m in type A8-NC115) **(Fig. 2.26)**. The thickness of single beds in facies C2 varies between 0.4 m and 2.0 m. Locally there is an indistinct mottling at the top of units with ghost burrows, and sharp basal bed boundaries are present in some of the horizons within this facies (*e.g.* 1452 m in type well A8-NC115)

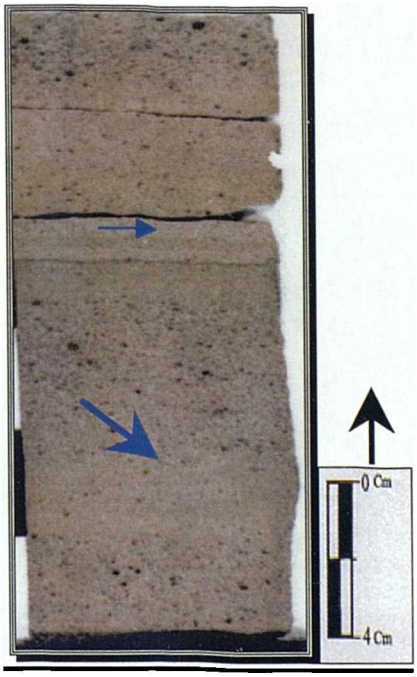

Fig. 2.26 Slabbed core sample from well A8-NC115, at 1454 m, showing the transition between truly structureless sandstone in the lower portion (large arrow) and laminated sandstone (small arrow) in the middle portion of facies C2.

In some cases the surfaces of amalgamation are very poorly defined and can only be inferred from subtle changes in sandstone properties. In these cases, the distinction between a bed and a unit is less clear (Galloway and Hobday, 1983).

The massive beds may or may not show an erosive lower surface containing abundant mudstone and siltstone intraclasts. With respect to massive sands, the term *bed* is used in its standard sense to mean a single identifiable stratum that is believed to have been deposited by one event. However, in many of the examples studied, a number of beds have clearly been amalgamated into a massive sandstone *unit* or *body*. Such units comprise, typically, from two to eight beds (rarely more).

In facies C2 rare, indistinct parallel subhorizontal laminations are visible. Sand to granule grade mudclasts may be scattered throughout this facies. These sediments of facies C2 may also contain rare, thin intervals of coarse-grained, more poorly sorted sandstone (at the base of units, *e.g.* 1457 m in type well A8-NC115) **(Fig. 2.27B)**, and fine-grained sandstone with stylolitized wispy clay partings at the top of some units (which in places display a fining-upward trend, within A-Field, (*e.g.* 1451 m in type well A8-NC115) **(Fig. 2.27A)**. The facies contains a well-preserved suite of trace fossils including the *Skolithos* ichnofacies with occasional bioturbation in the lower portion and some glauconitic sandstones (Fello, 1996).

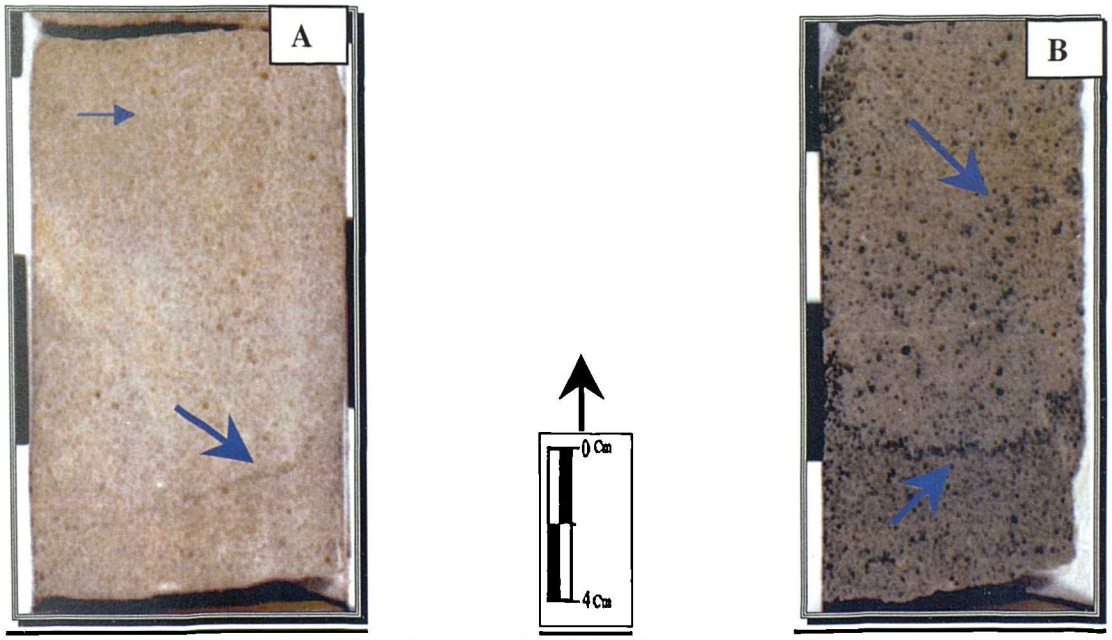

Fig. 2.27 Slabbed core samples from well A8-NC115: A) at 1451 m, showing the fine-grained sandstones (small arrow) with stylolitized wispy clay (large arrow). B) at 1457 m, showing the coarse-grained sand to granule grade (arrows) scattered in the lower portion of the facies C2, within A-Field.

Interpretation

Massive sandstones may form in response to depositional processes (Collinson, 1970; Turner and Monro, 1987; Lowe, 1988), or by post-depositional deformation (Allen and Banks, 1972; Doe and Dott, 1980; Allen, 1986). Meanwhile, some authors emphasize the thickness, some the structureless aspects, and others consider both important.

The combination of local bioturbation, some glauconite and burrows suggests that the facies C2 massive bedded sandstones were deposited in a marine shelf environment, mostly at a depth between the fairweather wave base and storm wave base or, even deeper (Lowe, 1982). Interpretation of the sedimentary structures of facies C2 suggests that some sandstone features developed in response to a hydraulic regime characterized by tidal currents and wave processes. Both processes operated simultaneously under fairweather and storm conditions (Johnson, 1977). The highest energy conditions occur within facies C2 when tidal currents were enhanced by storms.

The facies lacks hard body fossils but contains a well-preserved suite of trace fossils characteristic of shallow-marine environments. The trace fossils including the *Skolithos* ichnofacies assemblage is considered to be indicative of variable energy conditions in an open-marine setting between wave-base and storm wave-base (Ekdale *et al.*, 1984; Frey and Pemberton, 1984). Mottling and ghost burrows will normally remain in evidence, and the indistinct mottling of the massive sandstone at the top of units is probably due to water escape. Throughout facies C2, the transitional relationship between massive and faintly laminated sandstone indicates a genetic origin common to both (Jones and Rust, 1983).

Alternative explanations are that the laminae formed by marginal deceleration or "frictional freezing" of a high concentration flow. However, the deposits of massive type sand in facies C2 formed in this way may be several meters thick and are particularly prone to development of secondary water escape structures, because of their loose primary packing (Lowe, 1982).

The coarse/fine-grained alternation of sandstone within facies C2, is diagnostic of marine storm sedimentation. The storm processes had a decisive effect on sedimentation, not only producing characteristic storm layer deposits but also controlling the preservation of "fair-weather" tidal bedforms (Anderton, 1976). Following the arguments presented above this facies was deposited in an environment of strongly fluctuating currents, deposition generally occurring during periods of tidal current strength. The currents were stronger that those which produced facies C1 as is indicated by both the slightly greater grain-size and the predominance of upper flow regime parallel stratification (Banks, 1973).

The massive sandstone facies provides a link between purely tidal and purely wave dominated shelf sediments. The coarse-grained sandstones show similarities with many ancient tidal-shelf deposits (*e.g.* Allen and Narayan, 1964; Anderton, 1976) as do the fine-grained sandstones with ancient storm sediments (*e.g.* Goldring and Bridges, 1973). In facies C2, closely associated cross-bedded sands and sand/mud alternations, showing "turbidite" features, can therefore, be interpreted as shallow marine sediments of mixed tidal and storm origin (Anderton, 1976). Sedimentary structures observed within facies C2, such as irregular laminae and occasional ripples, suggest sedimentation under oscillatory waves or possibly wave reworking (Howard and Reineck, 1981). The sharp-based sandstone beds are indicative of rapid emplacement of sediment consistent with strong flow velocities (Reineck and Wunderlich, 1968).

2.3.3.3 Facies (C3): Ripple cross-laminated sandstone

Description

This facies has been found only in the southwestern part of the study area of the B-Field throughout NC 115 Concession within the Lower Member of the Mamuniyat Formation (M3). It is represented by the cored interval from 1465 m to 1483 m in type well B2-NC115 **(Fig. 2.3)**.

This facies is about 18 m thick. It consists of fine- to very fine and occasionally medium-grained sandstone, with locally developed thin, sandstone, irregularly interlaminated with grey to brown siltstones and shale. The sandstone is a light brownish to grey, moderately well-sorted.

Individual sand grains are rounded to subrounded, and silica cemented. Grain-size increases upward in facies C3 from about 0.12 mm to 0.22 mm in diameter. The fine-grained horizons are commonly slightly more argillaceous in character and are locally interbedded with cleaner sands. Occasionally the facies consists of homogenous very fine glauconitic sand units. Facies C3 is characterized by thick 3 to 4 m units of amalgamated fine- to medium-grained sandstones. The units usually have an erosive base and sharp tops, and are interbedded with parallel-laminated siltstones. Individual beds reach a maximum thickness of 1 m but are generally around 0.3 m. These sandstones are sometimes massive but usually contain faint parallel or wavy lamination and occasionally weak normal grading.

Burrows occur mainly in the upper portion of the shale and also in the sandstone. In the uppermost portion of facies C3 the interbedded shaly siltstones are massive to fissile, unlaminated, and show varying amounts of burrows. The amount of burrows normally increases upward in the section. They are predominately horizontal, < 1 cm in diameter, and filled with light grey siltstone or very fine sandstone. A few small narrow vertical burrows, < 1 cm long, belonging to the *Skolithos* and *Cruziana* ichnofacies, also occur in the sandstone. No specific trace fossils were identified in this interval.

Ripple cross-lamination dominates the internal architecture, but subordinate climbing ripple units, clay flasers (abundant in places) are also present. Some sandstone is massive or indistinctly laminated. Low angle cross-stratification is present in many of these sandstones and convolute lamination on a small-scale occurs throughout this facies. The cross-laminated sets of facies C3, which have undulose top and bottom surfaces, suggest that they were originally cross-laminated. They are equivalent to the wavy bedding of Reineck and Wunderlich (1968).

The upper surface of these bedsets within facies C3 shows well preserved ripple cross-lamination (*e.g.* 1470 m in type well B2-NC115) **(Fig. 2.28)**. The most common characteristic of the ripple-cross laminae in facies C3, is their lenticular geometry, and undulatory set boundaries, out of phase with one another. Inclination of the ripple form cross-laminae is the same as those of the set boundaries (Anderton, 1976).

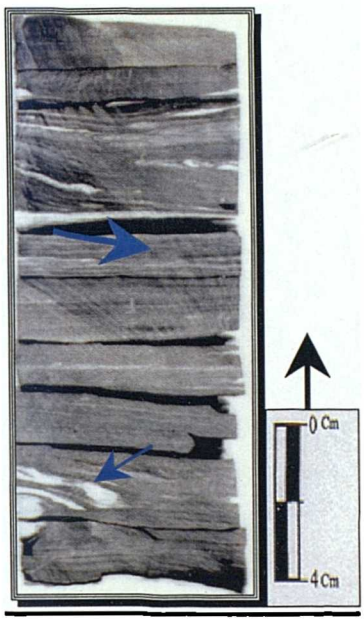

Fig. 2.28 Slabbed core sample from well B2-NC115, at 1470 m, showing the ripple cross-lamination (large arrow) and lenticular ripple cross-laminae (small arrow) in the lower portion of facies C3.

In profile, the lenticular ripple cross-lamination exhibits many of the features described by De Raaf *et al.* (1977), and considered by them to be characteristic of wave-formed ripples. These include bundled lenses, scooped and undulatory lower set boundaries, off-shooting and draping of foreset laminae, intricately interwoven cross-laminae and form discordance. These same features also occur in facies C3 of the Lower Mamuniyat Formation (M3). Facies C3 forms only a very minor proportion of the cored section and is unlikely to be significant in the uncored section. It comprises thin sandstone, with often isolated sets of current ripple cross-lamination or poorly defined wave ripples, closely associated with the sandstone of facies C2. In facies C3, changes in building direction along a single ripple train have not been observed.

Moreover, the internal sedimentary structures of this facies is cross-bedding with low angle and parallel lamination (*e.g.* 1475 m in type well B2-NC115) **(Fig. 2.29)**.

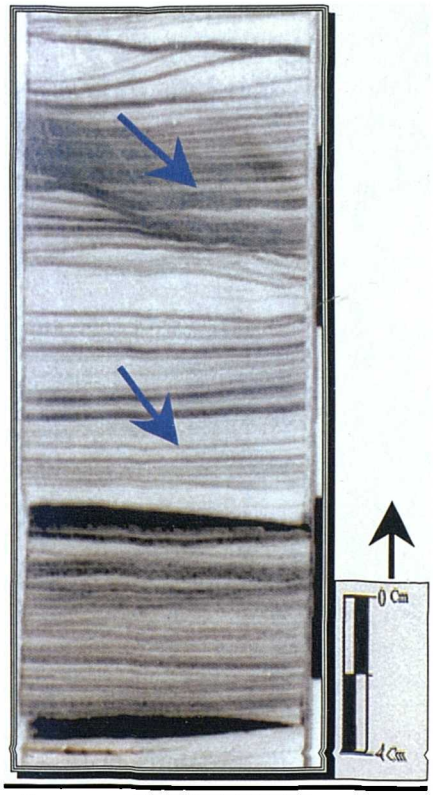

Fig. 2.29 Slabbed core sample from well B2-NC115, at 1475 m, showing the cross-bedding with low angle and parallel lamination (arrows).

Interpretation

Ripple cross-lamination is the dominant physical sedimentary structure formed in the nearshore facies according to Howard and Reineck (1981). The general sedimentary characteristics of facies C3 indicate a shallow marine origin, with deposition from tidally dispersed, storm generated suspension clouds (Rubin, 1987). The laminated and ripple cross-laminated facies may represent relatively proximal and distal storm-sand deposition respectively, and the mud facies may represent an area of shelf mud where storm-sand sedimentation was of very minor importance. The ripple facies may be compared directly with the North Sea storm-sand layers (Reineck and Wunderlich, 1968; Reineck and Singh, 1972).

The thick, planar sets of low angle parallel lamination are typical of beach face deposition (Hamblin and Walker, 1979). This interpretation is a logical continuation of the shallowing-upward sequences from facies C3 and C2 through facies C1. Thin, tabular sand beds, typically graded are common in Recent shelf sediments (Nelson, 1982) and from ancient sequences where they generally occur in the lower parts of storm-influenced deposits (Morton, 1981). The most common situation of facies C3 is for the sandstone to be intercalated within the marine siltstones and shales. The interlaminated sandstone and shale units in the upper portion of this facies suggests variable depositional conditions and periodic higher energy currents affecting a normally quiet-water environment (Hein *et al.*, 1991). The thick shale bed within B2-NC115 may have formed during a minor transgression and increased water depth.

Thus, the possible processes responsible for the deposition of the sandstone within the facies is the storm wave. During the passage of shallow water waves, net mass transport of water and entrained sediment in the direction of wave progradation occurs just above the substrate surface (Goldring and Bridges, 1973). The textural variations, sedimentary structures and biological features of the facies C3 (including sandstones and burrows) indicate single depositional events related to a waning current.

Other common processes responsible for sediment motion on marine shelves are storm generated currents, tidal currents and oceanic currents (Swift, 1969). Of these, storm generated currents are the most likely mechanism. Storms are generally recognized as the most powerful geologic agent in the nearshore shelf and over geologic time, most likely to leave an imprint in the rock record (Vos, 1977). Their ability to move sand-sized sediment on marine shelves has been demonstrated by Howard and Reineck (1981).

The ripple cross-laminated sandstone facies C3 possibly formed in a similar manner to nearshore shelf sandstones. However, in the lower shoreface, higher flow regime structures and less abundant siltstone indicate moderate wave surge currents in a shallower environment. Also sandstones probably underwent many reworking episodes before burial by a thin layer of finer sediment ensuring textural maturity.

Figure 2.30 shows the schematic and idealized sequence of sedimentary structures within sandstone beds of the nearshore shelf (Vos, 1977). The recognition of ripple cross-stratification is useful for environmental interpretation, because it developed in the coarse siltstone or fine- to very fine-grained sandstone deposited in a wave-dominated shallow-marine environment (Duke, 1985). Some sandstones lack structures either due to small contrasts in mean grain-size of the adjacent laminae, or an influx of rapidly deposited storm sand.

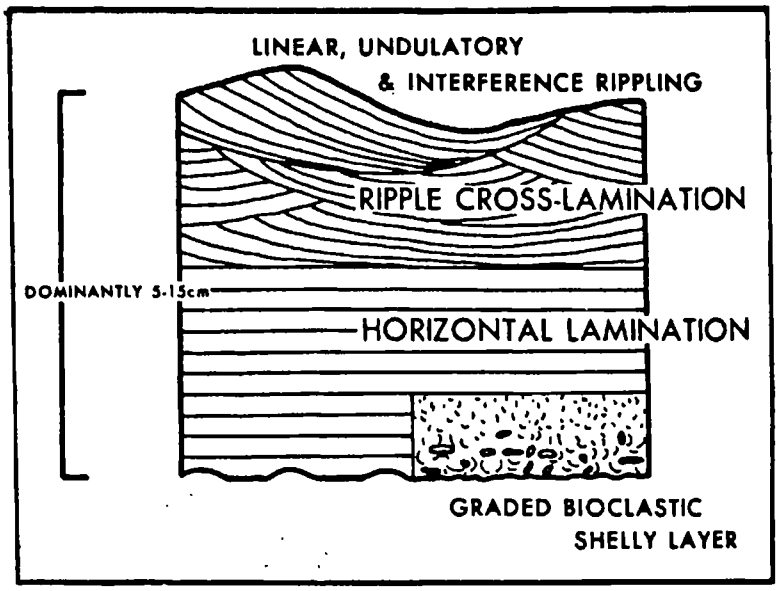

Fig. 2.30 Schematic and idealized sequence of sedimentary structures within the sandstone beds of the nearshore shelf facies found in the ripple cross-laminated sandstone facies throughout the Lower Mamuniyat Formation.

Both *Skolithos* and *Cruziana* within facies C3 are characteristics of shallow marine deposits. Meanwhile, very fine glauconitic sand is also a good indication of marine sediments (Visher, 1972). There are also relatively few burrows in the middle part of facies C3, which is probably due to rapid accumulation of the sediment. Hence there was little opportunity for reworking any particular exposed substratum (Graham, 1975). In facies C3 the sharp-based, laterally extensive thin sandstone with internal parallel lamination and cross-lamination within B-Field, particularly in type well B2-NC115, suggest the effects of wave-induced currents associated with storms (Jansa, 1972).

In facies C3, the ripple cross-laminated sandstones are similar to the shoreline association of storm-influenced sandstones described by Goldring and Bridges (1973). Storm-generated sands demonstrate distinctive proximal-distal relationships. Bed thickness, grain-size, and degree of amalgamation all decrease towards deeper water (Brenchley *et al.*, 1979). The frequency of disturbance of sediment by storms also decreases distally (Jago, 1980). The similarity of facies C3 to published accounts of similar sedimentary structures from elsewhere suggest that they have been formed in a shoreface environment (Graham, 1975). In facies C3 the ripple cross-laminated and burrowed fine sandstones towards the top of the trend may reflect a shallower depth of deposition. Moreover, the thinner, locally rippled and laminated sandstone beds are lower energy deposits, which may owe their origin to episodic flows of tidal or oceanic origin rather than storms (Turner, 1991).

The lack of hummocky and swaley cross-stratification in facies C3 during this time suggests that, the shelf was not subject to severe storms (*cf.* Castro *et al.*, 1985). This may reflect the shelf width, since wide shelves inhibit storm conditions and favour tidal action. Some of the tidal activity is seen in the sediments at the top of the overlying facies C1 and C2 sands in the Lower Mamuniyat Formation (M3). The ripple cross-laminated sandstone facies C3 in the Lower Mamuniyat Formation (M3), is interpreted to comprise the deposits of Lower energy distal storm events (**Table 2.3**).

2.3.3.4 Facies (C4): Bioturbated wavy-hummocky cross-stratified sandstone

Description

This facies occurs in each of the type wells of the study area. It is represented by the cored interval from 1458 m to 1506 m in type well A8-NC115, the cored interval from 1483 m to 1503 m in type well B2-NC115 and the cored interval from 1494 m to 1517 m in type well H4-NC115 (**Figs. 2.2, 2.3 and 2.4**).

Facies C4 is about 48 m, 20 m and 23 m thick within A8, B2 and H4-NC115, respectively. It is characterized by a light brownish grey/yellowish grey, fine- to very fine, locally medium-grained, quartz sandstone. This facies is mainly bioturbated throughout. Ichnofossils are predominantly small and horizontal with rare large subvertical burrows similar to *Skolithos*. The sand is moderately to well sorted, with poor to moderately poor visible porosity (25 %). This facies can be divided into two subfacies. Each facies and component subfacies are described separately below.

Subfacies (C4a): Bioturbated sandstone

Description: The Bioturbated sandstone subfacies occurs in all type wells of the study area. It is represented by the cored interval from 1489 m to 1495 m in type well A8-NC115, the cored interval from 1457 m to 1458 m in type well B2-NC115, and cored interval from 1514 m to 1517 m in type well H4-NC115 **(Figs. 2.2, 2.3 and 2.4)**. This subfacies typically consists of intensely burrowed, bioturbated sandstone (90-95%) with subordinate shale (5-10%), and thin beds of siltstones (average 2 cm to 3 cm thick, maximum 5 cm thick).

The sandstone is medium to dark-grey in colour, indicating a significant amount of organic matter. It is a fine- to very fine, locally medium-grained, well-sorted and mature sandstone with individual grains predominantly rounded to subrounded. These sandstones coarsen upward from very fine- to medium-grained, and they contain several types of burrow, including 0.5 cm to 1 cm diameter, sinuous horizontal burrows (*Thalassinoides*) (*e.g.* 1457 m in type well B2-NC115) **(Fig. 2.31)**, and 1 mm to 2 mm diameter, < 10 cm long, "worm-like" horizontal burrows.

The bioturbated sandstone contains a lower interval of rare planar-laminated and ripple-cross laminated, lenticular beds in which the laminae are commonly partly obliterated by intense *Skolithos* burrows and the *Cruziana* ichnofacies. Elsewhere the original primary sedimentary structures are completely obliterated by burrowing and biological action.

The subordinate shale is brown- to light brown-grey and locally black, with horizontal to subhorizontal and irregular wavy laminae < 1 cm thick. Burrows occur in the shale and are prominent on bedding surfaces. These are < 1 cm long, vertical to oblique and locally curved. Horizontal burrows, < 0.5 cm in diameter, filled by siltstone, also occur.

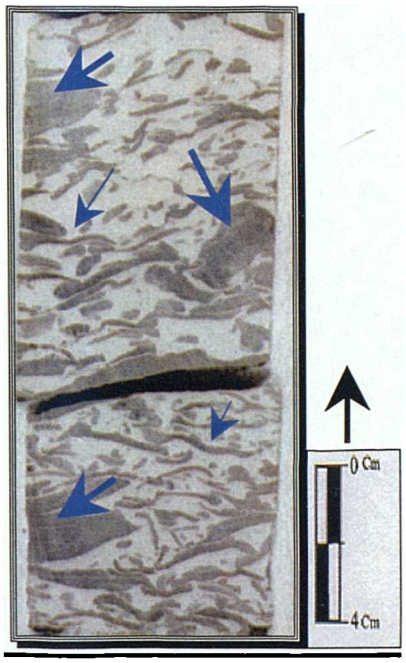

Fig. 2.31 Slabbed core sample from well B8-NC115, at 1457 m, showing the high intensity of bioturbation (large blue arrow) with burrows, dispersed in different directions (vertical and horizontal type small arrow).

Interpretation: In marine environments many of the parameters that govern the abundance and distribution of trace-makers, such as temperature, food supply and the intensity of wave or current agitation tend to change progressively with water depth. Therefore, the individual assemblages or ichnofacies constitute the basis for a relative scale of bathymetry (Basan, 1978).

In subfacies C4a, the occurrence of rare planar-lamination with wave ripple cross-lamination and the association of subfacies C4a with low energy event deposits of facies C3, suggest that the bioturbated sandstones were probably deposited under similar storm-dominated conditions inferred for this latter facies.

Extensive bioturbation, however, implies lengthy pauses or periods of relatively slow sedimentation between low storm- influenced energy events and suggests that the obliteration of depositional sedimentary structures probably occurred below fair-weather wave-base (Dott and Bourgeois, 1982). Bioturbation is extensive in most sedimentary facies, and bioturbated rock fabrics typically are well represented in core and outcrop samples.

As a general rule, non-marine deposits contain fewer trace fossils than marine deposits and thick, rapidly deposited beds contain fewer traces than slowly deposited ones (Basan, 1978). Soft ground ichnofacies tend to be differentiated from one another by variables that typically are depth related. In the bioturbated sandstone subfacies the *Skolithos* and *Cruziana* ichnofacies are representative of nearshore marine or coastal environments. For example, in the Cretaceous of the western Interior of North America, the inter-deltaic marine shoreface can be zoned ichnologically (**Fig. 2.32**) (Pemberton *et al.*, 1992).

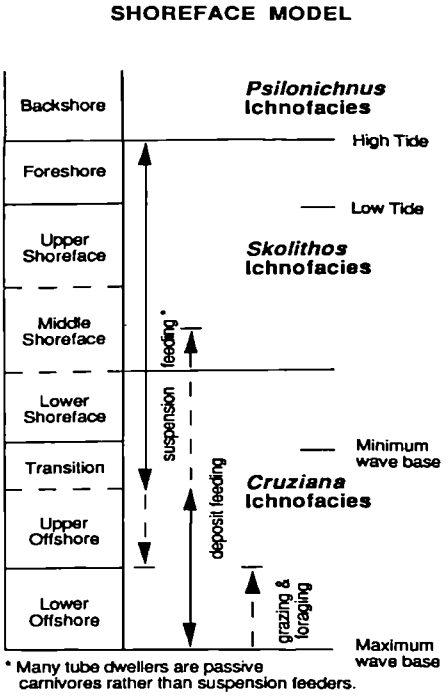

Fig. 2.32 Idealized shoreface model for ichnofacies, based mainly on facies observations in the Cretaceous Interior Seaway of the USA (Pemberton *et al.*, 1992).

In subfacies C4a the finer sediments may imply deposition in an offshore quieter shelf setting. This intense bioturbation is presumably due to a low rate of sedimentation (Reineck and Singh, 1973). Furthermore, bioturbation increases away from the shore as water depths increase and sediment becomes fine-grained. Similar patterns of bioturbation are characteristic of typical nearshore shelf sequences (Basan, 1978). The sandstone shows the presence of escape burrows. This subfacies is interpreted to represent deposition in a shallow marine shelf margin, with the presence of bioturbation indicating a relatively low energy environment with slow rate of sediment input.

In the middle section of subfacies C4a, the increase in sand content from the underlying laminated shale, indicates that generally they form part of the same progradational succession. The irregular alternation between sand and shale reflects alternating periods of high and low-energy. This interval suggests that these sediments were deposited by periodic, high-energy events in a low energy environment (Ainsworth and Crowley, 1994). The fluctuations in sediment supply and current velocity of the subfacies C4a, are typical of shelf storm events, as described by De Raaf *et al.* (1965).

Subfacies (C4b): Wavy-hummocky cross-stratified sandstone

Description: This subfacies is represented by the cored interval from 1483 m to 1485 m in type well B2-NC115 and the cored interval 1494 m to 1498 m in type well H4-NC115. It is characterized by a light brownish grey/yellowish grey fine- to very fine-grained, moderately to well sorted, and locally well indurated sandstone. The uppermost portion of subfacies C4b is characterized by thin (centimetre to decimetre-scale), erosionally-based, laterally continuous sandstone beds interbedded in the upper few meters with subfacies C4a. In some relatively thick beds (20-30 cm thick), the wavy-hummocky cross-stratified sandstone facies is very well developed (*e.g.* 1497 m in type well H4-NC115) **(Fig. 2.33B)**.

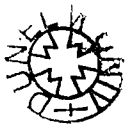

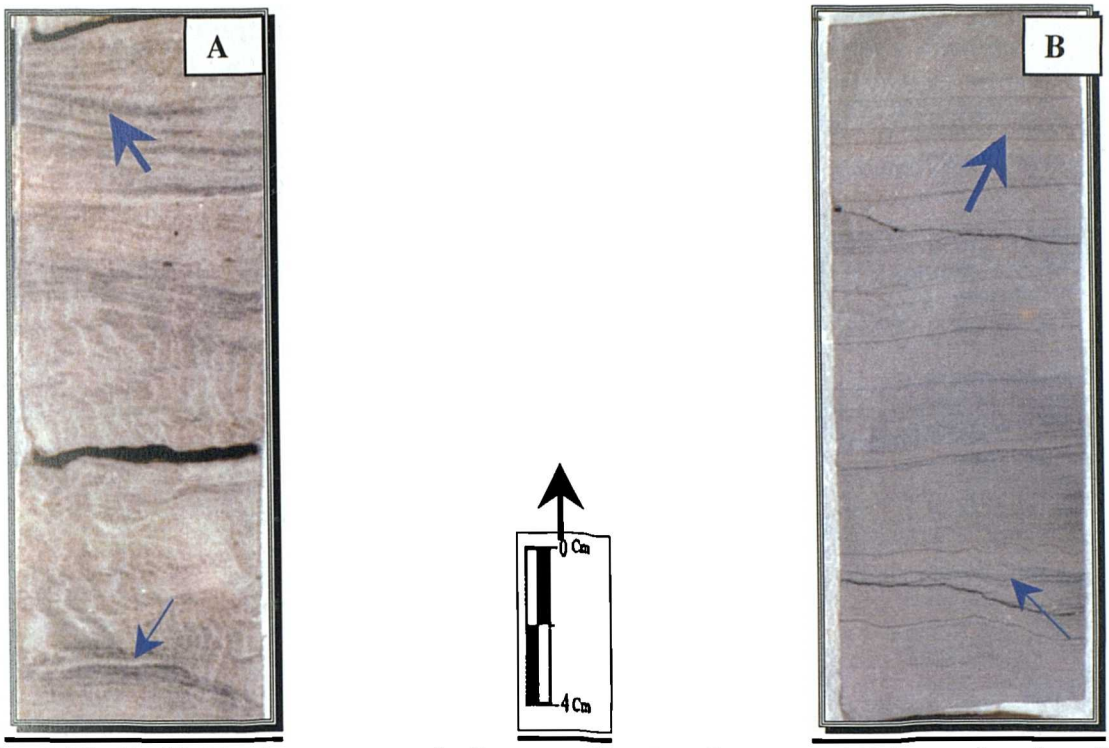

Fig. 2.33 A) Slabbed core sample from well B2-NC115, at 1485 m, showing the individual wavy-hummocky cross-stratified sandstone (large arrow) with burrows (small arrow). B) Slabbed core sample from well H4-NC115, at 1497 m, showing the planar-lamination (large arrow), with wave ripple cross-laminated, fine to very fine-grained sandstone (small arrows).

The average bed thickness of subfacies C4b is 15 cm. It is observed within type wells B2 and H4-NC115 (*e.g.* 1485 m in type well B2-NC115) (**Fig. 2.33A**). Burrowing is common in the sandstone but varies in intensity. Most beds are sparsely burrowed, but some sandstones are intensely bioturbated with consequent obliteration of primary sedimentary structures. Burrowing tends to be concentrated towards the tops of individual beds (toward subfacies C4a).

Interpretation: Hummocky cross-stratification was defined by Harms *et al.* (1975) as recording a bed configuration of unorientated, low-relief hummocks and swales with spacing of 1 m or more, developed in fine sands and silts. The spacing criterion, however, has been relaxed to include mm's-scale bedforms commonly described as small-scale hummocky cross-stratification.

Nonetheless, hummocky cross-stratification generally is considered to be an indicator of shoreface and shelf environments well above effective storm wave base (Duke, 1990). Hummocky cross-beds vary in thickness from a few centimetres to 5 or 6 m; bedsets may also be tens of meters thick. Hummocky-cross stratification is significant because it provides:

1) A potential bathymetric guide for the inner-shelf to lower shoreface transition;
2) Apparent evidence for large storm waves or tsunamis; and
3) Evidence of relative event frequency and rates of scouring, deposition, and burrowing.

Hummocky cross-stratification is important not only as an indicator of episodic large waves, but also for determining relative depth or position relative to shore (or a shoal). Although it probably forms across a wide depth range, its greatest preservation potential seems to be between fair-weather wave base and storm wave base, that is from a few to several tens of metres (Dott and Bourgeois, 1982). The occurrence of erosionally based sandstones vertically enclosed by subfacies C4a suggests that these sediments were deposited by periodic, high-energy events in a low-energy environment (Ainsworth and Crowley, 1994).

Planar-lamination, evidence of normal grading and the presence of wave-ripple cross-laminated tops to planar-laminated units are all consistent with deposition from decelerating, sediment-laden currents typically associated with storm events (Reineck and Singh, 1972; Goldring and Bridges, 1973). Moreover, in subfacies C4a, the downward decrease in burrowing suggests faunal activity in the upper portion of beds during fair-weather periods. The fact that wave ripple cross-lamination occurs in association with planar-laminated sands, and that other event beds of this subfacies C4b are composed entirely of wave ripple cross-lamination, implies deposition at least above storm wave base. The presence of hummocky cross-stratification within subfacies C4b also indicates that sandstones were at times affected by storm wave scouring.

Consequently, the sandstone in subfacies C4b is interpreted to be the product of intermittent, storm-generated currents capable of transporting sand-grade sediment in a relatively low energy offshore environment where they were susceptible to reworking by storm waves (Arnott and Southard, 1990). The occurrence of fine sand or silt at the top of hummocky beds, represents temporary reworking at low flow intensity, of the top of the bed by wave oscillation as storms waned. Fair-weather conditions followed (Dott and Bourgeois, 1982). These current variations could have been produced by the differing intensities and tracks of individual storm events relative to the site of deposition (Ainsworth and Crowley, 1994).

Interpretation of facies C4

In facies C4 horizontal lamination is present in the lower portion of the sandstone beds in the facies, and is occasionally overlain by wavy hummocky cross-stratification as in the shelf sandstone deposits. The abundance of trace fossils increases towards the top of the facies. Dominant types include *Skolithos* and *Cruziana,* characteristic of Seilacher's (1967) *Cruziana* ichnofossil assemblage (littoral zone to wave base). Although *Skolithos* and *Cruziana* are the most abundant trace fossils, they are not found together. The facies shows no evidence of subaerial exposure.

Trace fossils of the *Cruziana* ichnofacies reflect the activities of a benthic fauna of epifaunal and shallow burrowing infaunal detrital feeders. The behavioural response of animals to different energy levels and rates of sedimentation (Crimes, 1970) is thought to be responsible for the close association but mutual exclusiveness of *Skolithos* and *Cruziana.* Vertical burrows in the upper portion of the facies C4 possibly reflect attempts by animals to escape as water depths increased concomitant with deposition of the overlying transgressive marine shelf sand facies. In facies C4 the basal scoured surface and fine- to medium-grained sand lag may indicate storm activity and possible shallow marine shelf sand systems (Harms *et al.*, 1975), which could be related to distal rip currents. The occurrence of burrowing and bioturbation within facies C4 suggests a more-protected environment, possibly periods of reduced current activity with alternations of current and biogenic structures related to their differential energy level.

The contact between the bioturbated sandstone subfacies C4a and the wavy-hummocky cross stratification sandstone subfacies C4b is interpreted to represent fair-weather wave base of the shallow marine environment.

2.3.3.5 Facies (C5): Heterolithic

Description

The heterolithic facies C5 is present in all type wells of the study area. It occurs in the lower part of the cored succession of the Lower Mamuniyat Formation (M3) (**Table 2.3**). This facies is represented by the cored interval from 1506 m to 1527 m in type well A8-NC115, the cored interval from 1503 m to 1525 m in type well B2-NC115 and the cored interval from 1517 m to 1527 m in type well H4-NC115.

This facies is about 21 m, 22 m and 10 m thick within A8, B2 and H4-NC115 respectively. It consists of interbedded mudstone, siltstone and sandstone. Mudstones and siltstones make up over 60% of the facies and alternate with fine- to medium-grained, moderately well-sorted sandstone that occurs as lenticular, wavy units.

The entire facies shows a general coarsening-upward trend from fine- to medium-grained sandstone, which is light grey to brownish-grey, locally red to brown in colour. It is characterized by a scoured basal surface with local relief of up to 2.5 cm. Small-scale lenticular laminations of lighter coloured, coarse-grained siltstone and fine-grained sandstone occur throughout the facies.

Rarely, dark-grey shale with vertical-subvertical burrows and some bioturbation is present within the upper portion. The burrows are dispersed, and increase slightly in abundance upward through the facies. Most of the vertical and horizontal-subhorizontal burrows occur within the silty shale units of this facies (*e.g.* 1527 m in type well H4-NC115) (**Fig. 2.34**).

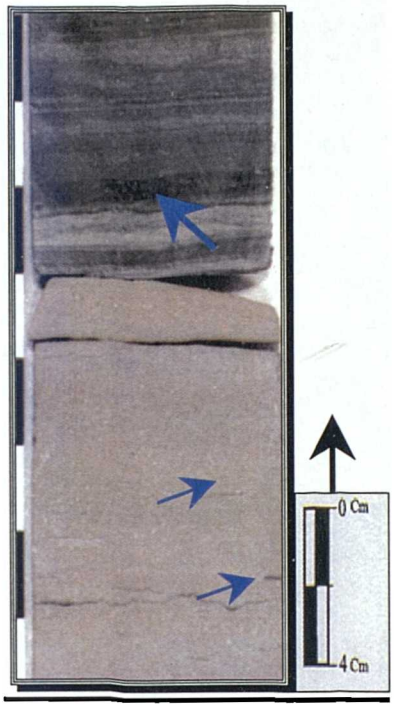

Fig. 2.34 Slabbed core sample from well H4-NC115, at 1527 m, showing the silty-shale bed present in the upper portion (large arrow), with local horizontal-subhorizontal burrows (small arrow).

The thickness of the sandstone beds is usually less than 10 cm thick, and shows, small-scale trough cross-beds and ripple marks (*e.g.* 1521 m in type well H4-NC115) **(Fig. 2.35B)**. Locally the sandstone contains soft sediment deformation structures, and occasionally vertical burrows and bioturbated. The facies C5 also contains very rare trace fossils (*e.g.* 1525 m, in type well A8-NC115) **(Fig. 2.35A)**.

This facies contains ripple cross-laminated **(Fig. 2.36A)** and rarely convolute lamination, particularly in the A-Field, where lenticular bodies of very-coarse grained sandstone are also present locally (*e.g.* 1507 m in type well A8-NC115). In contrast, trace fossils are locally present within the clean and thick sandstone beds.

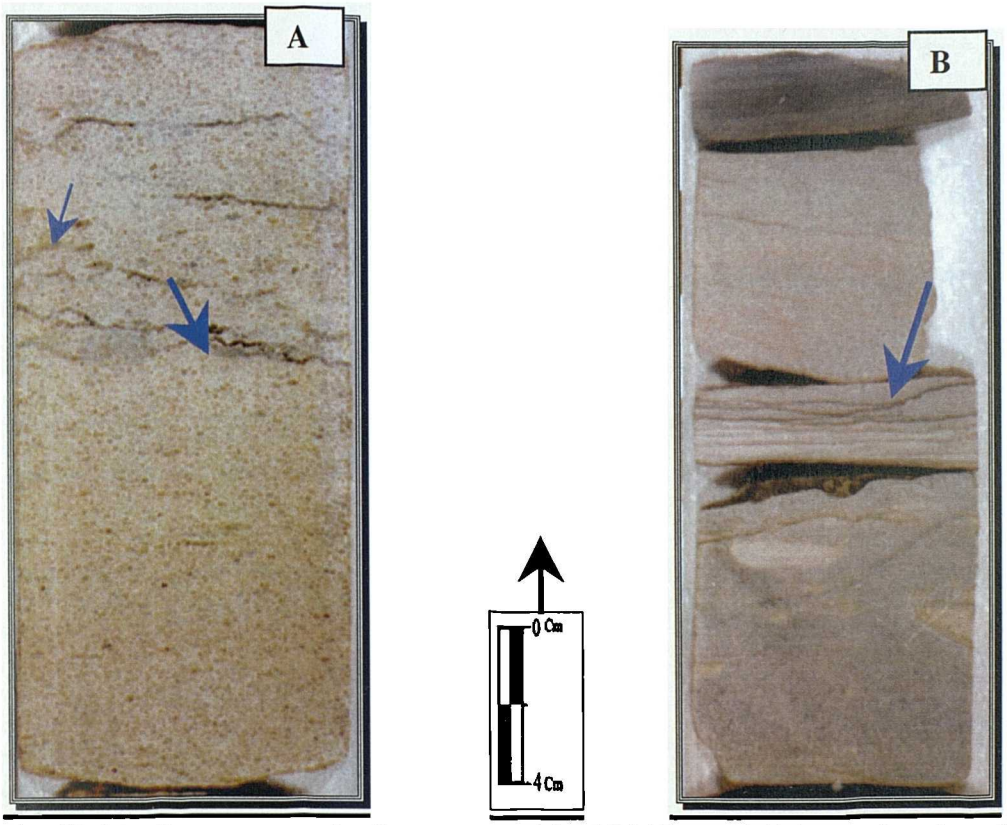

Fig. 2.35 A) Slabbed core sample from well A8-NC115, at 1525 m, showing the heterolithic facies. Note the horizontal burrow in the upper portion (small arrow) and some bioturbation (large arrow) in the middle portion of this facies. B) Slabbed core sample from well H4-NC115, at 1521 m, showing the sedimentary structures including small-scale trough cross-beds and ripple forms (large arrow).

Furthermore, subvertical burrows (*e.g. Skolithos* and *Cruziana*) have a complex to simple structure, and are filled with sand, silt and mud. These burrows are confined to the upper portion of the facies. (*e.g.* 1524 m, in type well H4-NC115) **(Fig. 2.36B)**. The effects of biogenic reworking can be seen in the light grey coloured mottling of the sand and the presence of medium quartz grains. Bioturbation has destroyed most of the primary sedimentary structures.

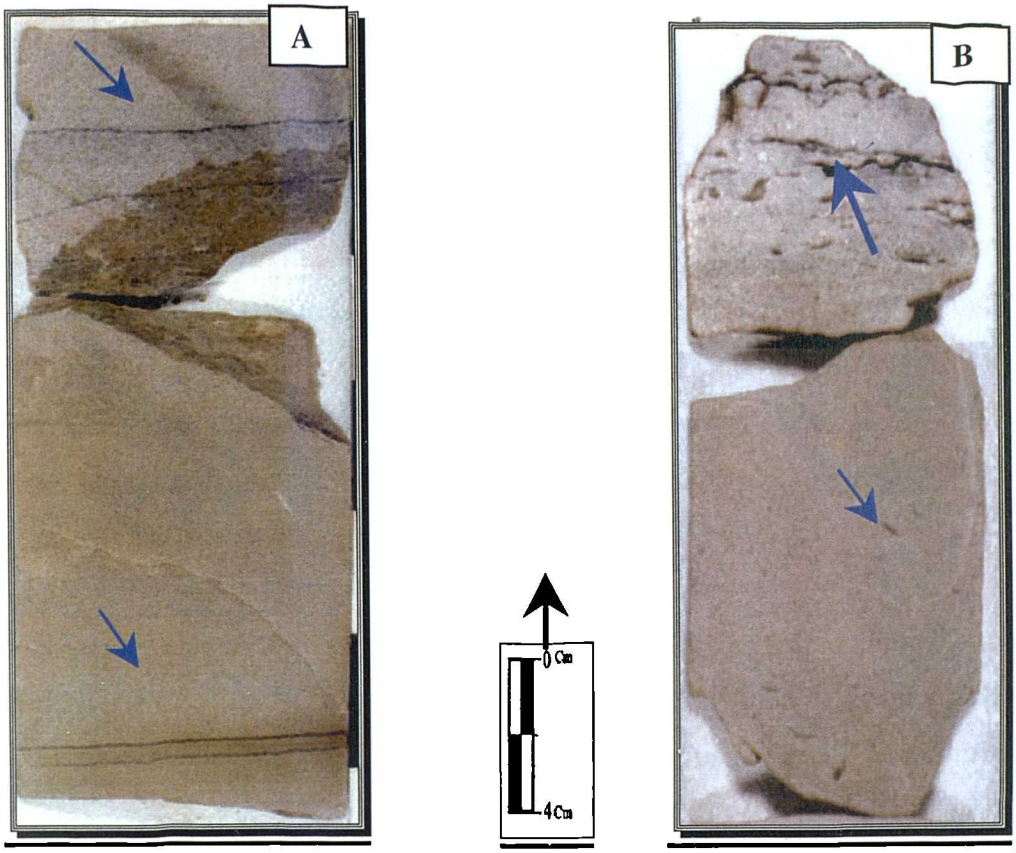

Fig. 2.36 A) Slabbed core sample from well A8-NC115, at 1507 m, showing the ripple laminated sandstone (arrows). B) Slabbed core sample from well H4-NC115, at 1524 m, showing the bioturbated sandstone within the upper portion (large arrows) with subvertical burrows (small arrow).

Interpretation

This facies consists of varicoloured heterolithic sediments, and contains bioturbation and trace fossils characteristic of an open-marine environment and alternating energy conditions (Howard and Reineck, 1981; Frey and Pemberton, 1984). The sediment texture, however, is largely a result of burrowing activity and the silty shale and mudstone imply an offshore shelf environment (Galloway and Hobday, 1983). In facies C5 the intensity of bioturbation has caused mixing of the lithologies, especially in the silty-shale beds. Burrowing organisms cause varying degrees of bioturbation, which in extreme instances, can thoroughly homogenise the sediments (Ekdale *et al.*, 1984; Frey and Pemberton, 1984).

2.3.3.6 Facies (C6): Claystone

Description

This facies is dominantly present in the lowermost part of the Mamuniyat Formation, throughout the El-Sharara Field (**Table 2.3**). It has been found in all the type wells of the study area within NC115 Concession. It is represented by the cored interval from 1527 m to 1542 m in type well A8-NC115, the cored interval from 1525 m to 1528 m in type well B2-NC115 and the cored interval from 1527 m to 1529 m in type well H4-NC115 (**Figs. 2.2, 2.3 and 2.4**).

In general the beds of this facies are more laterally persistent than facies C1 within the uppermost part of the Lower Mamuniyat Formation (M3), and can usually be traced for at least 50 km, within NC115 Concession. This facies is about 15 m, 3 m and 2 m thick within A8, B2 and H4-NC115 respectively, and it is gradational with the heterolithic facies C5. The entire facies is characterized by different colours, ranging from yellow and dark grey to black. A dark reddish brown ironstone bed is prominent at the top and along the base of the facies (*e.g.* 1527 m in type well H4-NC115).

This claystone facies is mainly represented by clay, which makes up over 90% of its composition, interbedded with lesser amounts of very fine-grained argillaceous sandstones and coarse-grained siltstones interbedded with very thin, 1 mm to 5 mm thick, fine-grained sandstone laminae. The fine-grained sandstone is well sorted, and planar laminated. The siltstone shows well-preserved small-scale ripple profiles (*e.g.* 1528 m in type well H4-NC115) (**Fig. 2.37B**).

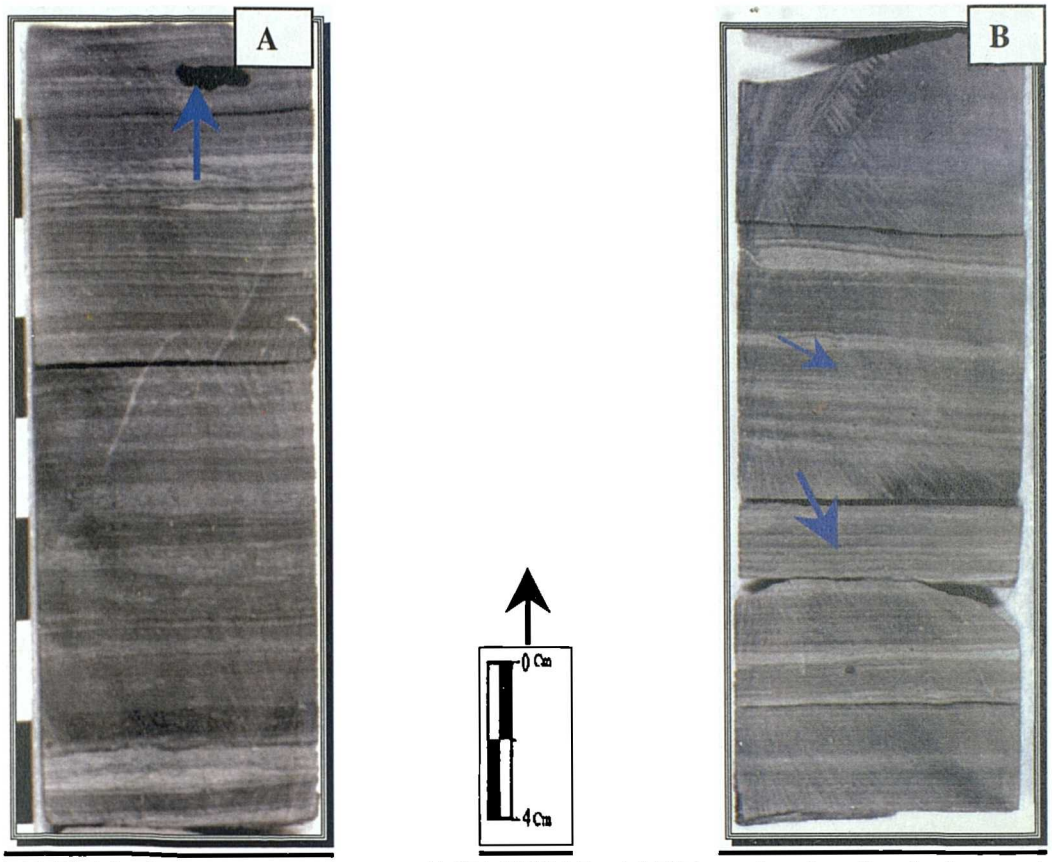

Fig. 2.37 A) Slabbed core sample from well H4-NC115, at 1527 m, showing the dark grey to black, parallel lamination of the claystone facies and organic fragments (arrow). B) Slabbed core sample from well H4-NC115, at 1528 m, showing the parallel lamination (small arrow) and micro wavy bedding of claystone (large arrow).

This unit exhibits soft-sediment deformation structures. Bioturbation is locally present in the middle portion of this facies and decreases upward concomitant with increased parallel lamination. Rare bioturbation (burrow forms are not identifiable) has been found in the lower portion of the facies where it partly obliterates primary lamination in the middle portion of claystone facies.

Other organic fragments are also locally present within the claystone facies C6 (*e.g.* 1527 m in type well H4-NC115) (**Fig. 2.37A**). Some isolated fine lenses of black organic matter up to 3 cm long are occasionally present. Several 1 cm to 2 cm thick beds of organic-rich, laminated black shale occur within the claystone facies in the study area, and can be traced laterally over a large area of the A, B and H-Fields.

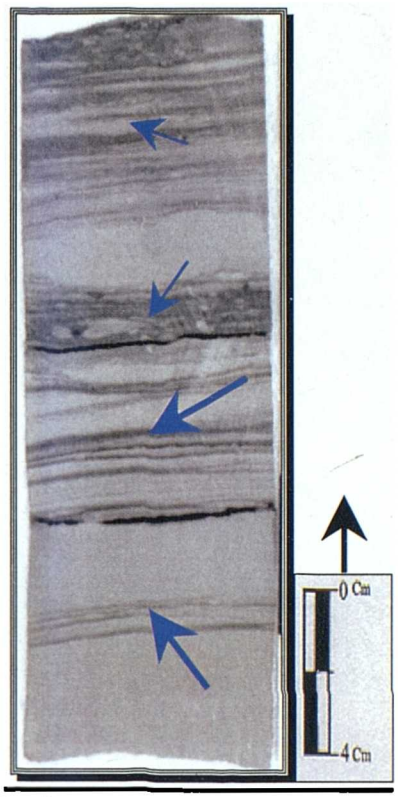

Fig. 2.38 Slabbed core sample from well H4-NC115, at 1526 m, showing the varying amounts of silt and clay (small arrow), with ripple cross-lamination and low angle cross-stratification (large arrow).

This facies is also characterised by the presence of randomly distributed shale and sand laminae, which range from 0.5 cm to 2 cm thick. In addition, in the first 3 m of this facies, there are intercalated layers of sandstone, 10 to 20 cm thick, with horizontal lamination or ripple cross-lamination, and low angle cross-stratification (*e.g.* 1526 m in type well H4-NC115) **(Fig. 2.38)**.

Interpretation

The facies, in the lowermost part of the Lower Mamuniyat Formation is dominated by claystone with subordinate and lesser argillaceous sandstones and non-calcareous siltstones. It is interpreted to have been deposited under low energy conditions in an open-marine environment.

The dominance of shale and thinner siltstone and sandstone indicate a shelf receiving mainly fine-grained detritus (Turner, 1980). Deposition is believed to have taken place below storm wave base on this shelf (Reineck and Singh, 1972). Parallel lamination and low-angle cross-stratification are interpreted to represent the deposition by storm events below fair-weather base (Harms *et al.*, 1975; Hamblin and Walker, 1979; Dott and Bourgeois, 1982). Some sandstones lack structure either due to small contrasts in mean grain-size of the adjacent laminae or rapid deposition. The thick shale bed within the facies from well A8-NC115 may have formed during a minor transgression and increased water depths (De Raaf *et al.*, 1965; Hein *et al.*, 1991).

The rare bioturbation and lack of body fossils imply an oxygen-deficient environment, unsuitable for supporting an extensive benthic fauna. Black claystone facies are characterized by variation in the oxygen conditions under which they accumulated. Nevertheless, the presence of these rare bioturbated sandstones may represent variable storm-influenced low energy conditions. The dark-grey to black colour of the claystone facies possibly represents the high content of very fine carbonaceous detritus, whereas the presence of horizontal laminae indicates deposition mainly from suspension under low-energy conditions. Mud and silt were probably washed onto the shelf by rivers, especially during flood events, and by shelf storm events.

The claystone facies shows subtle changes in colour from darker shale to lighter sandstone/siltstone indicating periodic changes in sedimentation rate from relatively slow to fast. The sand laminae and lenses probably record storm events on the shelf throwing sediment into suspension, followed by traction currents and the development of small ripple bedforms, subsequently preserved by fine suspension deposits (Reineck and Singh 1972). The facies is locally reddish brown in colour due to the presence of iron minerals within the sediment. Locally developed ironstone, however, typically accumulates in a marine or near marginal setting (Buchheim *et al.*, 2000). Furthermore, the laminae commonly have sharp bases and locally diffuse tops, features characteristic of shelf storm deposits (Figueiredo *et al.*, 1982).

2.4 Summary

Facies analysis of the Mamuniyat Formation is consistent with braided alluvial plain, marginal-marine and shallow-marine depositional models. Repetition of fluvial and marine facies is attributed to interaction of the fluvial and marine environments a cross a NW-SE coastline with episodes of progradation interspersed with transgression. The Mamuniyat Formation shows a general coarsening-upward trend as a result of seaward progradation and basinward-thinning (clastic wedge) to the northeast accompanied by a change from fluvio-continental to marginal marine and marine-neritic environments. The Mamuniyat sandstones were derived from a nearby tectonically active granitic basement source terrain, which was most probably the uplifted Ghat/Tikiumit basement Arch, which is only 150 km to the southwest of the Concession area NC115.

The Mamuniyat Formation is Ashgillian in age. It was deposited during the **Upper Ordovician Glaciation**, which covered large parts of Africa, including most of Libya. Evidence of this glaciation is seen in other Palaeozoic basins in Libya, but not in this part of the Murzuq Basin, because the ice was sourced from the southwest, and the study area was probably protected from the ice by the topographic high of the Ghat/Tikiumit Arch. This is discussed further in chapter seven.

CHAPTER 3

PETROLOGY AND DIAGENESIS

PETROLOGY AND DIAGENESIS

3.1 Introduction

3.1.1 Objectives

The main objectives of the petrographic study are to determine the mineral composition, maturity, sorting, grain roundness and porosity characteristics of the Mamuniyat Formation Sandstones throughout A, B and H-Fields of the El-Sharara Field, NC115 Concession, in order to:

1) Assess the spatial and temporal variations in mineral composition;
2) Classify the sandstones, using the scheme of Pettijohn *et al.* (1987);
3) Reconstruct the diagenetic history;
4) Determine source rock provenance and composition;
5) Assist interpretation of the sedimentary facies and depositional environment;
6) Evaluate the reservoir sequence and hydrocarbon potential of the Mamuniyat Formation; and
7) Examine the local and regional plate-tectonic setting of the Mamuniyat Formation and the Murzuq Basin.

3.1.2 Methods

This study is based on a total of 105 thin sections, collected from four wells in each of the three fields A, B and H. The number of thin sections per field is as follows: 40 from field A (**Fig. 3.1**); 30 from field B (**Fig. 3.2**); and 35 from field H (**Fig. 3.3**). The thin sections have been impregnated with blue resin in order to more accurately assess porosity, a technique that is particularly useful for sediments having more than 10% porosity. Impregnation was carried out according to the technique described by El-Hinnawi (1966).

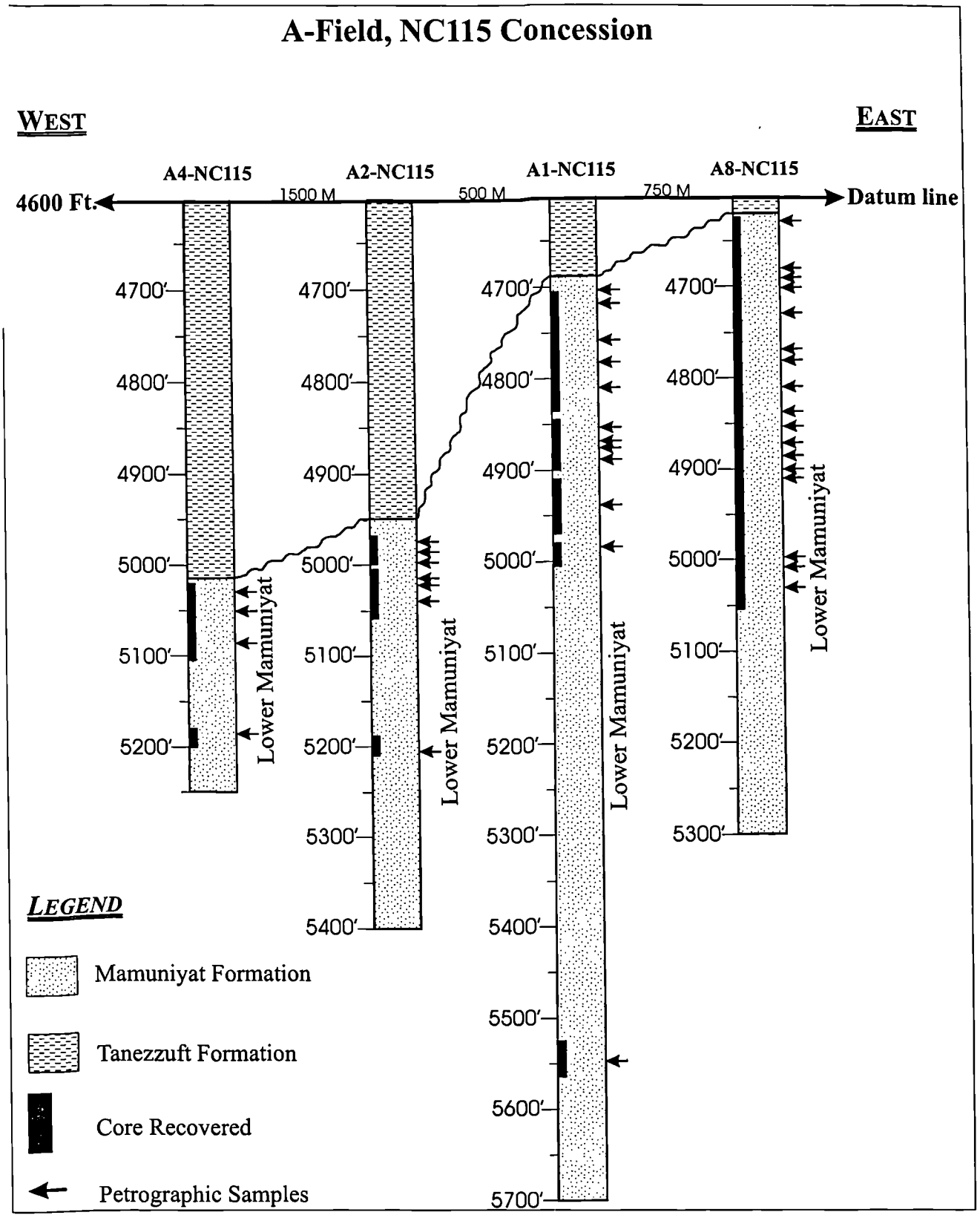

Fig. 3.1 Core coverage and location of petrographic samples from the Mamuniyat Formation in the four wells within the A-Field used in the study.

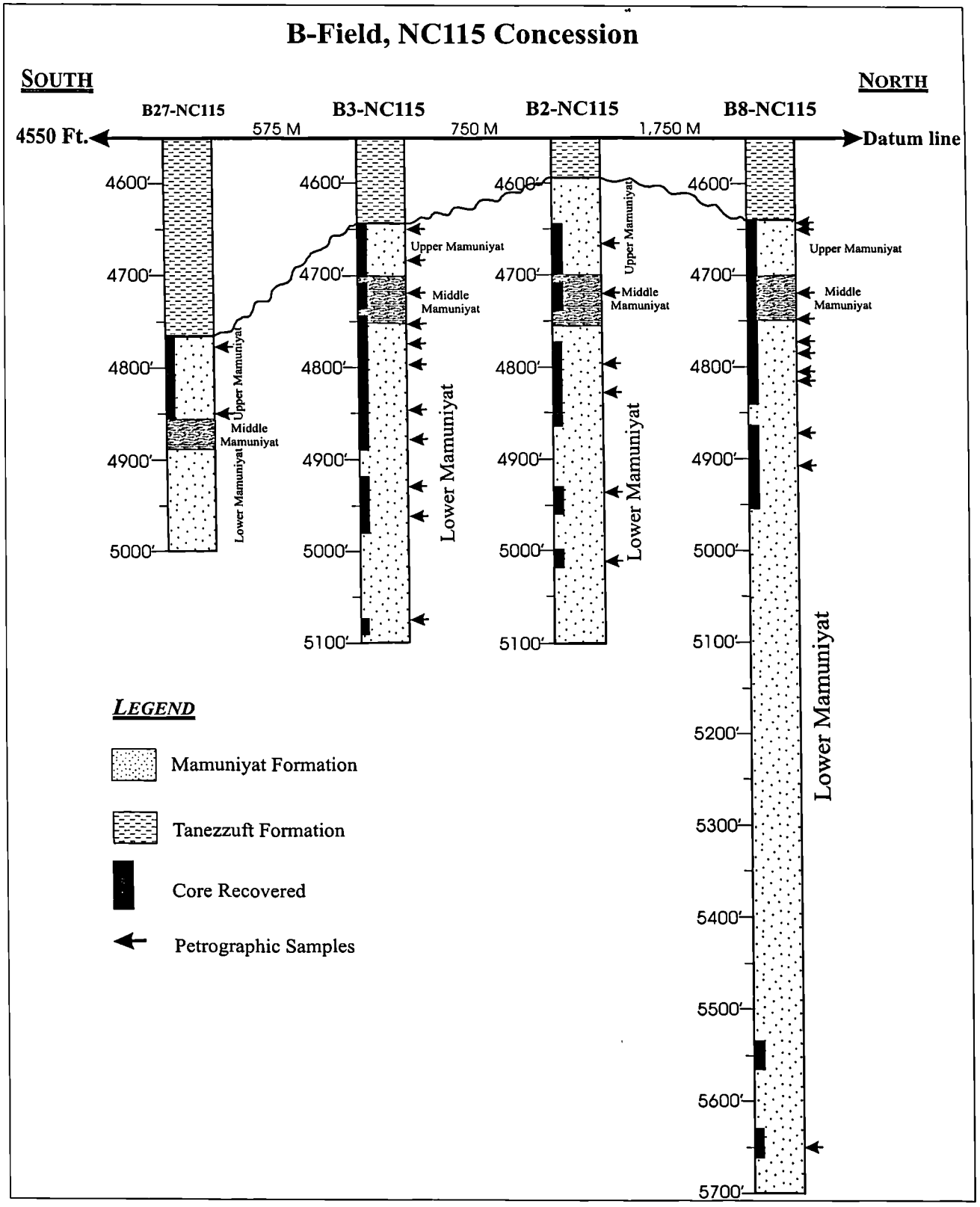

Fig. 3.2 Core coverage and location of petrographic samples from the Mamuniyat Formation in the four wells within the B-Field used in the study.

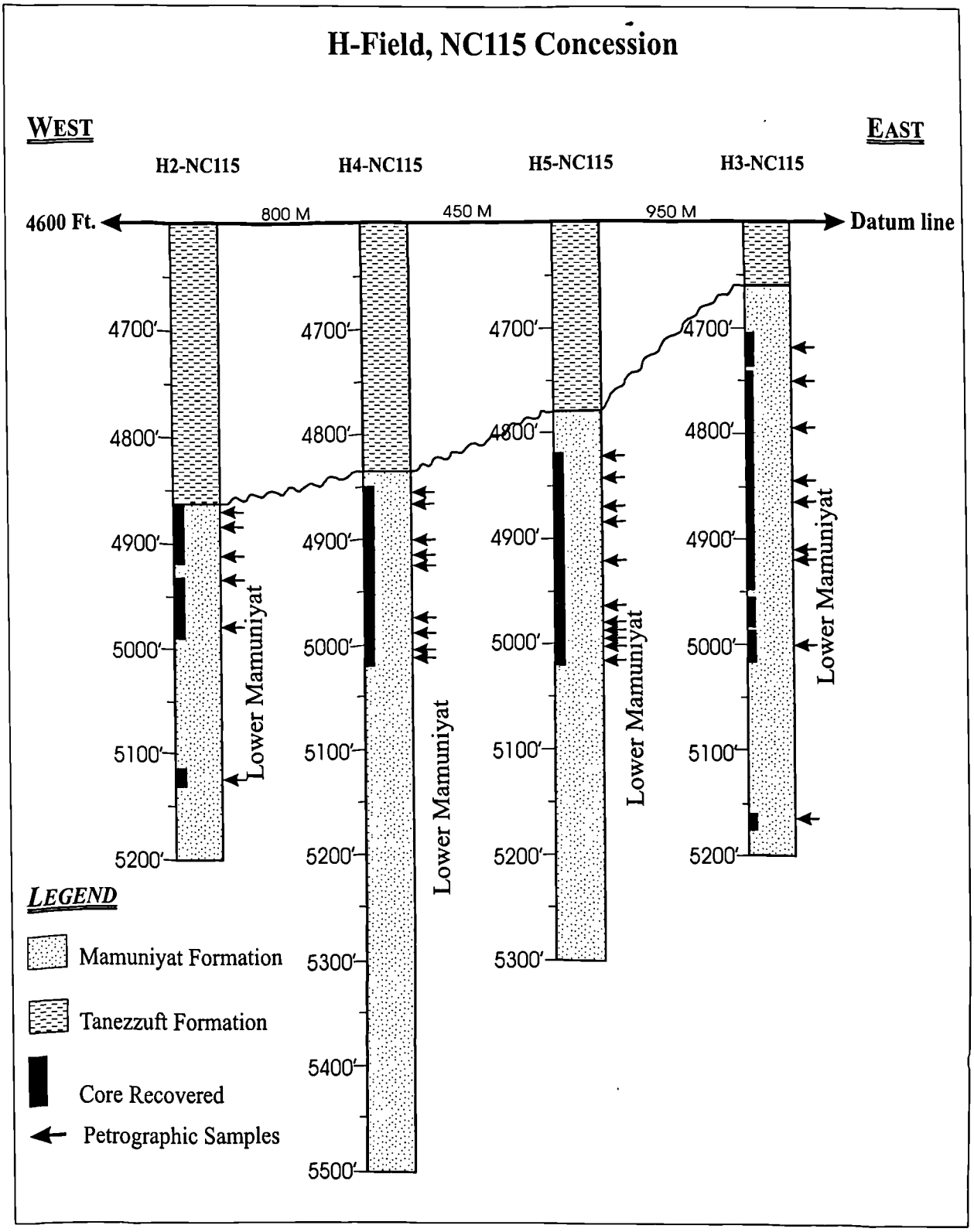

Fig. 3.3 Core coverage and location of petrographic samples from the Mamuniyat Formation in the four wells within the H-Field used in the study.

In the Mamuniyat Formation, each thin section was analysed according to standard modal analysis techniques in order to determine the percentage of the following minerals: quartz, rock fragments, feldspar, heavy minerals, mica, chert, dolomite, kaolinite, illite, chlorite, pyrite, matrix and bitumen. Grain-size was determined in thin section by using a micrometer eyepiece to measure the long axis of 150 quartz grains per slide throughout the A (**Fig. 3.4**), B (**Fig. 3.5**) and H-Fields (**Fig. 3.6**). These same thin sections were used to determine grain roundness and sorting within the Mamuniyat sandstones (**Tables 3.1, 3.2 and 3.3**).

Porosity measurement was estimated by standard modal analysis techniques, and the types of porosity in the Mamuniyat Formation were classified into three types for counting purposes: primary porosity, secondary dissolution porosity and microporosity. Additional information has been derived from the following wireline logs: BHC (Borehole Compensated Sonic), CNL (Compensated Neutron Log), GR (Gamma Ray), FDC (Formation Density) and SP (Spontaneous Potential Log). Colour photographs of the slabbed core have been used to assist in interpretation of the facies and depositional environments.

3.2 Compositional analysis

Detrital components for modal analyses were classified into monocrystalline quartz (Q), feldspar (F) and rock fragment (RF) (including detrital polycrystalline quartz grains). The omission of cement and matrix material from this classification removes the effects of diagenesis that may mask the maturity. The mineral composition of the Mamuniyat sandstone provides evidence of the composition of the source rocks and the diagenetic events that have affected the post-depositional burial history of the sandstone.

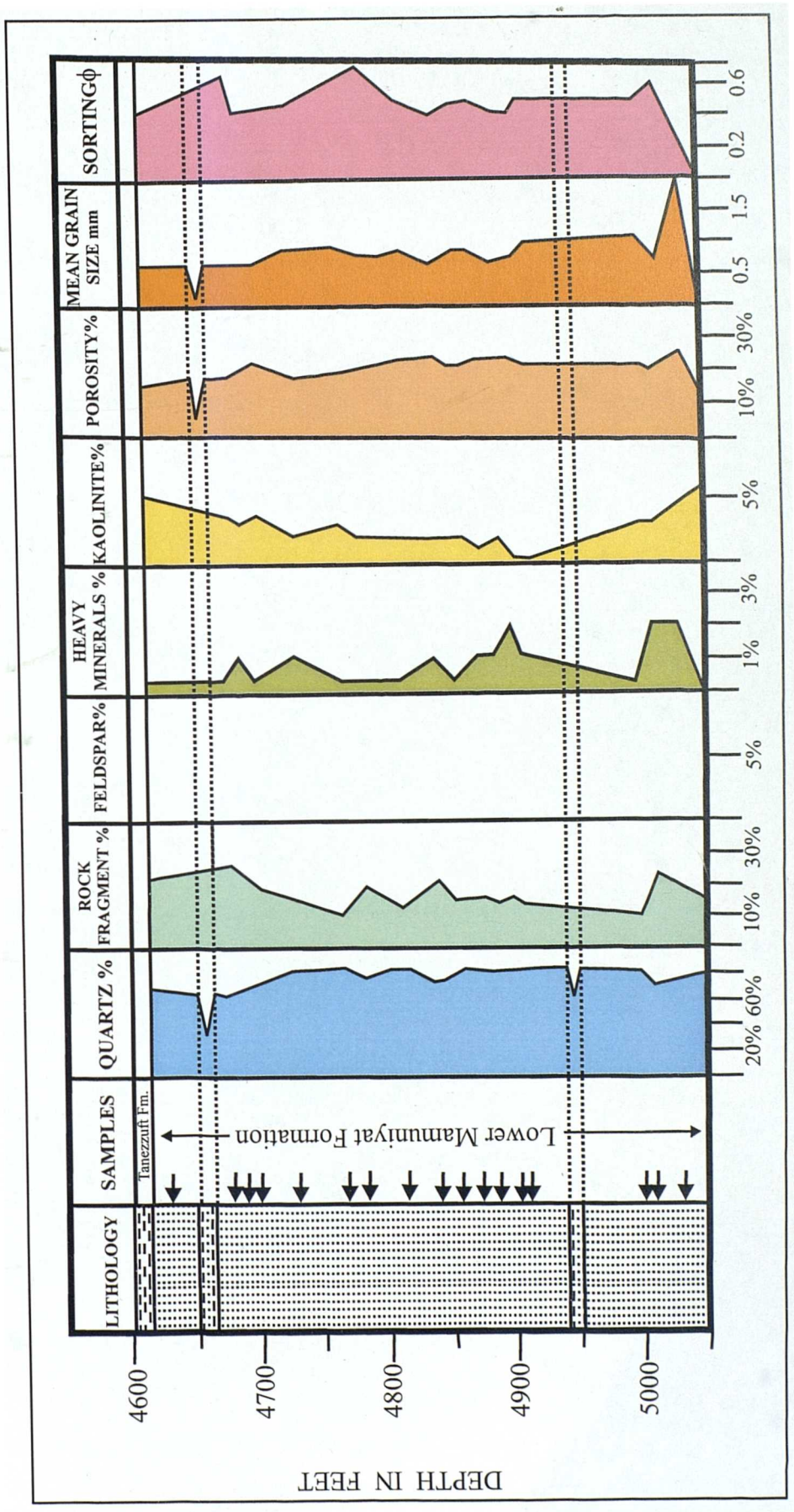

Fig. 3.4 Petrographic characteristics of the Mamuniyat Formation throughout A-Field, well A8-NC115, showing the sample points (arrows), quartz, rock fragment, feldspar content, heavy minerals, kaolinite clay, porosity, mean grain size (mm) and sorting.

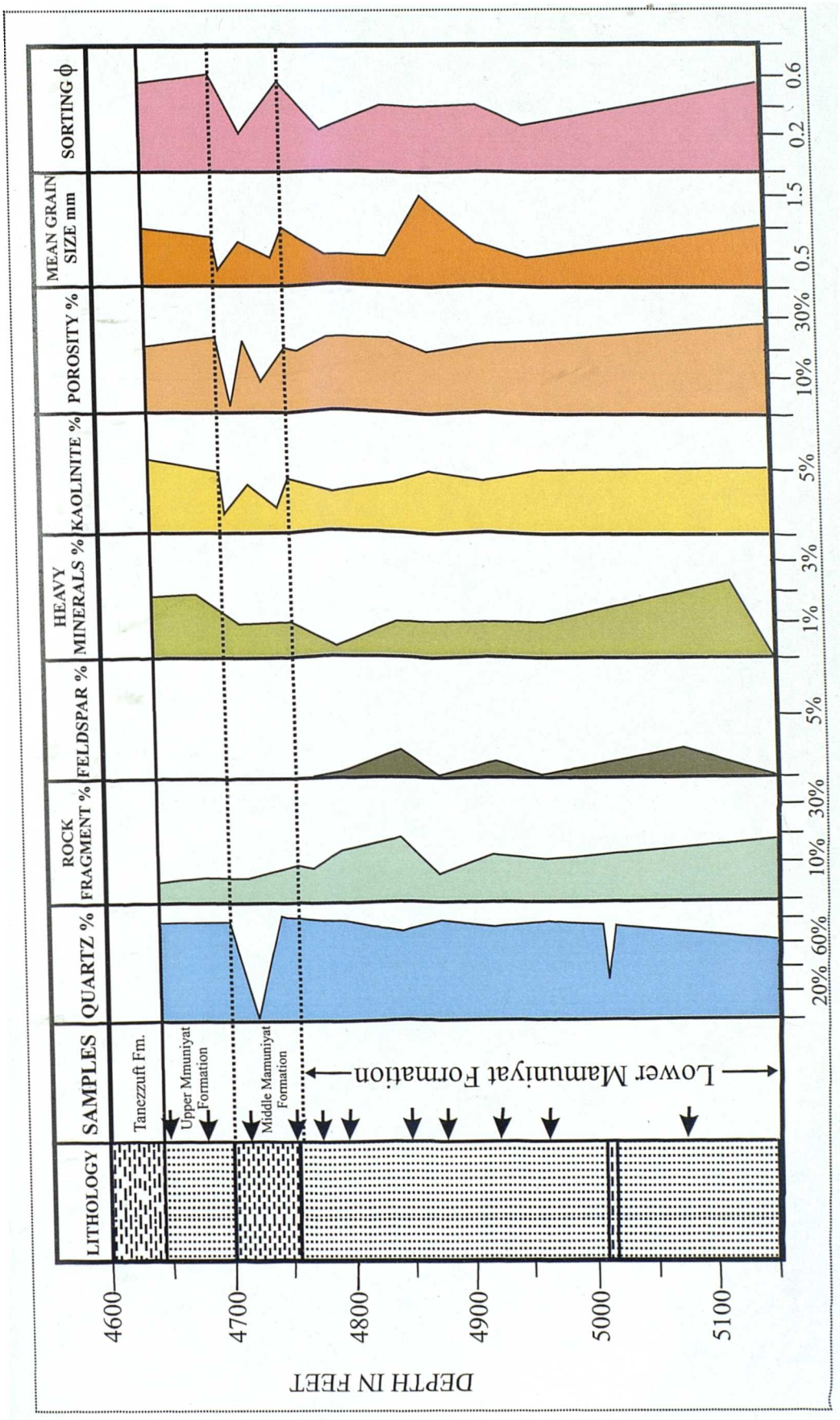

Fig. 3.5 Petrographic characteristics of the Mamuniyat Formation throughout B-Field, well B3-NC115, showing the sample points (arrows), quartz, rock fragment, feldspar content, heavy minerals, kaolinite clay, porosity, mean size (mm) and sorting.

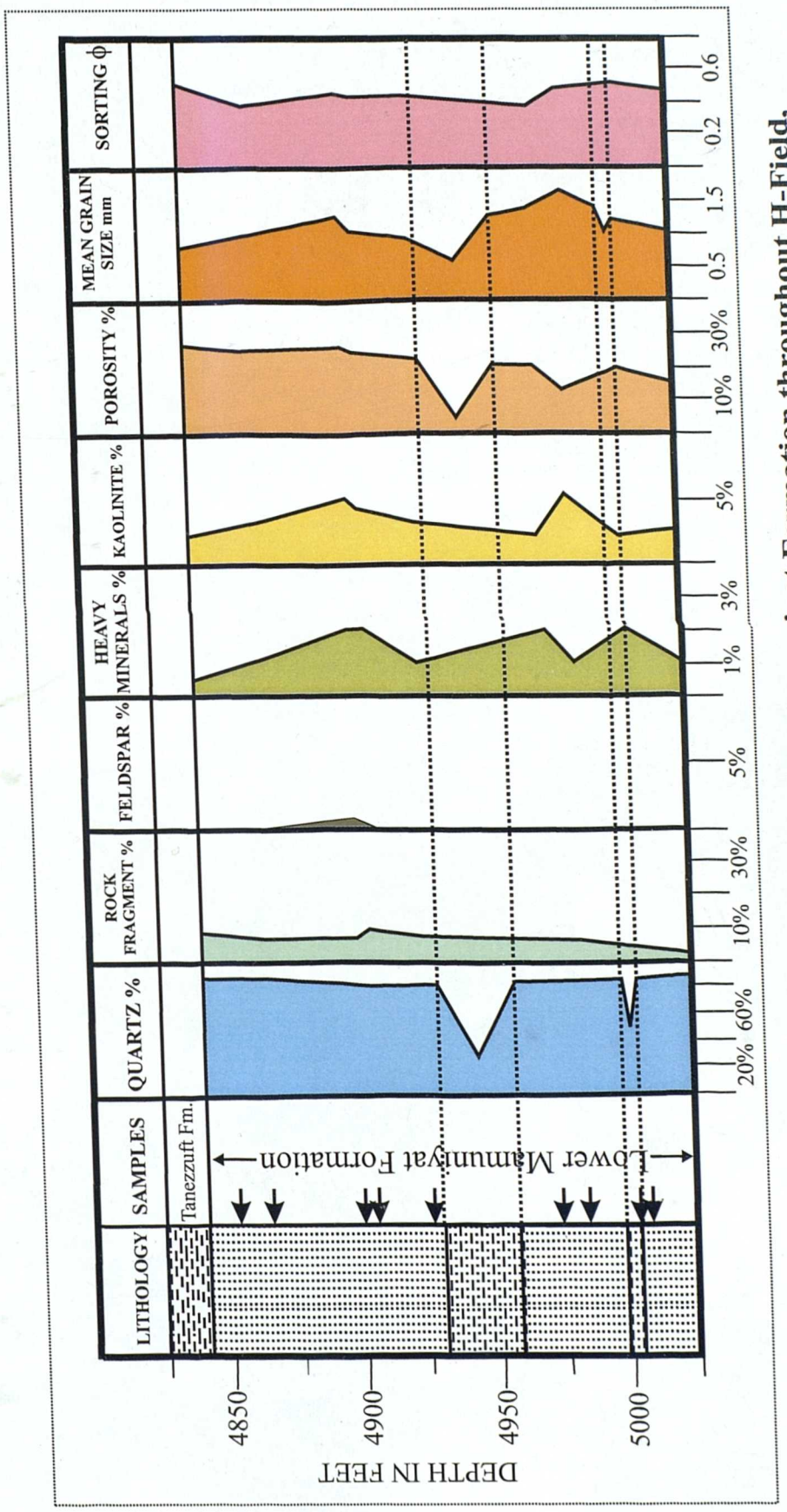

Fig. 3.6 Petrographic characteristics of the Mamuniyat Formation throughout H-Field, well H4-NC115, showing the sample points (arrows), quartz, rock fragment, feldspar content, heavy minerals, kaolinite clay, porosity, mean size (mm) and sorting.

The modal analysis was carried out using a Swift automatic point counter and mechanical stage. Approximately 300 grains were counted per slide, which were then recalculated to 100%. In comparing different sandstones, samples of a similar grain-size have been used,

3.2.1 Quartz

Quartz grains are the most common detrital constituents of most sandstone, making up between 65% and 95% of the detrital mineral composition (Blatt, 1982). This reflects its mechanical and chemical stability under a wide range of sedimentary conditions. Because quartz occurs in so many igneous and metamorphic rocks, attempts have been made to use it for source rock determination. The undulatory extinction of quartz grains appears as an irregular darkening of the crystal in thin section when rotated between crossed nicols. This results from distortion of the internal crystal lattice structure (Adams *et al.*, 1984). However, it has been demonstrated that quartz grains showing slight undulose extinction can be derived from most types of source terrains. The importance of undulatory extinction and the polycrystallinity of detrital quartz grains in provenance studies has been investigated by Blatt and Christie (1963).

Quartz is commonly divided into monocrystalline and polycrystalline types. Monocrystalline quartz refers to grains consisting of a single crystal and polycrystalline quartz refers to grains containing several crystals. The optical characteristics of mono - and polycrystalline quartz, together with the nature of their inclusions, their shape and grain boundaries are important in provenance determination (Pettijohn *et al.*, 1987). However, the most important characteristics used for differentiating quartz varieties under the microscope are undulatory extinction (Mackie, 1896) and types of inclusion (Gilligan, 1920).

Basu *et al.* (1975) re-examined undulose and polycrystalline quartz varieties, and compared universal stage with flat stage identifications. They concluded that careful petrographic analysis with a flat stage makes it possible to discriminate between quartz derived from plutonic and low and high grade metamorphic sources. Thus, the study of quartz varieties remains an important tool in provenance analysis, with the ratio of polycrystalline to monocrystalline quartz probably being the most important distinguishing parameter, followed by the ratio of undulatory to nonundulose grains and grain shape. Thus, quartz varieties can be useful in defining petrographic provinces (Pettijohn *et al.*, 1987).

The amount of stage rotation required for the entire crystal to pass from the greyish-white maximum birefringence colour of quartz to the extinction position depends on both the degree to which the crystal has been plastically deformed and the angular relationship between the c-axis of the crystal and the plane of the thin section (Blatt, 1982). In polycrystalline grains the individual grains are stretched and grain boundaries are sutured and show strong undulatory extinction. The sutures are believed to have formed by "static annealing", and the grains are highly strained (Voll, 1960). These grains are called sheared quartz or stretched metamorphic quartz.

In NC115 Concession, the Mamuniyat sandstones are composed mainly quartz grains, dominated by monocrystalline grains **(Plate 3.1A)** with subordinate amounts of polycrystalline grains **(Plate 3.1B)**. Quartz grains in the A-Field make up between 70% to 80% of the detrital components, in the B-Field they make up between 75% to 85% and in the H-Field they make up between 80% to 90%. The boundary between quartz grains under the microscope in the Mamuniyat sandstones is commonly straight in monocrystalline grains, which show straight to slightly undulose extinction. In the Mamuniyat sandstones undulatory quartz grains are very important. Approximately 10% quartz grains in the Mamuniyat sandstones show strong undulatory extinction on rotation of the stage by > 10° (Basu *et al.*, 1975). These strongly undulose quartz grains are more abundant in strained source rocks, especially metamorphic rocks.

In the Mamuniyat sandstone within A, B and H-Fields, the quartz overgrowths were recognised in thin section, either by dust rims between detrital grains and the overgrowth, or by the development of excellent rhombohedral crystal terminations growing into pore space. The quartz overgrowth cements in the Mamuniyat sandstones are easy to see **(Plate 3.2A)**. The contact types in the Mamuniyat sandstones are related to both particle shape and packing, and the packing depends on the spatial density of particles in a sediment accumulation. Most monocrystalline quartz grains have concavo-convex contacts, suggesting that these grains have undergone considerable compaction during burial. Very rare point contacts occur between monocrystalline quartz grains, with the contacts between polycrystalline grains being sutured contacts. The relative abundance of these various types of contact can be used as a rough measure of the degree of compaction and packing, and thus the depth of burial of the sandstone.

Moreover, in the Mamuniyat sandstones sedimentary quartz grains are not common within El-Sharara Field, but sedimentary chert grains occur which are subrounded to rounded, and which have a mean grain-size ranging between 0.13 mm and 0.5 mm (Schneiderohn, 1954). The detrital chert grains in the Mamuniyat Formation are seen as speckled grains composed of microcrystalline quartz grain **(Plate 3.6A)**.

In the Mamuniyat sandstones igneous quartz grains are uncommon throughout NC115 Concession, and only a few percent of quartz grains extinguish completely under crossed polars with less than 1° of stage rotation; an important indicator of quartz derived from igneous source rocks (Blatt and Christie, 1963). Metamorphic quartz grains are generally composite or polycrystalline quartz grains, and throughout the Mamuniyat Formation **(Plate 3.1B)**, they are characterized by relatively straight boundaries between equant grains, and straight to slightly undulose extinction (Krynine, 1940).

3.2.2 Feldspar

Feldspar minerals make up between 10% to 20% of the framework grains of the average sandstone, except in arkoses where it exceeds 25% (Pettijohn *et al.*, 1987). Feldspars are the second most abundant mineral in most sandstone, although their mechanical stability is less than quartz, because they are softer and strongly cleaved (Boggs, 1995). The alteration of feldspar has been considered to reflect climatic conditions prevailing at the time at the depositional site. Feldspar occurs in nearly all types of crystalline rocks, so that feldspar grains of sand-size can be derived from granitoid igneous rocks, gneisses and schists in large amounts. The percentage and type of feldspar in sandstone depends on the rate and type of tectonic activity, and on climate.

Feldspar is the second most important mineral in the Mamuniyat Formation, although it varies considerably in abundance throughout A, B and H-Fields. It is completely absent in A-Field and the amount of feldspar in B and H-Fields ranges from trace amounts to > 2%. (**Figs 3.4, 3.5 and 3.6**). The complex nature of feldspar minerals has resulted in their being subdivided into two categories on the basis of their chemical, physical and structural characteristics (Blatt, 1982): potash feldspars (Fk) and plagioclase feldspars (Fp) (Tucker, 1991). Both types occur in the Mamuniyat Formation sandstones.

1) Potash feldspar

This type of feldspar includes orthoclase, microcline and sanidine. These types are much more common in sandstones than plagioclase feldspar because potash feldspar has a greater chemical stability than plagioclase, and so the latter is preferentially altered in the source area. Although potash feldspars are generally considered to be more abundant in sedimentary rocks than plagioclase feldspars, the latter is more abundant in sandstones derived from plagioclase-rich volcanic rocks (Boggs, 1995).

Orthoclase grains are commonly untwinned or may show Carlsbad twinning. Refractive indices are below lakeside or quartz and their birefringence is less than that of quartz. They commonly show alteration to illite flakes, especially along cleavage planes (Blatt, 1982). Apart from optical tests orthoclase can usually be recognised by its dusty and partly altered appearance (to kaolinite or sericite), relative to the very clear and clean quartz grains. Because it may be difficult to distinguish orthoclase from quartz in sandstones it is often underestimated (Tucker, 1991).

Microcline is readily identified in thin section from its distinctive grid-iron (cross-hatch) twinning pattern formed by a combination of albite and periclinal twins. *Sanidine* is the same as orthoclase except that 2V is very small (Blatt, 1982). The perthites (a variety of feldspar consisting of intergrown orthoclase or microcline with albite) are conspicuous by the irregular blebs of plagioclase in the potash feldspar host. Perthites are generally a result of slow cooling, and therefore more typical of plutonic source rocks (Tucker, 1991). In the Mamuniyat Formation the most common type of feldspar is untwinned orthoclase characterized by low relief, cleavage, a biaxial optical figure with a moderate 2V, and evidence of partial to complete alteration of the grains. Moreover, in the upper part of the Mamuniyat sandstones, particularly in B-Field, coarse-grained sandstones generally contain more feldspar than fine-grained sandstones (Cadigan, 1961). This relationship could be simply a reflection of the difference in grain-size and not just the nature of the source rocks.

2) Plagioclase feldspar

Plagioclase feldspars are typically polysynthetically twinned (albite twinning). It is distributed throughout sandstones and commonly shows alteration to montmorillonite, especially along cleavage planes. Plagioclase may be concentrically compositionally zoned, reflecting changes in the albite and anorthite ratio (Blatt, 1982). The relative proportions of potassium and plagioclase feldspar may be controlled either by the relative abundance of those feldspars in the igneous and metamorphic source rock, or by differential stability in earth surface environments.

The anorthitic component of plagioclase is far less frequently encountered in continental source rocks than is the albitic component. This is a function of the relative abundance of intermediate and siliceous rocks at the surface of the continents (Pettijohn *et al.*, 1987).

Throughout the Mamuniyat sandstone, plagioclase feldspar is uncommon. It ranges from 1% to 2%, and the plagioclase is generally subordinate to microcline, particularly in the B-Field and a few wells in the H-Field. The plagioclase crystals are mostly lathe-shaped and twinned according to the albite or combined Carlsbad-albite law. The alteration of plagioclase is more common in the coarser grade sandstones and tends to take place initially along the borders of grains, which become frayed and corroded, or along twin planes.

3.2.3 Rock fragments

The composition of rock fragments depends basically on source rock geology and the durability of particles during transportation. In sandstones the fragments are commonly derived from fine-grained sedimentary and metasedimentary rocks, siliceous sedimentary rocks such as chert, and igneous rocks especially volcanic rocks (Tucker, 1982). Rock fragments make up between 15% to 20% of the detrital grains in the average sandstone (Boggs, 1995). The major types of rock fragment in sandstones are:

1) The argillaceous group, including shale, slate, phyllite, and schists;
2) Volcanic rocks including glass; and
3) The silica group consisting of quartz and chert.

The rock fragment content tends to be markedly size dependent, in that the proportion of such fragments increases with increasing size (Okada, 1966; Hunter, 1967). The abundance and type of rock fragment in ancient sands are much better known than in modern sands due primarily to the prevalence of thin-section analysis of sandstones.

Polycrystalline quartz grains composed entirely of quartz have been grouped with other quartz grains in many sandstone classifications. However, the nature of the quartz indicates a metamorphic origin and, in conjunction with other metamorphic rock fragments, it can be used to interpret source area composition. Rock fragments are relatively easy to identify, and they are more reliable indicators of source rocks types than individual minerals such as quartz or feldspar, which can be derived from different types of source rocks (Boggs, 1995). Several factors determine the rock fragment content: grain-size, provenance, maturity and age. In general, the rock fragment content is a function of grain-size as noted above, other things being equal (Shiki, 1959; Allen, 1962).

Rock fragments in the Mamuniyat Formation are uncommon, ranging from trace amounts up to 6% both in A, B and H-Fields **(Plate 3.4A)**. They consist of polycrystalline quartz rock fragments, with a few shale fragments. Most of the polycrystalline quartz grains in thin section are subrounded to rounded (**Tables 3.1, 3.2 and 3.3**).

3.2.4 Micas

The average abundance of coarse micas in siliciclastic sedimentary rocks is less than 0.5%, although some sandstone may contain 2% to 3%. Muscovite is chemically more stable than biotite and thus is commonly much more abundant in sandstones. Muscovite is commonly derived from igneous source rocks, and it is the most common mica seen in thin section. Micas are distinguished from other minerals by their platy or flaky habit (Tucker, 1991).

Mica is a minor constituent of the Mamuniyat Formation, with muscovite being the dominant type. It is easily identified by its platy nature and parallel extinction. It is colourless in plane-polarized light and shows bright second-order colours under crossed polars.

The distribution of muscovite in the Mamuniyat Formation ranges from trace amounts up to > 5% locally (**Tables 3.1, 3.2 and 3.3**). Detrital muscovite occurs as flakes between 0.15 mm and 0.55 mm long (**Plate 3.1A**). It is distinguished by its tabular appearance with individual crystals bent through compaction and deformation around quartz grains. The relatively high percent of muscovite in parts of the Mamuniyat Formation compared to the average sandstone, is probably a reflection of its higher resistance to chemical weathering than other mica types.

3.2.5 Clay minerals

Clay minerals make up only a small percentage (≤ 5%) of most sandstones, where they are present as part of the matrix. Because of their small size, clay minerals are compositionally diverse. They belong to the phyllosilicate mineral group, which is characterized by a two-dimensional layer structure arranged in indefinitely extending sheets (Boggs, 1995). Most clay minerals originate through subaerial weathering of silicate minerals. All of the major clay groups are found in weathered residues and soils. Exactly which clay occurs depends on the interaction of climate, geomorphology and parent rock. Humid climates and well-drained topographies lead to extensive weathering of feldspars and their silicates to kaolinite. Mafic silicates in many climates will weather to smectite, whilst illite forms mainly in intermediate to humid climates (Pettijohn *et al.*, 1987).

The clay minerals in the Mamuniyat sandstones are dominated by kaolinite, which is colourless in plane-polorized light, and grey-dark grey in cross-polarized light, with weak birefringence (**Plate 3.3B**). It partly fills both primary and secondary pore space (porosity shown with dark blue stained epoxy resin). Secondary porosity probably formed from feldspar crystals which were subsequently dissolved, leaving a residue of clays (Scholle, 1979). Clay minerals in sandstone are both detrital and authigenic, but the difference can rarely be identified with the petrological microscope. All the chief clay-mineral groups are represented in sandstones: kaolinite, illite, chlorite, smectites and mixed-layer clays. Detrital clays reflect the source-area geology, climate and weathering processes (Tucker, 1991).

Chlorite is common in sandstones. It may be either fresh or altered, and it can be readily identified under the microscope. Chlorite is characterized by its green colour, fair relief and weak birefringence. It is most readily recognised by its birefringence and morphology, but X-ray diffraction work is needed for detailed mineralogical studies (Scholle, 1979). In most sandstones chlorite is a minor constituent, except in some turbidite sandstones with strong volcanic rock components. Because of their thin sheet-like shape and consequent lower setting velocity, chlorite is associated with quartz grains of smaller sand or silt size (Doyle *et al.*, 1968, 1983). Other clay minerals present in the Mamuniyat Formation are illite and chlorite, which are present in amounts ranging from 2% to 3%. Illite can be identified by its needle-shaped crystals and strong birefringence. It is abundant in sedimentary rocks and is intermediate in composition between muscovite and montmorillonite.

Moreover, in the Mamuniyat Formation chlorite is precipitated in rare patches on detrital grains. All the chlorite comes largely from low-grade metamorphic rocks and the weathering and alteration of ferromagnesian minerals (**Tables 3.1, 3.2 and 3.3**).

3.2.6 Heavy minerals

Heavy minerals rarely make up more than 1% of a sediment or rock. In order to study them they must be separated out from loose sediment or disaggregated rocks and concentrated by liquids of high density such as bromoform (Leeder, 1982). Heavy minerals are divided into two common groups: non–opaque and opaque. The most common non-opaque heavy mineral grains include apatite, epidote, garnet, rutile, staurolite, tourmaline and zircon. Opaque heavy minerals include ilmenite and magnetite. They are chiefly silicates and oxides, many of which are very resistant to chemical weathering and mechanical abrasion (Tucker, 1991).

Heavy mineral suites usually contain both chemically stable and unstable minerals. Stable heavy minerals such as zircon and rutile can survive multiple recycling and are commonly rounded, indicating that the last source was sedimentary. Less stable minerals such as magnetite, pyroxene, and amphibole, are less likely to survive recycling.

Thus, heavy minerals are useful indicators of sediment source rocks because different types of source rocks yield different suites of heavy minerals. Heavy minerals are derived from a variety of igneous, metamorphic and sedimentary rocks (Boggs, 1995)

The study of heavy minerals can provide useful indications of provenance and tectonic events in the source area. Certain heavy minerals, such as garnet, epidote and staurolite are derived from metamorphic terrains, whereas others such as rutile, apatite and tourmaline indicate igneous source rocks. The specific gravity of heavy minerals is greater than 2.9, *i.e.*, higher than that of quartz and feldspar at 2.6. Heavy mineral can be dissolved out during diagenesis through intrastratal solution and because of this, older sandstones tend to have a less diverse heavy mineral suite. Although, heavy minerals can provide evidence as to the composition of the source rocks, they are affected by weathering, transportation, deposition and diagenesis (Morton, 1985).

Throughout the Mamuniyat Formation, two main types of non-opaque heavy minerals have been observed: zircon and tourmaline. Higher temperature and pressure in the burial diagenetic realm also cause heavy-mineral dissolution. The dissolution of grains with increasing depth is well documented by Milliken (1988) from Plio – Pleistocene sandstones in the Gulf Coast Region, USA. Special attention has been given to two of the commonest stable heavy minerals, zircon and tourmaline, in much the same way that quartz varieties have been studied in the hope of gaining greater effectiveness in provenance determination (Pettijohn *et al.*, 1987).

1) Zircon

Zircon is one of the most widely distributed accessory minerals in igneous rocks, and it also occurs in metamorphic rocks (Pettijohn *et al.*, 1987). Most zircon grains are colourless or occasionally pale-yellow. It is a ubiquitous component of sedimentary rocks, because of its great physical and chemical stability. Zircons in sedimentary rocks differ in composition and shape from those in igneous rocks. Shape and size are more important indicators of provenance than any other variables.

Tomita (1954) surveyed the literature on zircons and concluded that purple or rose-pink zircon comes only from Archean gneisses or granites; the colour was considered radiogenic, its depth or intensity increasing with age. Poldervaart (1956) studied zircons from sedimentary rocks in comparison with their distribution in igneous rocks and found that shape in relation to size may be a more important indication of provenance than another variables.

In the Mamuniyat Formation zircons are more abundant than any other heavy mineral, ranging from traces up to 3% (**Tables 3.1, 3.2 and 3.3**). They are resistant to mechanical and chemical weathering and usually occur as rounded detrital grains, commonly showing an abraded bipyramidal prismatic form. Moreover, zircon grain shape throughout the Mamuniyat Formation is mainly sub-rounded, indicating long distance of transport (**Plate 3.4B**).

2) Tourmaline

Tourmaline commonly occurs in granite pegmatites, or in granites which have undergone metasomatism by boron-bearing fluids. It also occurs in sediments adjacent to such granites, and as an accessory mineral in schists and gneisses. Although attempts have been made to use coloured varieties of tourmaline as an indication of provenance, there is no simple relationship between colour and composition or between composition and the type of igneous or metamorphic rock in which tourmaline is found (Pettijohn *et al.*, 1987). As shown by Potter and Pryor (1961), an occasional tourmaline grain may show a clearly defined rounded overgrowth.

Tourmaline throughout the Mamuniyat Formation occurs in trace amounts and it is characterized by colourless and pale green–olive green prismatic varieties with inclusions (**Plate 3.5A**). They are angular to poorly rounded prismatic crystals showing undulatory extinction and strong pleochroism.

3.2.7 Other constituents

1) Pyrite

Pyrite is distinguished from other opaque iron minerals by its yellowish colour in reflected light. Pyrite is present as disseminated grains and cubic crystals (Tucker, 1991). The pyrite crystals within the Mamuniyat Formation range in amounts from traces up to 1%. Although these grains are authigenic, rather than detrital, they show the typical yellow-gold metallic colour of pyrite **(Plate 3.5B)**. It is most common in marine sandstones, but it is only an accessory diagenetic mineral. Pyrite is commonly altered to goethite/limonite on surface weathering (Tucker, 1991).

2) Barite

Little is known of barite cement in sandstone, its geological distribution and the kinds of geochemical regimes in which it forms (Pettijohn *et al.*, 1987).

In the Mamuniyat sandstone barite is present as traces of a late crystallisation phase, that is thought to have occurred in connection with dewatering of the sandstones. It can also occur in association with the invasion of drilling mud solids, and is specially common in fluids expelled from coal-bearing shale-dominated sequences (Revelle and Emery, 1951).

3) Bitumen

Bitumens are solid substances occurring as seepages, surface accumulations and impregnations occupying the pore space of sandstones or other sedimentary rock, and in veins and dikes. They are black or dark brown and have a characteristic odour of pitch or paraffin (Boggs, 1995). Bitumen is black in plane polarized and cross polarized light and remains black/dark in reflected light. Bitumen can be seen filling primary and secondary pores, and coating detrital grains in many samples. In many of the samples, bitumen envelopes can be seen forming around detrital radioactive minerals such as zircon and pyrite.

Generally, the term bitumen is used for various solid and semi-solid hydrocarbons which are soluble in carbon disulphide, whether gases, easily mobile liquids, viscous liquids, or solids. The term is generally applied to any of the flammable viscid liquid, or solid hydrocarbon mixtures soluble in carbon disulphide (Krumbein and Pettijohn, 1938).

In the Mamuniyat sandstone solid bitumen envelopes can be seen coating detrital grains in many samples (**Plate 3.6B**). The solid bitumen content as recorded by thin section analysis varies from 0% up to 8%. The bulk of kaolinite clay present is completely enveloped by bitumen and in these cases occludes any microporosity that might have been associated with the kaolinite. Many samples above and below the perceived oil/water contact show bitumen emplacement. Bitumen commonly envelops pore-filling kaolinite clay. This would suggest that the majority of kaolinite in the Mamuniyat Formation had precipitated prior to bitumen emplacement and therefore provides an indication of the pore system at that time.

3.3 Classification

The status of sandstone classification has been reviewed by Klein (1963), McBride and Yeakel (1963) and Okada (1971), and most recently by Pettijohn, Potter and Siever (1987). The reader is directed to these works both for a historical review of the subject and for basic philosophies underlying sandstone classification and nomenclature. There are many sandstone classification schemes available but most use a triangular diagram with end members of Quartz (Q), Feldspar (F) and Rock fragments (RF).

The triangle is divided into various fields, and rocks with an appropriate modal analysis are given a particular name (Tucker, 1991). Basically there are many other kinds of particles which occur in sands and sandstone, but these are not considered essential in naming and classifying sandstones. Quartz occurs in several varieties, and feldspars and rock fragments are of various kinds. The matrix is the mud: fine-grained physically deposited material that occurs mostly as clay minerals and as quartz. Cement is the chemically precipitated filling of originally void spaces (Friedman and Sanders, 1978).

A widely used, simple classification of sandstones is presented by Pettijohn *et al.* (1987) based on the origin of the sandstone. Sandstones are divided into two major groups based on texture, that is, whether the sandstones are composed of grains only, the *arenites*, or whether they contain more than 15% matrix, forming the *wackes* (Tucker, 1991).

The sandstone of the Mamuniyat Formation can be classified according to Pettijohn *et al.* (1987) as mainly sublitharenite, with some quartz arenites and litharenites **(Fig. 3.7)**. Sublitharenites are perhaps the most abundant of all sandstones. These are quartz-rich, feldspar-poor, quartz-cemented sandstones. Rock particles from low-rank metamorphic and sedimentary sources are abundant (Pettijohn, 1975). Throughout the Mamuniyat sandstones the sublitharenites are characterised by their high quartz contents ranging between 80% to 90% (**Tables 3.1, 3.2 and 3.3**), dominated by monocrystalline quartz grains with subordinate amounts of polycrystalline quartz grains **(Plate 3.2B)**. They are well cemented with secondary quartz overgrowths. Although they are moderately well to well sorted, the grains are subrounded to rounded with a low sphericity. However, sublitharenites have high porosity values and the best reservoir potential.

Quartz arenites have 95% or more quartz grains, a rock–type referred to as orthoquartzites (quartzite is the low–grade metamorphic equivalent) (Tieje, 1921). They are commonly cemented by quartz deposited in optical continuity with detrital quartz. The quartz of the orthoquartzites is largely monocrystalline which display sharp rather than undulatory extinction (Blatt and Christie, 1963). The quartz grains are very well sorted and well rounded, and they are texturally and compositionally the most mature; polycrystalline grains are less stable and largely eliminated (Blatt, 1967). Quartz arenites are uncommon in the Mamuniyat sandstones **(Fig. 3.7)**, "except locally in the eastern part of H-Field, particularly H5–NC115" **(Table 3.3)**. These are characterised by a high quartz content of up to 95% or more, dominated by monocrystalline quartz grains with polycrystalline quartz grains locally abundant **(Plate 3.1B)**.

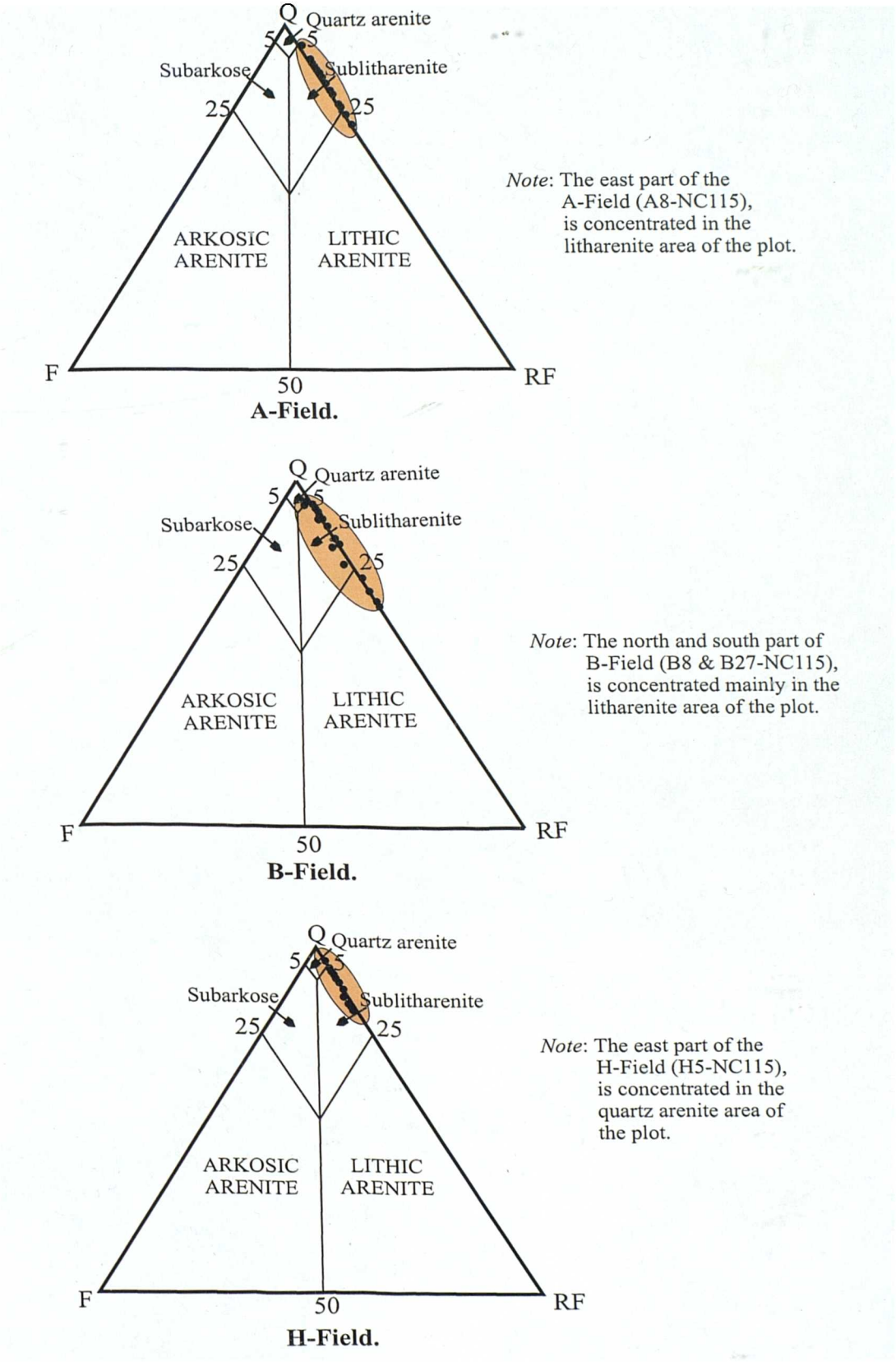

Fig. 3.7 Ternary QFRF plot showing the composition of thin sections from three oilfields, NC115 Concession. (Classification modified from Pettijohn *et al.*, 1987).

Note: Q = Quartz, RF = Rock fragment, and F = Feldspar.

They also contain more well–rounded and well–sorted grains, so that the textural maturity is also very high. Quartz overgrowths and calcite, usually in the form of poikilotopic calcite, are common cements (**Tables 3.1, 3.2 and 3.3**).

Litharenites are characterized by a rock fragment content in excess of feldspar (McBride and Yeakel, 1963). These are chiefly fragments of mud-rock and their low–grade metamorphic equivalents, and volcanic grains. Other components are flakes of mica, with some feldspar and abundant quartz. Litharenites account for 20% to 25% of all sandstones in the rock record.

They are uncommon in the Mamuniyat Formation (low abundance in some wells in A and B-Fields) (**Fig. 3.7**). They are dominated by polycrystalline quartz grains and rock fragments, and moderate porosity. However, they have little or no feldspar grains and they have a slightly coarser grain-size than the quartz arenites but with less quartz (ranging between 60% and 70%). The grains are mainly subrounded and well sorted. They contain up to 5% of kaolinite clay and minor amounts of other minerals such as mica (< 1%) and heavy minerals (< 4 %) (**Tables 3.1, 3.2 and 3.3**).

3.4 Provenance

Sandstone composition can be a useful indicator of the composition and tectonic setting of the source area (Swift *et al.*, 1991; Macdonald, 1993). With the exception of chert, nearly all silicate mineral grains in sandstones are derived ultimately from plutonic igneous rocks, gneisses, and schists (Blatt, 1982). The average igneous rock contains 12% to 24% quartz (Clark, 1924; Leith and Mead, 1915), whereas the average sandstone derived from the igneous rocks contains 67% to 70% quartz (Leith and Mead, 1915).

Quartz arenites may originate as first cycle deposits (Pettijohn *et al.*, 1987). They can also be a product of multiple recycling (Suttner *et al.*, 1981) of quartz grains from sedimentary source rocks or formed *in-situ* through extensive chemical weathering.

Quartz arenites are typically deposited in stable cratonic environments. Quartz arenites produced by persistent wave or current reworking were deposited on stable cratons and passive margins (Tucker, 1991; Boggs, 1995). The quartz arenites are also of granitic provenance. Indeed, virtually all the quartz in sands is ultimately derived from quartz-bearing plutonic rocks: "granite" in a very broad and loose sense (Pettijohn, 1975).

Lithic arenites generally reflect a wider provenance, supplied by a large drainage basin, which is most likely to have a diverse bedrock lithology. Estimates of recycling rates of sediments based on erosion rates and sediment volumes range from a little over 100 million years to almost 300 million years for mean sediment residence times (Garrels and Mackenzie, 1971; Blatt *et al.*, 1980).

These estimates represent mostly continental and continental margin processes, but a figure based on oceanic sediment alone would give a figure of about the same magnitude. Recycling through the lower crust and mantle via subducting slabs may involve some continental margin sediment that is sandy, but the volumes of sand are small compared to other sediments found on or at the edge of oceanic lithosphere. The recycling rates of sediments conclude that the operation of plate tectonics together with other sedimentary processes keep sand at or near the surface of the earth in continental crust once it arrives by sedimentary and igneous differentiation (Pettijohn *et al.*, 1987).

Ternary diagrams have been used to plot the Mamuniyat sandstone composition data for A, B and H–Fields (**Fig. 3.8**). These indicate that they were derived from similar parent rocks (source rock). Moreover, the Mamuniyat sandstone in the study area, formed under humid climatic conditions from plutonic and metamorphic rocks (Suttner *et al.*, 1981).

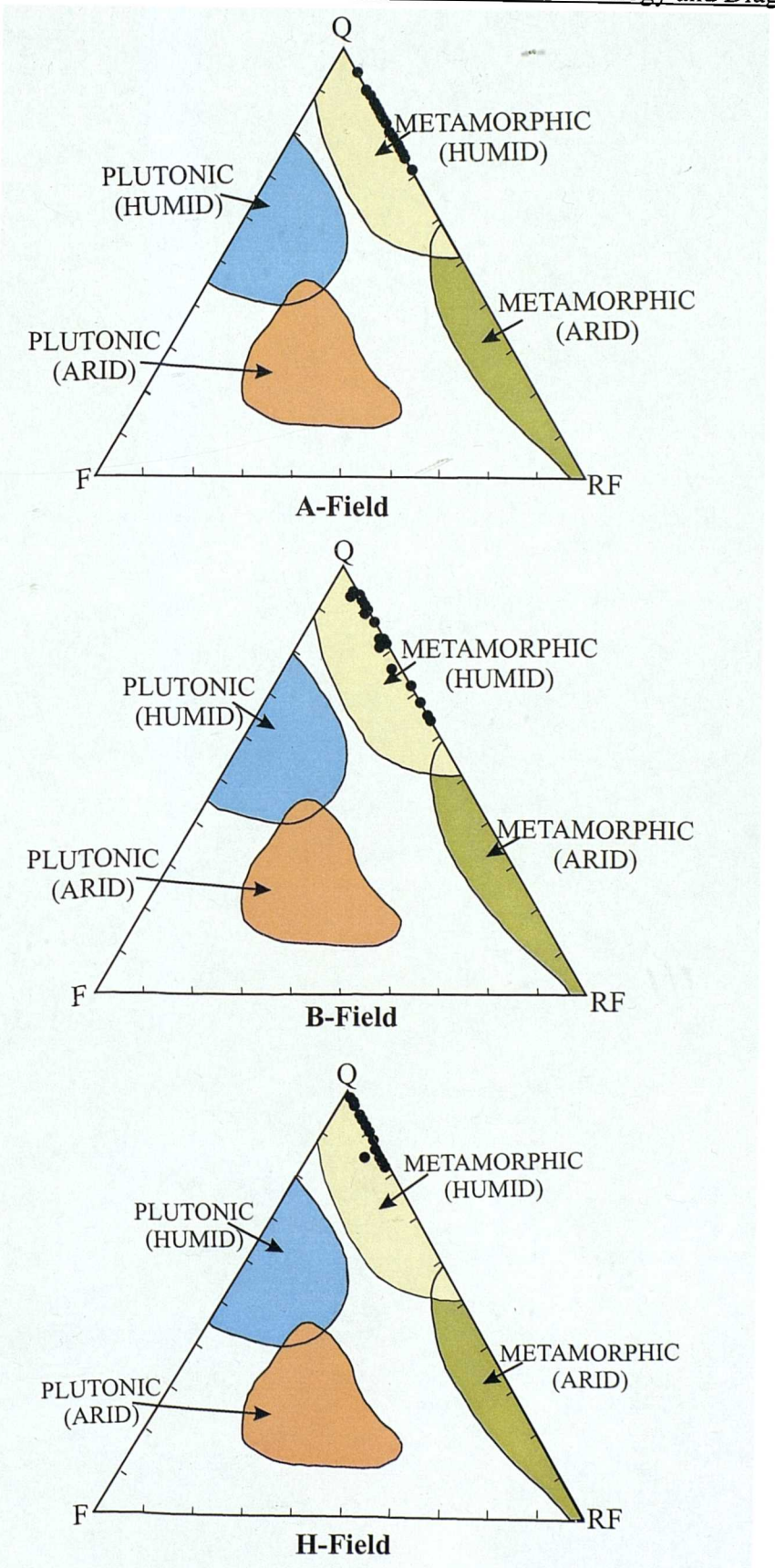

Fig. 3.8 Ternary QFRF plot showing the average composition of sandstone and source rock marked by metamorphic humid climate from A, B and H-Fields. (After Suttner *et al.*, 1981).

3.5 Diagenesis

Many of the major factors that control diagenesis, such as detrital composition, fluid composition and fluid flux, can be related directly or indirectly to physical, chemical and biological processes operating at the time of deposition. Each depositional environment produces a lithofacies with a specific limited range of physical and compositional characteristics that affect diagenesis (Visher, 1969; Boggs, 1995).

Once a sediment accumulates at its site of deposition, a great variety of post-depositional changes begin to take place. The term diagenesis is used to include all these changes, physical and chemical, up to metamorphism. Some aspects of packing are included and would be early diagenetic processes. The most important diagenetic phenomenon is cementation or lithification, whereby sediments become rocks (Richard and Davis, 1983). The term diagenesis was coined in 1888 by Von Gumbel and has been used in many senses since then. A complete review of the subject, its history, and its terminology has been given by Dunoyer de Segonzac (1968).

Authigenic or authigenesis refers to specific minerals and their formation. Authigenic is to some extent synonymous with diagenetic (Pettijohn *et al.*, 1987). Some diagenetic changes (physical, chemical and biological) occur at the water-sediment interface and are termed halmyrolysis, but the bulk of diagenetic activity takes place after burial. During deep burial the main diagenetic process are compaction and lithification (Blatt, 1982). There is no clear boundary between the realms of diagenesis and metamorphism; however, most workers commonly consider diagenesis to occur at temperatures below about 300° C.

Diagenesis can begin almost immediately after deposition, while sediment is still on the ocean or other basin floor, and may continue through deep burial and eventual uplift. Increase in geostatic (rock) pressure, hydrostatic (fluid) pressure, and temperature is a function of depth. Diagenesis in sandstones can be divided into three stages; Eodiagenesis, Mesodiagenesis and Telodiagenesis.

Eodiagenesis occurs at the surface prior to burial. *Mesodiagenesis* occurs in the sub-surface and is characterised by secondary porosity development, and *Telodiagenesis* refers to the effects of modern processes upon the sandstone after uplift (Boggs, 1995). Diagenetic processes begin immediately after deposition and continue until metamorphism takes over. This is when reactions are due to elevated temperatures (> 150 - 200° C) and / or pressure (Tucker, 1991).

The Mamuniyat Formation shows a variety of diagenetic phases. Mechanical compaction and chemical compaction include pressure dissolution and dissolution of minerals. The paragenetic sequence for the Mamuniyat sandstone is a composite sequence, observed from thin sections, which is given schematically in **Figure 2.9**. Authigenic phases preceding or post-dating the secondary porosity (for more detail see the porosity evolution) yield clues to the chemical (composition of the fluid phase) and physical (temperature and pressure) conditions responsible for dissolution.

3.5.1 Silica cementation

One of the most common types of silica cement is quartz overgrowth. Silica cement is precipitated around the quartz grains and in optical continuity, so that the grain and cement extinguish together under crossed polarisers. One important feature arising from the early quartz cementation of sandstones is that they are then able to withstand better the effects of compaction and pressure dissolution during later burial. In this way a moderate porosity can be preserved which may be filled later with oil or gas (Tucker, 1991).

From thin sections analysis, it can be demonstrated that the deposition of silica overgrowths occurred at an early diagenetic stage and continued to grow periodically throughout burial diagenesis, as evidenced by the preservation of primary intergranular volume. The source for this silica cementation is probably the dissolution of framework grains, since some extend into secondary pore spaces after dissolution of unstable detrital fragments.

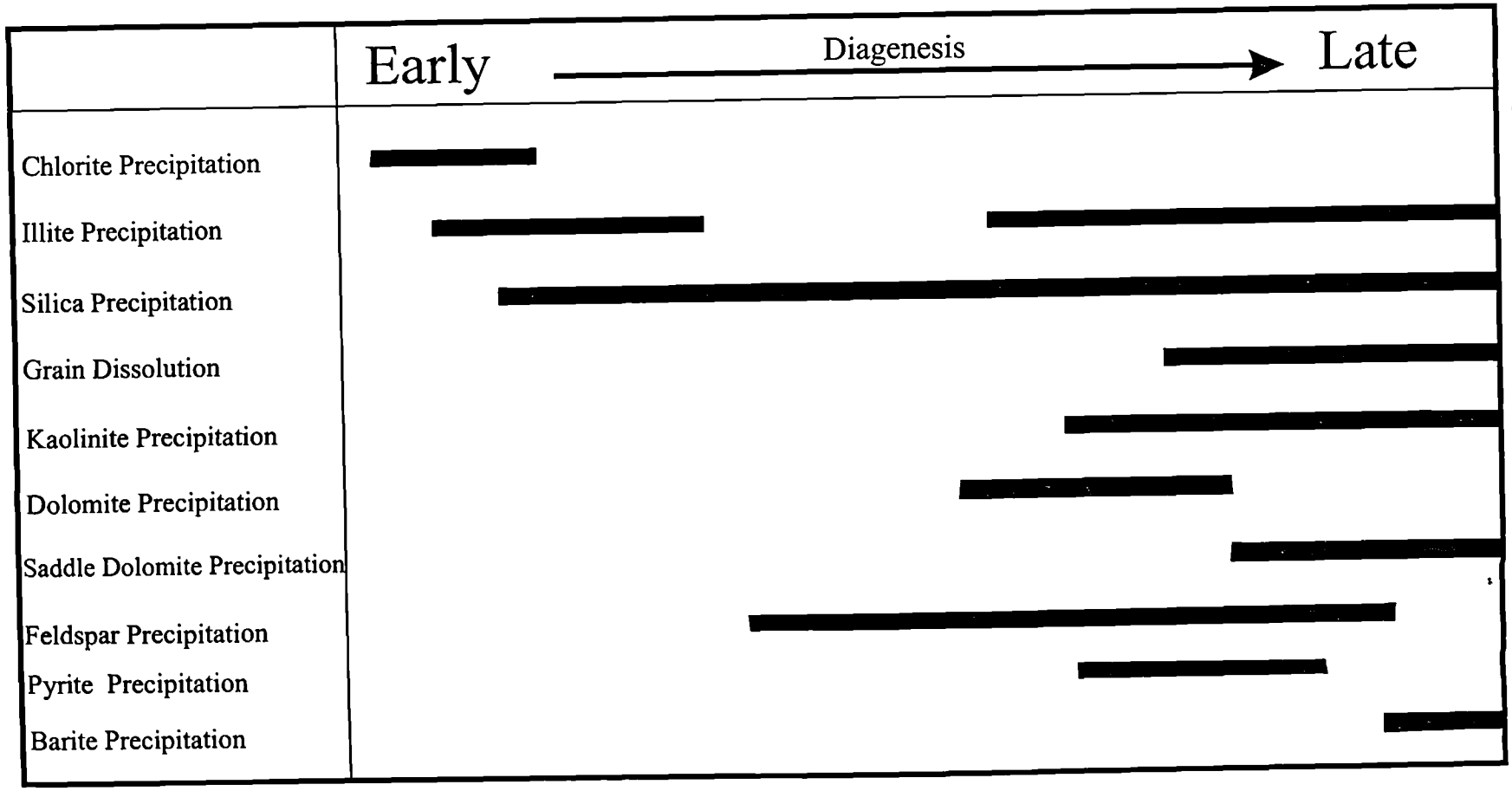

Fig. 3.9 Paragenetic sequence of diagenetic events in the Mamuniyat sandstone, NC115 Concession.

Note: Feldspar precipitation occurs only in B-Field, southwest of the study area.

Dissolution of feldspar grains is reported as a silica source for quartz cement, Although prismatic kaolinite pseudomorphs and oversize pores suggest that feldspar was an important detrital component on deposition, silica is also released by clay mineral authigenesis, *i.e.,* the breakdown of illite-smectite to illite, pressure solution of quartz grains at points of contact and the re-deposition of silica away from areas of stress, and feldspar decomposition (Blatt, 1979). During feldspar dissolution, kaolinite precipitates and silica is released, possibly due to an influx of acidic meteoric water and hence within a shallow diagenetic environment.

The early diagenesis of silica reduces the primary porosity. Reduction of pore space, but not of thickness, may result from precipitation of cement. Silica cementation, especially if early, may prevent mechanical compaction or solution at particle contacts. Both compaction and cementation are accelerated by high temperature, moving water solutions, and large pressure equivalent to large depths of burial. As a rule, porosity decreases with increasing depth of burial (Friedman and Sanders, 1978).

The dissolution is so extensive in some samples that no remnants of detrital grains remain with channelled and oversized pores common throughout. Moreover, the main factors favouring secondary porosity preservation and destruction are: the early flushing of meteoric water causing leaching of feldspar; and the transformation of kaolinite to illite, which may also cause the leaching of feldspar (Burley and Kantorowicz, 1986).

In the Mamuniyat Formation kaolinite is present in amounts ranging from 1% to 15%. It is abundant throughout most of the slides and is precipitated by circulating pore fluids following the alteration and dissolution of potash feldspar grains **(Plate 3.3B)**. For kaolinite precipitation the circulating water must be of a meteoric origin.

Kaolinite requires acid pore waters and low K^+, which can be produced by flushing of the sandstone by fresh water, either during an early burial stage, if the sediments are continental, or if marine, during uplift after a burial phase.

Kaolinite precipitation within marine sediments may also result from decomposing organic matter setting up a low pH. The ions for kaolinite precipitation are largely derived from the alteration of labile detrital minerals, in particular feldspars (Tucker, 1991).

3.5.2 Carbonate cementation

In most sandstones the volume of carbonate cement does not exceed about 30%, In some sandstones, however, the percentage of carbonate can be 50% to 60%, much greater than any postcompaction porosity in a rock composed only of quartz, feldspar and rock fragments (Dapples, 1975; Blatt, 1982). Carbonate cementation is favoured by increasing concentration of calcium carbonate in pore waters and increasing burial temperature. Precipitation is inhibited by increased levels of CO_2 in pore water, which may result from decomposition of organic matter in sediments during burial. Increased CO_2 levels (partial pressure) cause pore waters to become acidic and corrosive to carbonate minerals (Boggs, 1995).

Calcite and dolomite are abundant in sandstones as pore-filling and replacement cements of post-depositional origin. The primary and early diagenetic carbonate cement of many modern sediments may include magnesian calcite. In contrast, the calcite and dolomite of later diagenetic cements of sandstone are relatively pure, with no excess magnesium in the calcite and no excess calcium in the dolomite. Aragonite has not been reported as a precipitated cement in ancient sandstones, though it is well known in beach-rock in modern carbonate environments and aragonite-cemented modern sands (Tucker, 1982, 1991; Pettijohn *et al.*, 1987).

Calcite is one of the most common cements in sandstones, but other carbonate cements of more local importance are dolomite and siderite. The cement may vary from an even to patchy distribution, to local segregation and concretions. The latter have been called doggers. The two main types of calcite cement are poikilotopic crystals and drusy calcite spar (Tucker, 1991).

As a result of calcite precipitation there is commonly a displacement of grains (post quartz overgrowth) so that they appear to 'float' in the cement **(Plate 3.3A)**. Calcite may also be precipitated in cracks in grains and so force them to split (Dapples, 1975; Blatt, 1982). Carbonate cementation throughout the Mamuniyat Formation is rare and dolomite occurs in isolated patches of rhombic and saddle-shaped crystals. Dolomite cements vary from pore-filling microcrystalline rhombic to coarse anhedral mosaics and large poikilotopic crystals. In the Mamuniyat Formation the rhombic dolomite has precipitated in shallower burial conditions than the precipitation of saddle dolomite.

3.5.3 Saddle dolomite cementation

3.5.3.1 Introduction

Petrographic and chemical characteristics of saddle dolomite indicate a divergence from "normal" dolomite. It is an indicator also of higher diagenetic temperatures and is associated with sulfide mineralization and hydrocarbon occurrences (Tschermak, 1884; Dunsmore, 1973). As revealed by various reviews, saddle dolomite is considered as a late stage cement (Radke and Mathis, 1980). Thus, saddle dolomite in the Mamuniyat Formation enables us to more closely constrain the diagenetic history of the sediments, the salinity of the pore water, and determine the geothermal conditions.

3.5.3.2 Morphology

The morphology of saddle dolomite ranges from rhombohedral, with slightly curved faces through increasing face curvature to symmetrical saddle forms. It appears sometimes to be composed of subcrystals, which are an indication of the disruption of crystal surfaces (Radke and Mathis, 1980). The crystals are generally large (many millimetres) and have conspicuous curved crystal faces. In thin section, they have curved cleavage and undulose extinction (Tucker, 1991). In the Mamuniyat Formation the characteristics of saddle dolomite are: rhombic shaped dolomite crystals with the boundaries with adjacent subcrystals usually normal to the direction of growth.

3.5.3.3 Inclusions

Saddle dolomite is slightly calcium-enriched. Concentrations of iron and manganese are variable and reflect associations with the host suite or local conditions. Within individual growth laminae of a saddle dolomite crystal, composition is not uniform but changes away from edges and intersection points of crystal faces, which are more enriched in calcium. A calcium decrease away from these sites is compensated for by a corresponding increase of magnesium, iron and manganese (Dunsmore, 1973). The overall pattern of variations in composition is not known but would logically correspond to the pattern of growth-rate variations (Radke and Mathis, 1980).

Throughout the Mamuniyat Formation the saddle dolomite is of cloudy appearance due to the abundance of inclusions, and in thin section they show cleavage and undulose extinction (fluids or mineral relics).

3.5.3.4 Colour and optical properties

Saddle dolomite occurs in a variety of colours, but is most commonly white, pink and orange to red. The colour mainly depends upon trace element content. The colour of saddle dolomite in the Mamuniyat Formation appears brown, due to the oxidation of the iron (Beales, 1971; Radke and Mathis, 1980). Optical characteristics of the saddle dolomite include its sweeping extinction which is the main criteria distinguishing saddle dolomite from other carbonate minerals (Folk, 1977; Machel, 1987).

3.5.3.5 Occurrence of saddle dolomite

Saddle dolomite is associated with hydrocarbon occurrences, base-metal sulfide mineralization, fluorite and calcite. In addition, it commonly occurs in sulfate-rich carbonates. The mineral has greatest volumetric abundance in replacement bodies with geometries controlled by both faults and stratigraphic units.

Calcium adsorption on the growing saddle dolomite crystals is influenced by properties of the crystal as an entity, producing variations in composition that reflect crystal symmetry. It is the variations in concentration of the larger calcium cation, which initiate the lattice distortion. Both temperature and the chemistry of the mother fluids are considered to be the influential parameters in inducing polarized surface-charge on the crystal, which in turn controls the selective adsorption of calcium in particular sites (Radke and Mathis, 1980).

Throughout the Mamuniyat Formation, saddle dolomite commonly occurs in association with hydrocarbon reservoirs by filling the pore space between the grains and sometimes as a replacement **(Plate 3.5B)**. However, whenever clay minerals are present, saddle dolomite as a replacement phase is inhibited, although it is found altering the host mineral along its edge (Turner *et al.*, 1991).

Such an assurance reveals two paragenetic features. It demonstrates that saddle dolomite in the Mamuniyat Formation is late stage, at least later than clay rims. Moreover, the presence of iron altering the host minerals through their partial replacement by saddle dolomite is evidence that this type of alteration is a function of the diagenetic formation of saddle dolomite.

These conditions are compatible with the occurrence of saddle dolomite crystals in the Mamuniyat Formation. The crystals commonly show leaching which would suggest that there has been a change of formation waters undersaturated with respect to dolomite. The saddle dolomite commonly shows leaching followed by part enclosure of the crystals by silica. Subsequent to this phase of diagenesis dolomite continues to precipitate as saddle dolomite crystals. Saddle dolomite in previous studies is shown to occlude fractures and veins, which demonstrates a post-tectonic timing and a late stage origin (Radke and Machel, 1980; Machel, 1987).

3.5.3.6 Conditions of formation

There appears to be a general consensus today that liquid oil forms at the same temperature range as saddle dolomite from 60-150° C, consistent with depths of burial from 1500-4500 metres, (Philippi, 1965; Vassoyevich *et al.*, 1970), and high salinities 2 to 6 times that of normal seawater (Tisso *et al.*, 1971; Machel, 1987). In addition, high temperature conditions, established by the presence of saddle dolomite are confirmed by D.S.T (Drill Steam Test) on formation water. Such results have revealed temperatures from 105°-110°C (Edwards, 1991).

In the Mamuniyat Formation most of the thin sections which have been examined reveal that saddle dolomite occurs at average depths of 2280 meters, and that the depth of burial is the main factor controlling temperature in NC115 Concession.

3.5.3.7 Saddle dolomite precipitation

Saddle dolomite crystals in the Mamuniyat Formation are associated with hydrocarbon reservoirs, and are occasionally associated with pyrite (Beales 1971; Turner *et al.*, 1991). Moreover, the saddle dolomite crystals are associated with organic matter, which surrounds them (Lippmann 1973). In the Mamuniyat Formation saddle dolomite is precipitated as a passive void-filling cement. The crystals of saddle dolomite range from millimeter to centimetre-size and sometimes as scattered single crystals (Turner *et al.*, 1991).

3.5.4 Feldspar dissolution and overgrowth

Comparison of chemical conditions for diagenetic dissolution of feldspar with those for authigenic feldspar growth is overgrowth. It appears that both processes are common (Heald and Laresa, 1973; Pittman, 1979). Dissolution is related to porewater movements from undersaturated environments dominated by waters of meteoric origin that move downward and laterally in a basin. In these waters the Na^+/H^+ and K^+/H^+ activity ratios are low compared to silica activities.

Authigenesis is related to either local isochemical changes or to porewater movement that transports water high in Na^+/H^+ or K^+/H^+ ratio from lower formations (Pettijohn *et al.*, 1987). Although in Mamuniyat sandstones, feldspar is altered to clay minerals or replaced by calcite, in some instances feldspar overgrowths do grow on detrital feldspar grains.

Feldspar dissolution is most common on potash feldspar, but it also occurs on detrital albite grains. In the deeper burial environment, albitization of detrital plagioclase and K–feldspar takes place, with the required Na^+ probably coming from the breakdown of smectite to illite (Pettijohn *et al.*, 1987; Tucker, 1991).

3.5.5 Clay mineral authigenesis

In most sandstones the volume of authigenic clay minerals is small, certainly less than 5% of the rock volume. The prominent exception is volcaniclastic sandstones in which secondary clays can form the bulk of the rock. Clay minerals may be potassic (illite and its polymorphs), sodic and calcic (montmorillonite and its polymorphs), or devoid of alkali and alkaline earth cations (kaolinite and its polymorphs). Sandstones that contain matrix normally have two distinct peaks in their grain-size distribution: one in the sand size, the second in the clay size (Blatt, 1982).

Authigenic clay minerals reduce the space in pores, increase microporosity and the ratio of surface area to volume, and increase the physical resistance to fluid flow as crystals grow outward from pore walls, especially the long, fibrous, illite crystals. The abundance and kinds of authigenic clays, like the primary clays, should always be related to the sub-environments of a sandstone body (Pettijohn *et al.*, 1987).

Illite and kaolinite are the most common authigenic clays in sandstones, but montmorillonite, mixed–layer illite–montmorillonite and mixed–layer montmorillonite–chlorite also occur. Authigenic clay minerals occur as pore–filling cements and clay rims up to 50μm thick around grains.

The attenuation and absence of rims near and at grain contacts demonstrates their diagenetic origin. The precipitation of clay rims is usually an early or the first diagenetic event, often predating quartz overgrowths or calcite cementation (Tucker, 1991).

3.5.5.1 Kaolinite authigenic of the Mamuniyat Formation

Throughout the Mamuniyat Formation kaolinite is the most common authigenic clay mineral developed within the sandstones. It is a late stage authigenic mineral post–dating early quartz overgrowth. Kaolinite precipitation occurs as an alteration product from the dissolution of feldspar grains and from circulating pore fluid. Kaolinite develops as discrete particle clays (Pettijohn *et al.*, 1987) and forms a characteristic pattern of irregular stacked (booklets) of pseudo–hexagonal platelets which can be readily identified under the microscope.

The main conditions required for the deposition of kaolinite are sufficient porosity and permeability to allow the migration of interstitial water and adequate growth space, the presence of a source of aluminium and potassium such as potassium feldspar and the presence of organic matter to maintain a low pH (Scholle, 1979; Blatt, 1982). Kaolinite deposition is also favoured by the presence of partly degraded illite which acts as a receptor for potassium ions. Kaolinite is important in any sandstone reservoir since it reduces the intergranular porosity and behaves as a migrating fine within the pore network (Blatt, 1982).

In thin section, in the Mamuniyat Formation, kaolinite may line the pores in an orderly-arranged manner or completely fill the pore network system. Kaolinite deposition appears to bear no relation to feldspar decomposition and commonly develops in pores away from feldspars that are decaying to produce secondary porosity. However, circulating waters would locally transport the dissolved potassium and aluminium ion away from the dissolving feldspar to be deposited at the site of kaolinite accumulation such as pore throats.

3.5.5.2 Illite authigenic of the Mamuniyat Formation

Illite clay continues to precipitate as an intergranular cement, possibly during late stage deep burial diagenesis. Illite is commonly cited as having a detrimental effect on the reservoir potential of a sandstone reservoir due to its whisp–like growth habit across pores. This tends to increase the tortuosity of the flow path and hence decrease the permeability. Illite has a higher birefringence and normally is pore-lining (Tucker, 1991). The illite clay coats detrital quartz grains. Wispy terminations of clay extend into, and partially bridge pores. Although considerable porosity remains, much of it is isolated by the narrowness of the connecting pore throats (Scholle, 1979).

3.5.5.3 Chlorite authigenic of the Mamuniyat Formation

In the Mamuniyat Formation it is likely that poorly crystallised chlorite clay was precipitated in rare patches on detrital grains. This was post-dated by the precipitation of grain-coating illite clay exhibiting a short fibrous morphology. It is possible that the chlorite clay was altered to illite. Illite clay therefore began to form early in the diagenetic history of the sandstones. In many samples illite continued to accumulate until the pores were completely filled.

3.5.6 Pyrite cementation

Pyrite occurs in many sandstones as small cubes, clusters and framboids, but it is only an accessory diagenetic mineral. It is most common in marine sandstones. Pyrite is genetically related to a more or less amorphous common mineral, hydrotroilite (FeS) now called mackinawite, that is found in modern sediments under reducing conditions. FeS forms first by the bacterial reduction of sulfate in sea water and during early diagenesis is converted to FeS_2, pyrite, indicative of locally reducing condition (Berner, 1964). These have often been tied to a silled anoxic basin, but in the case of sandstone it is more likely that it is the presence of large amounts of organic matter that is responsible for the reduction (Pettijohn *et al.*, 1987).

3.5.6.1 Pyrite cementation of the Mamuniyat Formation

In the Mamuniyat sandstones the authigenic pyrite forms as cubes and framboids. The framboids are enclosed by a stage of silica cementation which in turn pre–dates dolomite precipitation and subsequent leaching of dolomite crystals. The close association of pyrite with its source of iron suggests that during the formation of pyrite there was no extensive circulation of ground water and that local reducing conditions were created within the sediment, possibly connected with a local rise in the height of the water table. Later pore fluids caused dissolution of much of this diagenetic pyrite creating a large amount of secondary porosity, which has, in many cases, been in-filled with late kaolinite authigenic clays.

3.5.7 Barite cementation

Throughout the Mamuniyat Formation barite occurs as traces of a late crystallisation phase and it is thought to occur in connection with dewatering of the sandstones. Barite is mixed within the drilling-mud and may invade the sandstones as a solid mineral phase. However, as bitumen post-dates the barite it must have been a discrete authigenic mineral phase.

3.6 Porosity evolution

The study of porosity is very important for reservoir rock assessment. Porosity is the percentage of pore space to the total volume of the rock (Pettijohn, 1957). Porosity in sandstone can be divided into three types: primary intergranular porosity, secondary porosity and microporosity.

Primary porosity is a direct reflection upon the deposition and compactional processes that the sediment has undergone during initial burial. Sandstones prior to burial have porosities ranging from 35% - 40%, but this is decreased through burial and increasing compaction of the sediments and through the deposition of authigenic cements and clay mineral diagenesis. Final values of irreducible primary porosity may be as low as 4.0% (Schmidt and McDonald, 1979).

In the Mamuniyat sandstone all three types of porosities occur. The mean primary porosities throughout A, B and H-Fields are 11.40%, 13.33% and 14.08% respectively **(Plate 3.6B)**. Hence, each field has suffered considerable loss through burial compaction.

Secondary porosity develops as a result of dissolution of unstable detrital grains and framework cement. Secondary porosity may be generated, destroyed and regenerated throughout the diagenetic evolution of a sandstone and there is evidence that this was the case with the Mamuniyat sandstone **(Plate 3.3B)**. Secondary porosity is predominant in the Mamuniyat sandstones within NC115 Concession, and is recognised in thin section from the partial or complete dissolution of unstable minerals and corroded grains.

In reservoir sandstones the vast amount of secondary porosity is generated by the dissolution of carbonate minerals. Secondary porosity occurring from early and late dissolution of former framework grains is common and has enhanced reservoir quality considerably. Direct dissolution of silicate minerals such as quartz and feldspar is thought to create little or no secondary porosity (Schmidt and McDonald, 1979), as such silicate minerals may be replaced by non–silicate minerals whose subsequent dissolution may be mistakenly attributed to the direct leaching of the silicate minerals.

In the Mamuniyat sandstones secondary porosity, occurring from the probable early and late dissolution of former framework grains, is common and has enhanced reservoir quality considerably. The dissolution is so extensive in some samples that no remnants of detrital grains remain with channelled and oversize pores common throughout. There is a limit to the amount of secondary porosity that can develop in any sandstone under specific conditions of stress because the supportive strength decreases with increasing porosity and the framework will ultimately fail. The mean secondary dissolution porosity for A, B and H-Fields is 7.15%, 5.40% and 3.34% respectively **(Plate 3.3B)**. Hence, each field has dissolution of unstable detrital grains and framework cement throughout the diagenetic evolution of the sandstone.

Microporosity is defined by pores with an aperture radius of less than 0.5μm, Microporosity may be associated not only with small pores but with some larger ones as well (Loucks *et al.*, 1977). Microporosity occurs within clay minerals and at pore throats and accounts for the irreducible water saturation of sandstone (Pitman, 1979).

Microporosity occurs as pores within kaolinite clay minerals, in association with authigenic clays, (with the exception of where bitumen cement has completely enveloped kaolinite clays) and partially dissolved quartz or lithic grains. Microporosity cannot be accurately estimated and the proportion of microporosity present typically accounts for the frequent underestimation of porosity when measured in thin section by point counting methods.

Throughout the mineralogical investigation of the Mamuniyat sandstones, the type of porosity was noted and expressed as a percentage of the total porosity for each sample. The mean total porosity (primary intergranular porosity + secondary dissolution porosity) for A, B and H-Fields, NC115, is 18.55%, 18.73% and 17.42% respectively. Generally, the average total porosities of the Mamuniyat Formation in NC115 Concession are 18.23%, based on point counting of 105 thin sections. No analysis of permeability for these samples has been attempted in this study and permeability data are not currently available.

The majority of the secondary porosity developed in the Mamuniyat sandstones is through the alteration of unstable detrital grains, especially feldspar. Secondary porosity after feldspars can readily be identified in thin section. Feldspar dissolution within the Mamuniyat sandstones is a continuous process and accounts for the remaining porosity after kaolinite deposition, which is important to the reservoir potential of the Mamuniyat sandstone at depth.

3.7 Comparison between A, B and H-Fields in NC115 Block

A petrographic study of the Mamuniyat sandstones within El-Sharara Field, northwestern flank of the Murzuq Basin, reveal similarities in composition, texture and porosity between A, B and H-Fields. The detrital components identified from the Mamuniyat Formation in A, B and H-Fields, are monocrystalline quartz with subordinate polycrystalline quartz. Feldspar grains are significantly absent in A-Field, but in B and H–Fields they are sufficiently abundant in orthoclase feldspar. Lithic grains, mica and heavy minerals are rare throughout the study area (Fello and Turner, 2001a).

Three types of cement, namely quartz overgrowth, carbonate and authigenic clay are recognised in the sandstones. Authigenic quartz is rare to very common, kaolinite and illite clays are common, but dolomite, pyrite and barite are very rare. Although primary intergranular porosity is common in most samples from the A, B and H-Fields, it is reduced in many places by secondary silica cement. Secondary porosity, due to the dissolution of former framework grains is present to abundant, and significantly enhances reservoir quality. Microporosity commonly occurs in association with authigenic clays, (with the exception of where bitumen has completely enveloped clays).

The reservoir quality in the Mamuniyat Formation is good to very good, especially in the upper part of the reservoir. Generally, the best reservoir unit is the coarse-grained deposits within the Mamuniyat Formation in NC115 Concession. Mudstone and muddy heterolithites 'considered non-reservoirs' are rare. Relatively clean sandstone makes up the majority of the reservoir interval. The authigenic clays play a locally significant part in reducing reservoir quality by filling or lining pore-space (especially illite and kaolinite), as does authigenic silica which serves to reduce, and locally occlude, interparticle porosity. Ordovician sandstone reservoir quality varies greatly. However, porosity as high as 20% has been observed. Although largely secondary and often tectonically induced, it is at least partially controlled by depositional facies.

Glacial and peri-glacial clastic deposits of the Mamuniyat Formation provide the best reservoir, infilling incised north-south aligned palaeo-valleys in the NC101 region (Boote *et al.*, 1998). These may have acted as efficient migration conduits into traps formed by updip facies changes and differential compaction. The north-western NC115 pools appear to be trapped within low-relief fault structures of Ashgillian age. Mid to late Tertiary uplift of the basin margins terminated further expulsion and encouraged extensive meteoric invasion and flushing (Boote *et al.*, 1998).

Solid bitumen envelopes can be seen coating detrital grains and authigenic minerals in many samples, especially the more porous coarser grained samples. Extensive drilling mud invasion into the majority of the reservoir sands has significantly reduced their porosity, and to some extent their permeability. There is a possibility of formation damage resulting from mud solids invasion and clay minerals.

3.8 Summary

A petrographic study of the Mamuniyat sandstones based on 105 thin sections from NC115 Concession reveals similarities in composition, texture and porosity between A, B and H-Fields. The detrital components identified from the Mamuniyat Formation in the three oilfields are monocrystalline quartz with subordinate polycrystalline quartz, rock fragments, feldspar, heavy minerals and kaolinite. Petrographic data derived from sandstone samples from cored intervals through the Mamuniyat Formation show that they are mainly sublitharenites, with some quartz arenites and litharenites. Compositional data for the three oilfields indicate that the sandstones were derived from a similar parent rock, but with differences in modal composition, textural attributes and porosity of the Lower, Middle and Upper Members of the Mamuniyat. These are attributed to temporal variations in source-area uplift, base-level change and sediment flux and accommodation space. The average total porosity of the Mamuniyat Formation is 18.0 %, based on thin-section analysis. No permeability analysis of these samples has been carried out, and permeability data are not currently available.

Modal Composition of samples from the Mamuniyat Formation, A-Field, NC115 Concession, Murzuq Basin, SW Libya.

WELL	DEPTH ft. (kb)	GEOLOGICAL FORMATION	TEXTURAL DATA					PORE TYPE (%)						CLASSIFICATION (Pettijohn et al., 1987)	POINT COUNTED DATA																							
			GRAIN SIZE			GRAIN SORTING	GRAIN ROUNDNESS	Porosity (%)	Primary (Intergranular)	Secondary					MINERALS COMPONENTS (%)							CEMENT (%)																
																						AUTHOGENIC MINERAL				AUTHIGENIC CLAY				OTHER					
			Minimum size	Mean size	Maximum size					Intragranular	Dissolution	Microporosity	Fracture		MONOCRYSTALLINE QTZ.	POLYCRYSTALLINE QTZ.	ROCK FRAGMENT	HEAVY MINERALS	MUSCOVITE MICA	FELDSPAR	CHERT	NON FERRO DOLOMITE	FERRO DOLOMITE	CALCITE	DOLOMITE	KAOLINITE CLAY	SERICITE / ILLITE CLAYS	CHLORITE CLAY	MATRIX	PYRITE	MAGNETITE	BARITE	BITUMEN	DRILLING MUD SOLIDS
A1	4702.70	Mamuniyat	F.S	C.S	V.C.S	MS	SR - R	22	15	-	7	-	-	Sublitharenite	72	8	5	2	-	-	-	-	-	-	-	6	-	2	-	1	-	-	Tr	-
	4717.13	Mamuniyat	F.S	G	M.S	WS	SA - SR	0	0	-	0	-	-	Lithic greywacke	52	7	1	1	2	-	-	-	-	-	-	-	-	-	35	-	-	2	-	-
	4758.14	Mamuniyat	F.S	V.C.S	V.C.S	PS	SR - R	17	14	-	3	-	-	Sublitharenite	76	13	6	1	-	-	-	-	-	-	-	3	-	Tr	-	Tr	-	-	-	-
	4784.39	Mamuniyat	F.S	C.S	V.C.S	MWS	SR - R	21	13	-	8	-	-	Sublitharenite	75	10	3	1	-	-	-	-	-	-	-	6	-	Tr	-	1	-	-	Tr	-
	4811.30	Mamuniyat	F.S	C.S	V.C.S	MWS	SR - R	23	13	-	10	-	-	Sublitharenite	68	18	4	1	-	-	-	-	-	-	-	5	-	1	-	-	-	-	Tr	-
	4853.94	Mamuniyat	F.S	V.C.S	C.S	MWS	SA - SR	23	13	-	10	-	-	Sublitharenite	74	15	2	1	-	-	-	-	-	-	-	4	-	1	-	-	-	-	3	-
	4869.69	Mamuniyat	V.F.S	C.S	G	MS	SA - R	23	11	-	12	-	-	Sublitharenite	67	17	3	2	-	-	-	-	-	-	-	5	-	Tr	-	-	-	-	5	-
	4873.63	Mamuniyat	V.F.S	C.S	G	MWS	SA - SR	24	15	-	9	-	-	Sublitharenite	65	18	3	1	-	-	-	-	-	-	-	6	-	1	-	-	-	-	4	-
	4888.06	Mamuniyat	F.S	V.C.S	C.S	MWS	SA - SR	19	12	-	7	-	-	Sublitharenite	77	11	5	1	-	-	-	-	-	-	-	3	-	-	-	Tr	-	-	2	-
	4939.90	Mamuniyat	F.S	G	M.S	VWS	SA - SR	20	15	-	5	-	-	Sublitharenite	72	10	3	2	-	-	-	-	-	-	-	6	-	-	-	2	-	-	4	-
	4995.02	Mamuniyat	F.S	V.C.S	V.C.S	MWS	SA - SR	18	11	-	7	-	-	Sublitharenite	75	9	2	1	1	-	-	-	-	-	-	4	-	-	-	2	-	-	2	-
	5548.65	Mamuniyat	F.S	V.C.S	C.S	WS	SA - SR	0	0	-	0	-	-	Lithic greywacke	42	8	2	2	4	-	2	-	-	-	-	Tr	-	-	38	Tr	-	-	-	-
A2	4975.66	Mamuniyat	F.S	C.S	V.C.S	MWS	SR - R	20	12	-	8	-	-	Sublitharenite	70	15	3	1	1	-	-	-	-	-	-	2	3	-	3	-	-	-	-	-
	4986.23	Mamuniyat	F.S	C.S	V.C.S	MWS	SR - R	15	10	-	5	-	-	Sublitharenite	76	16	3	Tr	1	-	-	-	-	-	-	1	1	-	-	-	-	-	-	-
	4997.97	Mamuniyat	F.S	G	M.S	WS	SA - SR	18	12	-	6	-	-	Sublitharenite	79	5	-	-	4	-	-	-	-	-	3	Tr	1	-	4	3	Tr	-	Tr	-
	5014.37	Mamuniyat	F.S	C.S	V.C.S	MWS	SR	0	0	-	0	-	-	Lithic greywacke	27	5	-	-	1	-	-	-	-	-	-	-	-	-	65	Tr	-	-	-	-
	5020.77	Mamuniyat	F.S	C.S	V.C.S	MWS	SR - R	14	10	-	4	-	-	Sublitharenite	77	15	Tr	1	1	-	-	-	-	-	-	1	Tr	-	-	1	Tr	-	Tr	-
	5038.82	Mamuniyat	F.S	C.S	V.C.S	WS	SR - R	13	8	-	5	-	-	Sublitharenite	75	12	-	3	1	-	-	-	-	-	-	4	2	Tr	-	1	-	-	-	-
	5202.10	Mamuniyat	F.S	G	M.S	WS	SR	22	15	-	7	-	-	Sublitharenite	80	8	1	3	2	-	-	-	-	-	1	3	-	-	-	1	1	-	Tr	-
A4	5028.15	Mamuniyat	F.S	V.C.S	C.S	MWS	SR - R	19	10	-	9	-	-	Sublitharenite	74	9	1	2	Tr	-	-	-	-	-	-	5	-	-	-	-	-	-	8	-
	5050.79	Mamuniyat	F.S	C.S	V.C.S	MWS	SR - R	18	12	-	6	-	-	Sublitharenite	71	18	1	2	-	-	-	-	-	-	-	6	-	-	-	1	-	-	Tr	-
	5084.91	Mamuniyat	F.S	G	M.S	WS	SR - R	20	11	-	9	-	-	Sublitharenite	68	9	2	2	1	-	-	-	-	-	-	15	-	-	-	2	Tr	-	-	-
	5185.30	Mamuniyat	F.S	V.C.S	V.C.S	MWS	SR - R	15	10	-	5	-	-	Sublitharenite	73	16	2	2	1	-	-	-	-	-	Tr	3	-	-	-	1		-	-	1
A8	4627.89	Mamuniyat	F.S	C.S	G	MWS	SR - R	16	10	-	6	-	-	Sublitharenite	69	22	1	Tr	Tr	-	-	-	-	-	-	5	-	-	-	-	-	-	3	-
	4678.09	Mamuniyat	F.S	C.S	G	MWS	SR - R	18	10	-	8	-	-	Litharenite	65	25	1	Tr	-	-	-	-	-	-	-	4	-	-	-	-	-	-	2	-
	4685.97	Mamuniyat	F.S	C.S	G	WS	SR - R	21	12	-	9	-	-	Litharenite	69	18	6	1	Tr	-	-	-	-	-	-	3	-	-	-	Tr	-	-	Tr	-
	4699.75	Mamuniyat	F.S	C.S	V.C.S	WS	SR	22	13	-	9	-	-	Sublitharenite	73	16	3	Tr	-	-	-	-	-	-	-	4	-	-	-	Tr	-	-	-	-
	4729.93	Mamuniyat	F.S	C.S	C.S	MWS	SR	17	11	-	6	-	-	Sublitharenite	81	9	5	1	Tr	-	-	-	-	-	-	2	-	-	-	Tr	-	-	-	-
	4768.81	Mamuniyat	F.S	C.S	V.C.S	MWS	SR - R	19	11	-	8	-	-	Sublitharenite	85	7	3	Tr	Tr	-	-	-	-	-	-	3	-	-	-	1	-	-	Tr	-
	4781.77	Mamuniyat	F.S	C.S	G	MS	SR	21	12	-	9	-	-	Sublitharenite	77	13	7	Tr	Tr	-	-	-	-	-	-	2	-	-	-	-	Tr	-	-	-
	4811.95	Mamuniyat	F.S	C.S	C.S	WS	SR - R	23	14	-	9	-	-	Sublitharenite	82	7	5	Tr	1	-	-	-	-	-	1	2	-	-	-	1	-	-	-	-
	4837.38	Mamuniyat	F.S	C.S	G	WS	R	24	14	-	10	-	-	Sublitharenite	73	15	8	1	-	-	-	-	-	-	-	2	-	-	-	1	-	-	-	-
	4851.32	Mamuniyat	F.S	C.S	V.C.S	MWS	SR - R	21	12	-	9	-	-	Sublitharenite	80	9	5	Tr	Tr	-	-	-	-	-	-	2	-	-	-	Tr	-	-	2	-
	4870.68	Mamuniyat	F.S	C.S	V.C.S	WS	SR - R	23	13	-	10	-	-	Sublitharenite	82	10	5	1	-	-	-	-	-	-	-	1	-	-	-	Tr	-	-	Tr	-
	4885.11	Mamuniyat	F.S	C.S	G	WS	SR - R	23	13	-	10	-	-	Sublitharenite	80	8	6	1	-	-	-	-	-	-	-	2	-	Tr	-	1	-	-	Tr	-
	4900.53	Mamuniyat	F.S	C.S	V.C.S	WS	SR - R	24	16	-	8	-	-	Sublitharenite	80	8	7	2	Tr	-	-	-	-	-	-	Tr	-	-	-	1	-	-	Tr	-
	4906.76	Mamuniyat	F.S	C.S	V.C.S	MWS	SR - R	21	14	-	7	-	-	Sublitharenite	84	9	4	1	1	-	-	-	-	-	-	-	-	-	-	Tr	-	-	Tr	-
	4996.65	Mamuniyat	F.S	V.C.S	C.S	MWS	SR - R	21	13	-	8	-	-	Sublitharenite	83	8	2	Tr	1	-	-	-	-	-	-	3	-	-	-	1	-	-	-	-
	5001.25	Mamuniyat	F.S	C.S	V.C.S	MWS	SR - R	20	12	-	8	-	-	Sublitharenite	70	15	8	2	-	-	-	-	-	-	-	3	-	Tr	-	1	-	-	-	-
	5027.00	Mamuniyat	F.S	G	C.S	WS	SR - R	25	15	-	10	-	-	Sublitharenite	75	11	4	2	-	-	-	-	-	-	-	5	-	Tr	-	1	-	-	-	-

Table: 3.1

Model Composirtion of samples from the Mamuniyat Formation, B-Field, NC115 Concession, Murzuq Basin, SW Libya.

WELL	DEPTH ft. (kb)	GEOLOGICAL FORMATION	TEXTURAL DATA					POROSITY TYPE (%)						CLASSIFICATION (Pettijohn et al., 1987)	POINT COUNTED DATA																							
			GRAIN SIZE			GRAIN SORTING	GRAIN ROUNDNESS	Porosity (%)	Primary (Intergranular)	Secondary					MINERALS COMPONENTS (%)							CEMENT (%)								OTHER							
																						AUTHOGENIC MINERAL				AUTHIGENIC CLAY MINERAL										
			Minimum size	Mean size	Maximum size					Intragranular	Dissolution	Microporosity	Fracture		MONOCRYSTALLINE QTZ.	POLYCRYSTALLINE QTZ.	ROCK FRAGMENT	HEAVY MINERALS	MUSCOVITE MICA	FELDSPAR	CHERT	NON FERRO DOLOMITE	FERRO DOLOMITE	CALCITE	DOLOMITE	KAOLINITE CLAY	SERICITE / ILLITE CLAYS	CHLORITE CLAY	MATRIX	PYRITE	MAGNETITE	BARITE	BITUMEN	DRILLING MUD SOLIDS	
B2	4667.00	Mamuniyat	F.S	C.S	V.C.S	WS	SR - R	22	17	-	5	-	-	Sublitharenite	84	5	4	-	-	-	-	-	-	-	-	3	1	2	-	-	-	-	-	1
	4720.74	Mamuniyat	F.S	V.C.S	C.S	MWS	SR	19	13	-	6	-	-	Sublitharenite	80	4	2	2	1	-	-	-	-	-	1	6	3	1	-	-	-	-	-	-
	4796.04	Mamuniyat	F.S	V.C.S	C.S	MWS	SA - R	17	10	-	7	-	-	Sublitharenite	76	7	4	2	1	-	-	-	-	-	1	4	4	Tr	-	-	-	-	-	-
	4828.52	Mamuniyat	F.S	C.S	V.C.S	WS	R - SR	18	13	-	5	-	-	Ltharenite	65	19	6	1	Tr	-	-	-	-	-	Tr	6	2	-	-	-	-	-	-	-
	4937.67	Mamuniyat	F.S	C.S	V.C.S	MWS	SR - R	21	15	-	6	-	-	Sublitharenite	83	6	3	1	Tr	-	Tr	-	-	-	1	3	2	-	-	-	-	-	-	-
	5010.31	Mamuniyat	F.S	C.S	V.C.S	MWS	SA - SR	18	13	-	5	-	-	Sublitharenite	77	7	2	2	1	1	-	-	-	-	Tr	5	2	1	2	-	-	-	-	-
B3	4650.21	Mamuniyat	F.S	V.C.S	C.S	MWS	SR	21	15	-	6	-	-	Sublitharenite	81	4	2	2	1	-	-	-	-	-	Tr	6	2	Tr	-	-	-	-	-	-
	4685.15	Mamuniyat	F.S	C.S	V.C.S	MWS	R - SR	24	17	-	7	-	-	Sublitharenite	82	5	2	2	1	-	-	-	-	-	Tr	5	2	1	-	-	-	-	-	-
	4720.08	Mamuniyat	F.S	C.S	V.C.S	WS	SR - R	23	16	-	7	-	-	Sublitharenite	85	5	2	1	1	-	1	-	-	-	-	5	-	-	-	-	-	-	-	-
	4752.51	Mamuniyat	F.S	C.S	V.C.S	MWS	R - SR	21	16	-	5	-	-	Sublitharenite	85	7	4	1	Tr	-	Tr	-	-	-	-	2	-	-	-	-	-	-	-	-
	4775.53	Mamuniyat	F.S	V.C.S	V.C.S	WS	R - SR	20	15	-	5	-	-	Sublitharenite	83	6	4	1	1	-	Tr	-	-	-	-	4	-	-	-	-	-	-	-	1
	4798.92	Mamuniyat	F.S	C.S	G	VWS	SR - R	23	18	-	5	-	-	Sublitharenite	80	12	4	Tr	-	Tr	1	-	-	-	-	3	-	-	-	-	-	-	-	Tr
	4848.86	Mamuniyat	F.S	C.S	V.C.S	WS	SR - R	23	15	-	8	-	-	Sublitharenite	70	16	4	1	Tr	2	1	-	-	-	-	4	-	-	-	-	-	-	1	1
	4877.60	Mamuniyat	F.S	V.C.S	M.S	WS	SR	20	9	-	11	-	-	Sublitharenite	80	5	2	1	1	-	1	-	-	-	-	5	4	-	-	-	-	-	-	-
	4922.35	Mamuniyat	F.S	C.S	V.C.S	WS	SR - R	21	18	-	3	-	-	Sublitharenite	75	10	4	1	-	1	Tr	-	-	-	-	4	1	-	-	-	-	-	3	1
	4962.80	Mamuniyat	M.S	C.S	G	WS	SR - R	22	17	-	5	-	-	Sublitharenite	79	7	5	1	-	-	1	-	-	-	-	5	1	-	-	-	-	-	-	1
	5075.40	Mamuniyat	F.S	C.S	V.C.S	WS	SA - SR	25	18	-	7	-	-	Sublitharenite	70	10	5	2	2	2	-	-	-	-	Tr	5	4	-	-	-	-	-	-	½
B8	4646.35	Mamuniyat	F.S	C.S	G	WS	R - SR	20	15	-	5	-	-	Litharenite	60	20	12	-	-	-	-	-	-	-	-	3	Tr	-	-	-	-	-	1	4
	4646.60	Mamuniyat	M.S	M.S	G	VWS	SR - R	25	19	-	6	-	-	Litharenite	57	21	11	1	-	-	1	-	-	-	Tr	3	2	-	-	-	-	-	2	1
	4719.55	Mamuniyat	M.S	C.S	V.C.S	WS	SR - R	17	13	-	4	-	-	Sublitharenite	79	12	4	1	Tr	-	1	-	-	-	-	1	-	-	-	-	-	-	-	1
	4748.83	Mamuniyat	F.S	V.C.S	C.S	MWS	SA - SR	12	7	-	5	-	-	Sublitharenite	70	5	3	2	2	1	-	-	-	-	-	5	3	-	10	-	-	-	-	-
	4772.17	Mamuniyat	F.S	V.C.S	C.S	WS	SA - SR	8	5	-	3	-	-	Sublitharenite	70	10	5	2	1	-	1	-	-	-	Tr	5	3	-	3	-	-	-	-	-
	4784.55	Mamuniyat	F.S	C.S	V.C.S	WS	SR	18	13	-	5	-	-	Sublitharenite	79	5	3	2	1	-	1	-	-	-	Tr	5	3	-	-	-	-	-	-	-
	4806.00	Mamuniyat	F.S	V.C.S	C.S	WS	SR	10	6	-	4	-	-	Sublitharenite	70	10	5	2	1	-	1	-	-	-	Tr	6	3	-	1	-	-	-	-	-
	4815.00	Mamuniyat	F.S	V.C.S	C.S	MWS	SR	8	5	-	3	-	-	Sublitharenite	75	5	3	1	1	-	1	-	-	-	2	5	3	-	3	-	-	-	-	-
	4864.50	Mamuniyat	F.S	C.S	V.C.S	MWS	SR - R	20	13	-	7	-	-	Sublitharenite	80	6	3	1	1	-	Tr	-	-	-	1	4	3	-	-	-	-	-	-	-
	4912.00	Mamuniyat	F.S	V.C.S	C.S	MWS	SR - R	18	13	-	5	-	-	Sublitharenite	85	3	2	1	-	2	1	-	-	-	1	3	2	-	-	-	-	-	-	-
	5650.00	Mamuniyat	F.S	V.C.S	C.S	MWS	SR - R	5	3	-	2	-	-	Lithic greywacke	60	6	1	1	1	-	Tr	-	-	-	1	2	2	-	25	-	-	-	-	-
B27	4776.00	Mamuniyat	F.S	M.S	V.C.S	VWS	R - SR	20	16	-	4	-	-	Litharenite	65	24	6		-	-	1	-	-	-	-	2	-	-	-	1	-	-	-	1
	4849.50	Mamuniyat	F.S	V.C.S	C.S	WS	SR - R	23	17	-	6	-	-	Sublitharenite	88	3	2	1	-	1	Tr	-	-	-	-	3	Tr	-	-	Tr	-	-	Tr	1

Table: 3.2

Model Composition of samples from the Mamuniyat Formation, H-Field, NC115 Concession, Murzuq Basin, SW Libya.

WELL	DEPTH ft. (kb)	GEOLOGICAL FORMATION	TEXTURAL DATA					PORE TYPE (%)						CLASSIFICATION (Pettijohn et al., 1987)	POINT COUNTED DATA																					
			GRAIN SIZE			GRAIN SORTING	GRAIN ROUNDNESS	Porosity (%)	Primary (Intergranular)	Secondary					MINERALS COMPONENTS (%)							CEMENT (%)								OTHER					
																						AUTHIGENIC MINERAL				AUTHGENIC CLAY MINERAL									
			Minimum size	Mean size	Maximum size					Intragranular	Dissolution	Microporosity	Fracture		MONOCRYSTALLINE QTZ.	POLYCRYSTALLINE QTZ.	ROCK FRAGMENT	HEAVY MINERALS	MUSCOVITE MICA	FELDSPAR	CHERT	NON FERRO DOLOMITE	FERRO DOLOMITE	CALCITE	DOLOMITE	KAOLINITE CLAY	SERICITE / ILLITE CLAYS	CHLORITE CLAY	MATRIX	PYRITE	MAGNETITE	BARITE	BITUMEN	DRILLING MUD SOLIDS
H2	4872.81	Mamuniyat	F.S	C.S	V.C.S	MWS	SR - R	24	17	-	7	-	-	Sublitharenite	82	5	6	2	1	-	-	-	-	-	-	3	1	-	-	-	-	-	-	-
	4885.60	Mamuniyat	F.S	C.S	V.C.S	WS	R - SR	24	18	-	6	-	-	Sublitharenite	85	3	2	2	1	-	-	-	-	-	-	2	1	1	-	Tr	-	-	-	1
	4912.67	Mamuniyat	F.S	C.S	C.S	WS	SA - R	25	20	-	5	-	-	Sublitharenite	85	3	3	3	1	-	-	-	-	-	-	2	2	-	-	1	-	-	-	-
	4939.24	Mamuniyat	F.S	V.C.S	C.S	MWS	SA - R	23	19	-	4	-	-	Sublitharenite	84	5	2	3	1	-	-	-	-	-	-	1	1	1	-	-	-	-	-	1
	4979.60	Mamuniyat	F.S	V.C.S	C.S	MWS	SA - R	24	20	-	4	-	-	Sublitharenite	80	5	4	3	1	-	-	-	-	-	-	2	Tr	3	-	Tr	-	-	-	1
	5127.89	Mamuniyat	F.S	V.C.S	C.S	WS	SA - R	15	10	-	5	-	-	Sublitharenite	81	5	3	3	1	-	-	-	-	-	2	1	1	2	-	-	-	-	-	Tr
H3	4719.43	Mamuniyat	F.S	V.C.S	C.S	WS	SR - R	5	4	-	1	-	-	Sublitharenite	60	7	4	4	3	1	-	-	-	-	1	6	-	3	11	-	-	-	-	Tr
	4750.60	Mamuniyat	F.S	V.C.S	C.S	WS	SR - R	10	8	-	2	-	-	Sublitharenite	61	7	5	2	2	1	-	-	-	-	Tr	5	-	3	11	-	-	-	-	-
	4793.25	Mamuniyat	F.S	V.C.S	M.S	WS	R - SR	2	2	-	0	-	-	Sublitharenite	58	5	5	2	6	1	-	-	-	-	-	5	-	2	15	-	-	-	-	-
	4845.74	Mamuniyat	F.S	V.C.S	C.S	MWS	SR - R	4	3	-	1	-	-	Sublitharenite	66	5	5	3	3	1	-	-	-	-	1	3	-	Tr	13	-	-	-	-	-
	4863.79	Mamuniyat	F.S	V.C.S	C.S	WS	SR - R	24	18	-	6	-	-	Sublitharenite	82	5	2	2	2	-	-	-	-	-	-	5	-	1	-	-	-	-	-	Tr
	4910.54	Mamuniyat	F.S	V.C.S	C.S	MWS	SR - R	22	16	-	6	-	-	Sublitharenite	80	4	5	1	2	-	-	-	-	-	-	6	-	1	-	-	-	-	-	Tr
	4921.20	Mamuniyat	F.S	V.C.S	M.S	WS	SR - R	24	19	-	5	-	-	Sublitharenite	83	4	2	2	2	-	-	-	-	-	-	4	1	1	-	-	-	-	-	Tr
	5001.58	Mamuniyat	F.S	V.C.S	C.S	MWS	R - SR	24	20	-	4	-	-	Sublitharenite	82	3	3	2	1	-	-	-	-	-	-	2	-	1	-	-	-	-	5	Tr
	5163.98	Mamuniyat	F.S	V.C.S	M.S	WS	SR	10	8	-	2	-	-	Sublitharenite	78	4	2	2	2	-	-	-	-	-	1	8	-	2	-	-	-	-	-	Tr
H4	4852.35	Mamuniyat	F.S	C.S	V.C.S	WS	R - SR	23	18	-	5	-	-	Sublitharenite	85	5	4	Tr	Tr	-	-	-	-	-	-	3	Tr	2	-	-	-	-	-	-
	4863.00	Mamuniyat	F.S	C.S	C.S	WS	R - SA	24	20	-	4	-	-	Sublitharenite	86	3	3	1	1	-	Tr	-	-	-	-	3	2	-	-	-	-	-	-	-
	4900.00	Mamuniyat	F.S	V.C.S	C.S	WS	SR - SA	25	20	-	5	-	-	Sublitharenite	80	3	3	2	2	Tr	-	-	-	-	2	5	2	-	-	-	-	-	-	-
	4913.50	Mamuniyat	F.S	V.C.S	C.S	WS	SA - SR	24	20	-	4	-	-	Sublitharenite	80	5	4	2	2	-	Tr	-	-	-	Tr	4	-	1	-	1	-	-	-	-
	4925.00	Mamuniyat	F.S	C.S	C.S	WS	R - SR	21	17	-	4	-	-	Sublitharenite	83	4	3	1	1	-	Tr	-	-	-	2	3	2	-	-	1	-	-	-	-
	4974.00	Mamuniyat	F.S	V.C.S	M.S	WS	R - SR	20	16	-	4	-	-	Sublitharenite	85	4	2	2	2	-	-	-	-	-	1	2	1	Tr	-	1	-	-	-	-
	4988.50	Mamuniyat	F.S	V.C.S	M.S	WS	SR	12	10	-	2	-	-	Sublitharenite	81	3	3	1	2	-	-	-	-	-	1	5	2	1	-	Tr	-	-	-	-
	5002.00	Mamuniyat	F.S	V.C.S	C.S	MWS	SR - R	19	16	-	3	-	-	Sublitharenite	86	3	2	2	2	-	-	-	-	-	Tr	2	1	1	-	1	-	-	-	-
	5006.00	Mamuniyat	F.S	V.C.S	C.S	MWS	SR - R	17	14	-	3	-	-	Sublitharenite	86	3	2	2	Tr	-	Tr	-	-	-	-	2	-	1	-	1	-	-	-	3
H5	4823.50	Mamuniyat	F.S	V.C.S	C.S	WS	SR	15	13	-	2	-	-	Sublitharenite	80	5	2	1	1	-	-	-	-	-	3	5	2	1	-	Tr	-	-	-	-
	4842.30	Mamuniyat	F.S	V.C.S	M.S	MWS	SR	2	2	-	0	-	-	Sublitharenite	60	4	3	Tr	2	Tr	-	-	-	-	-	13	7	1	10	-	-	-	-	-
	4871.75	Mamuniyat	F.S	V.C.S	C.S	WS	SR - R	6	5	-	1	-	-	Sublitharenite	75	4	3	1	1	-	-	-	-	-	1	3	2	1	8	-	-	-	-	-
	4884.50	Mamuniyat	F.S	V.C.S	C.S	WS	R - SR	18	15	-	3	-	-	Quartz arenite	80	4	2	1	1	-	-	-	-	-	2	4	2	2	2	-	-	-	-	-
	4922.75	Mamuniyat	F.S	V.C.S	C.S	WS	SR - R	21	19	-	2	-	-	Sublitharenite	82	4	2	1	1	-	-	-	-	-	-	4	3	1	-	-	-	-	1	-
	4962.00	Mamuniyat	F.S	V.C.S	M.S	WS	R - SR	19	16	-	3	-	-	Quartz arenite	88	3	1	Tr	1	-	-	-	-	-	-	4	2	1	-	-	-	-	-	-
	4986.00	Mamuniyat	F.S	V.C.S	M.S	WS	SR - R	23	20	-	3	-	-	Quartz arenite	89	3	1	Tr	1	-	Tr	-	-	-	-	2	3	1	-	-	-	-	-	-
	4992.00	Mamuniyat	F.S	V.C.S	M.S	WS	SR - R	20	16	-	4	-	-	Quartz arenite	91	2	1	Tr	1	-	-	-	-	-	-	3	2	-	-	-	-	-	-	-
	4997.00	Mamuniyat	F.S	V.C.S	M.S	WS	SR - R	14	13	-	1	-	-	Quartz arenite	88	2	1	Tr	Tr	-	-	-	-	-	Tr	2	2	-	-	-	-	-	5	-
	5000.50	Mamuniyat	F.S	V.C.S	M.S	MWS	SA - R	4	3	-	1	-	-	Sublitharenite	60	6	3	1	5	3	-	-	-	-	1	7	-	-	14	-	-	-	-	-
	5011.00	Mamuniyat	F.S	V.C.S	C.S	MWS	SR - R	23	18	-	5	-	-	Quartz arenite	92	1	1	1	1	Tr	-	-	-	-	1	2	1	-	-	-	-	-	-	-

Table: 3.3

PLATE: 3.1A.

Photomicrograph of medium-grained, moderately well sorted Lower Mamuniyat sublitharenite (K10-H10), B-Field, showing monocrystalline, rounded to subrounded quartz grains cemented by quartz overgrowths in optical continuity with detrital grains. The thin section also shows bright brown colour detrital grains of muscovite (I4-B3). XPL (X 4). Sample No. 14.

PLATE: 3.1B.

Photomicrograph of medium-grained, well sorted Lower Mamuniyat quartz arenite (D8-A9). The thin section shows a polycrystalline metamorphic quartz grain (G6-D7), H-Field. XPL (X 10). Sample No. 35.

PLATE 3.1 A & B

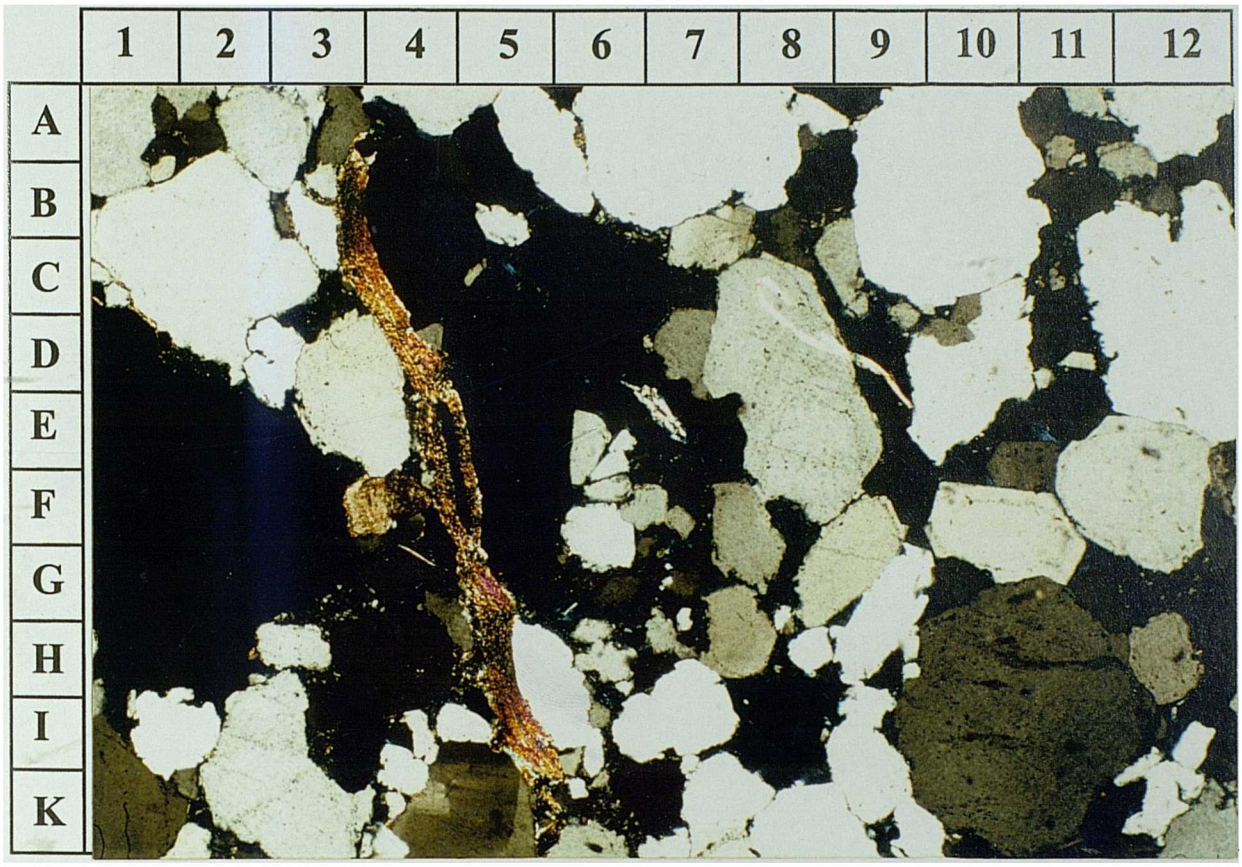

Well: B2-NC115 **Depth: 4828.52 Ft.**

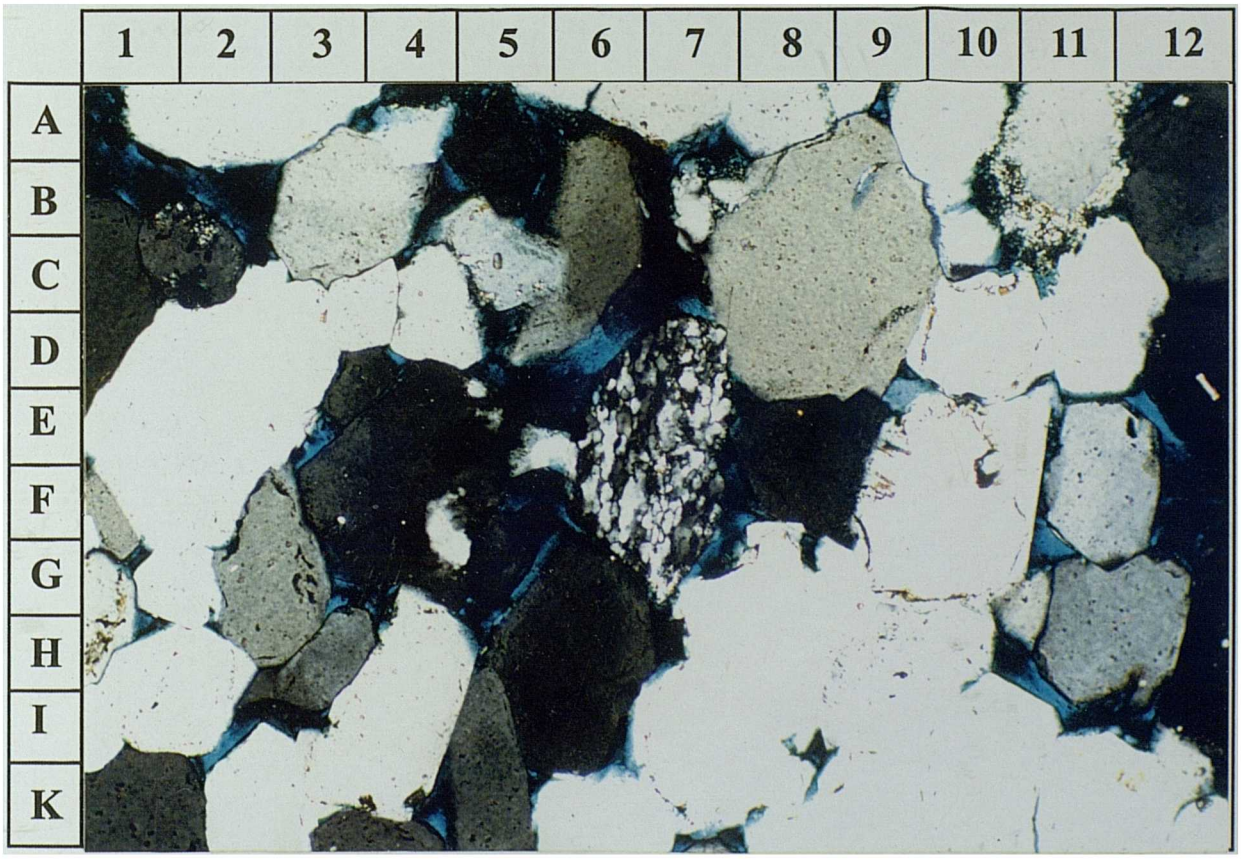

Well: H5-NC115 **Depth: 4884.50 Ft.**

PLATE: 3.2A.

Photomicrograph of Upper Mamuniyat sandstone, B-Field, showing quartz overgrowths (H9-C6) with well developed crystal face. Clay rims occur around detrital quartz grains. XPL (X 10). Sample No. 27.

PLATE: 3.2B.

Photomicrograph of Lower Mamuniyat sandstone showing monocrystalline quartz grains (C3 and B8) with subordinate amounts of polycrystalline quartz grains. XPL (X 10). Sample No. 15.

PLATE 3.2 A & B

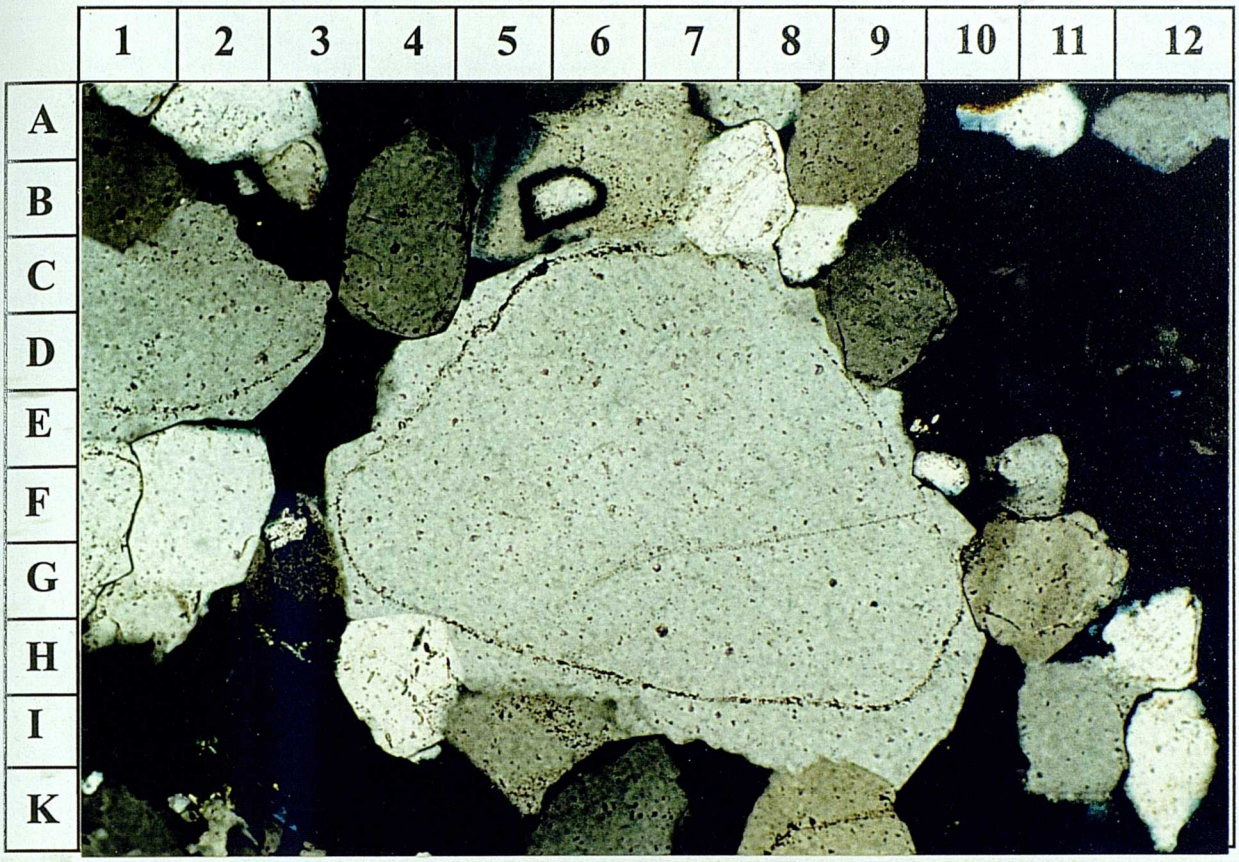

Well: B27-NC115 **Depth: 4849.50 Ft.**

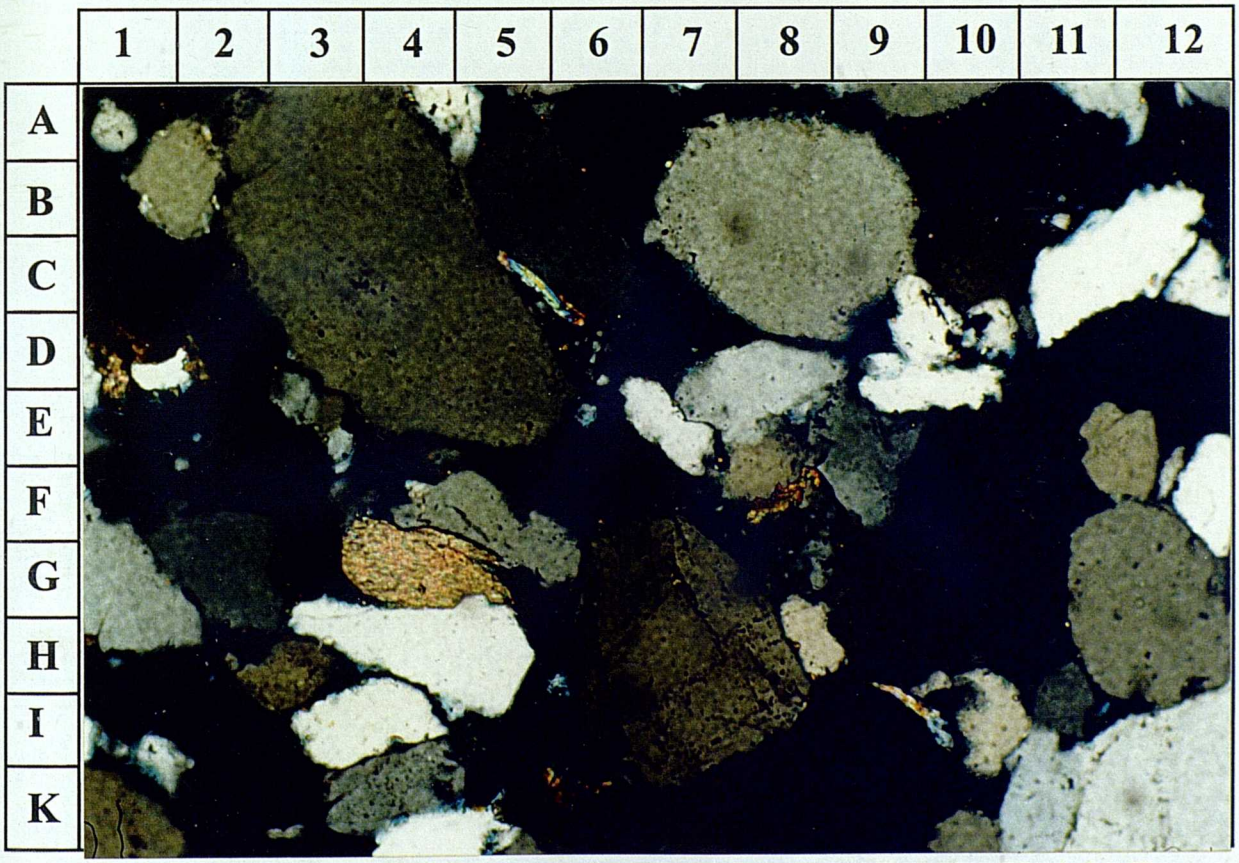

Well: B2-NC115 **Depth: 5010.31 Ft.**

PLATE: 3.3A.

Photomicrograph of Upper Mamuniyat sandstone showing secondary calcite displacing detrital quartz grains, so that the latter appear to "float" in the cement (G7-A9) (I4-D4). XPL (X 10). Sample No. 24.

PLATE: 3.3B.

Photomicrograph of Upper Mamuniyat Formation, B-Field, showing primary porosity (H6-G6) and secondary pore space porosity (F6-A7) (porosity shown with dark blue stained epoxy resin). XPL (X 10). Sample No. 8.

PLATE 3.3 A & B

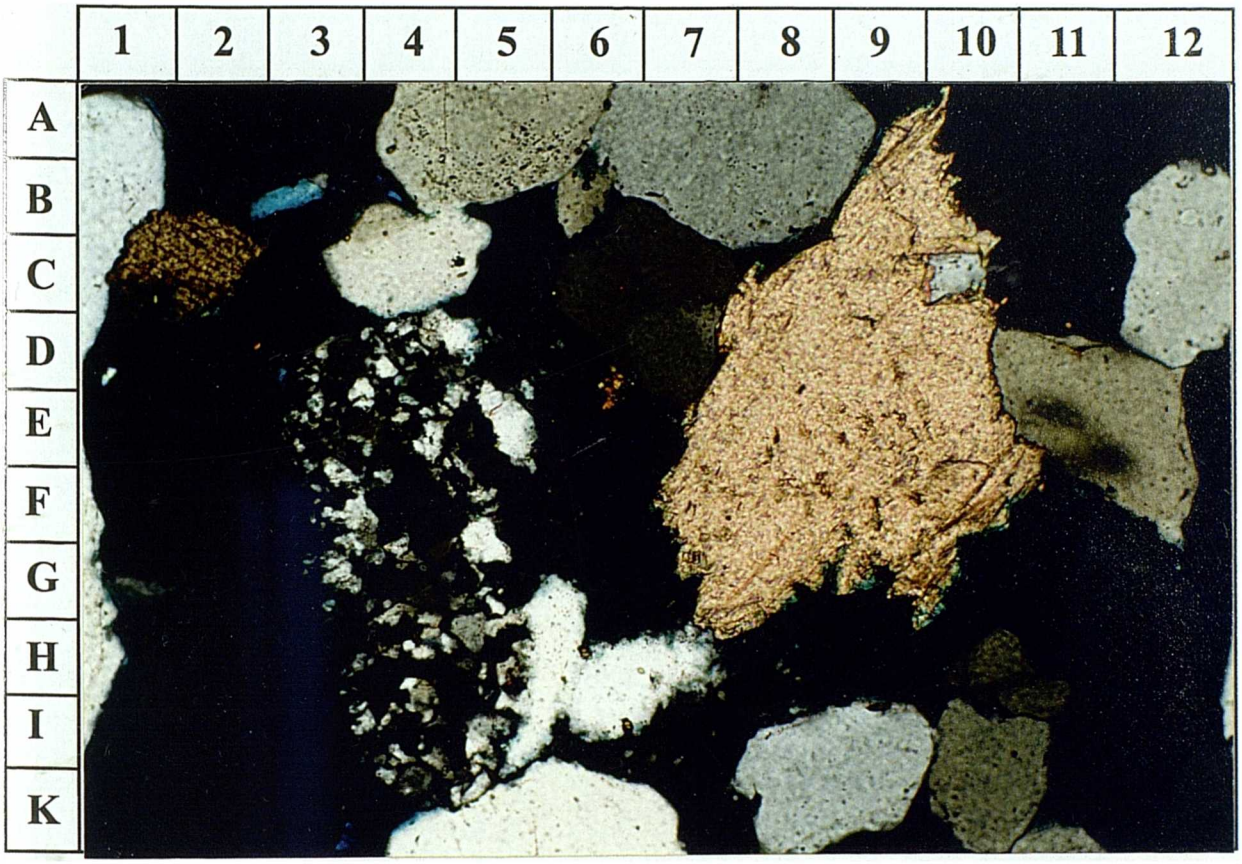

Well: B8-NC115 **Depth: 4784.55 Ft.**

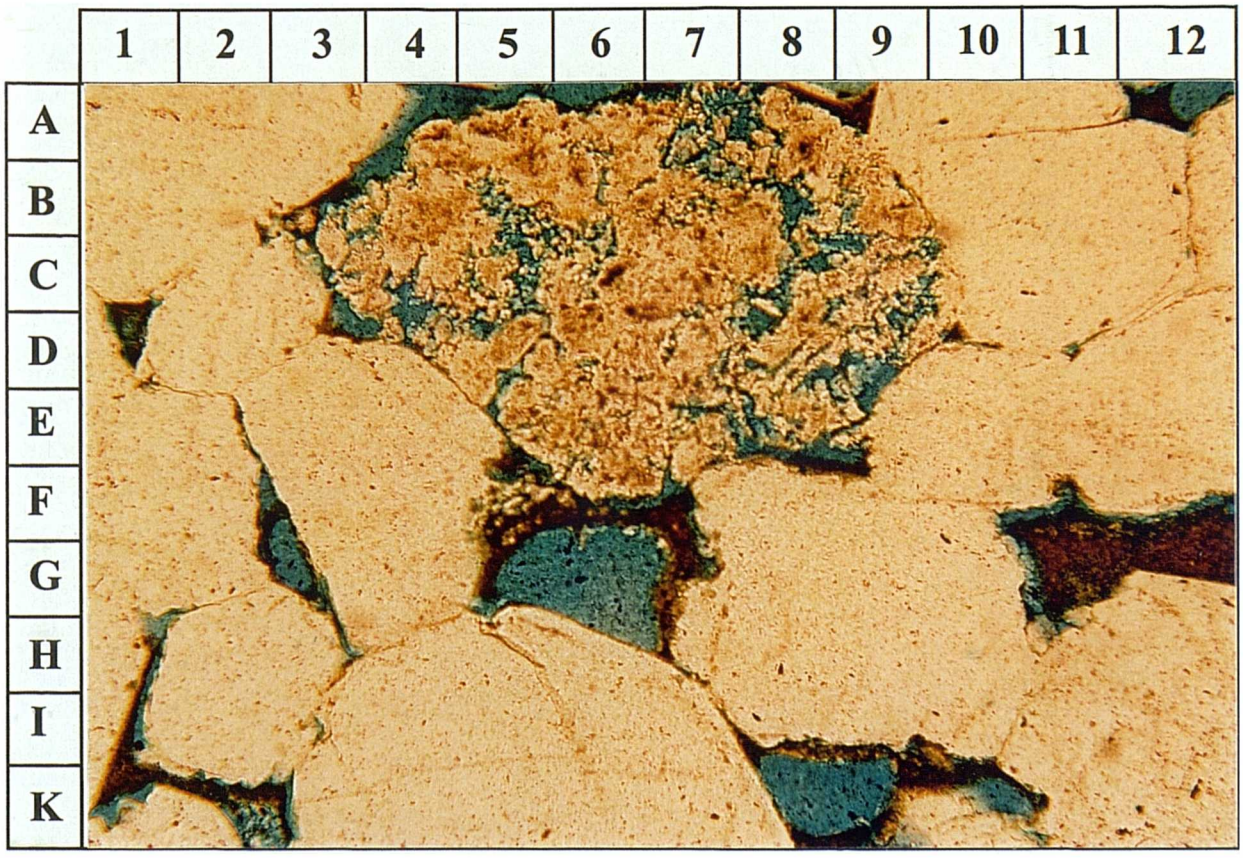

Well: B2-NC115 **Depth: 4667.00 Ft.**

PLATE: 3.4A.

Photomicrograph of Upper Mamuniyat sandstone, showing polycrystalline quartz grains (H7-A7) and coarse quartz grains with secondary overgrowths (E6, D7 and B7). XPL (X 10). Sample No. 16.

PLATE: 3.4B.

Photomicrograph of Lower Mamuniyat sandstone showing zircon grain (E3-D3) with strong to extreme birefringence and positive elongation. Zircon virtually never shows alteration but inclusions are common. XPL (X 10). Sample No. 36.

PLATE 3.4 A & B

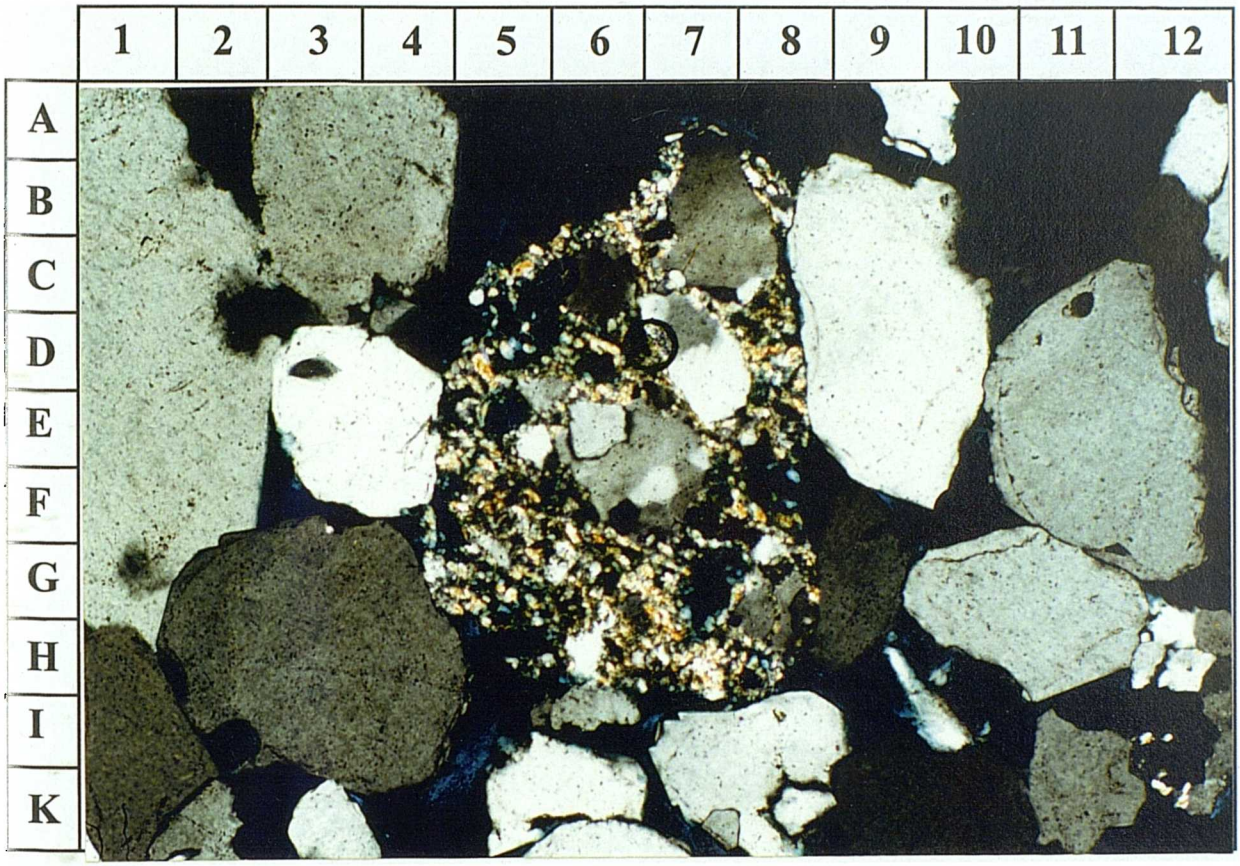

Well: B3-NC115 **Depth: 4752.51 Ft.**

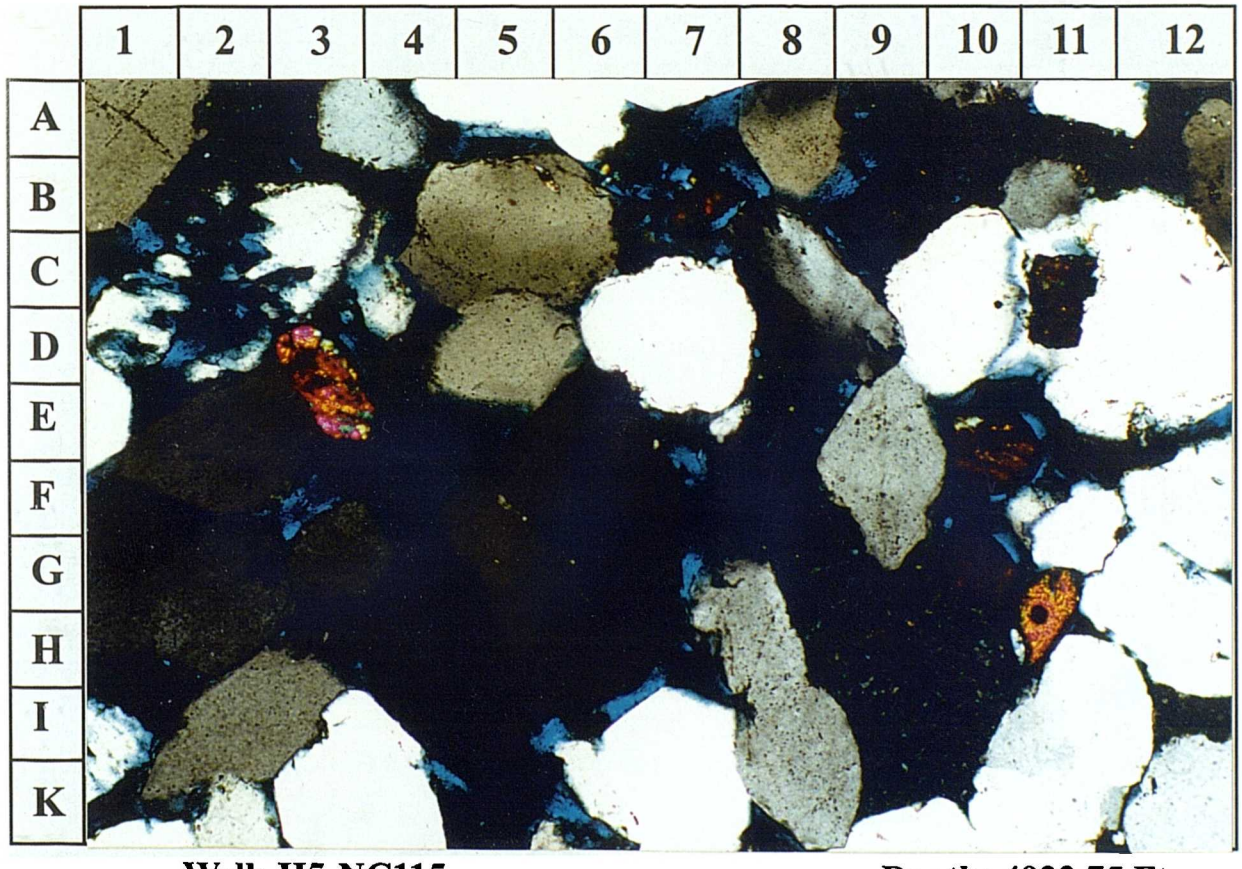

Well: H5-NC115 **Depth: 4922.75 Ft.**

PLATE: 3.5A.

Photomicrograph of Lower Mamuniyat sandstone showing a rounded tourmaline grain (E6-E7), characterized by moderate to strong birefringence and very poor cleavage, high relief and brown colour with extreme pleochroism (goes completely black with rotation of stage). PPL (X 10). Sample No. 7.

PLATE: 3.5B.

Photomicrograph of Lower Mamuniyat sandstone, H-Field showing a patch of saddle dolomite cement (E8-D6 and C6-B5). Pore-filling bitumen can be seen at (B3-A1). XPL (X 10). Sample No. 37.

PLATE 3.5 A & B

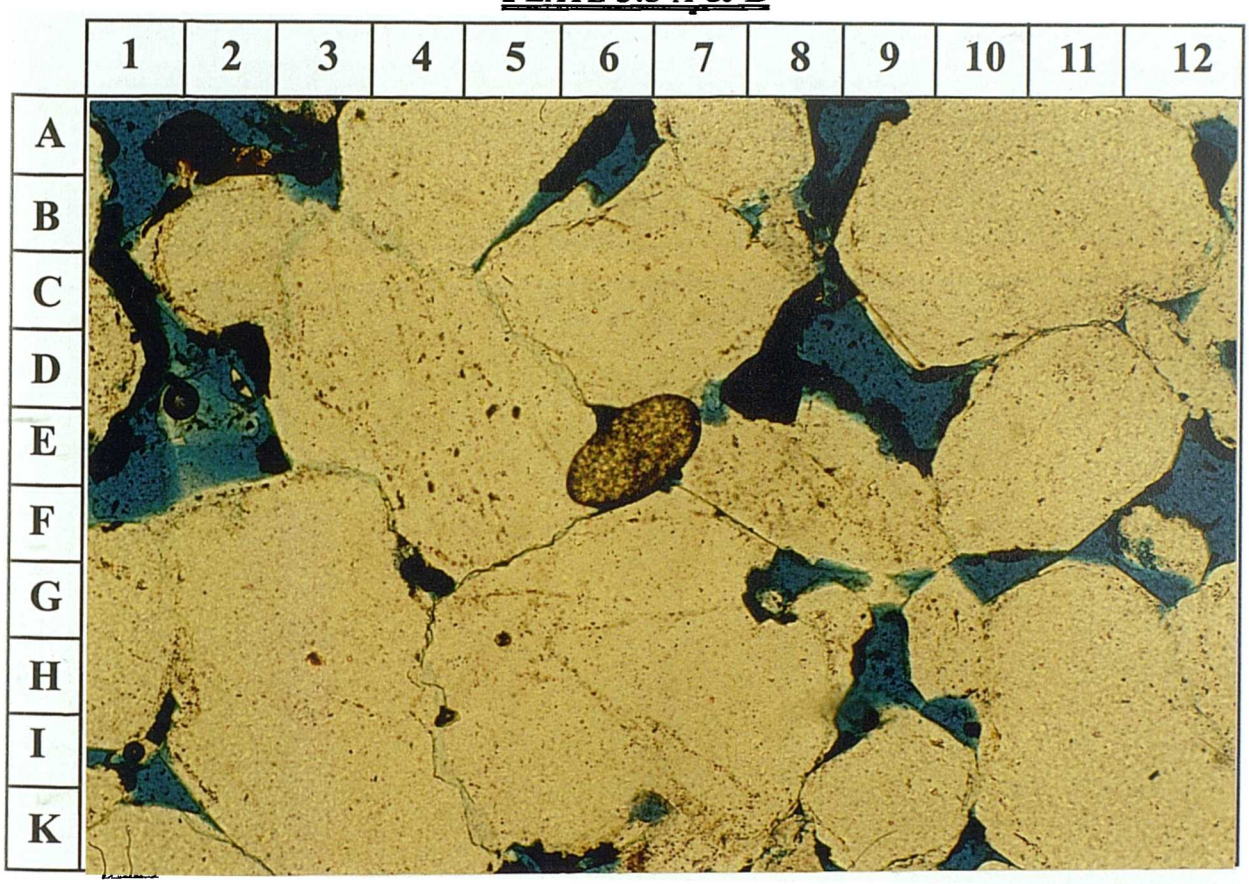

Well: A4-NC115 **Depth: 5028.15 Ft.**

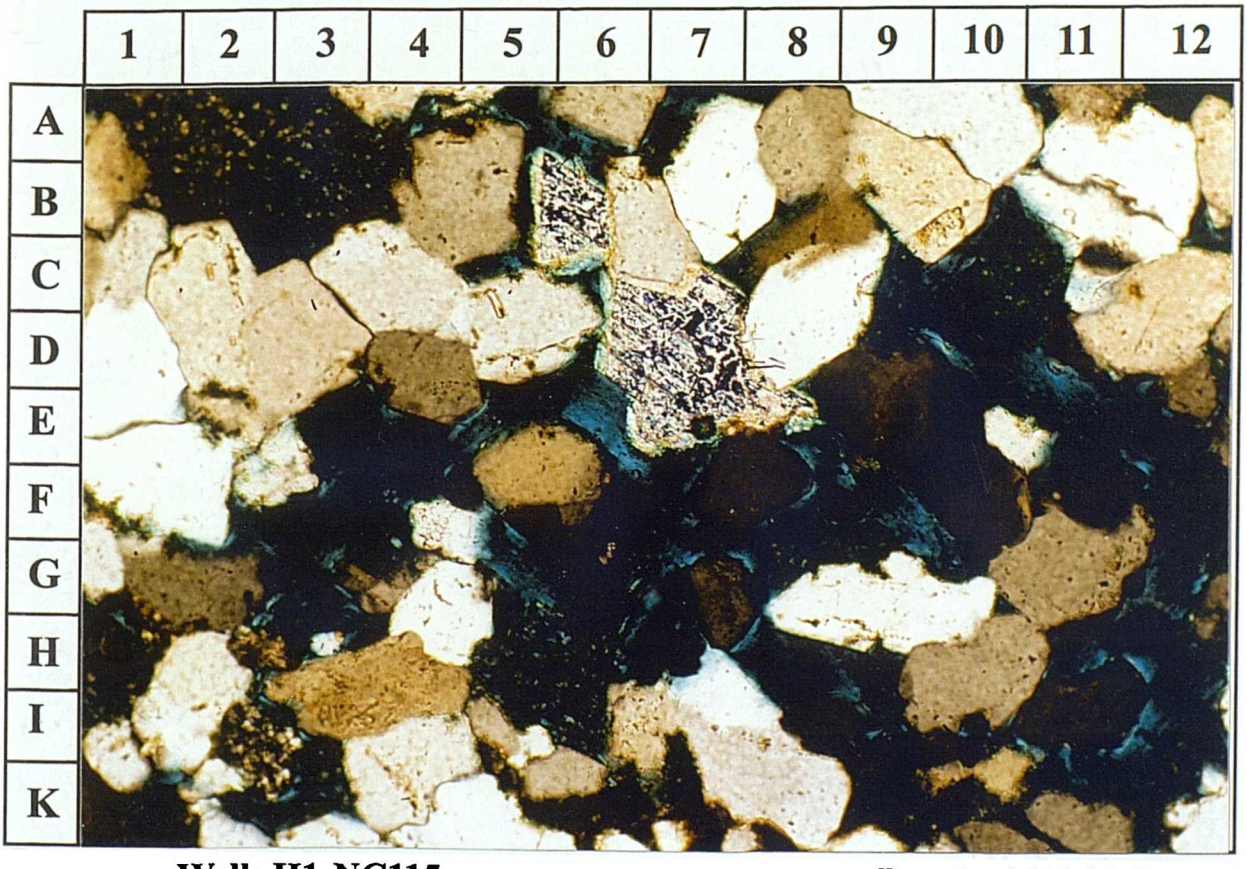

Well: H1-NC115 **Depth: 4671.20 Ft.**

PLATE: 3.6A.

Photomicrograph of Lower Mamuniyat sandstone, B-Field, showing detrital chert grain (F8-D7). XPL (X 10). Sample No. 13.

PLATE: 3.6B.

Photomicrograph of Lower Mamuniyat sandstone, B-Field, showing high primary porosity (blue stain) and pore-filling bitumen (black color) (E6-B7). PPL (X 4). Sample No. 25.

PLATE 3.6 A & B

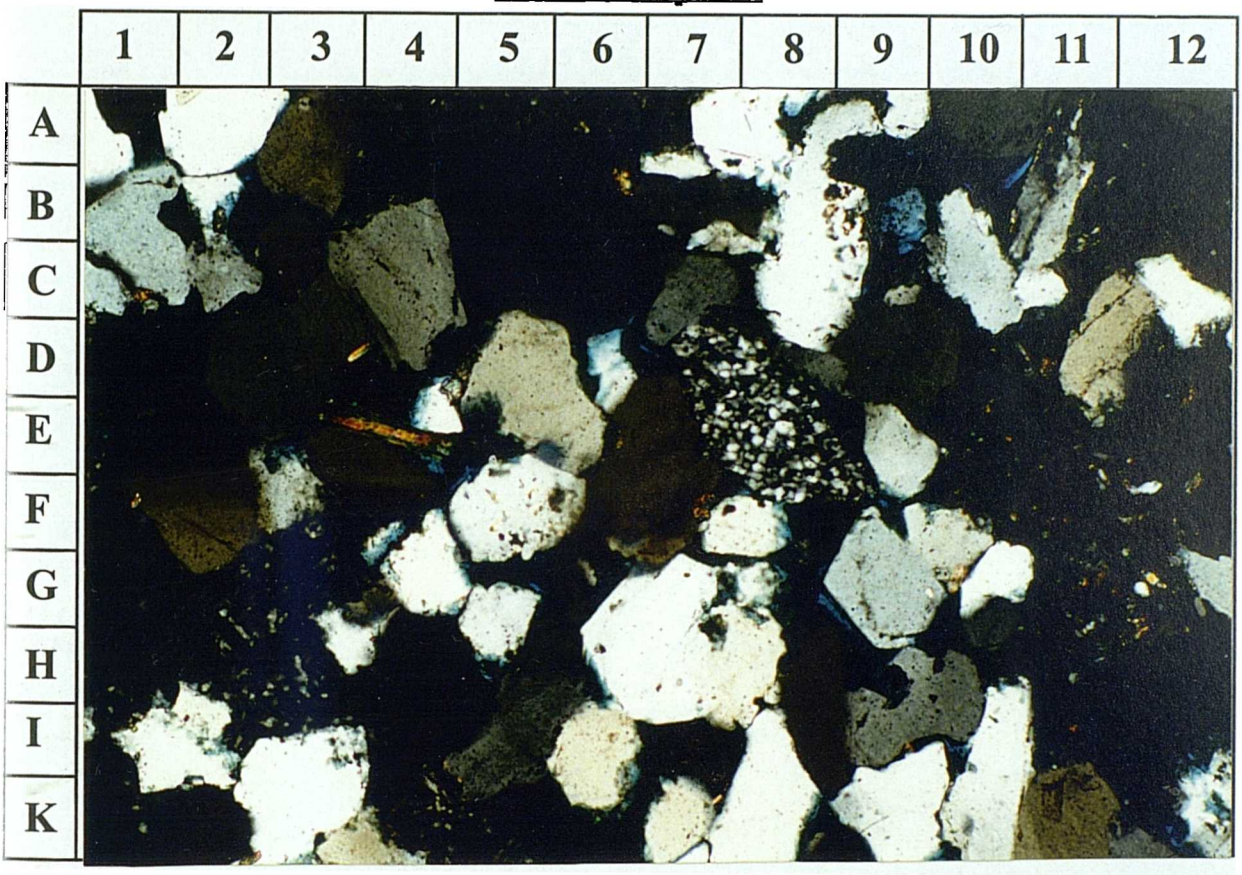

Well: B2-NC115 **Depth: 4720.74 Ft.**

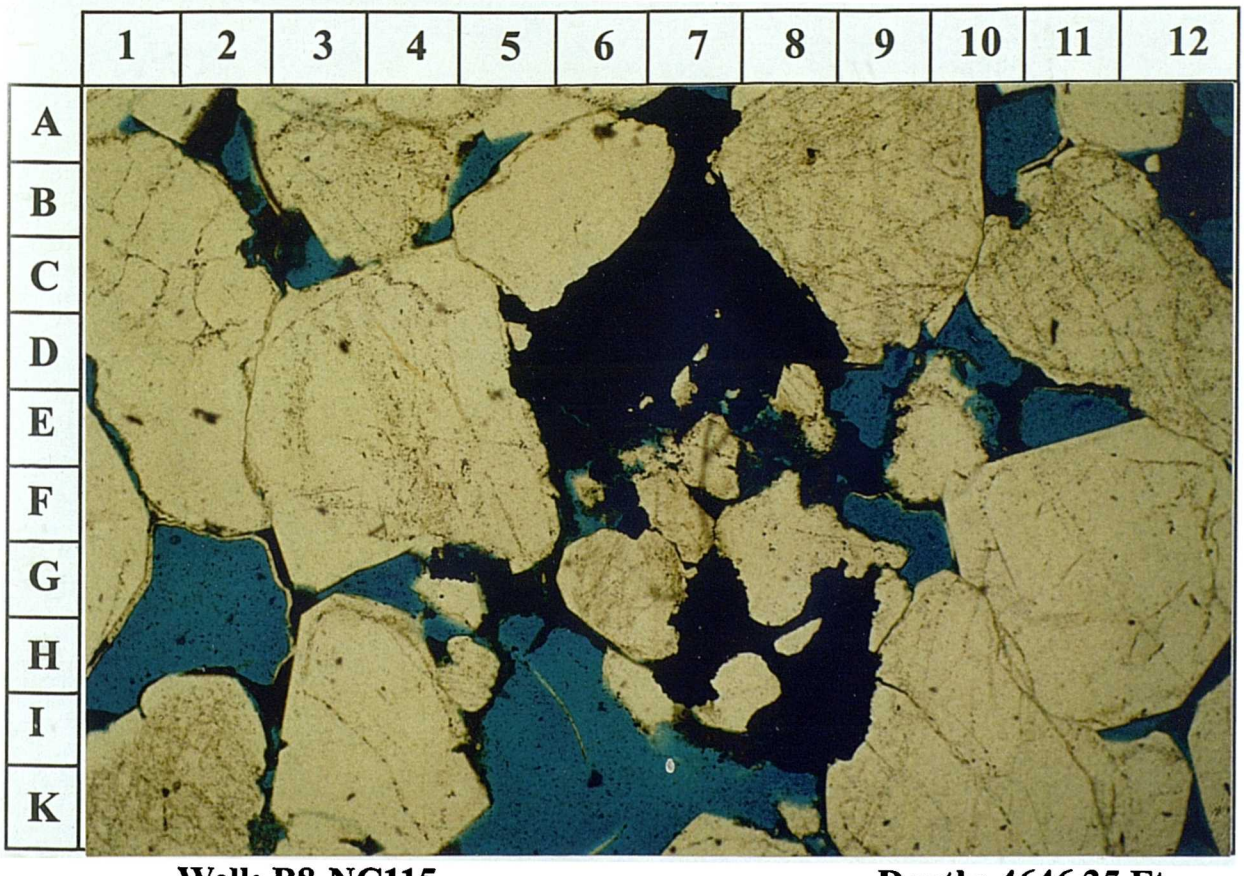

Well: B8-NC115 **Depth: 4646.35 Ft.**

CHAPTER 4

TEXTURAL PROPERTIES

TEXTURAL PROPERTIES

4.1 Introduction

4.1.1 Objectives

The term "textural properties of sandstone" refers to the size, shape (sphericity or form), roundness, grain surface features and fabric (packing and orientation) of grains (Pettijohn, 1975). Of these properties the size distribution of detrital clastic sediments has been most intensively studied in order to obtain information about the dynamic conditions of transport, and the depositional environment. One of the main objectives of textural research has been to identify the physical processes operating at the site of deposition from the textural characteristics of the sandstone (Visher, 1969).

Textural analysis in the Mamuniyat Formation sandstones includes quantitative data on the size, shape, surface texture, and the orientation of the grains. These fundamental data are then related to the physical processes and the depositional environment throughout A, B and H-Fields.

4.2 Grain-size

The term grain-size refers to the size of mineral particles that make up a rock or sediment. Although it is one of the most widely used terms in sedimentology the "size" of a particle is not uniquely defined except perhaps for only the most simple of geometric objects such as a sphere (diameter) or a cube (length of an edge) (Pettijohn *et al.*, 1987). Grain-size depends on the character of the source rocks, weathering processes, abrasion, and selective sorting during transportation (Lewis, 1983).

Generally, the number of grains to be counted per thin-section by most investigators is between 200 and 500 grains (Krumbein, 1935). Possibly as few as 100 to 200 measurements are necessary for a single analysis to satisfy specified confidence limits of the mean (Rosenfeld, 1950)

4.2.1 Techniques

For silica-cemented sandstones such as the Mamuniyat sandstones, the most suitable method for determining grain-size is in thin section under the microscope using a micrometer eyepiece graticule and point counter. A review of these techniques is given by McManus (1988).

A minimum of 150 grains must be measured for statistical accuracy. The long diameter of the sand grains was measured in each thin section and then grouped into 0.25ϕ classes, and the number frequency in percent plotted as a cumulative curve on arithmetic probability paper. This has the disadvantage that the grain diameters obtained from thin sections are not truly representative of the diameters of the loose grains due to the effects of random sectioning (Krumbein, 1935). Moreover, the efficiency of thin section analysis decreases from coarse to fine grades (Muller, 1967).

Experiments with completely spherical lead shot of uniform size embedded in wax on a glass slide show that the average radius computed from observed data was 0.763 of the actual radius. Thus, a correction factor must be used in order to convert grain-size in thin-section to that obtained by sieving. Even in rock studies by thin-section, non-homogeneity can be observed and taken into account when performing size analysis. For this purpose thin-sections or polished sections should always be cut perpendicular to bedding (Carver, 1971). One hundred and fifty grains per thin section were measured from A, B and H-Fields, respectively for comparative purposes. The results of the grain-size analysis were the corrected to their sieve equivalents according the method of Friedman and Sanders (1978).

4.2.2 Grain-size measurement

All methods of grain-size measurement are based on the premise that the constituent particles are spheres or that the measurements made can be expressed as diameters of equivalent spheres. Direct measurements of the particle diameter are commonly made, although the irregular shape of the fragment creates difficulties. Thus the measure chosen will reflect the object of study as well as the technique used. In general, one measure of size converts to another by expressing it in terms of a corresponding equivalent diameter. Unless otherwise specified, the term "size" as here used is the diameter of the grain in "mm" (Pettijohn *et al.*, 1987). Tables for conversion of millimetres to phi units have been published by Page (1955) and a program for the conversion on a programmable calculator by Lindholm (1979). Measurement of grain-size in loose grains has been described by Plumley (1948) who proposed a mounting technique, which permits three-dimensional measurement of sand grains.

The standard procedure for grain-size measurements under the microscope is to use an average intermediate grain length as the size. This may or may not be clearly related to factors such as transportability, settling velocity, or mass. Some detrital rocks have two pronounced sizes (bimodal), and this should be mentioned in the description of grain-size. The distribution of grain-sizes includes approximately two-thirds of the grains and it is normally expressed in phi units.

The phi symbol ϕ as originally adopted by Krumbein (1934), is used to denote a grade scale in which all divisions are equal in range. This adapts the grade scale for plotting grain-size data on arithmetic probability graph paper. The most common method is to use an ocular micrometer, which has been calibrated to the metric system with a stage micrometer. One could measure the largest apparent dimension by projecting the thin-section on a screen or from photomicrographs, but these methods involve one or more extra preparatory steps (Carver, 1971).

Grains-size investigation usually measure the largest apparent dimension of the grain (Krumbein, 1935; Rosenfeld, 1950; Friedman, 1958), or at least they choose a unique axis so that different rocks or sediments can be compared (Griffiths, 1961). Generally, measurements are usually recorded in millimetres or microns and then converted to phi (ϕ) units and plotted on graph paper. The size frequency distribution obtained in this way is a number frequency, and not a weight frequency as is obtained in sieved samples.

The estimation of errors inherent in grain-size analysis was first proposed by Wentworth (1933) and subsequently the sampling error was evaluated by Krumbein (1934). The last mentioned approach is of interest because of its general application to this, and other experimental techniques. Krumbein indicated that there were many sources of variation in grain-size analyses and strictly speaking there are many factors contributing to the variation, which were specifically cited by Krumbein (1935). These include sampling error, which is a function of homogeneity of the sediment, locality collected, kind of sampling (*e.g.* one phase, composite, *etc.*) and laboratory error.

The term "error" is used here in its statistical sense meaning variation and does not imply mistake although it will certainly include variations due to "mistakes". The difference between samples in terms of median diameters are still not significantly greater than the difference due to experimental procedure but the magnitude of variation has been very markedly reduced. Krumbein next reduced these errors to two large groups namely, variation associated with sampling an inhomogeneous sedimentary unit and variation associated with laboratory procedures of all kinds. As long as these errors or sources of variation are statistically independent, an experiment may be specifically designed to segregate them and estimate their individual contribution.

There is little doubt that the largest source of error in the phi percentile deviation is due to error in drawing and reading the cumulative curve in the region of the 90 percentile which in most natural rocks is found in the flat part of the curve (Griffiths, 1953). Every sediment samples a range of grain-size, and this variation must be characterised statistically so those samples may be compared and interpreted. It is therefore necessary to plot, in some way, frequency of occurrence against a measure of grain-size (Leeder, 1982).

4.2.3 Grain-size elements of statistical analysis

Once the grain-size distribution has been obtained then the sediment can be characterized by several statistical parameters: mean grain-size, mode, median grain-size, standard deviation, sorting and skewness. Nowadays the more precise parameters of Folk and Ward (1957) are applied to grain-size distributions measured in phi units rather than the simpler formulae of P. D. Trask, which are used with millimetres, but which are rarely used. The median grain-size, *i.e.* the grain-size at the 50^{th} percentile, is not as useful as the mean grain-size, which is an average value, taking into account the grain-sizes at the 5^{th}, 16^{th}, 50^{th}, 84^{th} and 95^{th} percentiles. The mode is the phi (or millimetre) value of the mid-point of the most abundant class interval. Where the grain-size distribution is perfectly normal and symmetrical, then the median, mean and mode values are the same.

These properties may be determined either mathematically by the method of moments or graphically by reading selected percentiles off the cumulative curves (both methods summarised by Krumbein and Pettijohn, 1938). In a suite of strongly bimodal samples, most of the grain-size frequency curves are very non-normal. Therefore, the commonly used graphic measures of mean size, sorting and other statistical parameters are inadequate, because they are based on only two or three points read-off the cumulative curve. Strongly non-normal curves require more detailed coverage regardless of their modality in order to assess their properties more accurately, as detailed below.

Mean size – Inman (1952) suggested ($\phi 16 + \phi 84$) / 2 as a measure of mean size. This serves quite well for nearly normal curves, but fails to reflect accurately the mean size of bimodal and strongly skewed curves. Therefore, as an alternative measure of means (Mz) the following formula has been used (Folk and Ward, 1957).

$$Mz = \frac{\phi 16 + \phi 50 + \phi 84}{3}$$

Here, $\phi 16$ may be considered roughly the average size of the coarsest third of the samples and $\phi 84$ as the average size of the finest third; the addition of the $\phi 50$ (the average of the middle third) thus completes the picture and gives a better overall representation of the true phi mean.

Mode – No good mathematical formula exists for accurate determination of the mode. The best approximation is probably that given by Otto (1939) but this works well only when the distribution is symmetrical in the region neighbouring the mode and fails in skewed curves. The mode is the phi (or millimeter) value of the mid-point of the most abundant class interval. Most sediments are unimodel, that is one class dominates, but bimodal and even polymodal sediments are not uncommon (Tucker, 1991). The maximum percentage occurring within a half-phi diameter range in any sample has been given the term "mode" concentration and may have some value as an auxiliary measure of the degree of sorting in the region about the mode (Folk and Ward, 1957).

Median – The median diameter is defined as the midpoint of the distribution. It is that diameter which is larger than 50 percent of the diameters in the distribution, and smaller than the other 50 percent. For its graphic determination, therefore, it is only necessary to draw a cumulative curve of sediment size and read the diameter value which correspond to the point where the 50^{th} percentile line crosses the cumulative curve (Krumbein and Pettijohn, 1938).

The median is a very misleading value and should be abandoned as a measure of average size inasmuch as it is based on only one point on the cumulative curve (Folk and Ward, 1957). Generally, the median grain-size, simply the grain-size at 50%, is not as useful as the mean grain-size which is an average value (Tucker, 1991).

Standard Deviation – The generally accepted definition of sorting is that the more closely a sediment approaches a single size in its frequency distribution the better sorted it is. The standard deviation has been used as a measure of sorting, and Inman (1952) followed Krumbein and Pettijohn (1938) in suggesting the following phi standard deviation

$$\sigma\phi = \frac{\phi 84 - \phi 16}{2}$$

For many normal curves this measure is adequate. However, it is based only on the central part of the distribution and ignores fully one-third of the sample, specifically the "tails" which offer some of the most valuable information. Although it would theoretically be best to include every thing from the first to the 99th percentile, Inman (1952) has shown that data are seldom reliable beyond the 5th and 95th percentiles. Hence, these percentiles provide a practical end point. Inasmuch as the spread between the 5th and 95th percentiles includes 3.3 standard deviations, and is a more reliable measure than that based only on the tails of the distribution.

$$\sigma\phi = \frac{\phi 95 - \phi 5}{3.3}$$

However, neither the $\phi 84 - \phi 16$ measure, nor the $\phi 95 - \phi 5$ measure is adequate by itself for complex bimodal sediments, and a superior overall measure of sorting may be obtained by combining the two and taking their average.

This measure, called the Inclusive Graphic Standard Deviation is given by the formula (Folk and Ward, 1957)

$$\sigma I = \frac{\phi 84 - \phi 16}{4} + \frac{\phi 95 - \phi 5}{6.6}$$

In discussing sorting, it is convenient to have a verbal scale, so that information may be communicated to non-specialists. Plotting of hundreds of analyses from many different environments has suggested the following divisional points:

σI	under - 0.35	very well sorted
σI	0.35 – 0.50	well sorted
σI	0.50 – 1.00	moderately well sorted
σI	1.00 – 2.00	poorly sorted
σI	2.00 – 4.00	very poorly sorted
σI	over – 4.00	extremely poorly sorted

With the exception of the lowest limit the scale is geometric with a ratio of 2. The frequent generalisation that sorting increases with transport is in many suites simply due to the fact that the mean size of a sediment changes with transport, and the improvement in sorting is dependent only on the decreasing mean size, not the distance. As Inman (1952) suggested, once the sediment attains a minimum of 6 (best sorting), if it continues to get finer it will "round the turn" on the curve and sorting will worsen with further transport. Generally, sorting improves along the sediment transport path. This is the case with desert sand, where grain-size also decreases down-wind (Lancaster, 1986).

Skewness – This is a measure of the symmetry of the distribution and visually is best seen from the smoothed frequency curve. Inman (1952) suggested two measures of skewness. The first, to determine the asymmetry of the central part of the distribution

$$\alpha\phi = \frac{\phi 84 + \phi 16 - 2\phi 50}{\phi 84 - \phi 16}$$

and the second, to measure the asymmetry of the extremes

$$\alpha 2\phi = \frac{\phi 95 + \phi 5 - 2\phi 50}{\phi 84 - \phi 16}$$

Again, a better measure of overall skewness may be obtained by averaging these two values using the Inclusive Graphic Skewness

$$SkI = \frac{\phi 16 + \phi 84 - 2\phi 50}{2(\phi 84 - \phi 16)} + \frac{\phi 5 + \phi 95 - 2\phi 50}{2(\phi 95 - \phi 5)}$$

The terms for skewness derived from the Folk and Ward (1957) formula are:

Sk	greater than + 0.30	strongly fine-skewed
	+ 0.30 to + 0.10	fine – skewed
	+ 0.10 to – 0.10	near – symmetrical
	- 0.10 to – 0.30	coarse – skewed
	greater than – 0.30	strongly coarse – skewed

In general, sediment becomes more negatively skewed (and finer grained) along its sediment transport path, whereas the source sediment (lag) becomes more positively skewed and relatively coarse (Pettijohn *et al.*, 1987).

4.3 Mamuniyat Formation

4.3.1 Thin section analysis

Techniques for quantitative thin-section analysis, including modal analysis for compositional data, are provided by Krumbein (1935), Chayes (1956), Griffiths (1961) and Carver (1971). Quantitative comparisons of thin section grain-size data are feasible, particularly when data are compiled by the same operator (to avoid operator bias in measurement procedures), and from rocks that do not differ greatly in packing or grain sphericity (which can influence apparent size distributions) (Lewis, 1983).

The grain-size of the Mamuniyat Formation has been determined by measuring the long axis of 150 quartz grains per slide, using a micrometer eyepiece and mechanical stage. These values were grouped into 0.25ϕ classes and the number frequency, converted into percentages and the values plotted on arithmetic probability paper. In the Mamuniyat Formation, the grain-size in mm for all the samples was plotted as cumulative frequency curves in order to calculate median diameter, mean parameter and sorting.

Moreover, the cumulative frequency plot can be use to estimate the percentages of suspension load, saltation load and traction load. Based on grain-size relationships the inflection points broadly correspond to the change over from one type of sediment to another. Visher (1969) first proposed that the inflection point between the two coarsest fractions separates grains that were always in contact with the bed, transported by sliding and rolling (surface creep) from grains transported by intermittent suspension (saltation). A second inflection point occurs between the saltation load and the suspension load (Pettijohn *et al.*, 1987).

These methods can be used to assess the depositional environments together with other information from sedimentary structures, facies and sequence stratigraphy. In addition, the sorting, size range, degree of mixing, and the point of truncation of these populations may provide insight into provenance, currents, waves and rates of deposition (Visher, 1969).

4.3.2 Interpretation of the cumulative curves

Udden (1914) observed that a geometric grade scale tends to symmetrisize the frequency curve. This observation stimulated interest in the nature of the size frequency distribution and the characteristic of the Mamuniyat grain-size curves. Krumbein (1934) observed that the size distribution of many clastic sediments was log normal, and he expressed the distribution as a Gaussian function in which log size was substituted for actual size.

Krumbein applied the tests for normality and found that the requirements were reasonably well satisfied by many sediments. The log normal character of a size distribution can be quickly assessed by use of a modified probability paper (Otto, 1939). The size frequency, expressed as weight percentage, is cumulated in the usual manner and plotted against the log of the size. Generally, the symmetrical cumulative curve plots as a straight line on logarithmic probability paper; when the curve does not plot as a straight line the distribution is asymmetrical (Krumbein, 1934).

Throughout, the Mamuniyat Formation within A, B and H-Fields, the cumulative curves do not plot as a single straight line, but plot as straight line components with intersection points. Based on the grain-size relationship the inflection points broadly correspond to the change over from one type of sediment transport to another **(Fig. 4.1)**. The reason for the non-normal curves of the Mamuniyat sandstone is believed to be simple mixing of two or more normal distributions by means of different hydrodynamic regimes as suggested by Mueller (1967) and Folk (1977).

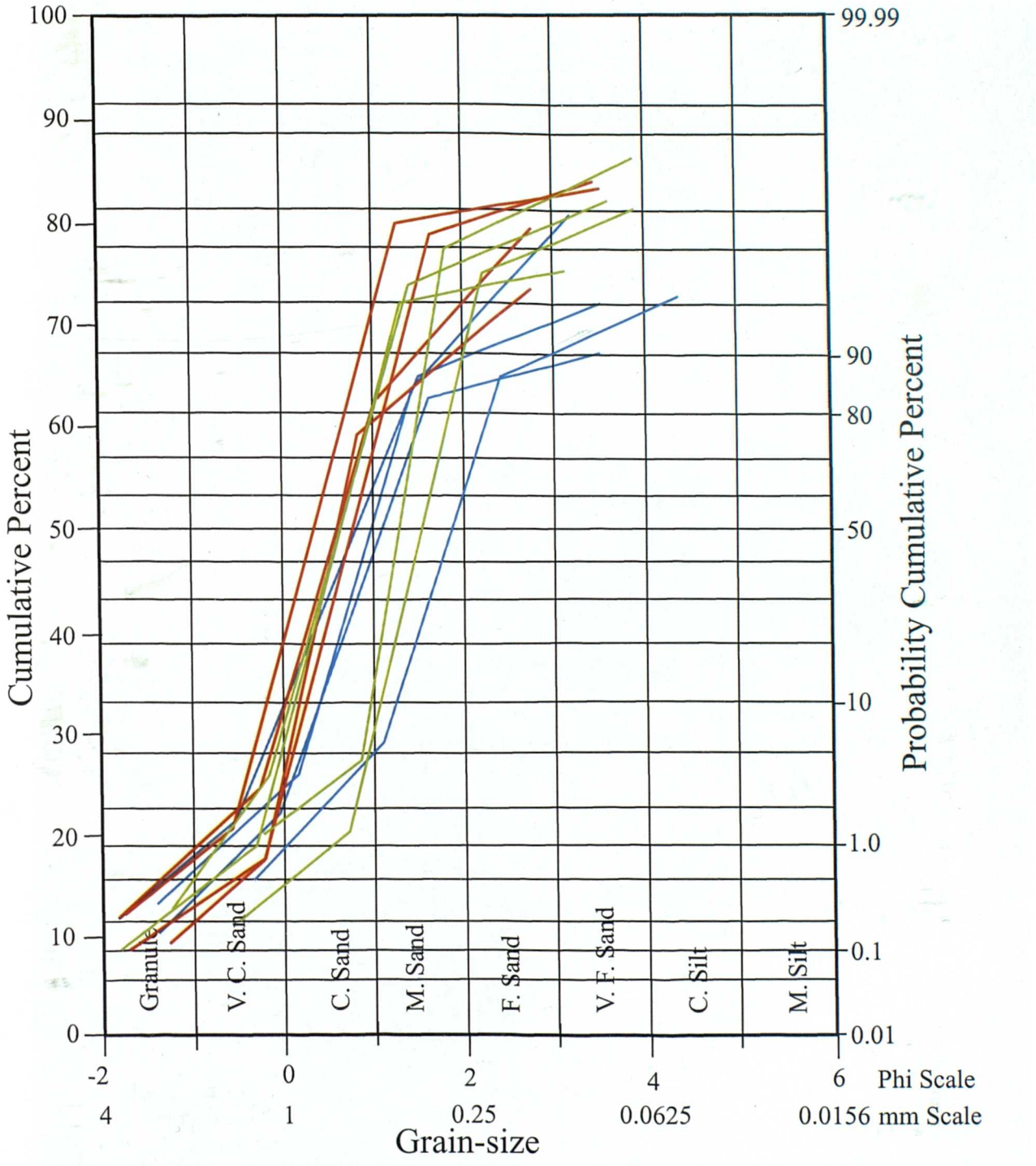

Fig. 4.1 Grain-size cumulative frequency curves for the Mamuniyat Formation based on thin section grain-size analysis plotted on lognormal probability paper, showing the tripartite subdivision of the curves, which may correspond to the suspension, saltation and traction populations.
A-Field: Blue; B-Field: Red; H-Field: Green.

The detrital quartz grain-size of the Mamuniyat sandstone is generally coarse- to very coarse-grained, ranging between 0.75 mm and 1.50 mm **(Tables 4.1, 4.2 and 4.3)**. The cumulative curves in the Mamuniyat Formation are predominantly bimodal with subordinate polymodal distributions (Pettijohn, 1975). Several efforts have been made to "dissect" the cumulative curves and separate the component populations (Tanner, 1959; Spencer, 1963; Visher, 1969).

4.3.3 Grain-size parameters

The grain-sizes in the Mamuniyat sandstones are of two distinct types. More than four-fifth of the grains are subrounded to rounded, and occasionally well-rounded; some of the grains are perfect spheres, and range from 0.6 mm to 1.5 mm in diameter. The other one-fifth of the grains, range from angular (in the 0.9 mm size range) to sub-angular (in the 1.2 mm grade).

This mixture provides some interesting evidence concerning the classification of Dapples (1975) who choose as a measure of sediment maturity, the percentage of well-rounded sand grains present in a deposit. In the Mamuniyat Formation, throughout A, B and H-Fields, **(Tables 4.1, 4.2 and 4.3)** the following statistical parameters described below have been used.

4.3.3.1 Mean grain-size

The mean grain-size of the Mamuniyat Formation indicates the average size of the sediment and is related to the kinetic energy of the medium of deposition. Generally the mean grain-size of the upper and lower Mamuniyat sandstones in NC 115 Concession, ranges from ϕ 0.45 to ϕ 2.28, and falls within the very coarse to fine sand grades according to the grain-size classification of Pettijohn *et al.* (1987). This wide range in grain-size reflects the local variation in hydraulic regime, which enabled coarse and fine fractions to be deposited side by side.

Well	Depth (ft)	Mean size	Sorting	5%	16%	50%	84%	95%
A1-NC115	4702.7	0.793	0.82	0.2	0.18	0.6	1.6	3.25
	4717.13	2.126	0.39	1.32	1.74	2.15	2.49	2.65
	4758.14	1.363	1.07	0.06	0.4	0.81	2.88	3.02
	4784.39	0.893	0.65	0.06	0.4	0.79	1.49	2.56
	4811.3	0.726	0.68	0.29	0.15	0.6	1.43	2.68
	4853.94	1.923	0.61	0.94	1.32	1.89	2.56	2.91
	4869.69	0.81	0.83	0.14	0.22	0.74	1.47	3.54
	3873.63	0.773	0.62	0.29	0.15	0.74	1.43	2.25
	4888.06	1.943	0.57	1.15	1.32	1.95	2.56	2.85
	4939.9	2.286	0.32	1.69	2	2.26	2.6	2.84
	4995.02	1.316	0.63	0.36	0.66	1.42	1.87	2.54
	5548.65	1.27	0.43	0.74	0.84	1.33	1.64	2.28
A2-NC115	4975.66	0.73	0.68	0.4	0.03	0.73	1.43	2.57
	4986.23	0.666	0.64	0.18	0.01	0.67	1.32	2.25
	4997.97	2.2	0.4	1.43	1.79	2.25	2.56	2.79
	5014.37	0.883	0.55	0.06	0.32	0.9	1.43	1.85
	5020.77	0.763	0.55	0	0.29	0.74	1.26	2.06
	5038.82	0.6	0.46	0.38	0	0.67	1.13	1.57
	5202.1	2.186	0.4	1.47	1.74	2.25	2.57	2.76
A4-NC115	5028.15	1.91	0.63	0.79	1.3	1.89	2.54	2.91
	5050.79	0.84	0.69	0.11	0.36	0.76	1.4	2.96
	5084.91	2.256	0.35	1.6	1.89	2.27	2.61	2.75
	5185.3	1.036	0.61	0.29	0.52	0.95	1.64	2.47
A8-NC115	4627.89	0.636	0.5	0.19	0.15	0.64	1.12	1.88
	4678.09	0.673	0.69	0.41	0	0.7	1.32	2.81
	4685.97	0.66	0.44	0.6	0.1	0.66	1.22	1.63
	4699.75	0.643	0.45	0.36	0.06	0.69	1.18	1.52
	4729.93	0.883	0.5	0.12	0.44	0.89	1.32	1.97
	4768.81	0.946	0.68	0.04	0.43	0.94	1.47	2.84
	4781.77	0.756	0.78	0.29	0.12	0.79	1.36	3.38
	4811.95	0.823	0.47	0.13	0.47	0.74	1.26	1.93
	4837.38	0.64	0.4	0.56	0.12	0.64	1.16	1.47
	4851.32	0.843	0.52	0.04	0.4	0.78	1.35	1.94
	4870.68	0.776	0.49	0	0.29	0.79	1.25	1.64
	4885.11	0.636	0.42	0.57	0.12	0.64	1.15	1.64
	4900.53	0.703	0.4	0.12	0.29	0.69	1.13	1.39
	4906.76	0.936	0.53	0.26	0.44	0.94	1.43	2.12
	4996.65	1.206	0.53	0.47	0.74	1.15	1.73	2.35
	5001.25	0.666	0.59	0.41	0.17	0.74	1.09	2.8
	5027	2.036	0.39	1.38	1.66	2.03	2.42	2.69

Table. 4.1. Grain-size characteristics of the Mamuniyat Formation, A-Field, NC115 Concession, NW Murzuq Basin.

Well	Depth (ft)	Mean size	Sorting	5%	16%	50%	84%	95%
B2-NC115	4667	0.766	0.42	0.03	0.38	0.74	1.18	1.51
	4720.74	1.346	0.55	0.38	0.84	1.36	1.84	2.33
	4796.04	1.066	0.55	0.25	0.52	1.13	1.55	2.19
	4828.52	0.56	0.47	0.46	0	0.56	1.12	1.74
	4937.67	0.79	0.53	0.14	0.26	0.79	1.32	1.89
	5010.31	0.886	0.69	0.15	0.4	0.79	1.47	2.95
B3-NC115	4650.21	1.033	0.57	0.22	0.6	0.94	1.56	2.4
	4685.15	0.933	0.64	0.22	0.44	0.89	1.47	2.74
	4720.08	0.89	0.45	0.18	0.51	0.84	1.32	2.12
	4752.51	0.586	0.63	0.39	0.14	0.5	1.12	2.9
	4775.53	1.01	0.44	0.38	0.64	0.99	1.4	2
	4798.92	0.556	0.32	0.52	0.13	0.59	0.95	1.25
	4848.86	0.58	0.46	0.26	0.06	0.62	1.06	1.64
	4877.6	1.57	0.42	1.09	1.22	1.43	2.06	2.45
	4922.35	0.766	0.45	0.06	0.32	0.79	1.19	1.6
	4962.8	0.57	0.37	0.59	0.21	0.47	1.03	1.69
	5075.4	0.8	0.44	0.06	0.4	0.76	1.24	1.6
B8-NC115	4646.35	0.566	0.36	0.65	0.14	0.47	1.09	1.45
	4646.6	0.45	0.11	0.98	0.76	0.37	0.22	1.18
	4719.55	0.586	0.4	0.2	0.15	0.59	1.02	1.39
	4748.83	1.253	0.57	0.6	0.8	1.12	1.84	2.64
	4772.17	1.256	0.48	0.57	0.89	1.19	1.69	2.44
	4784.55	0.726	0.4	0.05	0.32	0.74	1.12	1.38
	4806	1.136	0.42	0.4	0.79	1.12	1.5	1.99
	4815	1.28	0.5	0.51	0.84	1.2	1.8	2.24
	4864.5	0.976	0.51	0.22	0.51	0.99	1.43	2.06
	4912	1.14	0.56	0.28	0.64	1.12	1.66	2.32
	5650	1.293	0.54	0.47	0.84	1.2	1.84	2.37
B27-NC115	4776	0.466	0.29	0.38	0.25	0.29	0.86	1.27
	4849.5	1.086	0.43	0.43	0.76	1.03	1.47	2.12

Table. 4.2. Grain-size characteristics of the Mamuniyat Formation, B-Field, NC115 Concesson, NW Murzuq Basin.

Well	Depth (ft)	Mean size	Sorting	5%	16%	50%	84%	95%
H2-NC115	4872.81	0.946	0.52	0.22	0.52	0.89	1.43	2.18
	4885.6	0.776	0.36	0.12	0.47	0.74	1.12	1.43
	4912.67	0.91	0.45	0.32	0.51	0.89	1.33	1.94
	4939.24	1.003	0.56	0.32	0.57	0.96	1.48	2.51
	4979.6	1.476	0.55	0.87	1	1.36	2.07	2.75
	5127.89	1.033	0.46	0.3	0.64	1	1.46	2
H3-NC115	4719.43	1.42	0.49	0.81	1	1.32	1.94	2.47
	4750.6	1.146	0.45	0.47	0.76	1.12	1.56	2.12
	4793.25	1.836	0.49	1.13	1.36	1.79	2.36	2.69
	4845.74	1.353	0.54	0.78	0.89	1.18	1.99	2.54
	4863.79	1.256	0.41	0.79	0.94	1.19	1.64	2.33
	4910.54	1.516	0.51	0.84	1.05	1.41	2.09	2.49
	4921.2	1.596	0.46	1.12	1.24	1.43	2.12	2.74
	5001.58	1.593	0.55	0.89	1.06	1.52	2.2	2.64
	5163.98	1.68	0.45	1.12	1.25	1.6	2.19	2.56
H4-NC115	4852.35	0.623	0.44	0.35	0.05	0.66	1.16	1.43
	4863	0.963	0.37	0.32	0.6	0.97	1.32	1.61
	4900	1.253	0.46	0.79	0.89	1.13	1.74	2.42
	4913.5	1.06	0.43	0.45	0.78	1.01	1.39	2.26
	4925	0.923	0.44	0.36	0.6	0.91	1.26	2.18
	4974	1.366	0.37	1.05	1.11	1.25	1.74	2.47
	4988.5	1.643	0.49	1.08	1.18	1.5	2.25	2.57
	5002	1.396	0.55	0.69	0.89	1.3	2	2.48
	5006	1.456	0.54	0.84	0.96	1.32	2.09	2.55
H5-NC115	4823.5	1.136	0.43	0.6	0.79	1.06	1.56	2.18
	4842.3	1.71	0.54	1.06	1.15	1.64	2.34	2.65
	4871.75	1.31	0.48	0.74	0.94	1.24	1.75	2.56
	4884.5	1.086	0.36	0.74	0.82	1.01	1.43	2.1
	4922.75	1.273	0.48	0.74	0.85	1.18	1.79	2.37
	4962	1.506	0.39	1.06	1.19	1.43	1.9	2.5
	4986	1.37	0.39	1.01	1.06	1.26	1.79	2.4
	4992	1.426	0.42	1.01	1.12	1.26	1.9	2.48
	4997	1.57	0.47	1.05	1.18	1.4	2.13	2.56
	5000.5	1.57	0.52	1.01	1.08	1.43	2.2	2.63
	5011	1.286	0.5	0.72	0.87	1.15	1.84	2.45

Table. 4.3. Grain-size characteristics of the Mamuniyat Formation, H-Field, NC115 Concession, NW Murzuq Basin.

4.3.3.2 Median grain-size

The median grain-size of the Mamuniyat Formation is a measure of average particle size obtained graphically by locating the diameter associated with the mid-point of the particle-size distribution. However, the median is the grain-size in the middle of the population, the 50th percentile. Median values are easily determined from either a frequency curve or a cumulative curve, whereas the mode cannot be accurately determined from a cumulative curve (Richard and Davis, 1983).

Visher (1969) observed that most grain-size distributions show a coarse-grained population with a different mean and degree of sorting than the suspension and saltation sub-population. However, the Mamuniyat sandstones do not show this in that the saltation population includes the coarsest material in the distribution. The reason for this is unknown, but it may be related to removal of part of the coarsest fractions, and to the sorting shear at the depositional interface in deposits formed by continuous currents.

4.3.3.3 Standard deviation "Sorting"

Sorting is the selection, during transport, of particles according to their size, specific gravities and shapes. Statistically, sorting is expressed as the description of the particle sizes about the mean (Friedman and Sanders, 1978). The degree of sorting is a reflection of the energy level in the environment of deposition. It is one of the most useful parameters since it gives an indication of the effectiveness of the depositional medium in separating grains of different classes.

Estimates of sorting based on the 84th and 16th percentiles should be superior to ones based on the 95th and 5th percentiles, because they are closer to the central tendency. Folk and Ward (1957) combined each of these measures in their inclusive graphic standard deviation, $\sigma\phi$, which is the average of sorting based on both the central and exterior parts of the size distribution. One can also estimate sorting visually or measure it semiquantitatively in thin section (Pettijohn *et al.*, 1987).

In general a frequency curve of well-sorted sediment is sharp peaked and narrow. This means that only a few size classes are present. In contrast, the frequency curve of a poorly sorted sediment is low and wide; and many size classes are present (Friedman and Sanders, 1978). This depends on the availability of different size fractions in the source area without which the fluctuations in current velocity will not be recorded on the probability curve.

The sorting of sandstones from A, B and H-Fields in the Mamuniyat Formation, as measured by ϕ standard deviation (σ_1), gives values ranging from 0.11 ϕ, or very well sorted, to 1.07 ϕ, or poorly sorted, with an average of 0.59 ϕ. According to the sorting scale of Folk and Ward (op. cit.) and Friedman (1962), the Mamuniyat sandstones are moderately well sorted. As with mean grain-size, sorting values vary systematically from the upper Mamuniyat to the lower Mamuniyat Formation.

The upper Mamuniyat sandstones in NC115 Concession are the best sorted, with an average value of 0.49 and a range of values from 0.37 to 0.62, or well sorted to moderately well sorted. The middle and lower Mamuniyat sandstones are least well sorted with an average value of 0.90 and an average value from 0.54 to 1.44. Moreover, there is no significant difference in sorting between the northeastern and southwestern flank of NC115 Concession. The sorting characteristics of the Mamuniyat sandstones in the NW flank of the Murzuq Basin shows them to be mature to super-mature according to Folk's (1951) classification.

4.3.3.4 Summary of the grain-size parameters

Grain-size analysis is a routine procedure in many sedimentary studies, to characterize the sediment or rock and give information on depositional processes and environments. Grain-size analysis may also be used to distinguish between sediments of different environments and facies characteristics (Bridge, 1981; Komar, 1985; Pettijohn *et al.*, 1987).

Analysis of grain-size and sorting patterns of the Mamuniyat Formation shows a clear subdivision into three main members: Upper, Middle and Lower. The upper member of the Mamuniyat sandstones is generally coarser, but better sorted than the middle and lower members. This trend may be explained by comparison with grain-size distributions and sorting patterns of similar types of sandstone.

The comparison between Upper, Middle and Lower sandstones of the Mamuniyat Formation reveal variations in composition and textural properties, Although the differences are not great, they are significant in terms of their reservoir potential. The upper member of the sandstone is significantly coarser-grained than the middle and lower members within the Mamuniyat Formation (Maximum mean grain-size up to 1.50 mm in diameter). Moreover, the Upper member sandstones are better sorted and the Middle and Lower members of the Mamuniyat are least well sorted (Fello and Turner, 2001a).

4.3.4 Roundness

Roundness is related to the sharpness or curvature of the edges and corners of the grains. It is geometrically independent of sphericity. The roundness of sand-size particles is easiest to measure by matching the outlines of individual particles with photographs of two sets of standard sand particles, each set having different sphericity. The term roundness, however, has been used or misused in the literature and in many cases has been used interchangeably with shape (Russel and Taylor, 1937). The roundness is an important physical property of all sediments that may prove useful in determining the:

1) Depositional environment;
2) Morphology of the grains;
3) Nature of the source rocks;
4) Degree of weathering;
5) Degree of abrasion during transport; and
6) Corrosion or dissolution during diagenesis.

Roundness gives us some idea of the distance traveled by a particle prior to its deposition. In order to evaluate the validity of such ideas an accurate method of determining roundness must be adopted using a statistically operable roundness scale. For convenience the method should also be rapid. Hakon Wadell's method for determining the roundness of a particle (Wadell, 1935) involves dividing the average of the radii of the corners of the grain image by the radius of the maximum inscribed circle. This method is the most accurate yet proposed, but it is far too slow to be used in studying sediments on a large scale.

Russell and Taylor (1937) placed particles in roundness classes based on comparison with photographs of type grains. They presented five grade terms, which are: angular, sub-angular, sub-rounded, rounded and well-rounded. The divisions between the classes are characterized by certain numerical values from WADELL'S roundness grades.

Division class limits were not systematically chosen and the arithmetic means of the intervals were used as mid-points. These values do not provide the smaller subdivisions that are needed in the lower values. Pettijohn (1949) has modified the arrangement by using a "geometric" scale, and has rounded off the class limits in order to facilitate memory. Even this "geometric" scale does not provide small enough divisions in the lower roundness values.

Pettijohn (1975) differs from Russell and Taylor (1937) in that he groups particles into classes by using silhouettes rather than photographs for comparison. The comparison characterizes a three dimensional particle by a two-dimensional reference although the three dimensional aspects of small particles are easily observed under the microscope by raising and lowering the focal plane through the full thickness of the particle. A more complete picture of the roundness of a particle is obtained in this manner.

Krumbein (1941) relied entirely on visual comparison of the individual grains with silhouettes to arrive at an average roundness value for the samples. He proposed no class limits, but presented silhouettes for nine different roundness values. This method is rather slow and somewhat tedious. Since his roundness values are very close together, it is often difficult to decide which roundness value to assign to a particle. In determining the roundness of a sample, each particle is assigned to one of the classes depending on the photograph with which it most closely compares. An average roundness for the sample is determined by multiplying the number of particles in each class by the geometric mean of the class and dividing the sum of the products by the total number of particles counted. This method has been used in laboratory work and found to be at least as accurate as other methods proposed.

The geological significant importance of roundness was noted by Krumbein (1934) who shown that roundness increases with distance of travel more rapidly at first and then more slowly. Krumbein (1941) observed that the rate of change of roundness was a function of the difference between the roundness at any point and a certain limiting roundness, a value dependent in some measure on the material involved and the particular stream or beach regime. Roundness, in particular, reflects abrasion history, which in turn depends on such diverse geological controls as relief, kind of source rocks, transport process, and the mineralogy of the grain.

The roundness scale of Powers (1953) is also based on the premise that it is easier to detect differences in roundness for low values than for high values. As a result most roundness charts contain comparatively few divisions in the higher roundness values. Whatever the precise meaning of roundness, whether derived from abrasion mill experiments or from natural streams, rounding does increase with time (distance) most rapidly at first and then more slowly. However, there does seem to be a limiting roundness, in part related to the lithology of the material (Sneed and Folk, 1958).

Winkelmolen and Veenstra (1974) have made careful studies of another aspect of particle morphology called rollability – the minimum angle of slope, which will cause a grain to roll or fall. Rollability is a property derived from roundness and shape. Winkelmolen used such a device and concluded that plots of rollability against grain-size were helpful in discriminating between some beach and dune sands (Pettijohn *et al.*, 1987)

The roundness classes are groups of sedimentary particles from 0.0 (not rounded) to 1.0 (perfectly rounded). A commonly used visual roundness scale for the descriptive characterization of roundness according to Pettijohn's grades (1957) contains five classes: angular (0-0.15), subanglar (0.15-0.25), subrounded (0.25-0.40), rounded (0.40-0.60) and wellrounded (0.60-1.00). Since most particles, even freshly broken ones, have a finite roundness rarely less than 0.10, the lower limit of the angular class is not 0. The mid-point of the fragments in the angular class, therefore, is probably nearer 0.125 (Mueller, 1967).

The degree of rounding of a detrital particle depends on its size, physical characteristics, history of abrasion and later on corrosion or dissolution during diagenesis. Inasmuch as roundness is a function of size, determination of the percentage of angular or round grains should be made only with the same size fraction and mineral. Roundness provinces may also be defined by the angularity of heavy minerals, generally either zircon or tourmaline, as well as quartz.

Although, round overgrowths are decisive evidence of multicycle grains, they are usually so small in number as to be impractical for graphic mapping. Multicycle grains are easiest to recognizes with cathodo-luminescence (Sippel, 1968).

For environmental interpretations, roundness measures are more significant than sphericity or form. The shape of a grain is dependent on many factors including the initial mineralogy, the nature of the source rock, the degree of weathering, and to a lesser extent on the degree of abrasion during transport, and corrosion or dissolution during diagenesis. If derived directly from crystalline rocks they tend to be highly non-spherical and angular, with embayments and fractures. If derived from pre-existing sediments, would be more spherical and very well rounded, where as in a quartz-cemented sandstone, they would be moderately angular. If derived from sandstone with no quartz overgrowth cement then the grains would show inherited features (Pettijohn *et al.*, 1987) and in a very general way the degree of roundness increases with the duration of transport and reworking.

Roundness values throughout the Mamuniyat sandstones for A, B and H-Fields, **(Tables 4.4, 4.5 and 4.6)** were estimated from thin sections by comparison with the roundness chart of Pettijohn (1987) by determining the roundness of 150 grains per slide to compensate for any operator bias (Griffiths, 1953). The average roundness value of the Mamuniyat Formation sandstones ranges from 0.35 to 0.50 **(Tables 4.7, 4.8 and 4.9)**.

According to the descriptive characterization of roundness (Pettijohn *et al.*, 1987) the Mamuniyat Formation contains subrounded to rounded grains with individual grains showing the affects of abrasion **(Figs. 4.2, 4.3 and 4.4)**. Generally, the abrasion and roundness of sand in the Mamuniyat sandstone is related to maturity, in which moderate to high roundness values are generally regarded as evidence of a texturally mature to supermature sandstone (Folk, 1951).

4.4 Summary

The mean grain-size of the Upper, Middle and Lower Mamuniyat sandstones in NC 115 Concession, ranges from ϕ 0.45 to ϕ 2.28, and falls within the very coarse to fine sand grades. Throughout, the Mamuniyat Formation into A, B and H-Fields, the cumulative curves do not plot as a single straight line, but plot as straight line components with intersection points. Based on the grain-size relationship the inflection points broadly correspond to the change over from one type of sediment transport to another. The reason for the non-normal curves of the Mamuniyat sandstone is believed to be simple mixing of two or more normal distributions by means of different hydrodynamic regimes. The Mamuniyat sandstones are moderately well sorted. Moreover the Mamuniyat Formation contains subrounded to rounded grains with individual grains showing the affects of abrasion.

Well	Depth (ft)	Angular	Subangular	Subrounded	Rounded	Well rounded	Interpretation
A1-NC115	4702.7	1.3	20	50	21.3	7.3	SR - R
	4717.13	2	27.3	41.3	24	5.3	SA - SR
	4758.14	2	22	30.6	40.6	4.6	SR - R
	4784.39	2.6	18	37.3	35.3	6.6	SR - R
	4811.3	4	21.3	41.3	30	3.3	SR - R
	4853.94	4.6	23.3	44.6	22	5.3	SA - SR
	4869.69	2	31.3	33.3	30.6	2.6	SA - R
	3873.63	6	29.3	40	22	2.6	SA - SR
	4888.06	2.6	38	36	22	1.3	SA - SR
	4939.9	2.6	39.3	41.3	14.6	2	SA - SR
	4995.02	4	44.6	38	13.3	0	SA - SR
	5548.65	2.6	44.6	40	11.3	1.3	SA - SR
A2-NC115	4975.66	2.6	19.3	48.6	26	3.3	SR - R
	4986.23	0	18.6	50.6	30	0.6	SR - R
	4997.97	0	26	53.3	20.6	0	SA - SR
	5014.37	0	16.6	62	20	1.3	SR
	5020.77	0	16.6	42.6	38	2.6	SR - R
	5038.82	0	18.6	44.6	36	0.6	SR - R
	5202.1	0.6	21.3	53.3	24.6	0	SR
A4-NC115	5028.15	0.6	12	41.3	41.3	4.6	SR - R
	5050.79	2	18.6	37.3	38	4	SR - R
	5084.91	0	14	47.3	38	0.6	SR - R
	5185.3	0	20	40	40	0	SR - R
A8-NC115	4627.89	0.6	12	42	36	9.3	SR - R
	4678.09	0	16.6	43.3	36.6	3.3	SR - R
	4685.97	0	8.6	43.3	44.6	3.3	SR - R
	4699.75	0	9.3	50	37.3	3.3	SR
	4729.93	0	7.3	55.3	36	1.3	SR
	4768.81	0	7.3	47.3	42	3.3	SR - R
	4781.77	0	4	55.3	34	6.6	SR
	4811.95	0	10.6	41.3	45.3	2.6	SR - R
	4837.38	0	10	40	47.3	2.6	R
	4851.32	0	4.6	40	50	5.3	SR - R
	4870.68	0.6	3.3	49.3	41.3	5.3	SR - R
	4885.11	0	6	42	49.3	2.6	SR - R
	4900.53	0	8.6	40	44.6	5.3	SR - R
	4906.76	0	6.6	46.6	44.6	2	SR - R
	4996.65	0	6.6	40.6	48.6	4	SR - R
	5001.25	0	9.3	46	41.3	3.3	SR - R
	5027	0	8	48	42	2	SR - R

Table. 4.4. Degree of roundness, based on the descriptive characterization of roundness (After Russel-Taylor-Pettijohn) for the Mamuniyat Formation, A-Field, NC115 Concession.

NOTE:

Degree of roundness Russel - Taylor - Pettijohn	Degree of rounded (Wadell)	Geometric mid-point (approximated)
Angular	0 - 0.15	0.125
Subangular	0.15 - 0.25	0.2
Subrounded	0.25 - 0.40	0.315
Rounded	0.40 - 0.60	0.5
Well rounded	0.60 - 1.00	0.8

Well	Depth (ft)	Angular	Subangular	Subrounded	Rounded	Well rounded	Interpretation
B2-NC115	4667	0.6	18	44.6	32	4.6	SR - R
	4720.74	1.3	26.6	46.6	46.6	22.6	SR
	4796.04	0	32	37.3	29.3	1.3	SA - R
	4828.52	0.6	28	34	34.6	2.6	R - SR
	4937.67	0.6	20.6	44	28.6	6	SR - R
	5010.31	0	40	38	18	4	SA - SR
B3-NC115	4650.21	0	23.3	46.6	30	0	SR
	4685.15	0	23.3	38	38.6	0	R - SR
	4720.08	0	10	46	41.3	2.6	SR - R
	4752.51	0	13.3	40	46.6	0	R - SR
	4775.53	0	18	40.6	41.3	0	R - SR
	4798.92	0	12	44.6	39.3	4	SR - R
	4848.86	0	9.3	53.3	36.6	0.6	SR - R
	4877.6	0	19.3	59.3	21.3	0	SR
	4922.35	0	18.6	44.6	36.6	0	SR - R
	4962.8	0	10.6	51.3	34.6	3.3	SR - R
	5075.4	0	28	48	22	2	SA - SR
B8-NC115	4646.35	0.6	13.3	35.3	48	2.6	R - SR
	4646.6	0	8	54.6	34.6	2	SR - R
	4719.55	0	8.6	58	32	1.3	SR - R
	4748.83	0	29.3	58	12.6	0	SA - SR
	4772.17	0	32	60.6	7.3	0	SA - SR
	4784.55	0	12	61.3	24.6	2	SR
	4806	0	20	57.3	22.6	0	SR
	4815	0	15.3	65.3	19.3	0	SR
	4864.5	0	18.6	48.6	32.6	0	SR - R
	4912	0	14	51.3	34.6	0	SR - R
	5650	0	8.6	52.6	38.6	0	SR - R
B27-NC115	4776	0	8	42.6	47.3	2	R - SR
	4849.5	0	10	46	44	0	SR - R

Table. 4.5. Degree of roundness, based on the descriptive characterization of roundness (After Russel-Taylor-Pettijohn) for the Mamuniyat Formation, B-Field, NC115 Concession.

NOTE

Degree of roundness Russel - Taylor - Pettijohn	Degree of rounded (Wadell)	Geometric mid-point (approximated)
Angular	0 - 0.15	0.125
Subangular	0.15 - 0.25	0.2
Subrounded	0.25 - 0.40	0.315
Rounded	0.40 - 0.60	0.5
Well rounded	0.60 - 1.00	0.8

Well	Depth (ft)	Angular	Subangular	Subrounded	Rounded	Well rounded	Interpretation
H2-NC115	4872.81	3.3	20.6	42	27.3	6.6	SR - R
	4885.6	2	20.6	32.6	34.6	10	R - SR
	4912.67	2	27.3	38.6	31.3	0.6	SA - R
	4939.24	0.6	27.3	37.3	32	2.6	SA - R
	4979.6	0.6	27.3	36	34	2	SA - R
	5127.89	0	26.6	38	31.3	4	SA - R
H3-NC115	4719.43	0	11.3	41.3	46	1.3	SR - R
	4750.6	0	19.3	40.6	36.6	3.3	SR - R
	4793.25	1.3	14	40.6	41.3	2.6	R - SR
	4845.74	0.6	13.3	49.3	36	0.6	SR - R
	4863.79	0	8.6	41.3	48.6	1.3	SR - R
	4910.54	0	13.3	44	42	0.6	SR - R
	4921.2	0	10	41.3	46.6	2	SR - R
	5001.58	0	19.3	39.3	41.3	0	R - SR
	5163.98	0	24	46.6	29.3	0	SR
H4-NC115	4852.35	0.6	13.3	32	48	6	R - SR
	4863	0	25.3	32	42	0.6	R - SA
	4900	0	38	42.6	19.3	0	SR - SA
	4913.5	0	40.6	40.6	18.6	0	SA - SR
	4925	0	15.3	35.3	49.3	0	R - SR
	4974	0	16.6	38	45.3	0	R - SR
	4988.5	0	22.6	48.6	28.6	0	SR
	5002	0	17.3	40.6	39.3	2	SR - R
	5006	0	20	43.3	36	0.6	SR - R
H5-NC115	4823.5	0	24	49.3	26.6	0	SR
	4842.3	0	21.3	49.3	29.3	0	SR
	4871.75	0	16	45.3	38.6	0	SR - R
	4884.5	0	16	35.3	48.6	0	R - SR
	4922.75	0	10	46	42.6	1.3	SR - R
	4962	0	14.6	38	47.3	0	R - SR
	4986	0	14.6	46.6	36.6	2	SR - R
	4992	0	16.6	48	34	1.3	SR - R
	4997	0	10.6	46	43.3	0	SR - R
	5000.5	0	24	42	34	0	SA - R
	5011	0	12	44	44	0	SR - R

Table. 4.6. Degree of roundness, basedon the descriptive characterization of roundness (After Russel-Taylor-Pettijohn) for the Mamuniyat Formation, H-Field, NC115 Concession.

NOTE

Degree of roundness Russel - Taylor - Pettijohn	Degree of rounded (Wadell)	Geometric mid-point (approximated)
Angular	0 - 0.15	0.125
Subangular	0.15 - 0.25	0.2
Subrounded	0.25 - 0.40	0.315
Rounded	0.40 - 0.60	0.5
Well rounded	0.60 - 1.00	0.8

Well	Depth (ft)	Angular	Subangular	Subrounded	Rounded	Well rounded	Interpretation
A1-NC115	4702.7	1.3	20	50	21.3	7.3	SR - R
	4717.13	2	27.3	41.3	24	5.3	SA - SR
	4758.14	2	22	30.6	40.6	4.6	SR - R
	4784.39	2.6	18	37.3	35.3	6.6	SR - R
	4811.3	4	21.3	41.3	30	3.3	SR - R
	4853.94	4.6	23.3	44.6	22	5.3	SA - SR
	4869.69	2	31.3	33.3	30.6	2.6	SA - R
	3873.63	6	29.3	40	22	2.6	SA - SR
	4888.06	2.6	38	36	22	1.3	SA - SR
	4939.9	2.6	39.3	41.3	14.6	2	SA - SR
	4995.02	4	44.6	38	13.3	0	SA - SR
	5548.65	2.6	44.6	40	11.3	1.3	SA - SR
	Average	*3.025*	*29.91*	*39.47*	*23.91*	*3.51*	*SA - SR*
A2-NC115	4975.66	2.6	19.3	48.6	26	3.3	SR - R
	4986.23	0	18.6	50.6	30	0.6	SR - R
	4997.97	0	26	53.3	20.6	0	SA - SR
	5014.37	0	16.6	62	20	1.3	SR
	5020.77	0	16.6	42.6	38	2.6	SR - R
	5038.82	0	18.6	44.6	36	0.6	SR - R
	5202.1	0.6	21.3	53.3	24.6	0	SR
	Average	*0.45*	*19.57*	*50.71*	*27.88*	*1.2*	*SR*
A4-NC115	5028.15	0.6	12	41.3	41.3	4.6	SR - R
	5050.79	2	18.6	37.3	38	4	SR - R
	5084.91	0	14	47.3	38	0.6	SR - R
	5185.3	0	20	40	40	0	SR - R
	Average	*0.65*	*16.15*	*41.47*	*39.32*	*2.3*	*SR - R*
A8-NC115	4627.89	0.6	12	42	36	9.3	SR - R
	4678.09	0	16.6	43.3	36.6	3.3	SR - R
	4685.97	0	8.6	43.3	44.6	3.3	SR - R
	4699.75	0	9.3	50	37.3	3.3	SR
	4729.93	0	7.3	55.3	36	1.3	SR
	4768.81	0	7.3	47.3	42	3.3	SR - R
	4781.77	0	4	55.3	34	6.6	SR
	4811.95	0	10.6	41.3	45.3	2.6	SR - R
	4837.38	0	10	40	47.3	2.6	R
	4851.32	0	4.6	40	50	5.3	SR - R
	4870.68	0.6	3.3	49.3	41.3	5.3	SR - R
	4885.11	0	6	42	49.3	2.6	SR - R
	4900.53	0	8.6	40	44.6	5.3	SR - R
	4906.76	0	6.6	46.6	44.6	2	SR - R
	4996.65	0	6.6	40.6	48.6	4	SR - R
	5001.25	0	9.3	46	41.3	3.3	SR - R
	5027	0	8	48	42	2	SR - R
	Average	*0.07*	*8.15*	*45.31*	*42.4*	*3.84*	*SR - R*
A1, A2, A4& A8 - NC115	*Average*	*1.08*	*17.48*	*44.12*	*34*	*3.13*	*SR - R*

Table. 4.7. Average roundness (%) of the Mamuniyat Formation, within type wells of A-Field, NC115 Concession.

Well	Depth (ft)	Angular	Subangular	Subrounded	Rounded	Well rounded	Interpretation
B2-NC115	4667	0.6	18	44.6	32	4.6	SR - R
	4720.74	1.3	26.6	46.6	22.6	2.6	SR
	4796.04	0	32	37.3	29.3	1.3	SA - R
	4828.52	0.6	28	34	34.6	2.6	R - SR
	4937.67	0.6	20.6	44	28.6	6	SR - R
	5010.31	0	40	38	18	4	SA - SR
	Average	*0.52*	*27.53*	*40.75*	*27.52*	*3.52*	*SR*
B3-NC115	4650.21	0	23.3	46.6	30	0	SR
	4685.15	0	23.3	38	38.6	0	R - SR
	4720.08	0	10	46	41.3	2.6	SR - R
	4752.51	0	13.3	40	46.6	0	R - SR
	4775.53	0	18	40.6	41.3	0	R - SR
	4798.92	0	12	44.6	39.3	4	SR - R
	4848.86	0	9.3	53.3	36.6	0.6	SR - R
	4877.6	0	19.3	59.3	21.3	0	SR
	4922.35	0	18.6	44.6	36.6	0	SR - R
	4962.8	0	10.6	51.3	34.6	3.3	SR - R
	5075.4	0	28	48	22	2	SA - SR
	Average	*0*	*16.88*	*46.57*	*35.29*	*1.14*	*SR - R*
B8-NC115	4646.35	0.6	13.3	35.3	48	2.6	R - SR
	4646.6	0	8	54.6	34.6	2	SR - R
	4719.55	0	8.6	58	32	1.3	SR - R
	4748.83	0	29.3	58	12.6	0	SA - SR
	4772.17	0	32	60.6	7.3	0	SA - SR
	4784.55	0	12	61.3	24.6	2	SR
	4806	0	20	57.3	22.6	0	SR
	4815	0	15.3	65.3	19.3	0	SR
	4864.5	0	18.6	48.6	32.6	0	SR - R
	4912	0	14	51.3	34.6	0	SR - R
	5650	0	8.6	52.6	38.6	0	SR - R
	Average	*0.05*	*16.34*	*54.81*	*27.89*	*0.72*	*SR - R*
B27-NC115	4776	0	8	42.6	47.3	2	R - SR
	4849.5	0	10	46	44	0	SR - R
	Average	*0*	*9*	*44.3*	*45.65*	*1*	*R - SR*
B2, B3, B8& B27 - NC115	*Average*	*0.123*	*18.286*	*48.276*	*31.713*	*1.45*	*SR - R*

Table. 4.8. Average roundness (%) of the Mamuniyat Formation, within type wells of B-Field, NC115 Concession.

Well	Depth (ft)	Angular	Subangular	Subrounded	Rounded	Well rounded	Interpretation
H2-NC115	4872.81	3.3	20.6	42	27.3	6.6	SR - R
	4885.6	2	20.6	32.6	34.6	10	R - SR
	4912.67	2	27.3	38.6	31.3	0.6	SA - R
	4939.24	0.6	27.3	37.3	32	2.6	SA - R
	4979.6	0.6	27.3	36	34	2	SA - R
	5127.89	0	26.6	38	31.3	4	SA - R
	Average	*1.42*	*24.95*	*37.42*	*31.75*	*4.3*	*SA - R*
H3-NC115	4719.43	0	11.3	41.3	46	1.3	SR - R
	4750.6	0	19.3	40.6	36.6	3.3	SR - R
	4793.25	1.3	14	40.6	41.3	2.6	R - SR
	4845.74	0.6	13.3	49.3	36	0.6	SR - R
	4863.79	0	8.6	41.3	48.6	1.3	SR - R
	4910.54	0	13.3	44	42	0.6	SR - R
	4921.2	0	10	41.3	46.6	2	SR - R
	5001.58	0	19.3	39.3	41.3	0	R - SR
	5163.98	0	24	46.6	29.3	0	SR
	Average	*0.21*	*14.8*	*42.7*	*40.85*	*1.3*	*SR - R*
H4-NC115	4852.35	0.6	13.3	32	48	6	R - SR
	4863	0	25.3	32	42	0.6	R - SA
	4900	0	38	42.6	19.3	0	SR - SA
	4913.5	0	40.6	40.6	18.6	0	SA - SR
	4925	0	15.3	35.3	49.3	0	R - SR
	4974	0	16.6	38	45.3	0	R - SR
	4988.5	0	22.6	48.6	28.6	0	SR
	5002	0	17.3	40.6	39.3	2	SR - R
	5006	0	20	43.3	36	0.6	SR - R
	Average	*0.07*	*23.22*	*38.22*	*36.27*	*1.02*	*SR - R*
H5-NC115	4823.5	0	24	49.3	26.6	0	SR
	4842.3	0	21.3	49.3	29.3	0	SR
	4871.75	0	16	45.3	38.6	0	SR - R
	4884.5	0	16	35.3	48.6	0	R - SR
	4922.75	0	10	46	42.6	1.3	SR - R
	4962	0	14.6	38	47.3	0	R - SR
	4986	0	14.6	46.6	36.6	2	SR - R
	4992	0	16.6	48	34	1.3	SR - R
	4997	0	10.6	46	43.3	0	SR - R
	5000.5	0	24	42	34	0	SA - R
	5011	0	12	44	44	0	SR - R
	Average	*0*	*16.34*	*44.53*	*38..63*	*0.42*	*SR - R*
H2, H3, H4& H5 - NC115	*Average*	*0.314*	*19.185*	*41.217*	*37.414*	*1.465*	*SR - R*

Table. 4.9. Average roundness (%) of the Mamuniyat Formation, within type wells of H-Field, NC115 Concession.

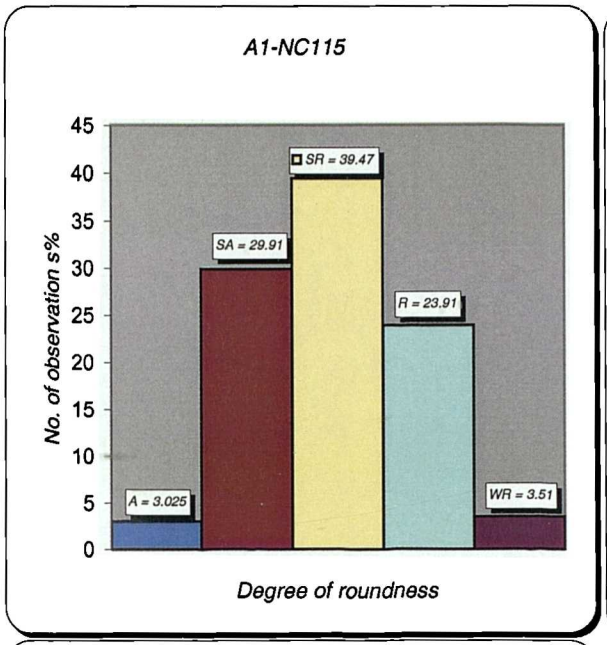

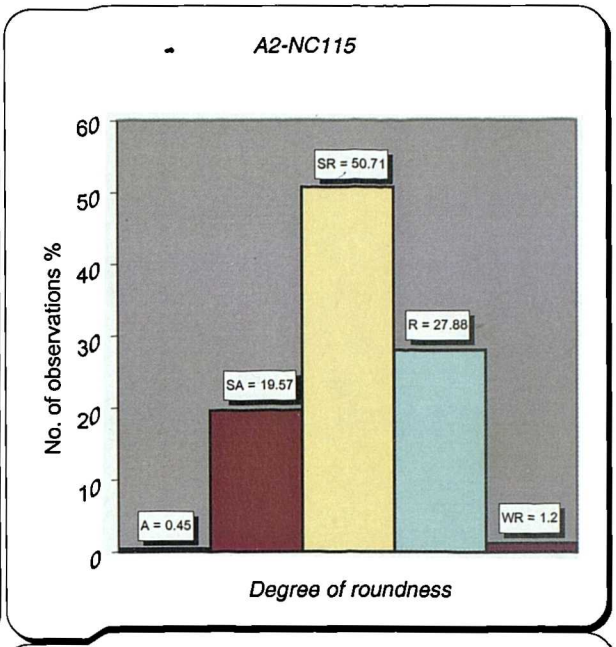

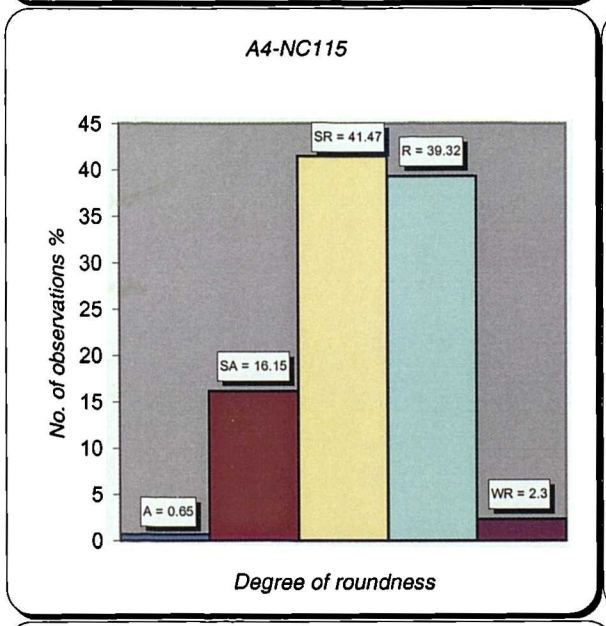

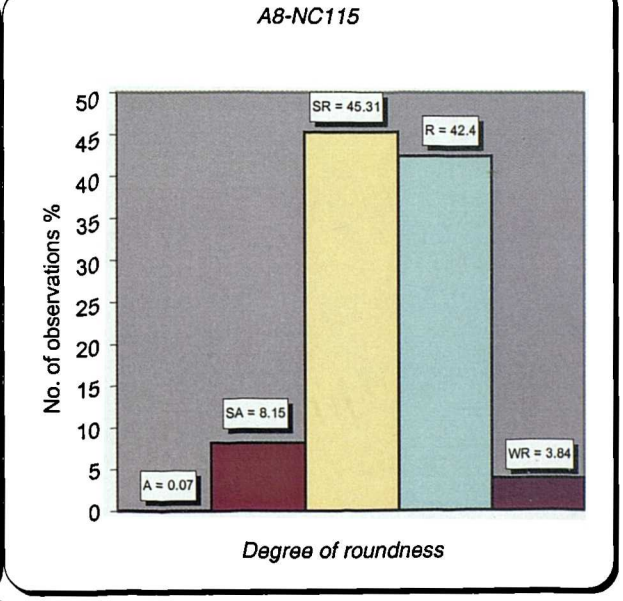

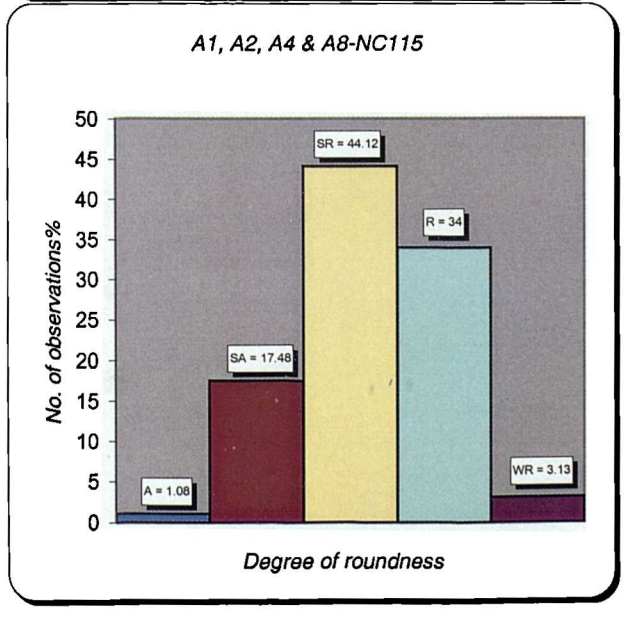

Note: Degree of roundness for the descriptive characterization of roundness.
(After RUSSEL - TAYLOR - PETTIJOHN).

Degree of roundness Russel - Taylor - Pettijohn	Degree of roundness (Wadell)	Geometric mid-point (approximate)
Angular (A)	0 - 0.15	0.125
Subangular (SA)	0.15 - 0.25	0.2
Subrounded (SR)	0.25 - 0.40	0.315
Rounded (R)	0.40 - 0.60	0.5
Well rounded (WR)	0.60 - 1.00	0.8

Fig. 4.2. Schematic average roundness of the Mamuniyat Fm, A-Field, NC115 Concession.

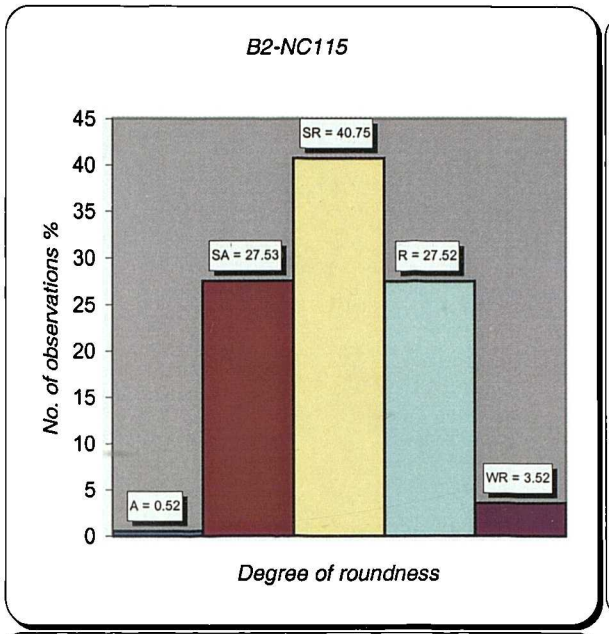

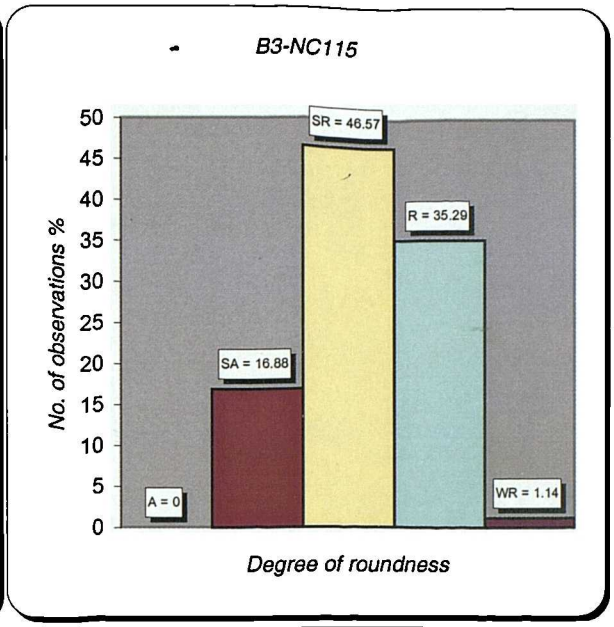

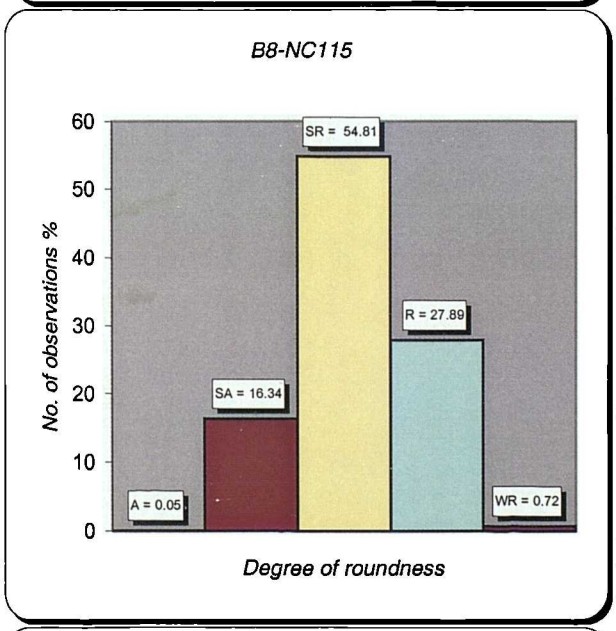

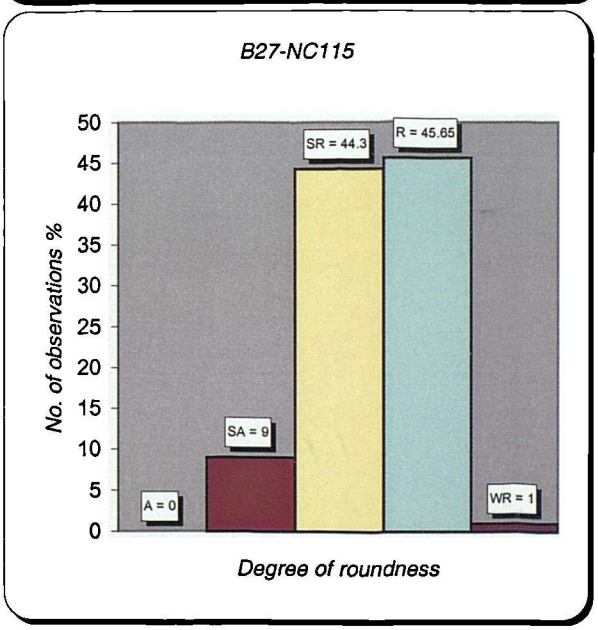

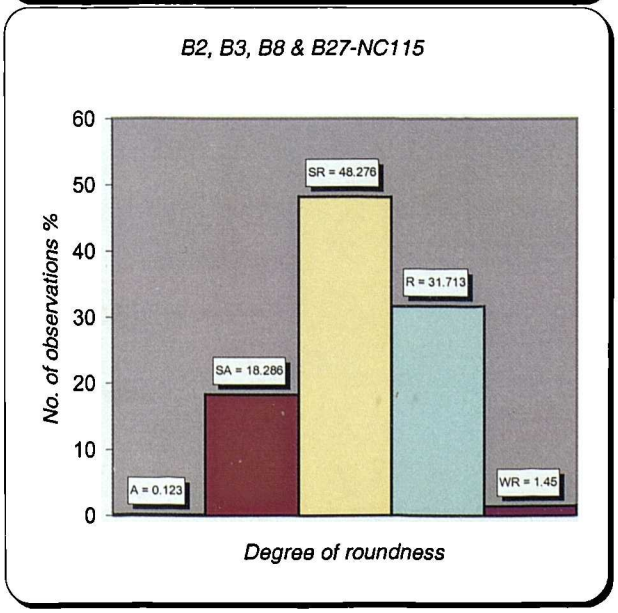

Note: Degree of roundness for the descriptive characterization of roundness.
(After RUSSEL - TAYLOR - PETTIJOHN).

Degree of roundness Russel - Taylor - Pettijohn	Degree of roundness (Wadell)	Geometric mid-point (approximate)
Angular (A)	0 - 0.15	0.125
Subangular (SA)	0.15 - 0.25	0.2
Subrounded (SR)	0.25 - 0.4	0.315
Rounded (R)	0.4 - 0.6	0.5
Well rounded (WR)	0.6 - 1.00	0.8

Fig. 4.3. Schematic average roundness of the Mamuniyat Fm, B-Field, NC115 Concession.

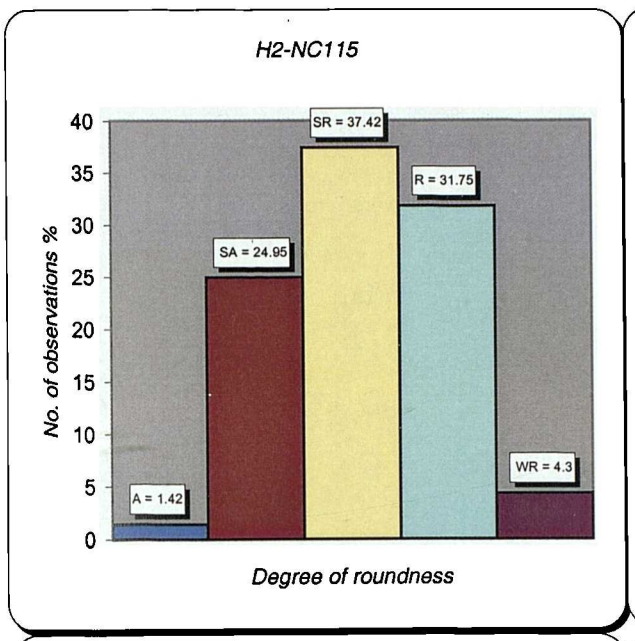

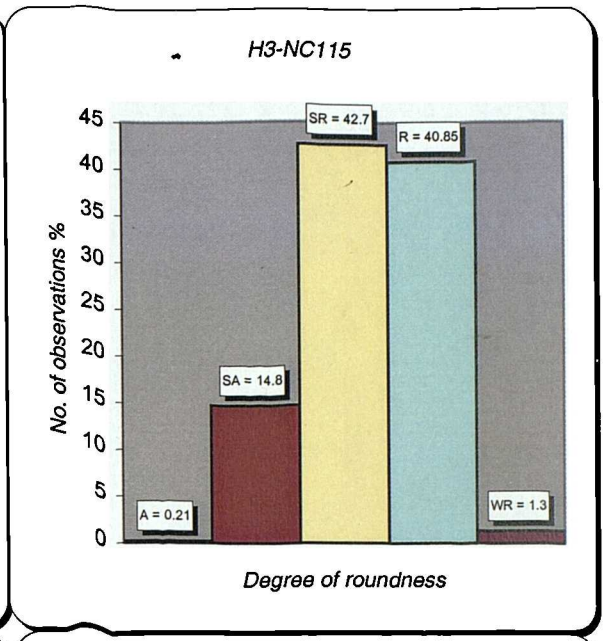

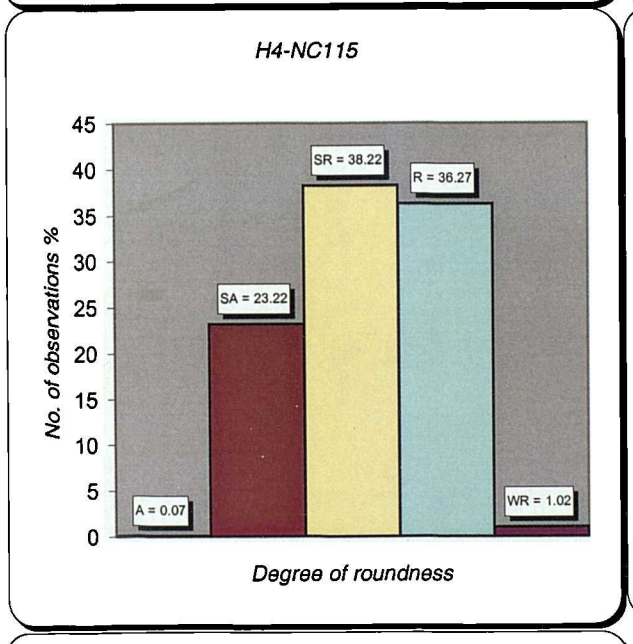

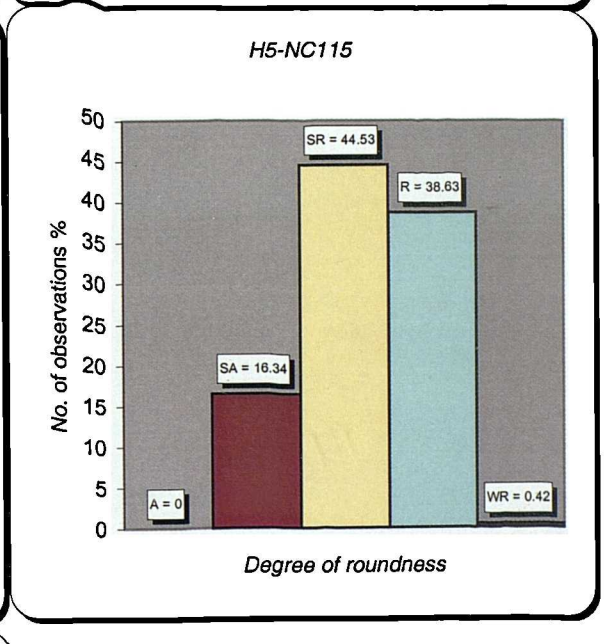

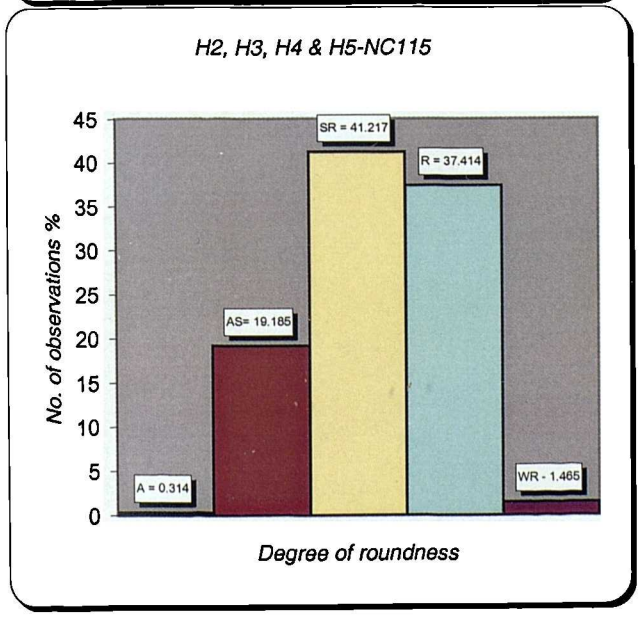

Note: Degree of roundness for the descriptive characterization of roundness.
(After RUSSEL - TAYLOR - PETTIJOHN).

Degree of roundness Russel - Taylor - Pettijohn	Degree of roundness (Wadell)	Geometric mid-point (approximate)
Angular (A)	0 - 0.15	0.125
Subanglar (SA)	0.15 - 0.25	0.2
Subrounded (SR)	0.25 - 0.40	0.315
Rounded (R)	0.40 - 0.60	0.5
Well rounded (WR)	0.60 - 1.00	0.8

Fig. 4.4. Schematic average roundness of the Mamuniyat Fm, H-Field, NC115 Concession.

CHAPTER 5

SEQUENCE STRATIGRAPHY

SEQUENCE STRATIGRAPHY

5.1 Introduction

In recent years, there has been a new approach to the study of sedimentary strata, that of Sequence Stratigraphy, which looks at sedimentary packages on a much larger scale to elucidate their internal and external geometry. Concepts have come from seismic stratigraphy, where onlap, offlap, downlap relationships can be demonstrated relatively easily on seismic sections (Payton, 1977).

Sequence stratigraphy is the study of genetically related facies within a framework of chronostratigraphically significant surfaces and related strata bounded by a surface of erosion or non-deposition, or their correlative conformities (Van Wagoner *et al.*, 1988). Research in the area of sequence stratigraphy has re-vitalized the subject of facies analysis because of the importance of documenting vertical and lateral facies changes in the rock record, and it has re-emphasized the importance of precise chronostratigraphic correlation. Analysis of vertical lithofacies profiles has become a vital tool for investigating the lateral migration of depositional systems. Lateral correlation is essential in order to trace individual sequences across a basin and to reconstruct the way in which contemporaneous, laterally adjacent depositional systems have become integrated into regional systems tracts.

Sequence stratigraphy is currently one of the most rapidly developing areas of sedimentary geology. A major research focus at the present time is the development of quantitative models that relate sequence stratigraphy to crustal behaviour during basin subsidence, and to the effects of regional (tectonically driven) and global (eustatic) sea-level changes. The essential ideas of sequence stratigraphy and terminology are summarised in AAPG Methods in Exploration 7 (Van Wagoner *et al.*, 1990).

Sequence stratigraphy is based on a cyclic stacking hierarchy (**Fig. 5.1**) of deposition, bounded above and below by unconformities (Emery and Myer, 1996). The constituent sequences and their boundaries are interpreted to form cycles related to fluctuation in relative sea-level (Dual and Vail, 1992). Four types of stratigraphic cycles are recognised by Duval and Vail (1992).

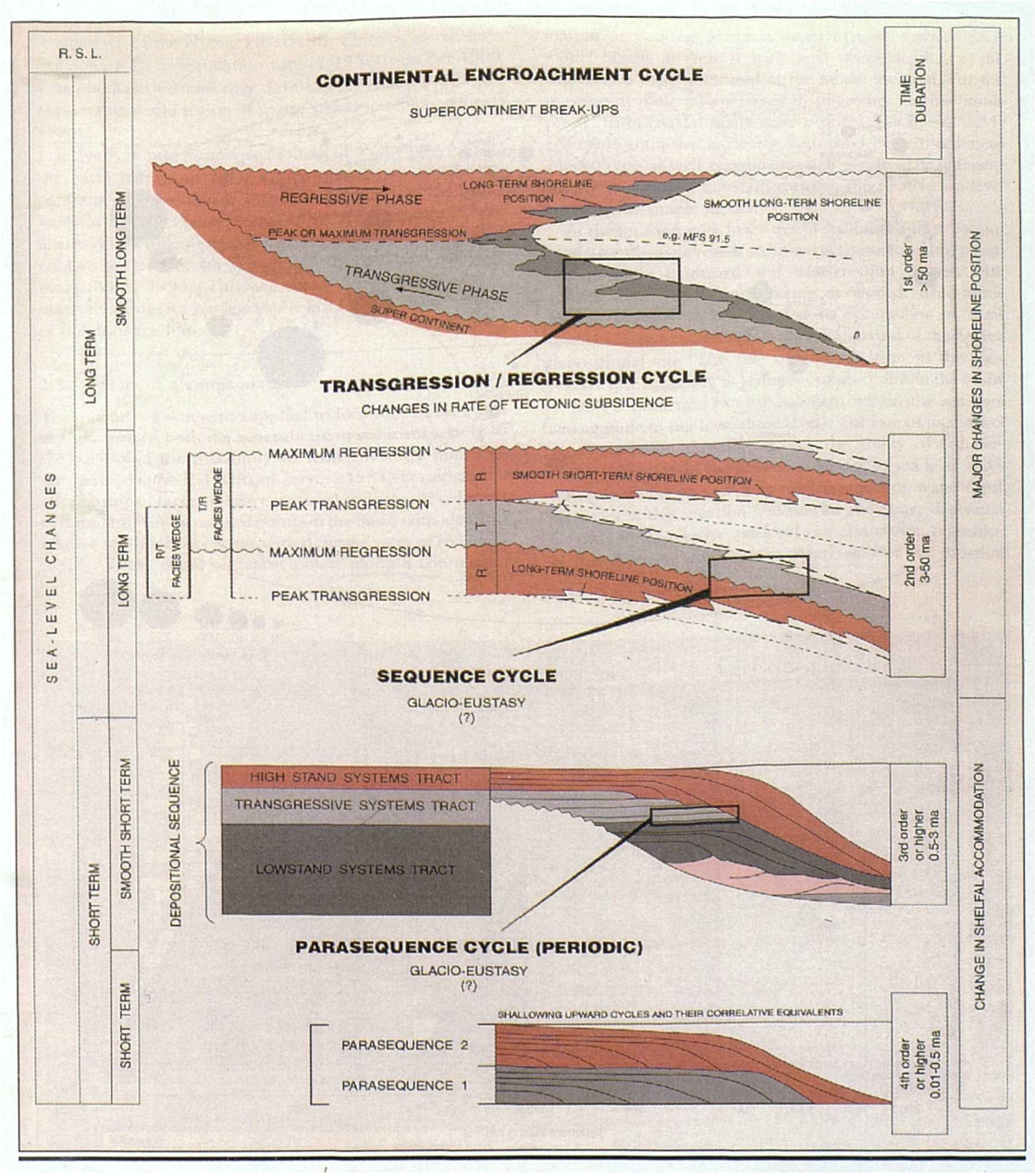

Fig. 5.1 Hierarchy of stratigraphic cycles (After Duval and Vail, 1992).

5.2 Historical development

1930s. Cyclicity has long been recognised as a feature of sedimentary successions by geologists. For example, many fluvio-deltaic successions consist of shallowing upward cycles (cyclothems) bounded by fossiliferous shales and limestone's (*e.g.* Phillips, 1836). In the context of sequence stratigraphy, it is interesting to note the heated argument in the 1930s-1950s about the best surface to define these cyclothems in Upper Carboniferous rocks. Many European geologists preferred to use condensed marine shale and limestone horizons (flooding surface in modern sequence stratigraphic terms) to define sedimentary cycles, whereas some North American geologists preferred to use regionally-extensive unconformities (sequence boundaries in modern sequence stratigraphic terms) at the base of deeply eroded fluvial sandstones (*e.g.* Weller, 1930; Wanless and Shepard, 1936).

1949. Sloss *et al.* (1949) were the first to formally propose the concept of the unconformity bounded sequence, although these authors acknowledged that this was not a new idea even then. Sloss and co-workers sub-divided the sedimentary succession of the North American craton from late Precambrian to Holocene rocks into six sequences, which they were able to correlate across the entire craton. These sequences exhibit all the parameters of the modern definition (Mitchum *et al.*, 1977). Although Sloss's ideas found little acceptance at the time, they formed the basis of modern sequence stratigraphy.

1977. The next major development in the evolution of modern sequence stratigraphy was the publication of the concepts of seismic stratigraphy by a team of Exxon researches led by Vail (Vail *et al.*, 1977). In a series of articles these authors presented the concepts of unconformity bounded sequences applied to, and documented with seismic reflection data. In this work, Vail *et al.* (1977) cited eustatic sea-level change as the primary driving mechanism for the stratal geometries observed in seismic sections.

Considerable effort was subsequently put into the global correlation of sea-level changes and the construction of a sea-level chart which could be used for absolute dating purposes (*e.g.* Haq *et al.*, 1988). The Exxon research group came under considerable criticism for the global sea-level chart – indeed, most of the problems faced by workers trying to gain acceptance for sequence stratigraphic concepts have stemmed from a widespread distrust of the global sea-level chart.

1988. The application of sequence stratigraphy was widened by the development of models, which explained seismic stratal geometries using the concept of accommodation space (Jervey, 1988; Posamentier *et al.*, 1988; Posamentier and Vail 1988). These models were not only applicable to seismic data but also provided a basis for understanding and predicting stratal geometries and facies relationships at a much higher resolution – including outcrop, cores and well logs. These concepts and models were summarised in a more accessible, if somewhat simplistic form, in Van Wagoner *et al.* (1990).

1990s. Since the publication of the accommodation space concept and resultant models, research has concentrated on two areas:

1) Much work has been directed at integrating facies models developed in the 1960s-1970s with sequence stratigraphy; and
2) Research has also shifted from the search for the "global" sequence to examine the effects of local/regional tectonics and sediment supply on the development of sequences.

Consequently, the development of a sequence stratigraphic framework is now a preliminary step in explaining many other features of sedimentary successions. As a result of the application of sequence stratigraphy, many mature oil fields are being re-examined with a view to renewed production, and many "classical" geological sites are being re-interpreted. For example, the Upper Carboniferous fluvio-deltaic cyclothems which received much attention and arguments during the 1930s are being re-examined– albeit with a modern knowledge of sedimentology and stratigraphy!

5.3 Methodology

The sequence stratigraphic method of dividing the sedimentary record into packages of genetically related sediments resulting from relative sea-level change was developed in passive continental margin siliciclastic successions (*e.g.* Mitchum, 1977; Vail *et al.*, 1977; Van Wagoner *et al.*, 1988; Vail *et al.*, 1991). The high-resolution sequence stratigraphic approach is a powerful methodology to unravel the fine scale stratigraphic architecture of sedimentary systems. This approach has found widespread application in siliciclastic systems (*e.g.* Van Wagoner *et al.*, 1988; Wilgus *et al.*, 1988) and more recently also in shallow water carbonates (*e.g.* Pomar, 1991).

This approach is based on four steps. The first step is the detailed description of the different facies types and their interpretation in terms of depositional environments. In particular the estimation of the paleo-bathymetry is important in order to recognize the trends of increase or decrease in accommodation space (*e.g.* Jervey, 1988).

The second step is the identification of special surfaces (*e.g.* subaerial exposure surface, ravinement surface, flooding surface, hardgrounds, and firm ground) and their sequence stratigraphic interpretation in terms of sequence boundaries, flooding surface and maximum flooding surface.

The third step is the correlation and hierarchicalisation of depositional sequences. The correlation is based on the identification of sedimentary surfaces and volumes which have a stratigraphic significance (*i.e.* which represent time units or surfaces). Based on the environmental or bathymetric changes across limiting surfaces, the transgressive or regressive character of the depositional sequences is determined. The amount of shift of the facies belts along the surfaces, in combination with the character of the surface (*e.g.* stratigraphic hiatus, flooding surface, short-term emission surface) determines the order (and therefore importance) of the depositional sequence.

Vail *et al.* (1991) and Haq *et al.* (1988) proposed a subdivision of depositional sequences into cycles from a 1st to 6th orders, which are primarily based on time. These orders are recognised hierarchies of sea-level cycles and durations as follows:

- 1st order (duration 50 + Ma);
- 2nd order (duration 3 - 50 Ma);
- 3rd order (duration 0.5 – 3 Ma);
- 4th order (duration 0.08 – 0.5 Ma);
- 5th order (duration 0.03 – 0.08 Ma); and
- 6th order (duration 0.01 – 0.03 Ma).

The final step is the construction of (a high resolution) sequence stratigraphic model based on correlation of cycles of increasing and decreasing accommodation potential across the different environments. This confirms the different orders of depositional sequences, and in particular, the importance of their bounding surface. The surfaces are the time lines and the model shows the (predictable) variability of the facies in between them, and accurately reflects the geometrical relationships of the various sediment packages.

By constraining the geometrical relationships in this manner, predictions can also be made about the diagenetic alteration patterns. The resulting model can then be tested and possibly refined or changed, when more data becomes available, such as additional outcrop sections (or wells) or new data sets such as geochemical, palaeontological and mineralogical observations.

The constituent sequences and their boundaries are interpreted to form cycles related to fluctuations in relative sea-level (Duval and Vail, 1992). Four types of stratigraphic cycles are recognised by Duval *et al.* (1992).

1) Continental encroachment cycles

These are defined as first order cycles. They have a duration of > 50 Ma (**Fig. 5.1**). Continental encroachment cycles are defined on the basis of the relative extent to which the continents are covered by sedimentary rocks at the time of deposition (Duval and Vail, 1992). First-order continental encroachment cycles have been attributed to tectonic-eustasy (*i.e.* changes in ocean basin volume induced by continental break-up and aggradation.

2) Major transgressive-regressive facies cycles

These cycles are defined on the basis of changes in the shoreline position and have durations of 3-50 Ma. They are defined as second-order cycles (**Fig. 5.1**). Second-order transgressive and regressive facies may be produced by regional tectonic change such as change in the rate of subsidence and uplift related to the rate of sea-floor spreading, and change in size of ocean basins (Duval *et al.*, 1992).

3) Sequence cycles

These are defined as third order cycles and have durations of 0.5-3 Ma (**Fig. 5.1**). These cycles are related to changes in shelfal accommodation space and are probably caused by glacio-eustasy (Vail *et al.*, 1991). They are composed of lowstand, transgressive and highstand systems tract and are bounded by sequence boundaries.

4) Parasequence cycles

These cycles represent shallowing-upward facies bounded by a surface of abrupt deepening (**Fig. 5.1**). Duval and Vail (1992) suggested that the parasequence cycles range from the fourth to the sixth order and have durations of 0.1-0.5 Ma. Parasequence cycles are the building blocks of the systems tract in third order sequences.

A schematic outcrop or well-log profile of the strata deposited during the orders of these eustatic sea-level cycles is illustrated in **Figure 5.5**. This scheme depends on the interaction between the rate of eustasy and subsidence, *e.g.* fourth-order cycles deposit a sequence or parasequence; fifth-order cycles deposit a parasequence or have no depositional expression (Van Wagoner *et al.*, 1988). Fourth-order sequences have been observed within sequence sets in Pennsylvanian strata of the western and central United states, Cretaceous strata of the western United States, and most of the Tertiary strata in the northern Gulf of Mexico (Van Wagoner *et al.*, 1990).

5.4 Sequence stratigraphic techniques

Sequence stratigraphy divides the sedimentary record into a number of sequences bounded by unconformities, and their correlation conformities, termed Sequence Boundaries (SB). A sequence represents sedimentary deposits or rocks deposited during one cycle of relative sea-level change. A sequence can be divided into separate parts, termed systems tracts that define the parts of the sequence in terms of rising or falling relative sea-level. Systems tracts are demarcated by key surfaces.

Sequence stratigraphy is a precise methodology to subdivide, correlate and map sedimentary rocks. The basic units of sequence stratigraphy are depositional sequences, systems tracts and parasequences, which develop on time scales of 0.5 – 5 Ma and 0.01 – 0.5 Ma respectively (Vail *et al.*, 1991), as detailed above.

The Lowermost Systems Tracts (LmST) contain those sediments deposited during falling relative sea-level between the SB and Transgressive Surface (TS). The TS represents the first significant flooding of the basin margin during rising relative sea-level. The Transgressive Systems Tracts (TST) represent sedimentation between the TS and the maximum rate of relative sea-level rise, which corresponds to the Maximum Flooding Surface (MFS). Sediments deposited during the rising, highest and falling relative sea-level of the half-cycle between the MFS and successive SB are assigned to the Highstand Systems Tracts (HST) (Brown and Fisher, 1977).

Smaller-scale packages of genetically related conformable sediments that are bounded by flooding surfaces are parasequences. These are the basic building blocks of sequences and stack to form systems tracts.

Van Wagoner *et al.* (1988) in their overview of the fundamentals of sequence stratigraphy, defined an unconformity as "a surface separating younger from older strata, along which there is evidence of subaerial-erosional truncation and, in some areas, correlative submarine erosion, or subaerial exposure, with a significant hiatus indicated". They went on to say that "this definition restricts the usage of the term unconformity to significant subaerial surfaces and modifies the definition of unconformity used by Mitchum (1977)". This earlier definition referred to both subaerial and submarine erosional truncation and was thought to be too broad by Van Wagoner *et al.* (1988).

The terminology developed from near-shore siliciclastic sequences recognises two types of sequence and sequence boundary, classified by erosional and basin-onlap architecture. These sequences are characterised by subaerial exposure and a downward shift in coastal onlap, with the more major type 1 sequence exhibiting a concurrent subaerial erosion surface associated with stream rejuvenation and a basinwards shift in facies (Van Wagoner *et al.*, 1988). The LmST is termed Lowstand Systems Tracts (LST) if overlying a type 1 SB and a Shelf-margin System Tract (SmST) if overlying a type 2 SB. Within the TST individual parasequences and parasequence sets are retrogradational, onlapping the basin margin and consequently the SB. Consequently, the TST is composed of a package of sediments with a retrogradational architecture. The HST is characterised by an aggradational and subsequently progradational geometry with prograding clinoforms downlapping on to the underlying MFS (**Fig. 5.2**).

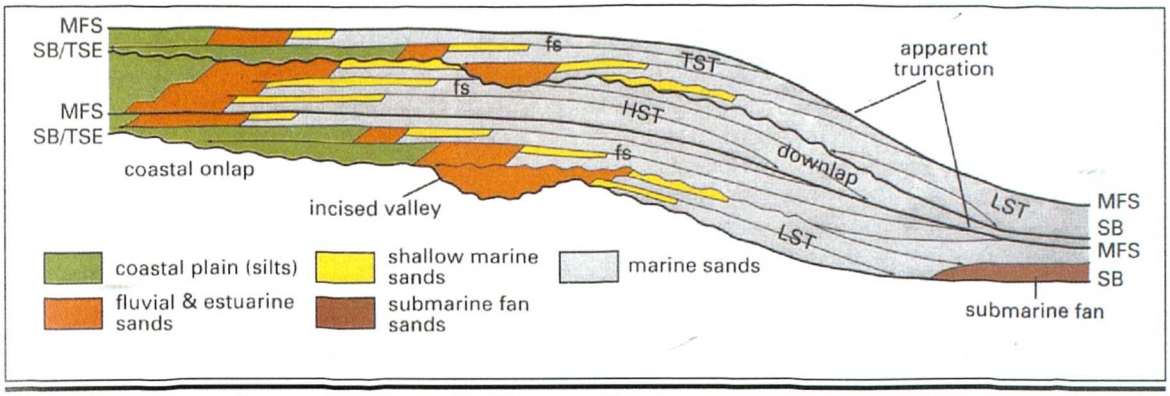

A) The sequence-lithological scheme and sequence tracts (After Rider, 1996).

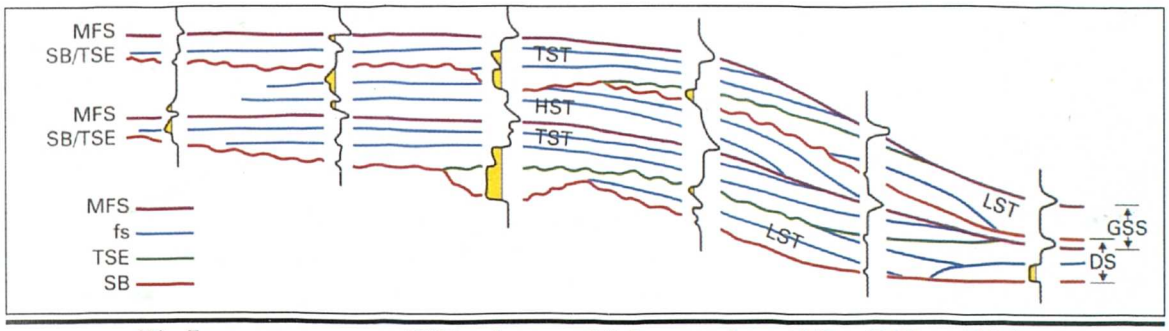

B) Log gamma-ray (GR) scheme with key surface (After Rider, 1996).

Fig. 5.2 The depositional model of sequence stratigraphy defined for the DS, depositional sequence (After Exxon) and the GSS, genetic stratigraphic sequence (After Galloway):
A) The sequence has a lithological scheme with sequence tracts; and
B) The same model with gamma ray log traces and key surfaces. MFS = maximum flooding surface: TSE = transgressive surface of erosion: SB = sequence boundary: FS = flooding surface. LST, TST, HST, = Lowstand, Transgressive, Highstand Systems Tract (After Rider, 1996).

Sequence stratigraphic analysis develops a chronostratigraphic framework of cyclic, generally related strata. A sequence is bounded by a surface of stratal discontinuity or their correlative conformities. These surfaces are created by erosion or nondeposition on the shelf and an associated increase in both supply and grain-size of the sediment deposited in the basin. Sequence and systems tract boundaries are always present in the rock record, although at times in certain situations they may be subdued or one boundary may be a composite of many.

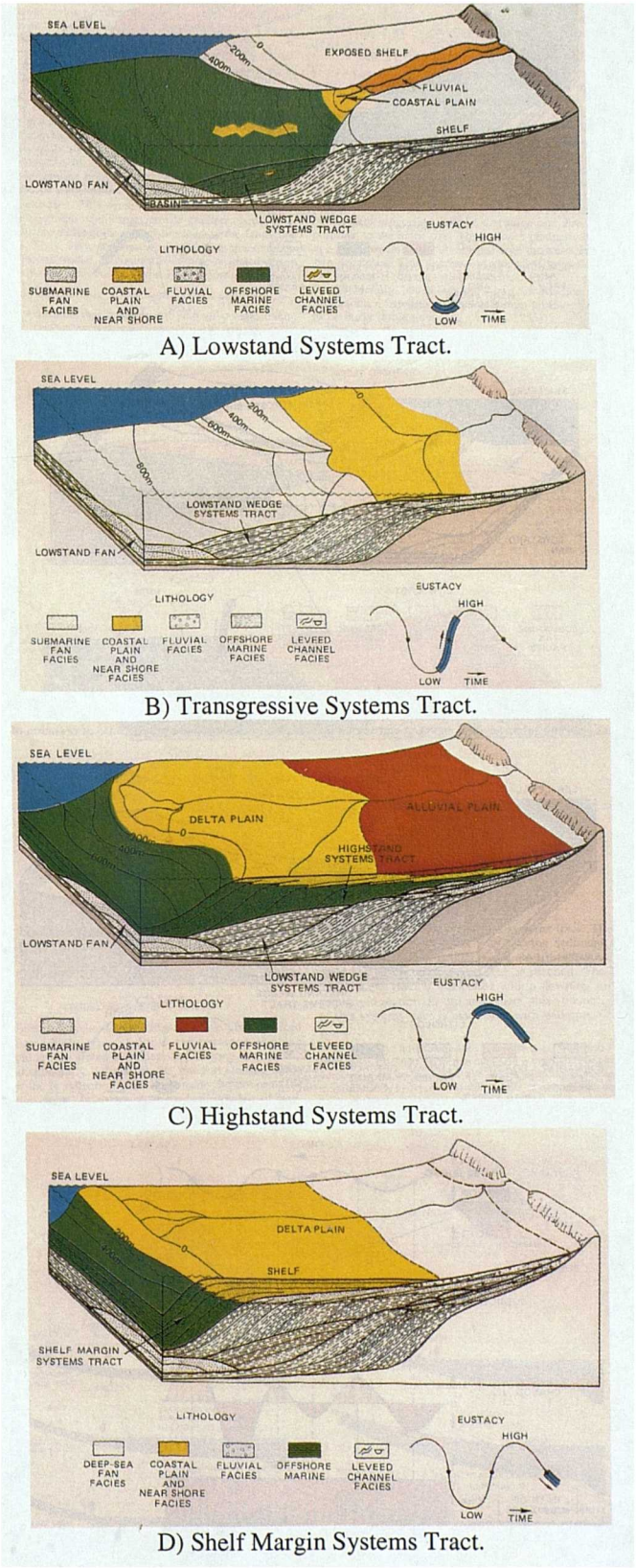

Fig. 5.3 Idealized block diagrams showing systems tracts and their relation to the eustatic sea-level curve (After Posamentier *et al.*, 1988).

A systems tract is a set of linked contemporaneous depositional systems. Each systems tract is bounded by a physical surface that is, in part, a discontinuity marking the boundary of a similar set of accommodation patterns such as sigmoidal to oblique, oblique to aggradational, or retrogradational (Posamentier *et al.*, 1988; Posamentier and Vail, 1988; and Jervy, 1988). Depositional systems within each systems tract are linked by changes in sedimentary facies (Posamentier and Vail, 1988) (**Fig. 5.3**).

Of the four types of systems tracts, only three will be present in any one sequence. A Type 1 sequence has a Type 1 sequence boundary at its base and is composed of a lowstand, transgressive and highstand systems tract. A Type 2 sequence has a Type 2 sequence boundary at its base and is composed of a shelf-margin, transgressive, and highstand system tract. Depositional sequences and system tracts are chronostratigraphic intervals because they represent all the rocks deposits within a particular interval of time. Each boundary is age-dated at the minimum hiatus where the strata are conformable. The interval of time between the lower and upper conformities defines the time period over which the rocks were deposited (**Fig. 5.4**).

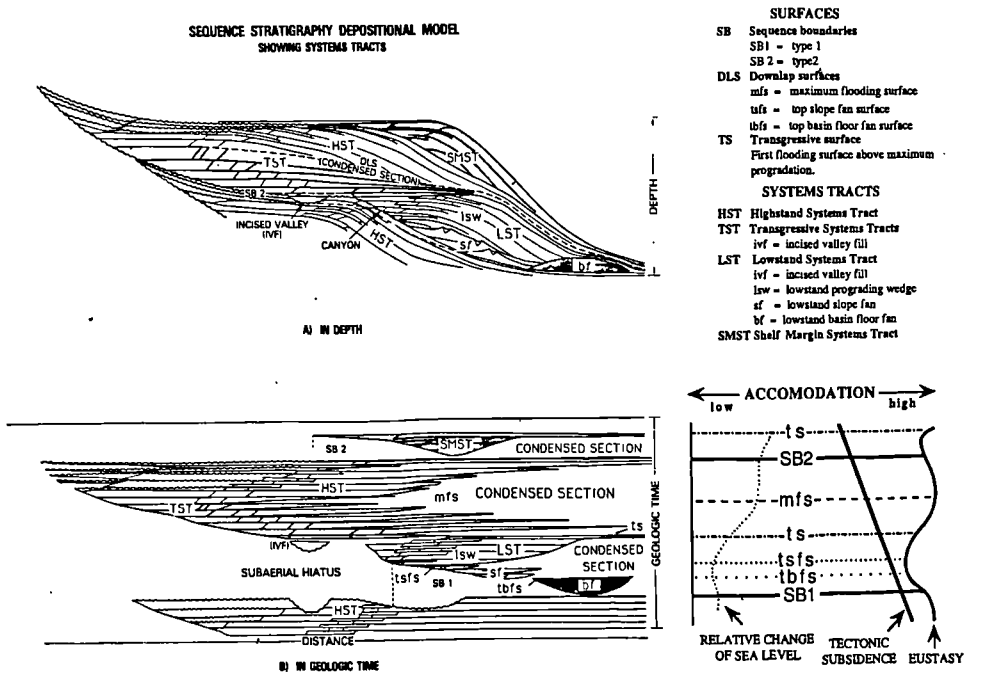

Fig. 5.4 Diagrammatic sketch of sequences and systems tracts in depth and geologic time in relation to tectonic subsidence, sea level and relative changes of sea level (After Vail *et al.*, 1991).

Sequence stratigraphic studies from basins around the world indicate that chronostratigraphic intervals defined in this way are global (Vail *et al.*, 1977, 1984; Bartek *et al.*, 1990). These intervals are defined on the basis of physical stratigraphy from seismic, wells or outcrop data and dated by biostratigraphy to identify the age of the interval.

5.5 Sequence stratigraphic procedure and interpretation

The following sequence stratigraphic procedure for interpretation of palaeogeography, geologic history, stratigraphic signature and resource evaluation is recommended by Vail (1987) (**Fig. 5.5**).

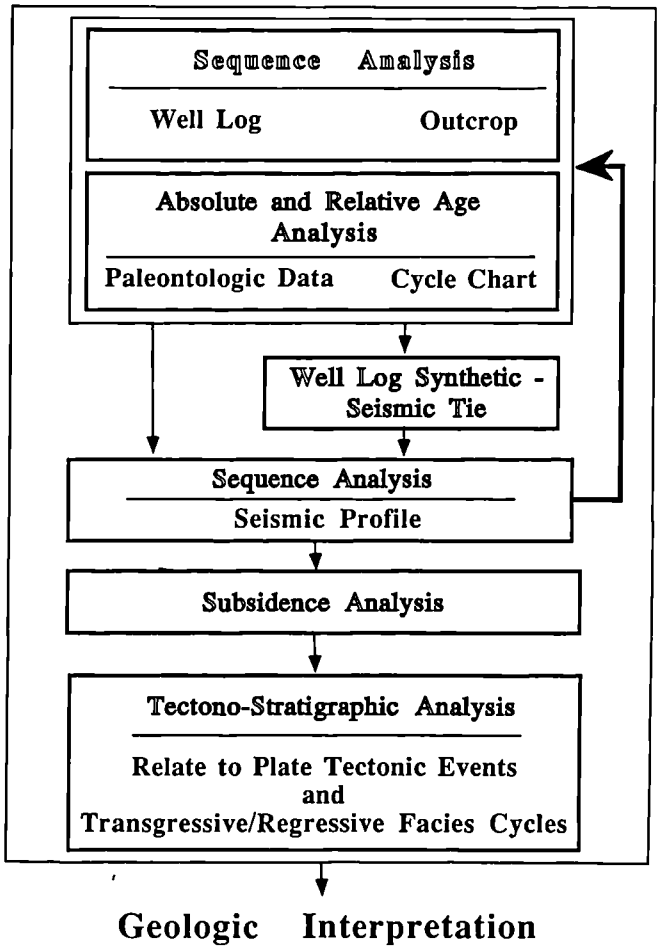

Fig. 5.5 Sequence stratigraphy interpretation procedure (After Vail *et al.*, 1991).

1) Determine the physical chronostratigraphic framework by interpreting sequence, system tracts and parasequences and/or simple sequences on outcrops, well logs and seismic data and age data with high resolution biostratigraphy;
2) Construct geohistory, total subsidence and tectonic subsidence curves based on sequence boundary ages;
3) Complete a tectono-stratigraphic analysis including:
   - Relate major transgressive-regressive facies cycles to tectonic events;
   - Relate changes in rates of tectonic subsidence curves to plate-tectonic events;
   - Assign a cause to tectonically enhanced unconformities;
   - Relate to the tectonic subsidence curve;
   - Map tectono-stratigraphic units;
   - Determine style and orientation of structures within tectono-stratigraphic units; and
   - Simulate geologic history.
4) Define depositional systems and lithofacies tracts within systems tracts and parasequences or simple sequence;
5) Interpret palaeogeography, geologic history and stratigraphic signatures from resulting cross-section, maps and chronostratigraphic charts; and
6) Locate potential reservoirs and source rocks for possible sites of exploration.

5.6 Sequence stratigraphic signatures

The depositional patterns of sequence stratigraphy are controlled by three main factors: tectonism, eustasy and sedimentation. The signatures of each of these can be distinguished by understanding the distribution of each of these variables in terms of their effects on the stratigraphic record in time and space (Vail *et al.*, 1991). Sequence stacking patterns result from interaction of these factors.

Tectonic and eustasy processes result in relative changes of sea-level, which control the space available for sediments (accommodation space) and the distribution of facies within such a genetically related package (Posamentier *et al.*, 1988; Van Wagoner *et al.*, 1988).

5.6.1 Tectonism

Tectonism has the greatest influence on increasing or reducing accommodation space. Also, when coupled with climate, it controls the type and amount of sediments filling that space (Vail *et al.*, 1991). The stratigraphic signature of tectonism results from a wide range of processes and has the most profound effect on accommodation. Tectonism is characterized by active processes related to plate interactions, and equilibration responses to conditions created by the active processes.

First-order tectonic events result from thermodynamic processes in the asthenosphere, which drive the plates and deform the earth's crust and upper mantle. Crustal extension and transtension, crustal shortening and transpression. Their stratigraphic signatures are uplifts and sedimentary basins.

Second-order tectonic events are characterized by changes in subsidence rates during the evolution of a sedimentary basin. They may result from local thermodynamic perturbations. These changes in subsidence rate apparent on tectonic subsidence curves are either concave-upward, or convex-upward. The stratigraphic signatures of both curves are major transgressive-regressive facies cycles.

Third-order tectonic events are folding, faulting, and magmatic activity. The stratigraphic signatures of these events is tilted and ruptured strata. They are associated with penecontemporaneous events such as slides, slumps, magaturbidites, bentonite beds, datable extrusive lava flows, and intrusive sills and dikes (Vail *et al.*, 1991).

5.6.2 Eustasy

Relative sea-level is a term used here for sea-level relative to a datum plane, here taken to be the sediment-water interface. Relative sea-level change therefore, encompasses eustatic changes in sea-level and changes resulting from sediment accumulation, compaction, winnowing and erosion coupled with changes resulting from localised tectonic movements.

Five orders of eustatic cycles have been identified in the geologic record including continental flooding cycles (first order) and four orders of sequence cycles with periodicity ranging from 5 My to 10 Ka (second to fifth order) (Hallam, 1977; Vail *et al.*, 1977; Fischer, 1982).

5.6.2.1 Continental flooding cycles

Continental flooding cycles are defined on the basis of major times of encroachment and restriction of sediments on the cratons. They represent first-order eustatic cycles and their stratigraphic signature is the megasequence. There are two Phanerozoic continental flooding surface cycles (Hallam, 1977; Vail *et al.*, 1977; Fischer, 1982). The first begins in the uppermost Proterozoic and ends in the latest Permian.

The two continental flooding cycles are recognisable on all continents and are believed to be global. The cause of these cycles is believed to be tectono-eustasy (change in ocean basin volume). Other factors that contribute to changes in ocean basin volume are continental collisions, subduction of trenches, submarine magmatism, and sediment infill. Pitman (1978) estimated that the maximum rate of tectono-eustatic change caused by a combination of all these variables would be 1.2 – 1.5 cm/1000 years.

Second-to fifth-order eustatic cycles are recorded by sequence cycles, systems tracts, and periodic parasequences or sequence. They are believed to be glacio-eustatic cycles (Vail *et al.*, 1977; Bartek *et al.*, 1990) with a smaller magnitude, but higher frequency than tectonically induced transgressive-regressive facies cycles.

5.6.2.2 Sequence stratigraphic cycles

Sequence stratigraphy recognises different types of cyclicity (Van Wagoner *et al.*, 1990; Vail *et al.*, 1991) (**Fig. 5.6**).

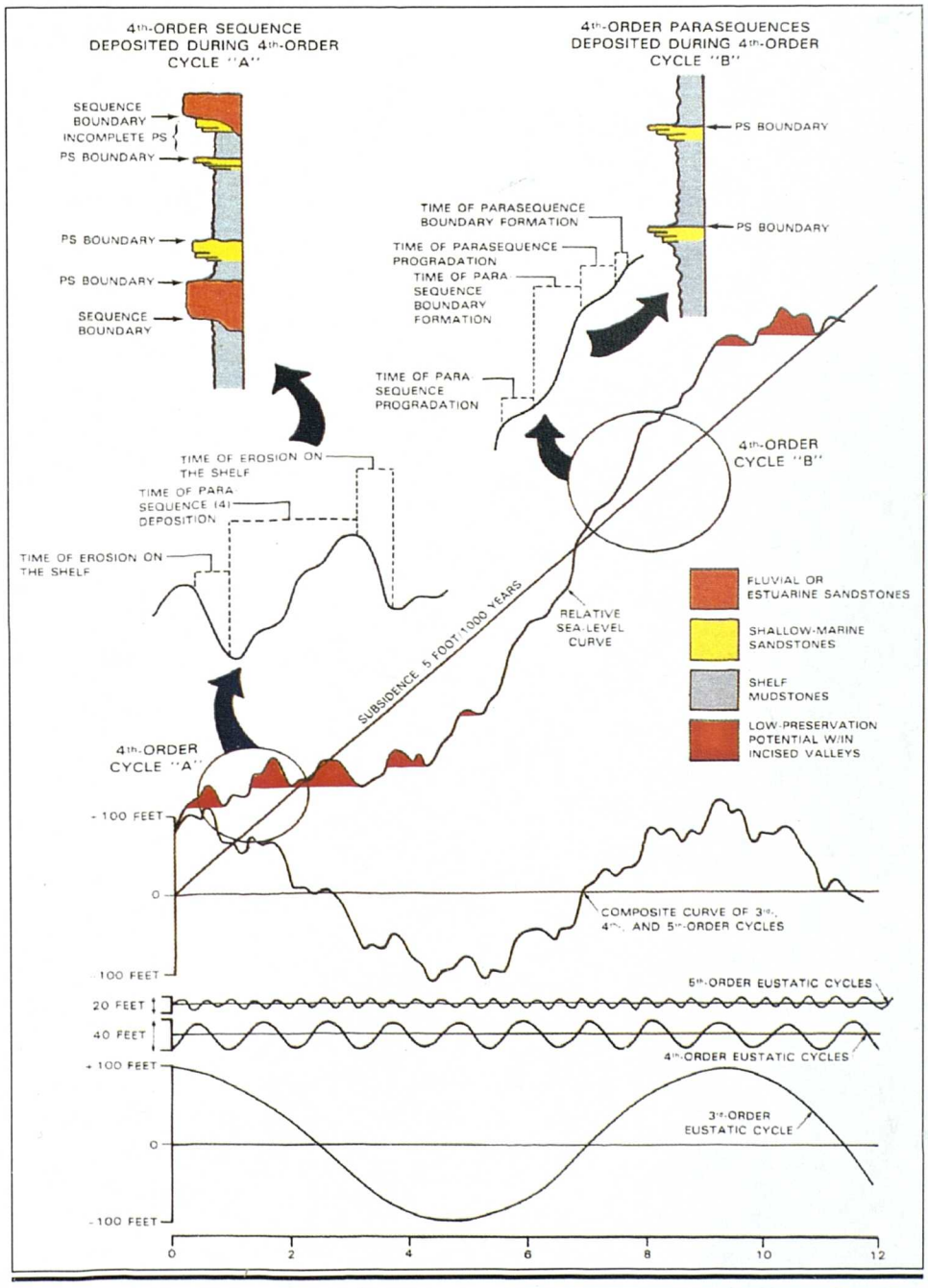

Fig. 5.6 Interaction of eustasy and subsidence to produce parasequences and sequences (After Van Wagoner *et al.*, 1990).

The relationship between this hierarchy of eustatic cycles, subsidence and the deposition of sequences and parasequences is illustrated in **Figure 5.6**. In this figure, a third-order eustatic cycle (approximately one million years) is added to fourth-order cycles (approximately 50000 years) to form a composite eustatic curve (Van Wagoner *et al.*, 1990). Two types of fourth-order cycles, designated cycle "A" and cycle "B", compose the relative change in sea-level curve. Fifth-order cycles superimposed on the fourth-order cycle form parasequences bounded by marine flooding surfaces.

5.6.3 Sedimentation

Sediment fills the space created by a relative rise of sea-level. Sediments are deposited episodically and are local in distribution. The stratigraphic signature of the sedimentologic effect is the depositional system. Depositional systems are composed of laminae, laminae sets, beds and bed sets, and episodic parasequences (Campbell, 1967).

The objective of sequence stratigraphy is to identify and correlate the genetic chronostratigraphic sequences, systems tracts, and parasequences, and then relate them to the depositional systems and lithofacies tracts. Application of this procedure to many different types of basins has shown a close relationship between the type of systems tract and the dominant depositional systems: Highstand, Transgressive, Lowstand and Shelf margin (Vail *et al.*, 1991)

5.7 Sequence stratigraphic setting of the Mamuniyat outcrops in the Murzuq Basin

5.7.1 Introduction

This section summarises the principle results of a geological field trip, carried out on behalf of, and in conjunction with Repsol Exploration (Murzuq) and Partners (TOTAL, OMV and SAGA), which focuses principally on the Ghat and western Qarqaf areas. The main objective of this study was to develop sequence stratigraphic models for the Upper Ordovician, summarising the relationships between the principal rock units, *i.e.* the Mamuniyat and Melez Shuqran Formations (**Fig. 5.7**).

The depositional sequences reflect decreasing glacial influence throughout the Upper Ordovician (Ashgillian). However, apart from probable glacial dropstones found in the early Melez Shuqran, no direct evidence was found for glaciation in the Murzuq Basin during the Upper Ordovician. Nevertheless, fluctuations in the size and position of the ice sheets are thought to have had a degree of control on the relative sea-level at the time and thus sediment architecture (McDougall and Martin, 1998).

5.7.2 Sequence stratigraphy boundary recognition

During the Upper Ordovician the study area was subject to a dynamic interplay of tectonics, localised sediment supply and glacial eustasy associated with the advance and retreat of ice sheets. This resulted in the development of complex, superimposed relative sea-level cycles, which, due to localised tectonics during isostatic rebound are not applicable over large areas *i.e.* one area may be undergoing glacial downwarping whilst another several tens to hundreds of kilometres away may be uplifting isostatically (McDougall and Martin, 1998).

Posamentier and Vail (1988) specifically state that before applying sequence stratigraphic concepts, local tectonics, sediment flux and physiography must be taken into account. Furthermore, throughout the Upper Ordovician Mamuniyat and Melaz Shuqran Formations.

Five unconformity-bounded sequences have been identified (McDougall and Martin, 1998). With a single exception these sequences approximate to the previously outlined formations and all exhibit at least some incision at their base (**Fig. 5.7**). They are summarised as follows:

- Sequence 1 (Melez Shuqran);
- Sequence 2 (Lower Mamuniyat);
- Sequence 3 (Middle Mamuniyat);
- Sequence 4 (Middle Mamuniyat); and
- Sequence 5 (Upper Mamuniyat).

Initial interpretations suggest that sequences 1, 2, 3 and 5 are of a similar order, whereas sequence 4 may be of a higher order. Due to a lack of rigorous biostratigraphic control the correlation of the sequences from one area to another can be problematic. However, there are distinct marker horizons that can be traced around the basin. In the absence of such markers, facies unique to various formations may be used in sequence identification (McDougall and Martin, 1998).

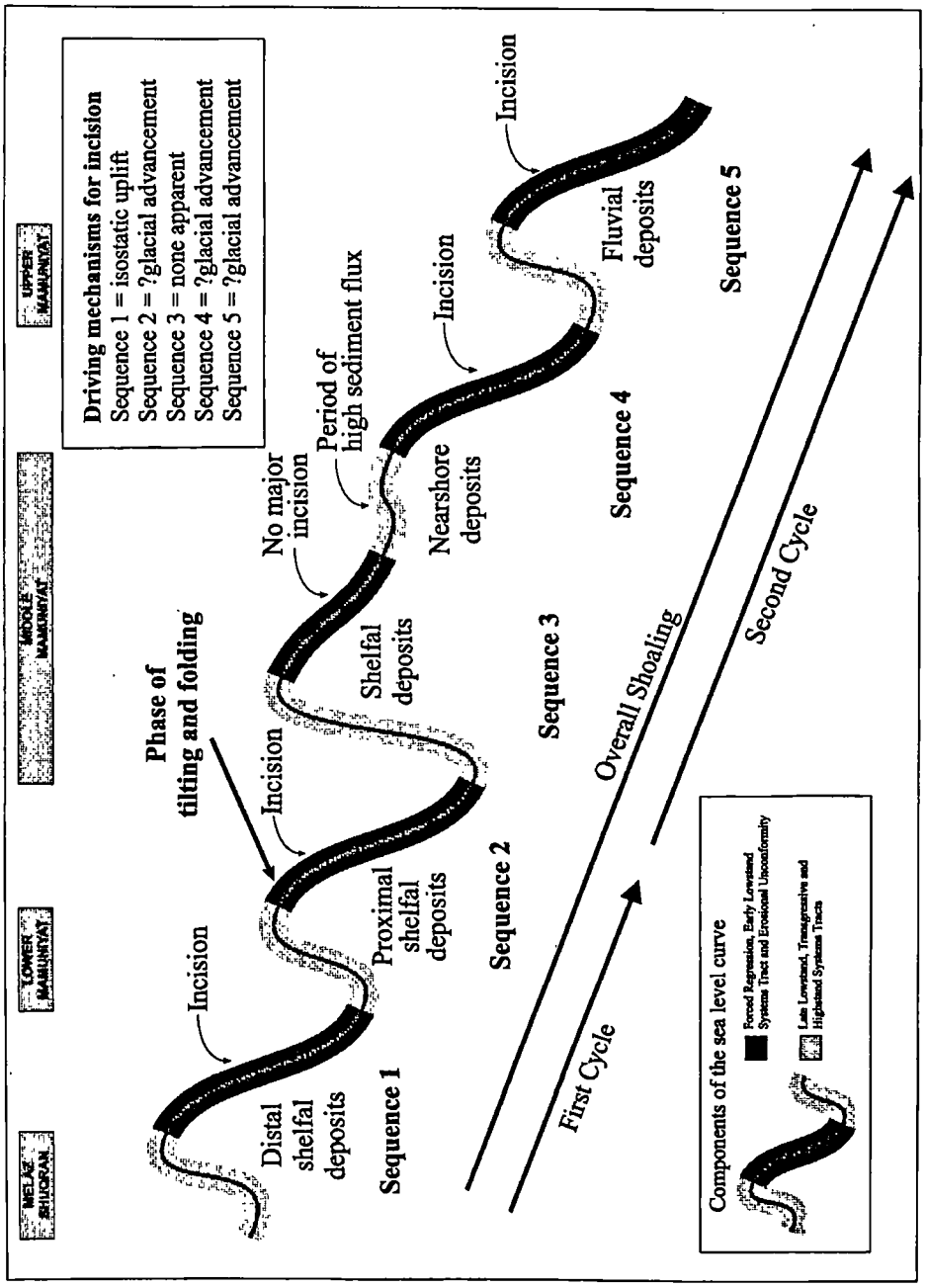

Fig. 5.7 Relative sea-level fluctuations through the Upper Ordovician (After McDougall and Martin, 1998).

5.8 Sequence stratigraphy of the Mamuniyat Formation, NC115 Concession, on the NW flank of the Murzuq Basin

5.8.1 Introduction

This part attempts to place the sedimentary section within the Upper Ordovician (Ashgillian) Mamuniyat Formation, NC115 Concession, in a sequence stratigraphic context (Vail *et al.*, 1977). The main emphasis of this section is placed on the role and importance of unconformity bounded sediment packages. Additional objectives are the identification and interpretation of transgressive-regressive alternations and the assessment of the effect of global variations in eustatic sea-level in controlling facies development. Most sedimentary units in NC115 Block, NW flank of the Murzuq Basin are relatively easily distinguished as they exhibit progressive rather than sharp lateral facies changes, and can thus be correlated over long distances within A, B and H-Fields.

The Mamuniyat Formation consists mainly of clastic rocks, which show an increased marine influence toward the northeast. It is dominated by proximal braided stream deposits in the southwest giving way to fluvial-marginal marine and shelf deposits in the northeast (discussed in Chapter Two). Over the last four decades, fluvial sedimentology has developed from modern geomorphological studies (*e.g.* Leopold and Wolman, 1957), through the development of facies models and description of case studies (*e.g.* Miall, 1978) to an increasing understanding of how fluvial systems develop and change over time, as a response to tectonism, climate and sea-level (*e.g.* Posamentier and Vail, 1988).

It should be noted that the framework presented here is the first attempt at applying sequence stratigraphic concepts to NC115 Concession and, in view of the scale of the study, it should be regarded as a preliminary study, and a basis for further, more refined analysis. For example, some correlations that will undoubtedly change with time and more detailed subdivision should ultimately become possible, as more data becomes available.

The increasing interest in sequence stratigraphy has diverted effort from routine facies studies towards analysis of the relationship between alluvial architecture and available accommodation space (*e.g.* Shanley and McCabe, 1991; Posamentier and Allen, 1993). High resolution sequence stratigraphy of the Mamuniyat Formation, based on colour photographs of the slabbed cores and wireline log data, is increasingly recognized as a powerful technique for correlating and predicting stratigraphy in the subsurface of A, B and H-Fields (McDougall and Martin, 1998; Fello and Turner, 2001b).

The wireline logs used in the correlation are mostly Sonic Log (ΔT) and Gamma Ray (GR), supplemented by Spontaneous Potential (SP) and Resistivity Logs (RT). Data from 12 oil wells were used in confirming the facies interpretations. An important component of the investigation of the Mamuniyat Formation is to evaluate the relative influence of factors that controlled deposition in the Murzuq Basin, such as eustatic sea-level change, tectonics and sediment supply rates (Posamentier and Vail, 1988).

5.8.2 Objectives

The main objectives of this sequence stratigraphic study are to apply and interpret the depositional environments of the Mamuniyat Formation for the first time, by using variations in facies tracts and stacking patterns in relation to changes in base level, in order to:

1) Assess the vertical and lateral variations in the sedimentary succession which are controlled by relative sea-level changes, and to provide a chronostratigraphic framework for sedimentary facies and facies associations;
2) To present a sequence stratigraphical model for the Mamuniyat sediments throughout NC115 Concession, for the first time;
3) To present relative sea-level curves for the interval studied and compare these to curves available in the literature;
4) To obtain a higher degree of stratigraphic resolution by studying the different scales of depositional sequence and their lateral continuity; and

5) To define the geometrical aspects of the Mamuniyat sandstone system within this refined stratigraphic framework.

5.8.3 Terminology

The sequence stratigraphic terminology used throughout the Mamuniyat Formation study is that defined by Mitchum (1977), Posamentier and Vail (1988), Van Wagoner *et al.* (1988), Mitchum and Van Wagoner (1991) and Miall (1991). Mitchum (1977) defines a sequence as a relatively conformable, genetically related succession of strata bounded by unconformities or their correlative conformities. This definition holds true whatever the sequence's frequency, duration or stratigraphic thickness. Sequence stratigraphy has provided new insights into how and why sequences develop and has been most successful in interpreting marine sequences, but has not been applied widely to non-marine deposits. The sequence stratigraphic models developed for non-marine (fluvial) sequences by Posamentier and Vail (1988) have not been rigorously tested. However, Miall (1991) produced a detailed critique of their model, particularly with regard to the basic concepts of equilibrium profile changes.

Posamentier and Vail (1988) describe two sequences of fluvial clastic deposits related to relative sea-level changes. Type 1 sequences are composed of incised valley fills comprising fluvial deposits with a linear or sinuous distribution pattern, typical of lowstand and early highstand system tracts. Widespread, unconfined fluvial deposition on broad floodplains does not occur until after the incised valleys are filled, followed by transgressive deposits. Type 2 sequences are characterized by widespread fluvial deposition only during late highstand, and there are no incised valleys.

Posamentier and Vail (1988) qualify their descriptions by stating that their models are generally applicable. However, before being applied to the Mamuniyat Formation, NW flank of the Murzuq Basin, they need to be modified to account for local factors such as tectonics, climate and variations in sediment supply, which was most probably related to the uplifted Ghat/Tikiumit Arch to the SW of NC115 Concession.

5.8.4 General sedimentary features

The Mamuniyat Formation consists almost entirely of siliciclastics, with significant radioactive shale developed only in the Middle Mamuniyat strata (M2), throughout southwest NC115, particularly in the B-Field. The Mamuniyat Formation can be seen to comprise a sand-dominated coarse- to very coarse and occasionally medium- to fine-grained fluvial-marginal marine sand system with marine shelf environments increasing upwards through the succession. It also coarsens-upwards overall as relative water depth decreased.

The Mamuniyat Formation and the underlying Melez Shuqran Formation are biostratigraphically dated as Upper Ashgillian and Lower Ashgillian respectively (Pierobon, 1991). These two formations are genetically related *i.e.* they represent deposition within the same cycle of deposition but in different environmental settings: fluvial and shelf respectively (Fello and Turner, 2001a). They can be considered, therefore, to be a single "Sequence" bounded at the base and the top by unconformity surfaces. The Melez Shuqran Formation comprises a number of condensed sets of parasequences, particularly at its base where it is shale dominated and represents more distal (outer shelf?) deposits, overlain by the more proximal sand-prone Mamuniyat Formation.

5.8.5 Preliminary sequence stratigraphy of the Mamuniyat Formation

5.8.5.1 Ideal depositional sequences

An idealised Mamuniyat depositional sequence has been derived from a combination of field observations, correlations from the literature, and the wireline logs for NC115 Concession. It is thought that many sequences, but principally those of gently subsiding basin margins, are produced by second to third-order rises and falls of sea-level, against a background of steady subsidence (Haq *et al.*, 1987; Wilgus *et al.*, 1988) (**Fig. 5.8**). Throughout, A, B and H-Fields, the mixed fluvial-marginal marine and shelf marine character of the Mamuniyat Formation suggests that they were deposited along the margins of a continental seaway (Turner and Monro, 1987; Fello and Turner, 2001b). The Mamuniyat succession, therefore, provides an opportunity to compare sedimentary architecture across a wide spectrum of coeval depositional environments within three oilfields (discussed in Chapter Two), and is particularly amenable to sequence stratigraphic analysis which was developed specifically for passive continental margin sequence (Van Wagoner *et al.*, 1990).

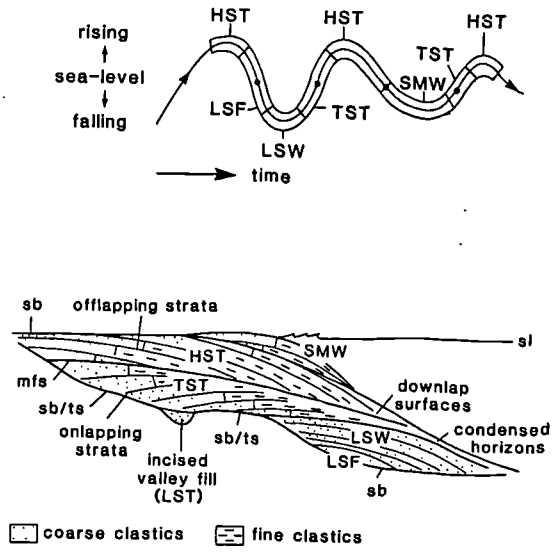

Fig. 5.8 Sequence stratigraphy, systems tracts and relative sea-level changes. Upper graph shows the systems tracts and the relative sea-level change curve. Lower graph shows the sequence stratigraphic depositional model for a siliciclastic shelf on a gently subsiding basin margin (After Haq *et al.*, 1987; Van Wagoner *et al.*, 1988 and Tucker, 1991).

5.8.5.2 Depositional framework

The Mamuniyat sediments generally show an uncomplicated structure and commonly show a cyclical nature, with individual facies and formations often very laterally extensive. Variations that occur tend to be gradual and can usually be related to basement and tectonic configurations. These patterns are characteristic of a cratonic domain (Fello, 1996; Fello and Turner, 2001a). Recognition of sequence boundaries and maximum flooding surfaces and their fluvial equivalent in the Mamuniyat Formation is a necessary condition before systems tracts can be appropriately discussed within three oilfields A, B and H-Fields.

Transgressive, highstand and lowstand systems tracts can be identified on the basis of geometric and sedimentologic criteria within fluvial-marginal marine and shallow marine strata in the Mamuniyat Formation. In the Mamuniyat Formation, particularly in the B-Field (*e.g.* B2-NC115), the top of the lowstand systems tract is defined by a transgressive surface (TS) at the top of the Upper Mamuniyat and base of the Tanezzuft Formations, particularly in B-Field, SW of NC115 Concession (**Fig. 5.12**).

The Tanezzuft Formation (Llandoverian), where it unconformably overlies the Mamuniyat Formation, is composed of shale with the hot shale member occurring locally at the base (**Fig. 5.12**). These sediments were deposited in restricted to open marine conditions associated with an early Silurian marine transgression. Moreover, the Tanezzuft Formation represents a regional, possibly global marine transgressive event that extends over the entire North Africa Craton, including the Murzuq Basin.

The highstand systems tract has been identified in all type wells of the study area throughout the El-Sharara Field. It is significantly truncated by the overlying sequence boundary at the base of the Upper Mamuniyat in B-Field (**Fig. 5.12**). This boundary hereafter referred to, as the Upper Mamuniyat sequence boundary unconformity, is a type-1 sequence boundary formed during a fall in sea level.

The sequence boundary represents a fundamental basinward shift in facies caused by erosion of a subaerially exposed shelf, with the underlying sediments of the Middle Mamuniyat within B-Field located between marginal marine deposits and the sequence boundary. The SB does not appear to be represented in the Lower-? Mamuniyat Formation in A and H-Fields.

This sequence boundary marks the base of the lowstand systems tract in the upper part of the Mamuniyat Formation, and is overlain by a prograding, coarsening-upward parasequence interpreted here, on the basis of sequence stratigraphic principles, as the fluvial deposits of a lowstand systems tract within B-Field, (*e.g.* B2-NC115) (**Fig. 5.12**). This abrupt transition from predominantly fine-grained marginal marine strata (Middle Mamuniyat), to medium and coarse to very coarse-grained fluvial strata (Upper Mamuniyat), indicates a marked alteration in hydraulic character and/or a change in the rate of fluvial aggradation (Leeder, 1978; Bridge and Leeder, 1979).

Similarly, the abrupt change in the degree of fluvial stacking and net : gross (sandstone : shale) ratio across an erosional surface of regional extent suggests a marked alteration in accommodation potential (Posamentier and Vail, 1988) and rates of alluvial aggradation (Bridge and Leeder, 1979). Taken together, these factors support this interpretation as a sequence boundary. Fluvial sediments deposited at this time are characterized by increased channel-fill sandstone (Posamentier and Allen, 1993).

The approach taken by Galloway (1989) in his discussion of genetic stratigraphy is to subdivide the stratigraphic succession at condensed sections (CS) or maximum flooding surfaces (MFS) (in the terminology of Posamentier and Vail, 1988). Within the condensed section, the maximum flooding surface, representing the time of maximum flooding, is nonetheless an important surface in sequence stratigraphic analysis. It separates the transgressive systems tract from subsequent highstand systems tract.

The maximum flooding surface (MFS) within NC115 Concession is overlain by the lower part of an incompletely exposed highstand system tract. In the Mamuniyat Formation, the maximum flooding surface is defined by the *Glauconitic* sandstone bed (Fello, 1996). If this interpretation is correct then the top of the succession belongs to an incompletely exposed or eroded highstand systems tract. The deposition and distribution of the facies within parasequences are controlled by different factors including rate of relative sea-level change, rate of subsidence and sediment supply. Furthermore, when the rate of accommodation development on the shelf decreases to less than the sediment supply, progradation of the depositional shelf break resumes and the highstand systems tract is established (Posamentier and James, 1993).

5.8.6 Sequence stratigraphic architecture of the Mamuniyat Formation

5.8.6.1 Introduction

Throughout the NC115 Concession, on the NW flank of the Murzuq Basin, over 120 closely spaced production oil wells were drilled, making it possible to achieve an exceptionally accurate level of correlation. The conceptual stratigraphic architecture of the Mamuniyat reservoir is based on first principles. The use of these principles has enhanced an understanding of geological relationships within a time-stratigraphic framework throughout A, B and H-Fields. Along with the general acceptance of these concepts, however, has come a number of problems that are addressed in the study area of NC115 Concession.

The Upper-Ordovician "Ashgillian" section of the Mamuniyat Formation within NC115 Concession has been divided into three major sequences. As a regional generalization, the Mamuniyat Formation exhibits thickness variation and lateral facies changes that are traceable and predictable in the subsurface. Although the sedimentary properties of the Mamuniyat Formation change continuously away from the basin edge, the depositional setting of the Mamuniyat Formation has been divided into an upper braid plain (proximal) a lower braid plain (distal) and a shallow marine shelf and nearshore environment.

Periodic uplift and base level changes led to basinward progradation of braided fluvial systems followed by marine transgressive events from the NE, across a storm-influenced shallow-marine shelf (discussed in Chapter Two).

5.8.6.2 Sequence stratigraphic analysis of the A-Field, (A8-NC115)

❖ *Transgressive systems tract*

The transgressive systems tract (TST) has been found in the Lower Mamuniyat Formation (M1) within A-Field, particularly in type well A8-NC115. It generally consists of fine- to medium-grained sandstone with alternating mottled and bioturbated zones and locally developed and burrowed planar cross-beds. The facies characteristics of these sandstones resemble shallow marine shelf deposits formed under storm and fair weather conditions, as discussed in Chapter Four. A tentative sequence stratigraphic analysis of the type well A8-NC115 is shown in **Figure 5.9**. However, parasequences, the fundamental building blocks of the sequence stratigraphy analysis, are poorly developed in the TST, and not easy to recognise.

The base of the TST is not seen here. However, it is bounded above by a thin bed of glauconitic sandstone with interbeds of black shale at the uppermost part of the Lower Mamuniyat Formation. It is interpreted as a condensed section corresponding to a maximum flooding surface (MFS), defining the boundary between the transgressive systems tract beneath and highstand systems tract above.

The vertical stacking pattern of the Lower Mamuniyat sandstone preserves part of sequence 1 and includes a shallow marine shelf, which reflects low-energy conditions. The sand proportions increases upward through the sequence and is interpreted to represent deposition in response to progradation under an increasing energy level (Van Wagoner *et al.*, 1988). The vertical stacking pattern of this package suggests that the shoreline prograded, probably during source area uplift and base-level fall, concomitant with an increase in sediment supply to the shelf (Van Wagoner *et al.*, 1990; Swift *et al.*, 1991).

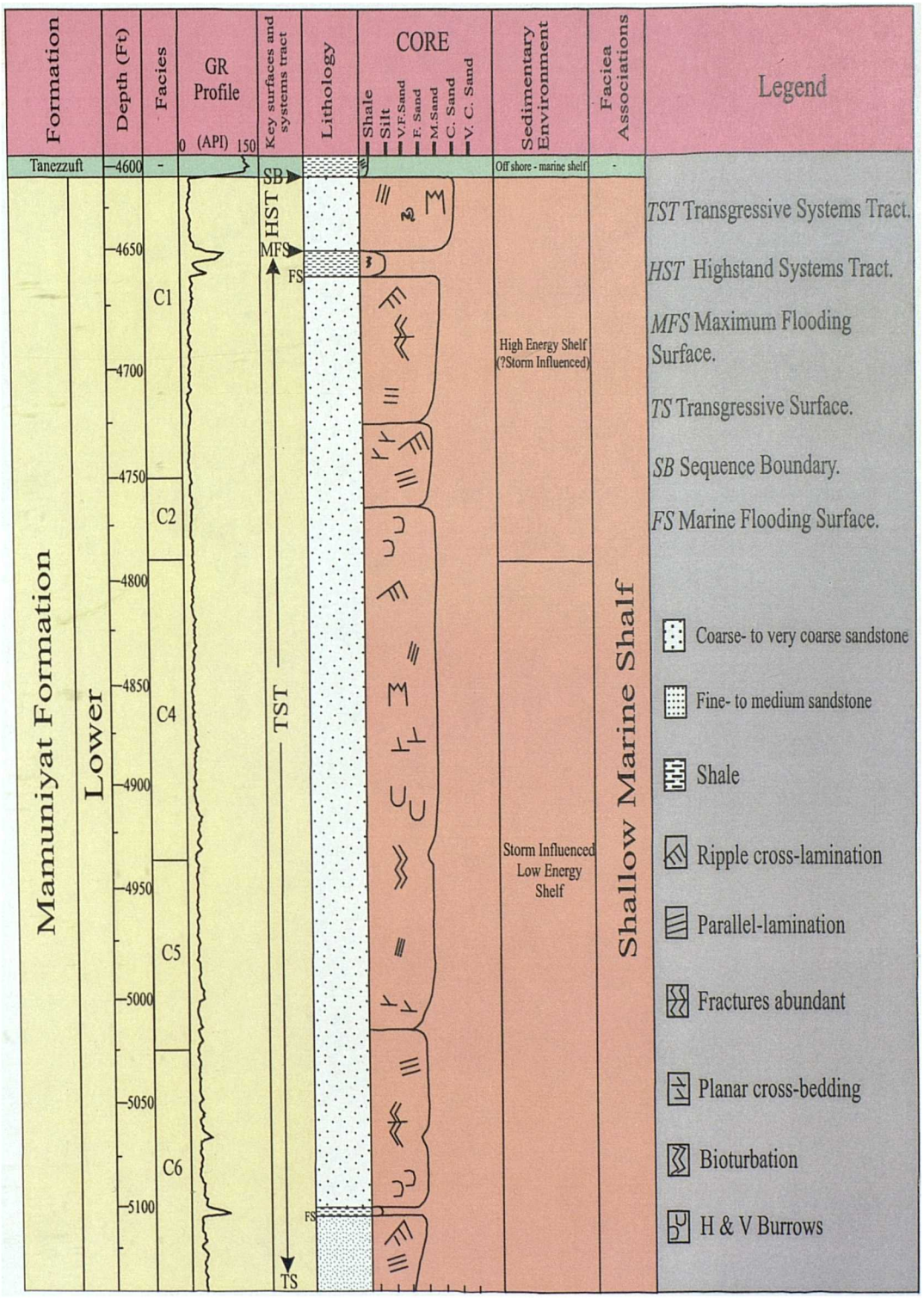

Fig. 5.9 Lithological log and sequence stratigraphic systems tract of the Mamunyiat Formation in type well A8-NC115.

❖ *Highstand systems tract*

The highstand systems tract (HST) within A-Field particularly in well A8-NC115, is a relatively thin bed (≈ 10-15 cm thick), and characterized by coarse-grained quartz sandstone with interbeds of silty shale. Significant thickness variations throughout A-Field reflect a strong tectonic control on sedimentation. The sandstone coarsens-upward, and marks the progradational component of the highstand stage. These sediments represent both shallow-marine and fluvially-influenced depositional systems. The presence of glauconitic sandstone (Fello, 1996) within the HST indicates a shallow-marine environment and deposition under anaerobic or reducing conditions (Pettijohn, 1957). Thus, the appreciable spiky pattern through the gamma-ray log values in the uppermost portion of the Lower Mamuniyat sandstone, result from this high concentration of glauconite (**Fig. 5.9**).

The incompletely exposed thin marine shales and intercalated thick sandstone that overlie the maximum flooding surface are interpreted to be related to progradation during deposition of highstand deposits above as accommodation space began to decreases relative to sediment supply (**Fig. 5.9**) (Van Wagoner *et al.*, 1990).

5.8.6.3 Sequence stratigraphic analysis of the B-Field, (B2-NC115)

❖ *Transgressive systems tract*

The transgressive systems tract (TST) is present in all oil wells particularly in type well B2-NC115, within the B-Field. It is characterized by alternations of fine- to medium-grained sandstone and shale, with increasing shale content up the section. In the type well fine alternations of bioturbated sandstones and shale pass up into shales, with the degree of bioturbation increasing upwards. In the subsurface core of this well, the TST is composed of fine cross-bedded sandstone at the base of the lower Mamuniyat Formation, passing up into alternations of medium sandstone and black shale in the middle Mamuniyat Formation (**Fig. 5.10**).

The alternating zone consists of bioturbated fine-grained hummocky cross-stratified sandstone and black greyish silty shales with glauconitic sandstone. The TST is bounded below by a transgressive surface (TS), which is inferred to occur beneath the bottom of the well, and above by a maximum flooding surface (MFS) (e.g. B2-NC115). These sediments become finer grained upwards, as the rate of sea-level rise outpaced sedimentation.

Parasequences are defined as a relatively conformable succession of genetically related beds or bedsets bounded by marine flooding surfaces and their correlative surfaces. In addition to these defining characteristics, most parasequences are asymmetrical shallowing-upward sedimentary cycles (Haq *et al.*, 1987). In B-Field, in the southwest of the study area, a transgressive surface (TS) marks the bottom of the transgressive systems tract in the Lower Mamuniyat succession. This is overlain by four progradational-stacking patterns, represented by coarsening-upward quartzose sandstone parasequences, particularly in type well B2-NC115. These sandstone parasequences are re-interpreted here, on the basis of sequence stratigraphic principles, as the shallow marine shelf and marginal marine deposits of a transgressive systems tract (**Fig. 5.10**).

The parasequence boundaries in type well B2-NC115 are marked by an abrupt change from fine- to medium-grained sandstone below to coarse-grained sandstones above (Turner, 1998). The maximum flooding surface (MFS) within B2-NC115 is marked here by a thin interval of radioactive shales and/or glauconitic sandstone, characterized by a very high gamma-ray peak. In (B-Field) the shoreline during maximum flooding probably lay to the southwest of NC115 Concession (A and H-Fields), where the equivalent shallow marine environments.

❖ *Highstand systems tract*

The highstand systems tract (HST) in type well B2-NC115 is made up of thin beds of medium–grained sandstone with radioactive shale. It consists of quartzose sandstone with interbeds of silty shale, passing upward into radioactive shales and/or glauconitic sandstone.

The HST is bounded below by a maximum flooding surface (MFS), and above by a sequence boundary. In type well B2-NC115, the HST is bounded at the top by a subaerial erosion surface, interpreted as a type-1 sequence boundary (SB) (Van Wagoner *et al.*, 1990), which clearly suggests a period of relative sea-level fall. The sediments present below this sequence boundary represent the upper part of sequence 1 (**Fig. 5.10**).

Throughout the B-Field, the HST interval contains fine- to medium-grained rippled and trough cross-bedded sandstone with dark shale and siltstone interbeds, which occur within the uppermost part of the middle Mamuniyat Formation, and which were deposited in a prograding marginal marine environment. Bioturbation is locally common in the middle Mamuniyat Formation in this area. Furthermore, the sedimentary structure and the fauna indicate shallow marine to nearshore environments (Reineck and Singh, 1972; Pemberton *et al.*, 1992).

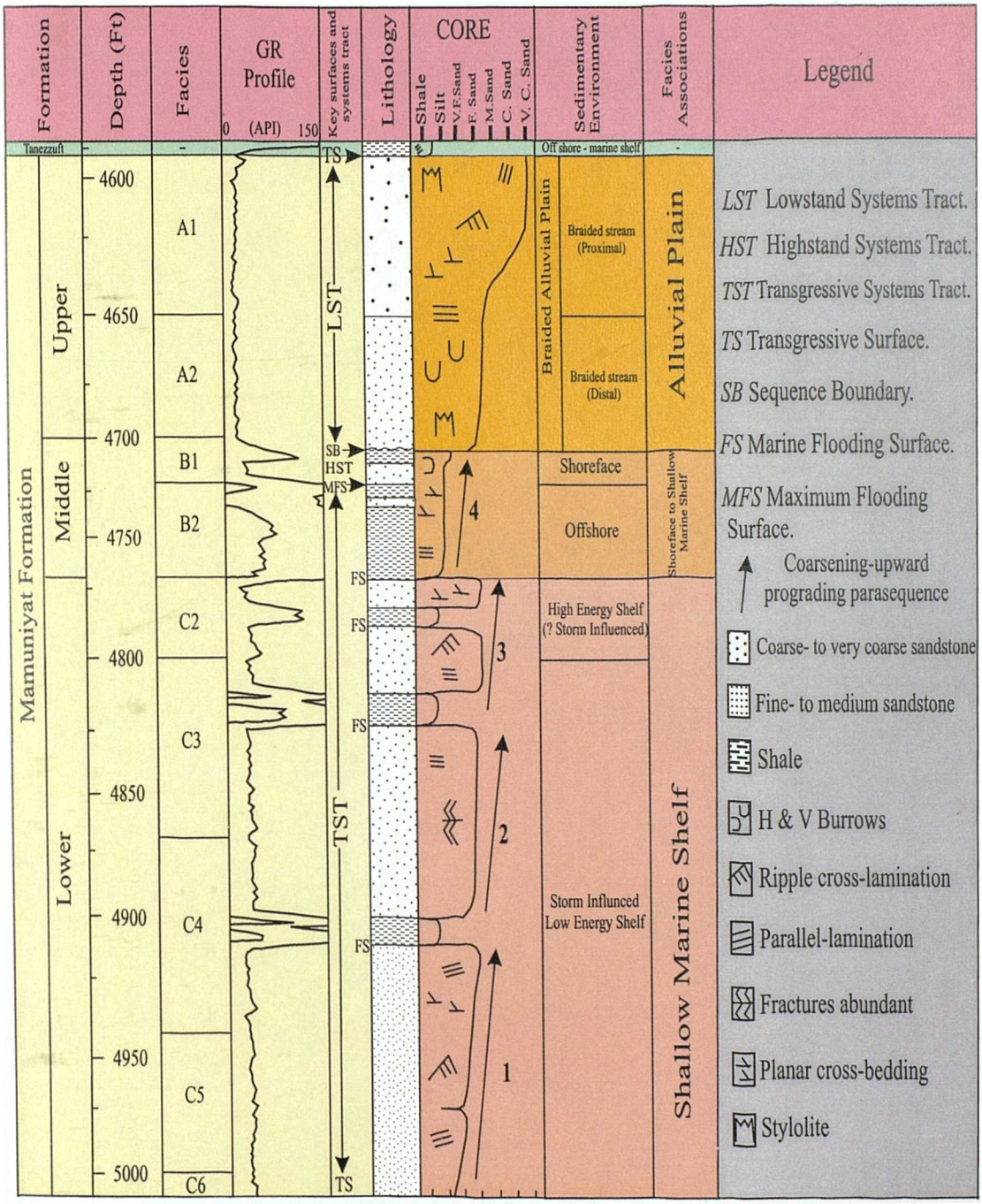

Fig. 5.10 Lithological log and sequence stratigraphic systems tract of the Mamunyiat Formation in type well B2-NC115.

❖ *Lowstand systems tract*

As discussed previously in chapter two (Facies B1 and B2), the core available from type well B2-NC115, shows well-preserved shoreface sandstones (Facies B1) of the uppermost portion of the Middle Mamuniyat succession (M2), underlain by marginal marine deposits (Heterolithic-claystone Facies B2). It appears that the shoreline migrated basinward and that the sequence represents shoreface progression under conditions of relative sea-level rise, high subsidence or minimal sediment supply and reworking of the shoreface sands (Elliott, 1986; Galloway, 1989; Reading, 1996).

The upper part of the Mamuniyat Formation (M1) in B-Field consists of a lowstand systems tract (LST). The uppermost part of type well B2-NC115 is made up of coarse-grained, trough cross-bedded sandstones deposited by high energy braided stream systems, representing sandstones deposited by sand-rich, high energy distributary channels, which continuously infilled accommodation space. They are characterized by coarsening-up sequences (from distal to proximal deposits), and represent a lowstand systems tract within B-Field, southwest NC115 Concession (**Fig. 5.10**).

Evidence of fluvial processes is negligible in the other two oilfields in NC115 Concession (A and H-Fields) probably due to distance from the source area. In addition, the preservation of fluvial sediments within B-Field depends on the rate of sea-level rise, marine processes and sediment supply from hinterland tectonics. Posamentier and Vail (1988) specifically state that before applying sequence stratigraphic concepts, local conditions regarding tectonics, sediment flux and physiography must be taken into account.

5.8.6.4 Sequence stratigraphic analysis of the H-Field, (H4-NC115)

❖ *Transgressive systems tract*

From core studies in H-Field, particularly type well H4-NC115, the Lower Mamuniyat Formation, has been interpreted as shallow marine shelf (**Fig. 5.11**). The transgressive systems tract (TST) within H4-NC115, is bounded below by a transgressive surface (TS), which is inferred to occur beneath the bottom of the well and above by a maximum flooding surface (MFS).

Above the transgressive surface are several parasequences, clearly defined by coarsening-upward sandstones, which tend to thicken upwards and show a progradational-stacking pattern. Relative rise in sea-level continued until the maximum flooding surface, which is represented by the boundary between the transgressive systems tract and highstand systems tract within H4-NC115 (**Fig. 5.11**). A correlative zone of high gamma radiation observed regionally in the subsurface section is shown in several parasequences and is interpreted as a condensed section.

A general decrease in sand/shale ratio is observed within the Lower Mamuniyat Formation throughout the northeastern part of NC115 Concession particularly between two type wells H4-NC115 and A8-NC115, consistent with a trend from shallow to deep water environments, probably associated with sea-level rise or a back-stepping shoreline (Fekirine and Abdallah, 1998). Furthermore, throughout the El-Sharara Field, northwestern flank of the Murzuq Basin, the clastic wedge of the Lower Mamuniyat Formation becomes thinner and finer-grained toward the northeast area (A and H-Fields). The northeastward decrease in the proportion of sandstone to shale reflects distance from the granitic basement source terrain, which was most probably the uplift Ghat/Tikiumit Arch to the SW of NC115 Concession (Fello and Turner, 2001a).

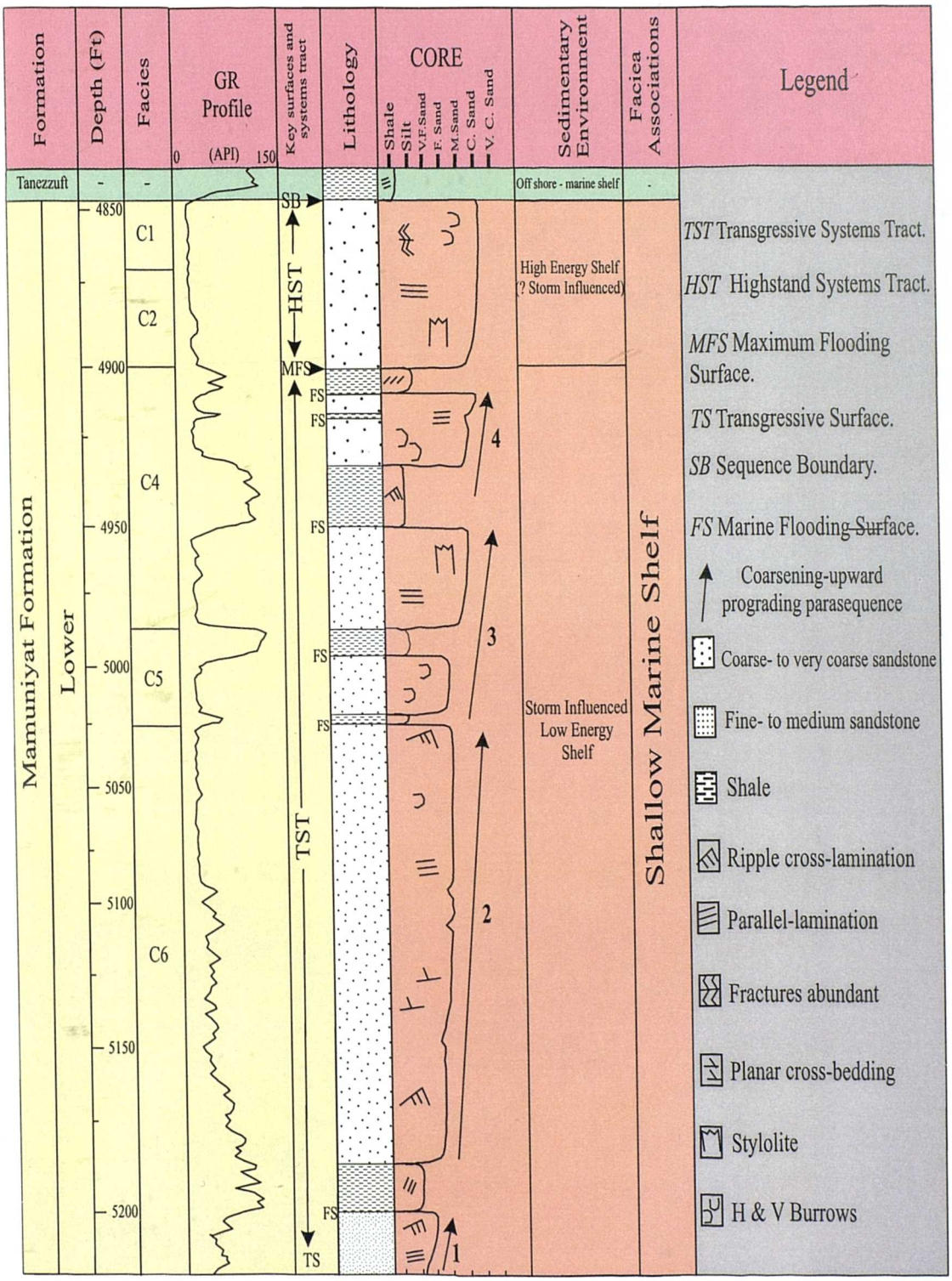

Fig. 5.11 Lithological log and sequence stratigraphic systems tract of the Mamunyiat Formation in type well H4-NC115.

❖ *Highstand systems tract*

The highstand systems tract (HST) throughout the H-Field is represent by coarsening-upward quartzic sandstones, within the uppermost part of the Lower Mamuniyat Formation (M3). Again, a progradational parasequence stacking pattern is evident. A shallow marine to nearshore environment in H-Field is indicated by the sedimentary structures and the fauna (discussed in Chapter Two).

The HST in type well H4-NC115 is significantly truncated by the overlying sequence boundary (SB) at the base of the Lower Silurian (Tanezzuft Shale Formation) (**Fig. 5.11**). The Tanezzuft shale, above the Mamuniyat Formation, records a major transgressive event of regional and economic significance (Fello and Turner, 2001b).

The TST within H4-NC115 is characterized by coarsening-upward sandstones suggesting a progradational stacking pattern and shallowing interval. The uppermost sandstone of the Lower Mamuniyat Formation is interpreted as representing shallow marine and high energy shelf environments. In the El-Sharara Field, the thickness of the lower Mamuniyat Formation is variable because of irregular topography on the unconformity, which may have been related to highs and lows caused by tectonic activity.

During highstand progradation, throughout H4-NC115, minor changes in relative sea level affected Lower Mamuniyat deposition. Sharp, locally correlative, basal contacts of sandstone intervals in the lower Mamuniyat may represent minor episodes of relative sea-level fall during an overall highstand progradation. The coarsening-upward cycles may have been caused by relative sea-level variations during the Lower Mamuniyat Formation.

5.8.7 Sequence stratigraphic model of the Mamuniyat Formation

The B-Field sandstones were deposited in a subsiding area with high input of sand from the adjacent granitic basement source terrain, which was most probably the uplift Ghat/Tikiumit Arch to the SW of NC115 Concession (discussed in Chapter Two). Shallow marine shelf facies of the Lower Mamuniyat Formation, progradational within A and H-Fields in the northeastern part of NC115 Concession, are correlative with thick fluvial-marginal marine facies of the B-Field sandstone farther to southwest of NC115 Concession (Fello and Turner, 2001a) (**Figs. 5.12**).

Periodic uplift and base level changes led to the basinward progradation of braided fluvial systems followed by marine transgressive events from the NE, across a storm-influenced shallow marine shelf (discussed in Chapter Two). The shallowing-upward change from dominantly marginal marine (Middle Mamuniyat Formation) to mostly fluvial (Upper Mamuniyat Formation) deposits, which occurs in B-Field, reflects the shift to more proximal environments during basinward progradation (Castle, 1998).

The Upper Ordovician deposits of the Mamuniyat Formation can be correlated in sequence stratigraphic terms across three type wells A8, B2 and H4-NC115 the provides an alternative means of viewing Mamuniyat reservoir stratigraphy model.

In the study area and according to this correlation between type wells A8, B2 and H4-NC115 (**Fig. 5.12**). The sequence stratigraphic model of the Mamuniyat Formation can be divided into three main types of systems tracts; the Lower Mamuniyat Member corresponds to a transgressive systems tract (TST) as relative sea level rises and sediments reflood the entire shelf surface, the upper part of the Middle Mamuniyat Member corresponds to a highstand systems tract (HST) and the Upper Mamuniyat Member, which is confined to the B-Field, records lowstand conditions (LST). The overlying Tanezzuft shale is placed in the transgressive systems tract of the second sequence.

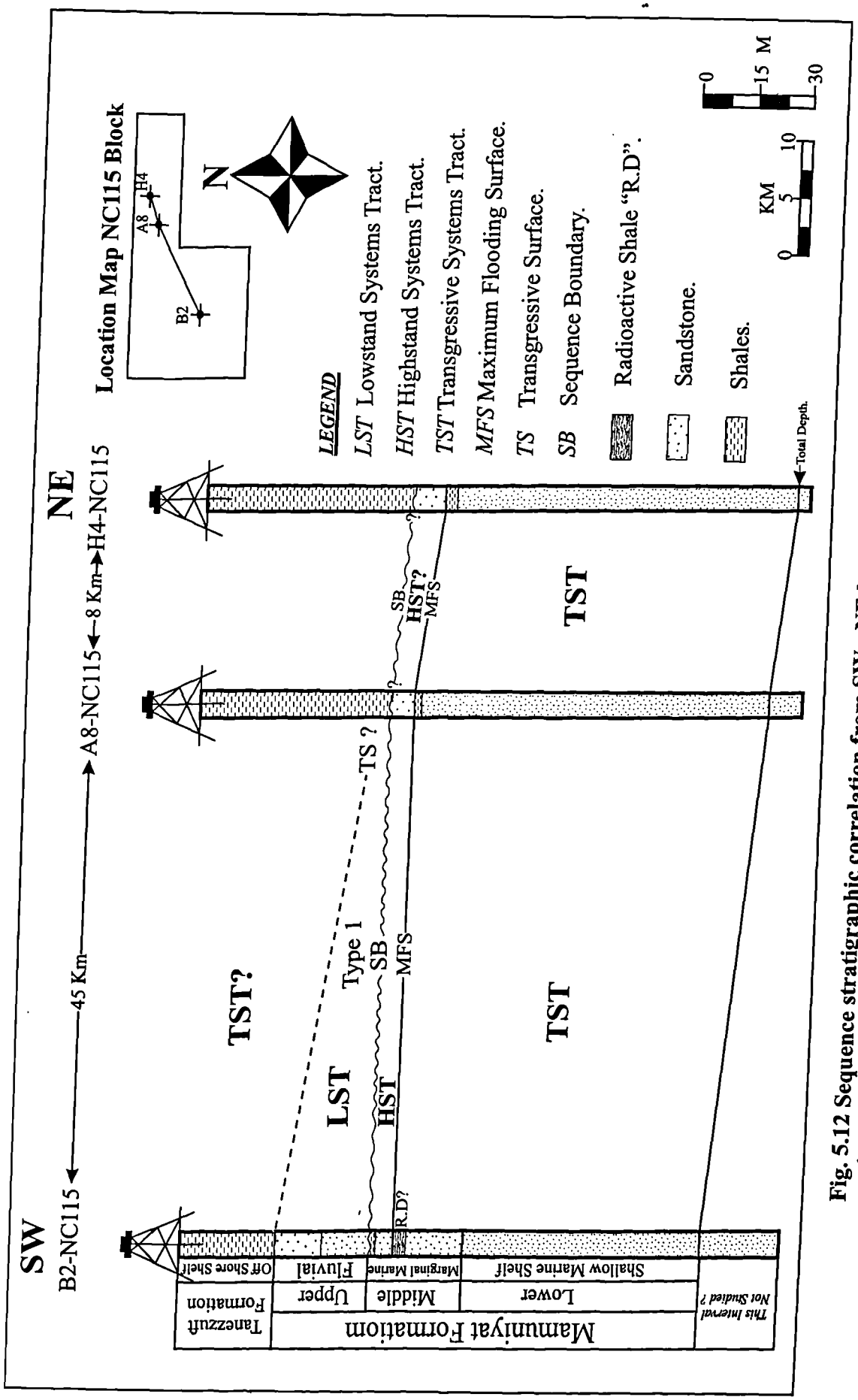

Fig. 5.12 Sequence stratigraphic correlation from SW - NE based on three oil wells A8, B2 and H4, within the El-Sharara Field. Lithologies recognized are based on core data and log signatures.

Sequence stratigraphic analysis of the Mamuniyat Formation in the three oilfields, emphasises the role of unconformity-bounded sediment packages. These are interpreted in terms of regional tectonic events, especially the Taconic orogenic event in the latter part of the Ordovician period, and changes in shelf physiography in response to relative fluctuations in sea level, which in turn affected stream equilibrium profiles. Transgressive, highstand and lowstand systems tracts have been identified within the biostratigraphically, poorly constrained Mamuniyat Formation, thereby allowing for a more accurate correlation between the three oilfields.

A tentative subsurface sequence stratigraphic model of the Mamuniyat succession in NC115 Concession is shown in **Figure 5.12**. However, no attempt has been made to interpret the Upper Ordovician of the Mamuniyat subsurface on the northwest flank of the Murzuq Basin in sequence stratigraphic terms, because it is incompletely succession in NC115 Concession and poorly understood. Moreover, these strata contain no diagnostic index fossils. Thus, the identification of sequence boundaries is of paramount importance in attempting to define a regional sequence stratigraphic framework.

5.9 Regional implication of the sequence stratigraphy

The Cambro-Ordovician strata in Libya, Algeria and Saudi Arabia is characterized by a high proportion of coarse clastic rocks, which were deposited within continental fluvial-marginal marine and shallow marine shelf environments (Bennacef *et al.*, 1971; Turner, 1980; Clark-Lowes, 1985; Pierobon, 1991; Fekirine and Abdallah, 1998; Adamson, 1997, 1999; Fello and Turner, 2001b).

The Lower Palaeozoic succession in Libya is conventionally divided into a number of stratigraphic units of formational status that generally retain the same name throughout Libya, irrespective of changes in facies and depositional environment. The concepts of sequence stratigraphy have not been widely applied to the lower Palaeozoic sedimentary rocks of Libya and several misconceptions exist in the literature.

The implications of this study are that the subsurface distribution of the Upper Ordovician "Ashgillian" Mamuniyat reservoir facies in NC115 Concession, on the northwest flank of the Murzuq Basin, can now be more accurately predicted on the basis of the foregoing sequence stratigraphic modelling. Sequence stratigraphic interpretation of the Mamuniyat succession has led to a grater understanding of sandstone thickness distribution within the three oilfields A, B and H-Fields, and increased confidence in correlations with adjacent Palaeozoic basins. At the same time it allows geometrical relationships to be more tightly constrained.

In Libya, the (entire) lower Silurian shale unit is termed the Tanezzuft Formation. Whilst these shales reach a maximum thickness of 700 m in the Ghadames Basin in NW Libya (Klitzsch, 1995) and 500 m in the Murzuq Basin in SW Libya (Pierobon, 1991), in exposed sections around the Kufra Basin, SE Libya, thicknesses never exceed 130 m (Bellini *et al.*, 1991). According to the sequence stratigraphic model for NC115 the Lower Silurian Tanezzuft Shale Formation is located either at the base of, or well within a Transgressive systems tract (TST), with the Upper Mamuniyat Formation, which is confined to the B-Field forming a Lowstand systems tract (LST) beneath. Stratigraphic events are intimately related to tectonic phases and in some cases to major transgressive and regressive cycles of relative sea-level change, some of which are documented worldwide, and eustatically controlled.

The Northern African basins have been affected by various episodes of intracontinental deformation. A system of partly interconnected basins with intervening uplift was created as a result of intraplate tectonism and lateral stresses associated with vertical movements, a feature common to many continental regions (Park, 1988). The structural development of the Murzuq, Ghadames and Kufra Basins area are characterized by at least five major tectonic phase, namely the Pan-African orogeny, Infracambrian extension, Cambrian-Late Carboniferous sagging, Late Carboniferous "Variscan" intraplate uplift and Early Cretaceous rifting (Luning *et al.*, 1999).

The top of the Upper Ordovician sandstone throughout the Murzuq, Ghadames and Kufra Basins is marked by a regional unconformity between the top of the Ashgillian Mamuniyat Formation and the base of the Llandoverian Tanezzuft Formation. Throughout B-Field southwestern part of the study area, an unconformity in places is characterized by coarse- to very coarse-grained, non-stratified sandstone of the Upper Mamuniyat Formation with soft sediment deformation, which constitute the Lowstand systems tract (LST) of the rising global sea-level of the Llandoverian Tanezzuft Formation. In type well B2-NC115 southwest El-Sharara Field, a regional unconformity appears at the top of the Lowstand systems tract, defined by a transgressive surface (TS) at the top of the Mamuniyat sandstone and base of the Tanezzuft shale.

The lower Silurian in the Murzuq, Ghadames and Kufra Basin is represented by a widespread hemipelagic shale unit, which was deposited during a major transgression, after the melting of the late Ordovician ice cap (Bellini and Massa, 1980). The major flooding surface (FS) beneath the shales is considered to be the Transgressive surface (TS) which separates an upper Ordovician sandstone-dominated Lowstand systems tract (LST) from an uppermost Ordovician to lower Silurian shale-dominated Transgressive Systems Tract (TST), which is confined in B-Field, southwest of the study area.

Above the transgressive sequence, black shale intercalated with subordinate fine-grained sandstone and siltstone represents the lowermost part of the Tanezzuft Formation (Fello and Herzog, 1996). Deposited in response to relative sea-level rise and increase in water depth, interpreted as Type 2 sequence boundary (Van Wagoner *et al.*, 1990). The Type 2 sequence boundary is characterized only by a change in stacking patterns from progradational in the underlying lowstand systems tract, fluvial system (Upper Mamuniyat), to aggradational in the overlying transgressive systems tract off shore shelf (Tanezzuft Shale) (discussed in Chapter Two). Detecting this shift in fluvial to marine sections can be quite difficult, and many Type 2 sequence boundaries probably go undetected (Van Wagoner *et al.*, 1990).

The maximum flooding surface (MFS) caps the transgressive systems tract and marks the turnaround from retrogradational stacking in the transgressive systems tract to aggradational or progradational stacking in the early highstand systems tract. The maximum flooding surface represents the last of the significant flooding surfaces found in the transgressive systems tract and is commonly characterized by extensive condensation and the widest landward extent of the marine condensed facies (Van Wagoner *et al.*, 1990).

Throughout, the El-Sharara Field, a Maximum flooding surface (MFS), occurs in the three main oilfields of the study area particularly in B-Field, in the southwest of the study area. During the final stage of the transgression in the Middle Mamuniyat Formation, the maximum flooding surface was deposited in the lower part of the Middle Mamuniyat Formation. Such (hot shales) display a strong positive response on gamma ray logs (Van Wagoner *et al.*, 1990). Furthermore, the uppermost part of the Middle Mamuniyat Formation represents by the Highstand systems tract (HST), which is composed of thin bed of shale, siltstone and sandstone with the sand/shale ratio depending on the position of the shelf (*e.g.* B2-NC115) (**Fig. 5.12**).

A drop in sea-level during the uppermost Mamuniyat Formation (M1) leads to the development of a major sequence boundary (SB) particularly in the southwest part of the El-Sharara Field shelf, characterized by a change in deposition from marine to fluvial sandstone (discussed in Chapter Two).

During the later stages of the Early Silurian sea-level rise, palaeo-oceanographic conditions changed towards a more oxygenated state, possibly related to the weakening of a prominent Early Silurian North Gondwana upwelling system (Finney and Berry, 1997). After this change, major organic-rich shale deposition ended (Boote *et al.*, 1998).

The distribution of these formations, however, was controlled by the creation of sub-basins in the Murzuq and Ghadames Basins. These eustatic and tectonic events and their corresponding signatures developed an ideal source rock–reservoir–seal scenario that now makes the Murzuq Basin a new frontier for hydrocarbon exploration in southwest Libya, particularly within NC115 Concession (Repsol Oil Operations), NC186, NC187 and NC190 (Repsol YPF Madrid) and NC174 Concession (Lasmo).

Throughout the lower Palaeozoic, specially the Upper Ordovician–Early Silurian cycles, signatures and megasequence events within the Murzuq (southwestern), Ghadames (western) and Kufrah Basins (northeastern) Libya, are identical to those reported from the Illizi Basin, SE Algeria, and NW Saudi Arabia (Clark-Lowes, 1985; Turner, 1998; El-Hawat and Basan, 1998; Fekirine and Abdallah, 1998; Adamson, 1999). These similarities however, are attributed to their relative distance from Gondwana glaciation centres, in that the latter areas were closer to these centres, whereas western Libya was in a more distal position, where periglacial fluvial and marine conditions prevail (Clark-Lowes, 1985).

5.10 Summary

Sequence stratigraphic analysis of the Mamuniyat Formation emphasises the role of unconformity-bounded sediment packages. These are interpreted in terms of regional tectonic events, especially the Taconic orogenic event, and changes in shelf physiography in response to relative fluctuations in sea level, which in turn affected stream equilibrium profiles. Transgressive, highstand and lowstand systems tracts have been identified within the biostratigraphically, poorly constrained Mamuniyat Formation, thereby allowing for a more accurate correlation between the three oilfields. Stratigraphically the Mamuniyat has been divided into a Lower, Middle and Upper part, each assigned informal member status. In terms of this subdivision the Lower Mamuniyat corresponds to a transgressive systems tract when sediment was deposited concomitant with a relative rise in sea level, flooding the entire shelf.

During the final stage of this transgression a radioactive shale unit, recording a maximum flooding surface was deposited in the lower part of the Middle Mamuniyat. The upper part of the Middle Mamuniyat corresponds to a highstand systems tract, and the Upper Mamuniyat, which is confined to the B-Field, records lowstand conditions. The Tanezzuft Shale, above the Mamuniyat Formation, records a major transgressive event of regional and economic significance, providing both source and seal for primary Lower Palaeozoic sandstone hydrocarbon reservoir targets.

CHAPTER 6

WIRELINE LOG TRENDS

WIRELINE LOG TRENDS

6.1 Introduction

The application of wireline well logs to recognition and inter-well correlation of facies and their sedimentological interpretation is governed by the resolving powers of the different logging tools relative to measured sedimentation rates and log trend periodicities. One of the most obvious and earliest geological uses of wireline logs, apart from the determination of lithology, was the interpretation of vertical successions of strata. The optimum approach is to use core data and well logs together, a strategy that requires knowledge of the limitations and capabilities of well logs in recording trend phenomena throughout NC115 Concession. Together with drill cuttings, such logs provide a basic suite of information about the lithology, petrophysical properties and pore-fluid content of the strata penetrated (Galloway and Hobday, 1983).

Sequence stratigraphic analysis of wireline logs is an important component of analysing a subsurface data set. Log data allow lithology and depositional environment to be placed on the seismic section, thus linking seismic facies, rock properties and sedimentological facies. Sequence stratigraphic analysis of wireline log data is neither easy nor unambiguous. Some systems tract boundaries may have a subtle expression on logs, and may even be hard to recognize in core (Emery and Myers, 1996).

6.2 Objectives

Field application of wireline log trends ideally requires the use of both log and core information, a strategy which reflects the current trend in earth science towards a more meaningful integration of data measured at vertical and lateral intervals in sedimentary successions to divide the strata into cycles; these cycles are thought to be controlled by relative sea-level changes. The most important wireline log trends, therefore, are those which show progradation, retrogradation and aggradation.

The main purpose of this chapter is to review the use of wireline logs in facies analysis, to define various characteristic motifs and to integrate them with core data. This chapter takes the geology further in describing how logs can be used for facies and sequence stratigraphy analysis. Modern subsurface geological analysis can, and should, employ a thorough and sophisticated analysis of well log data.

6.3 Log suite used in sequence stratigraphy

This section contains a brief explanation of principles behind each of the different types of wireline log used in this study and discusses the geological information, which can be obtained from each log. Log patterns may be used at three levels of interpretation:

1) Determination of vertical sequence and bedding architecture;
2) Recognition and mapping of log facies; and
3) Interpretation of depositional environment.

One of the most obvious and earliest uses of wire-line logs, beyond the determination of basic lithology, is the interpretation of vertical sequence. The characteristic erratic, upward-coarsening, and upward-fining textural patterns of aggradational, progradational and lateral accretion bedding geometries are readily recognized on electrical and gamma logs (Galloway and Hobday, 1983).

Sequence analysis is concerned with the inference of depositional controls on sedimentary successions. Sequence analysis of a log suite must therefore concentrate on logging tools that measure depositional parameters. It is important to be aware of the potential pitfalls involved in attempting to obtain stratigraphic information from log response (Rider, 1996). A suite of wireline logs over an interbedded succession of siliciclastics for individual log curves are discussed below.

6.3.1 Gamma ray logs (GR)

Units: API

Gamma ray measures the total natural gamma-ray emission of the formation. The emission is primarily from radioactive isotopes of potassium (K), Thorium (Th) and Uranium (U). The log is dependent on the formation mineralogy; for example, some formations contain (K-Feldspar, glauconite, biotite, illite and muscovite) and give a strong Potassium (K) kick. The gamma-ray log is one of the most useful logs for sequence stratigraphy analysis, and is run in most wells. The radioactivity of the rock, measured by a gamma tool, is generally a direct function of clay-mineral content, and thus grain-size and depositional energy. Gamma-ray logs are often used to infer changes in depositional energy, with increasing radioactivity reflecting increasing clay content with decreasing depositional energy (Emery and Myers, 1996).

6.3.2 Sonic velocity logs (DT)

Units: μS/ft

Sonic principles are used to determine the relative proportion of fluid and (rock) solids in a formation, and hence the porosity. Sonic waves are transmitted into the formation and received by the tool. Their transit time (velocity) varies with the hardness and density of the formation. Velocity increases with clay compaction and hence is a good indicator of abnormal pore pressure transitions.

6.3.3 Formation density logs (RHOB)

Units: gm/cm^3

The tool emits medium energy gamma-rays, which collide with electrons in the formation, losing energy and scattering at each collision. A detector counts the returning gamma rays. The number of collision is a function of the formation electron density, which is proportional to the formation bulk density (RHOB). RHOB is useful in identifying evaporites and other mono-mineralic formations.

6.3.4 Spontaneous potential logs (SP)

Units: mV

Spontaneous potential logs measure the natural electric voltage in a formation, indicating the water salinity and giving a related indication of permeability. The SP log works best where there is a good resistivity contrast between the mud filtrate and the formation water. Opposite impermeable shale the SP curve usually shows a more-or-less straight line on the log, known as a shale base line, and any differentiation within the shale is best done on gamma or resistivity logs.

6.3.5 Resistivity induction logs (RT)

Units: Ω/m

Resistivity logs measure the bulk resistivity of the rock, which is a function of porosity and pore fluid. A highly porous rock with a conductive (saline) pore fluid will have a low resistivity, whereas non-porous rocks, or a hydrocarbon-bearing formation, will have a high resistivity. Resistivity trends are excellent indicators of lithology trends, provided the fluid content is constant. Resistivity logs often are excellent for correlating within shale successions, or within clean sandstones with uniform gamma-ray response (Emery and Myers, 1996).

6.4 Analysis of wireline log trends

A number of distinctive trends, recognised frequently on wireline logs, can be used to estimate lithology. Log trends may be observed as a change in the average log reading, or from shifts in the sand or shale base line. Gamma-ray log shapes are often used by geologists to determine sandstone grain-size trends and hence depositional facies (**Fig. 6.1**). However, for the simple methodology of relating shapes to facies to be valid, there must be consistent relationships between gamma-ray log value and clay content, and between clay content and grain-size (Cant, 1984, 1992; Rider, 1990, 1996).

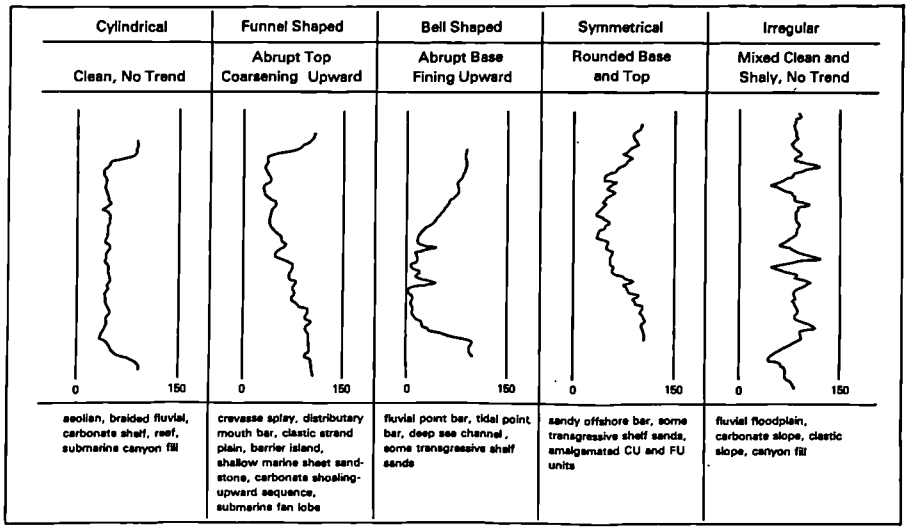

Fig. 6.1 The most idealized gamma-ray (SP) curves. Depositional environment characteristics are shown below each curve (After Cant, 1984).

Gamma-ray shapes may represent clean sandstone, interbedded sandstone with shale, and abrupt and gradational contacts. The gamma log has limited use in carbonate facies analysis where it can indicate fluctuations in clay content (Selley, 1985). Furthermore, the gamma-ray log shapes are often used by geologists to determine sandstone grain size trends and hence depositional facies. Using the log shapes, therefore, requires implied relationships. There are three main principals to the relationships between the gamma-ray and clay content as shown below.

1) The relationship of gamma-ray response to clay content;
2) The relationship of clay content to grain-size; and
3) The relationship of grain-size sequence to depositional facies.

6.4.1 Geological interpretation of the Mamuniyat Formation from gamma-ray log

The gamma-ray log does not vary because of change in grain-size; it varies (often) because of changes in clay content (the same is true for the SP). However, sedimentological interpretations based on gamma-ray log shapes require the log to vary with grain-size (**Fig. 6.2**). This involves undeclared assumptions:

1) Gamma-ray variation is related to clay volume change; and

2) Clay volume changes are related to grain-size differences.

In petroleum borehole logging, the commonest natural radioactivity (by volume) is found in shale (clay). A high gamma-ray value frequently means shale. A typical shale analysed by a spectral gamma-ray tool shows that each of the three elements: potassium (K), uranium (U) and thorium (Th), is contributing to indicate a high clay content, and an analysis of shales in general shows the relative contribution of each element to the overall radioactivity (Rider, 1996).

The high gamma-ray reading indicates shale content or it may indicate radioactivity from feldspar in arkosic sandstone, as well as heavy minerals in lag deposits. The unit for radioactivity logging is the API (American Petroleum Institute) which conventionally increases to the right (**Fig. 6.2**).

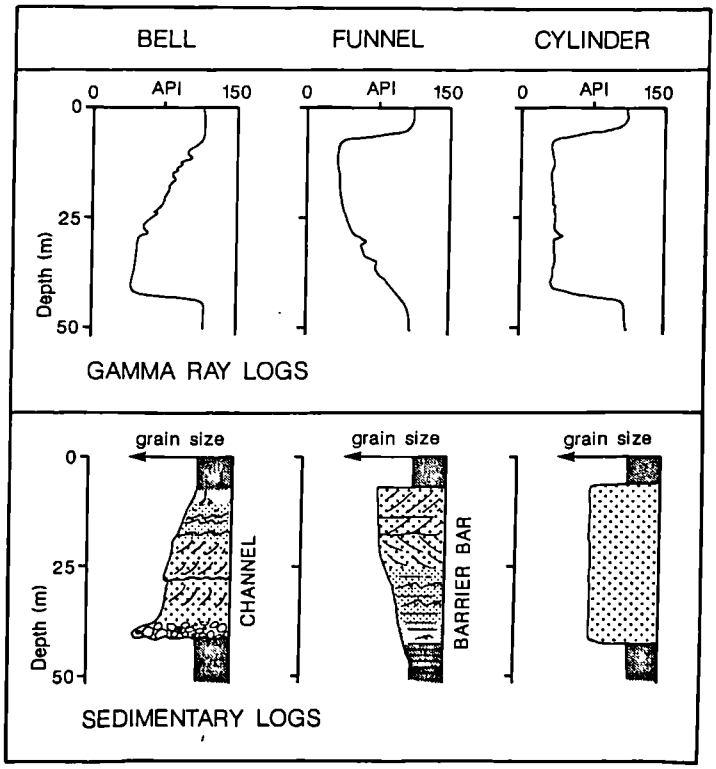

Fig. 6.2 The three principle gamma-ray log shapes and their corresponding sedimentary interpretation (After Rider, 1990).

The attractive idea that log shapes indicate sandstone depositional environments is too simplistic. The most useful wireline log curves in the Upper Ordovician succession of the Mamuniyat Formation is the gamma-ray log. This is because it is a common wireline log in NC115 wells and has better resolution than most other logs.

Figures 6.3, 6.4 and 6.5 show a suite of wireline logs from three different wells A8, B2 and H4-NC115 that have been used to select the different lithologies in the Mamuniyat succession. For example, the gamma-ray log clearly identified and distinguished between Upper, Middle and Lower sections of the Mamuniyat Formation only in B-Field, southwest of the El-Sharara Field (**Fig. 6.4**).

Gamma-ray log shapes may be use to determined sandstone grain-size, depositional environment facies and the deposition between sands and shales in mixed siliciclastic sequences (Rider, 1990). Several principal gamma-ray log shapes are frequently used as a basis for identifying depositional facies, especially sandstone. A number of distinctive trends are commonly recognized on wireline logs as shown below.

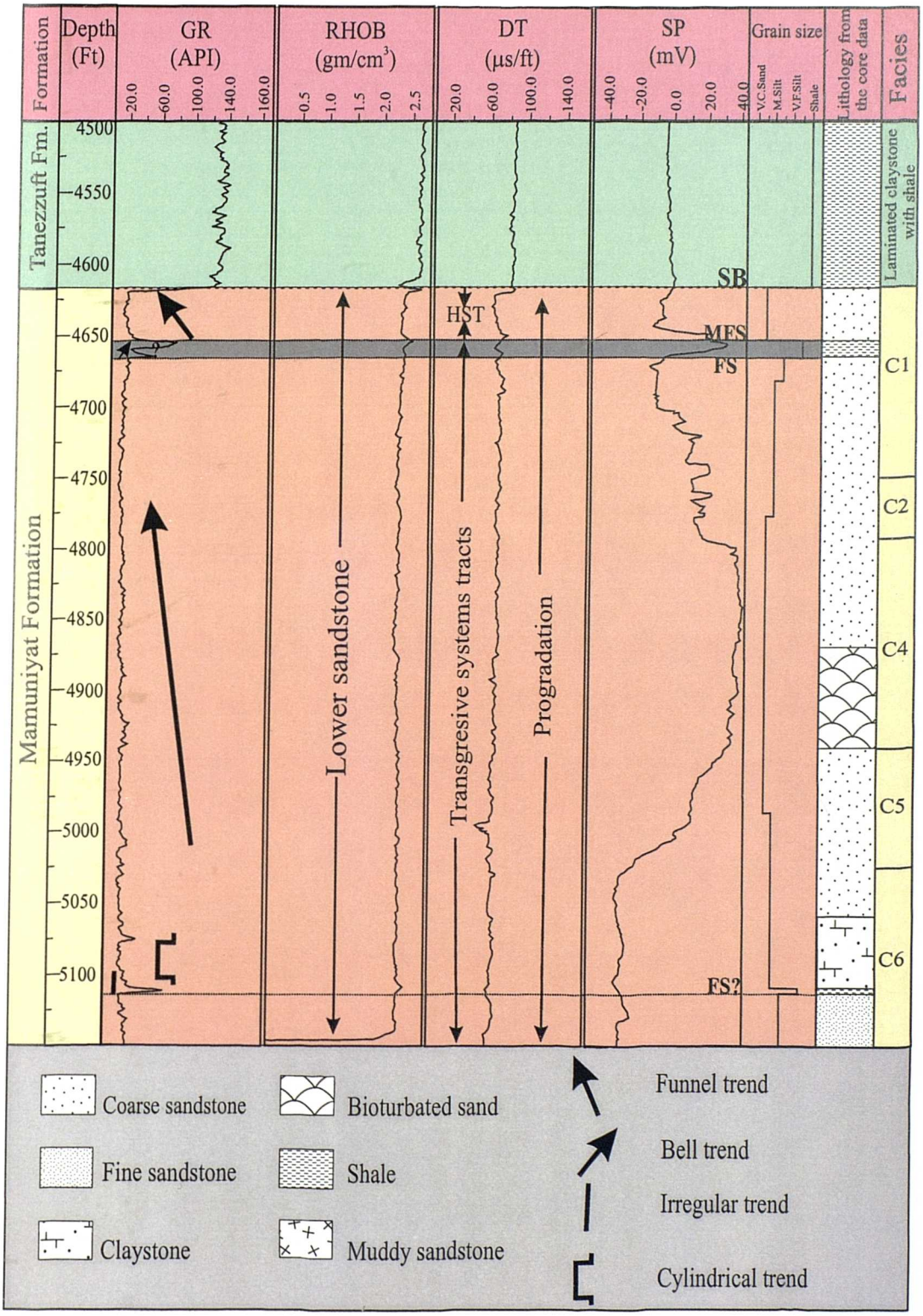

Fig. 6.3 Wireline logs from type well A8-NC115. Gamma-ray log (GR), Formation density (RHOB), Sonic velocity (DT) and Spontaneous potential log (SP) related to core lithology, and trends in systems tracts.

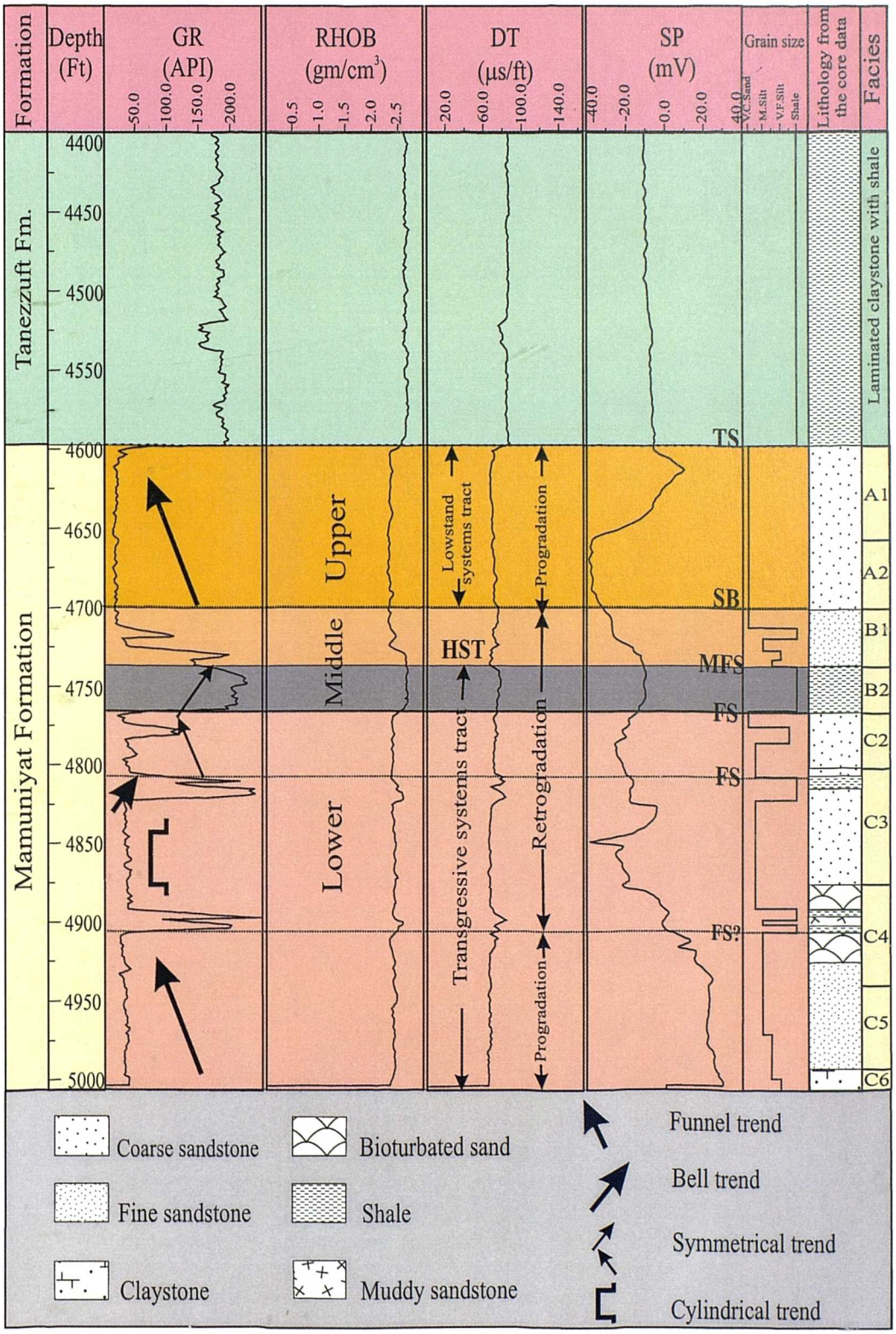

Fig. 6.4 Wireline logs from type well B2-NC115. Gamma-ray log (GR), Formation density (RHOB), Sonic velocity (DT) and Spontaneous potential log (SP) related to core lithology, and trends in systems tracts.

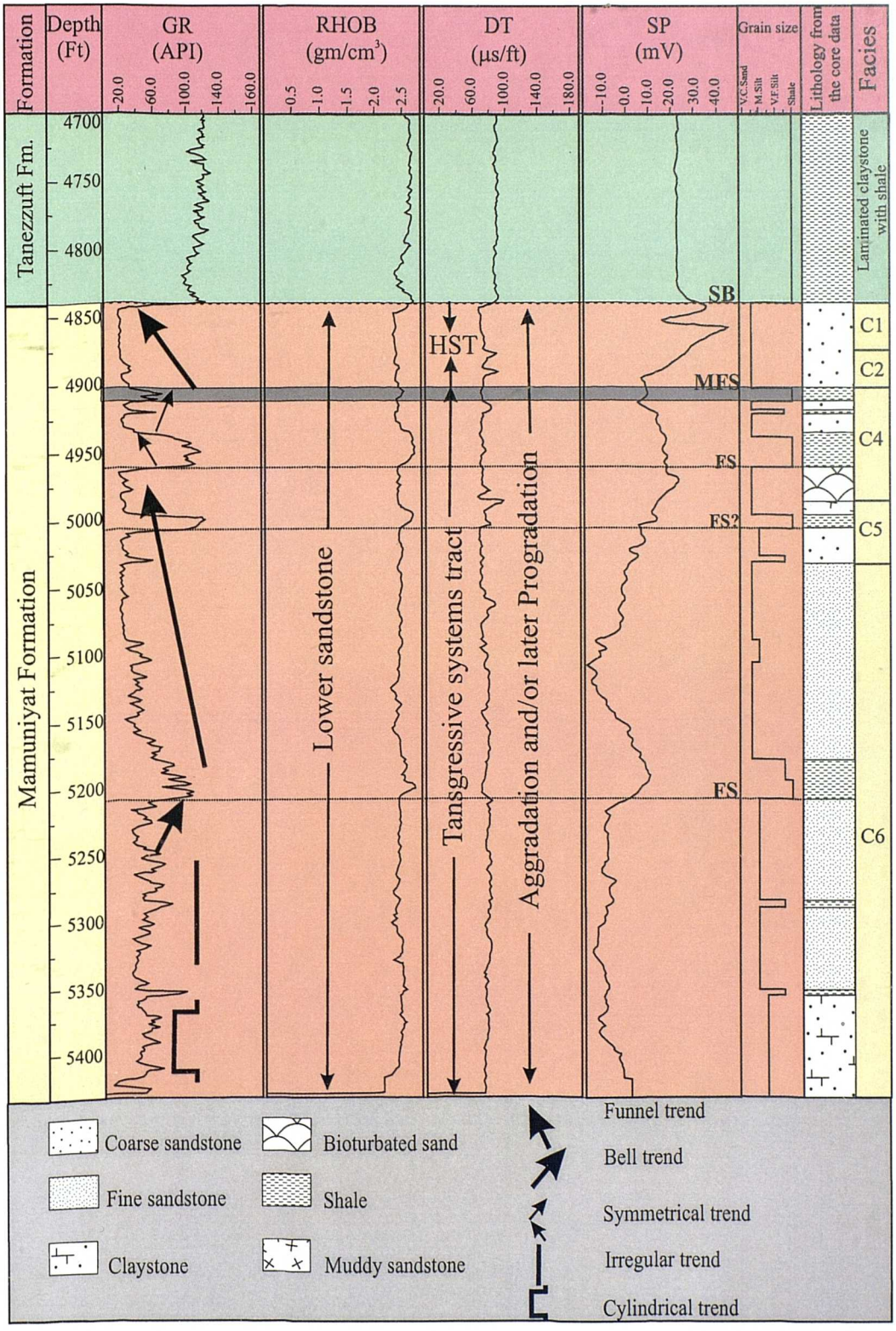

Fig. 6.5 Wireline logs from type well H4-NC115. Gamma-ray log (GR), Formation density (RHOB), Sonic velocity (DT) and Spontaneous potential log (SP) related to core lithology, and trends in systems tracts.

1) ***Bell trends:*** These show a progressive upward increase in the gamma-ray log reading and a gradual upward decrease in grain-size trend indicating increasing clay content (*e.g.* change from sandstone to shale). Such trends may represent deposition in channel or transgressive marine facies (Rider, 1990), for example, the transgressive marine shale in the lowermost section of the Middle Mamuniyat Formation (M2). This shape is recognized in type well B2-NC115 (**Fig. 6.4**);
2) ***Funnel trends:*** These show a gradual upward decrease in the gamma-ray reading representing a gradual upward change to a coarse-grained lithology, related to a gradual increase in grain-size indicative of a decrease in clay content. For example, from mudstone to sandstone or from mudstone to coarse-grained carbonate. This trend has been clearly recognized in the Lower Mamuniyat Formation (M3), and is related to a gradual increase in sandstone grain-size from fine to coarse within most wells of NC115 Concession, particularly in the study area. (**Figs. 6.3, 6.4 and 6.5**);
3) ***Cylindrical trends*** (Boxcar log trend): These consist of low gamma-ray values with a constant reading, set within a higher gamma-ray background value. The boundaries with overlying and underlying shale are abrupt. This type of trend is commonly recognized in shallow marine sediments. Within the study area this shape is recognized in the Lower Mamuniyat Member (M3) in type wells A8, B2 and H4-NC115 (**Figs. 6.3, 6.4 and 6.5**);
4) ***Symmetrical trend*** (Bow trend): These consist of funnel trends, overlain by a bell trend of similar thickness with no sharp break between the two. It is not common in the study area, but may be present in type well H4-NC115, northeast of the study area (**Fig. 6.5**); and
5) ***Irregular trend*** (mixed clean and shaly): No systematic change is observed, and they lack the clean character of the boxcar shape. This trend may represent aggradation of a shale or silt succession (Emery and Myers, 1996). Such a trend is seen in the lowermost part of the lower Mamuniyat sandstone succession in A8 and H4-NC115 (**Figs. 6.3 and 6.5**).

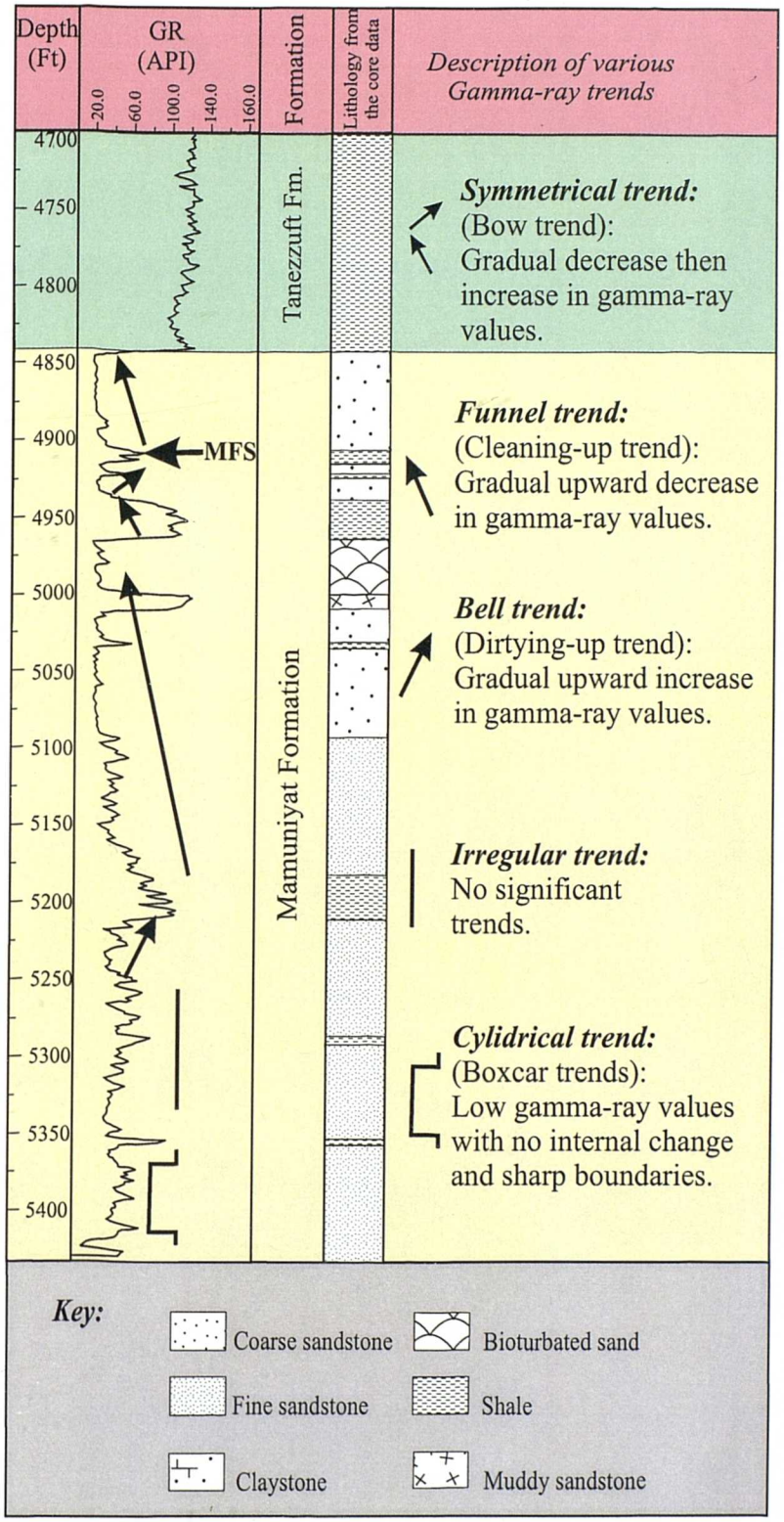

Fig. 6.6 Wireline Gamma-ray log trends from type well H4-NC115. Maximum flooding surface (thick arrow). Top of the Mamuniyat Formation based on data from Repsol Oil Operations (Fello and Herzog, 1996).

More recently log shapes have been used as a tool for sequence stratigraphy (Van Wagoner *et al.*, 1990; Rider, 1996; Emery and Myers, 1996; Ahmadi, 1997), with variations in log shape (generally gamma-ray), indicating facies relationships within parasequences, parasequence stacking patterns or facies changes at sequence boundaries.

The obvious relationship being suggested when gamma-ray log shapes are used in facies analysis is that gamma-ray changes faithfully correlate with grain-size variation. Low log values indicate coarse grain-size while high values indicate fine grain-size (Serra and Sulpice, 1975; Selley, 1976). However, the gamma-ray tool does not measure grain-size: it measures natural radioactivity (**Fig. 6.6**).

Since the gamma-ray log is frequently an indicator of clay (shale) content, gamma-ray log shapes can be explained in term of variations in clay (shale) content. A bell shaped log, where the gamma-ray value increases regularly upwards from a minimum value, should indicate increasing clay content: a funnel shape, with the log value decreasing regularly upwards, should show the reverse, a decrease in clay content (Rider, 1996).

The sedimentological implication of this relationship leads to a direct correlation between facies and log shape, not just for the bell shape and funnel shape as described above, but for a whole variety of shapes. Numerous publications show the log shapes expected or found in various facies (Galloway and Hobday, 1983; Vail and Wornardt, 1990; Van Wagoner *et al.*, 1990; Cant, 1992). They all depend on the relationship between log shape and grain-size trends in sandstone bodies.

A bell shape indicates a fining-upward sequence, which may indicate an alluvial/fluvial channel but also, a transgressive shelf sand. A funnel shape is a coarsening-upward succession which may be indicate a deltaic progradation or a shallow marine progradation (**Fig. 6.7**). The shapes come from the diminution in bed thickness associated with diminution in grain-size, rather than the direct change in grain-size itself (Rider, 1996).

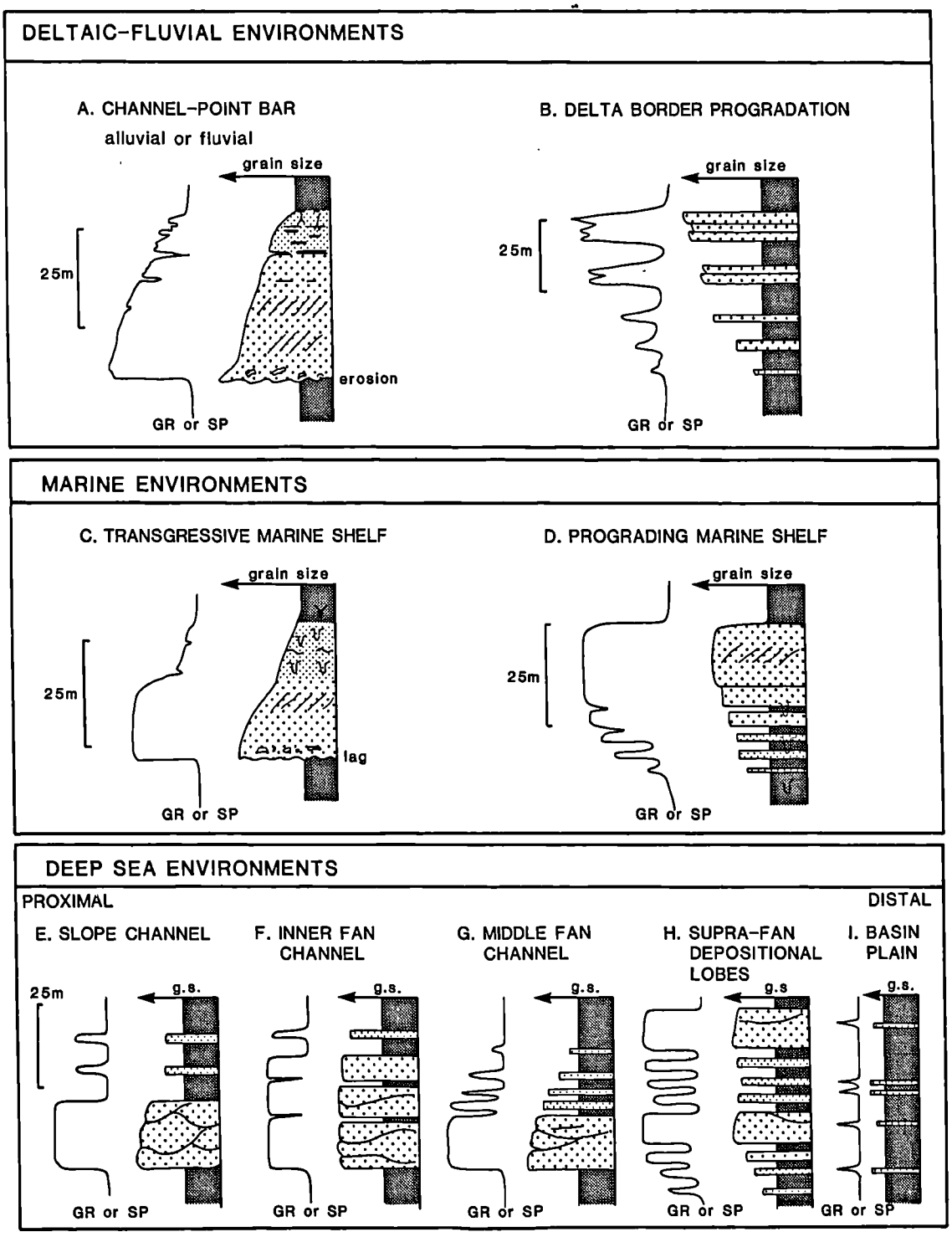

Fig. 6.7 Facies indication from gamma-ray (or SP) log shapes. These are idealized examples of both log shape and sedimentary facies (After Rider, 1996).

6.5 Generalized stratigraphic sequence analysis of the Mamuniyat Formation, from wireline log trends

6.5.1 Introduction

During drilling of most of the exploration and development wells in NC115 Concession area, the drilling company, Geomin Oil Service Company, provided the wireline logging services. However, the age of their equipment and their apparent inability to follow the necessary instrument calibration procedures, as per manufactures guidelines, raised serious doubts about the accuracy of the recorded log data (Fello and Herzog, 1996).

As a result of these doubts, a second logging contractor, Schlumberger Wireline Logging Company, was used to log the primary reservoir interval the "Mamuniyat Formation", and deeper sections in Concession NC115. Schlumberger was also in a position to provide more sophisticated logging equipment such as the ARI and FMI logging tool. The ARI data greatly increased the accuracy of the Sw calculations and the FMI provided important information on sedimentary structures, faulting and fracturing within the Mamuniyat Formation at the reservoir interval in the El-Sharara Field.

The wireline logs used in the correlation within NC115 Concession are mostly Gamma-ray (GR) supplemented by Spontaneous potential (SP) and Resistivity log (RT) (Fello and Herzog, 1996). Cleaning-upward sandstone sequences within NC115 wells, are the most common wireline log trends for the Mamuniyat sandstone units, although bow and boxcar trends are present in many cases within El-Sharara Field (**Fig. 6.6**). The most important wireline log trends, therefore, are those which show progradation, retrogradation and aggradation (**Fig. 6.8**).

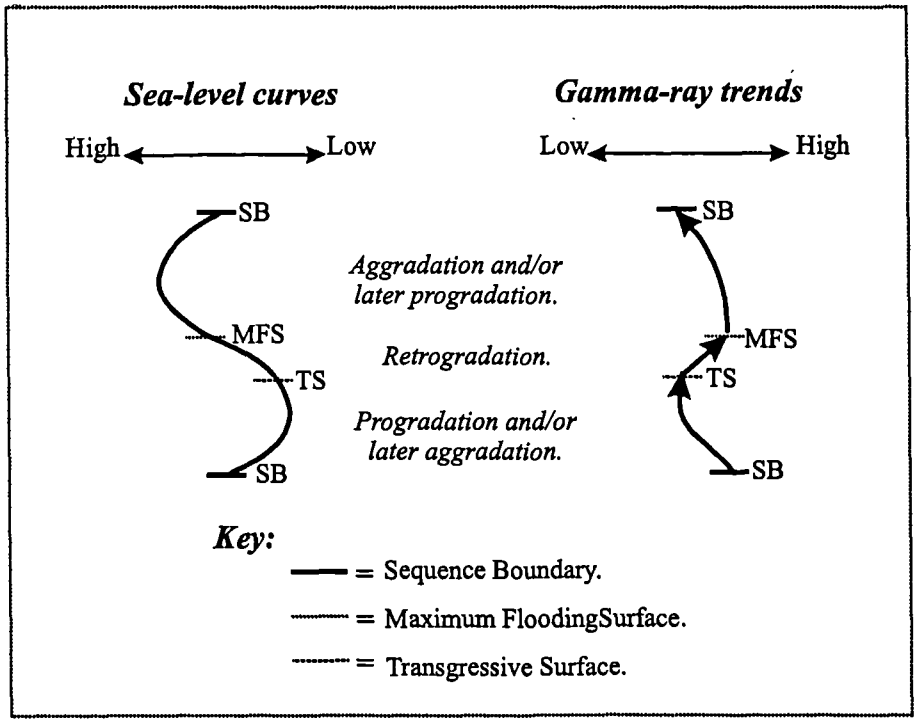

Fig. 6.8 Idealized wireline log trends in sequence stratigraphic analysis of the study area.

Wireline log trends are currently one of the most rapidly developing areas of study in the El-Sharara Field. The lowermost part of the Upper Ordovician "Ashgillian" is defined by a transgressive systems tract, which is represented by a progradation trend, which may or may not show aggradation towards the top, particularly in type well H4-NC115 (**Fig. 6.5**). Highstand systems tracts, represented by a retrogradational trend, particularly in the uppermost section of the Middle Mamuniyat Formation and lowstand systems tract, characterized by a progradational gamma-ray trend, occur throughout the Upper Mamuniyat Formation, particularly in type well B2-NC115 (**Fig. 6.4**).

6.5.2 Sequence stratigraphic interpretation of the Mamuniyat Formation from wireline log trends

The concept of sequence stratigraphic analysis that has been applied in this study is based on Van Wagoner *et al.* (1990), Mitchum *et al.* (1990), Posamentier and Allen (1993), Emery and Myers (1996), Miall (1996) and Rider (1996).

The region of study was drilled by over 120 exploration and production wells since the 1980s. The high-resolution sequence stratigraphic framework developed in this analysis is based on wireline log data from 12 oil wells. To cross-check the wireline interpretation and place the wells in depositional context sedimentological analyses of more than 310 met (1016 ft) of slabbed core from three type wells A8, B2 and H4 from the three oilfields A, B and H, was carried out (discussed in Chapter Two).

Rider (1996) shows the schematic wireline log characteristic for the sequence stratigraphic interpretation of wireline log patterns (**Fig. 6.9**). This model indicates the key sequence stratigraphic surface (sequence boundary, maximum flooding surface and transgressive surface) (discussed in Chapter Five) that can be used to interpret these key surface in the study area of the Mamuniyat sequence as follows:

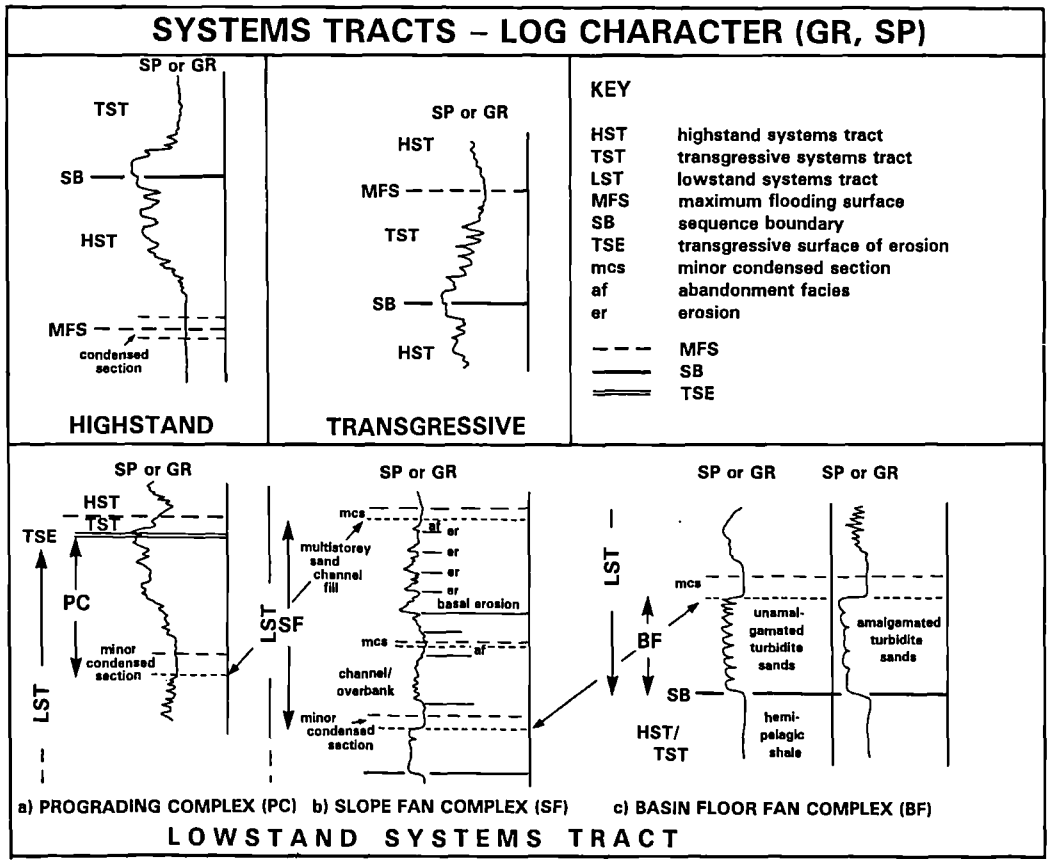

Fig. 6.9 Model log patterns for sequence tracts, with possible sequence stratigraphic interpretation. The upper part (HST and TST) represents the interpreted systems tracts within the study area (After Rider, 1996).

1) ***Sequence Boundary (SB):*** This results from a fall in relative sea-level and may be difficult to recognize from the well log alone (Emery and Myers, 1996). A sequence boundary is an unconformity and its correlative conformity; it is a laterally continuous, widespread surface covering at least an entire basin and seems to occur synchronously in many basins around the world (Vail *et al.*, 1977; Vail *et al.*, 1984; and Haq *et al.*, 1988).

   A sequence boundary separates all of the strata below the boundary from all of the strata above the boundary (Mitchum, 1977), and has chronostratigraphic significance. Correlation of sequence boundaries on well-log cross sections provides a high-resolution chronostratigraphic framework for facies analysis (Van Wagoner *et al.*, 1990). The sequence boundary may represent abrupt upward change from progradation to retrogradation in the succession.

   A sequence boundary may result from an abrupt change in log response in sandstone units or may be marked by change in shale type in the shale section (Rider, 1996). In the study area the sequence boundary is immediately followed by the lowstand systems tract particularly in type well B2-NC115. It is characterized by erosion of the subaerially exposed shelf;

2) ***Maximum Flooding Surface (MFS):*** This is represented by the maximum landward extent of marine deposits; it is immediately followed by the highstand systems tract (Miall, 1996). It can also be identified from a gamma-ray peak (high gamma-ray values) on bell and funnel trends respectively (*i.e.* where these are fining-upward and coarsening-upward respectively, the maximum flooding surface may be a gamma-ray maximum). It should not be assumed that every gamma-ray peak is a maximum flooding surface (Emery and Myers, 1996).

In the study area the maximum flooding surface appears in both core and wireline logs throughout A, B and H-Fields, particularly in type wells A8, B2 and H4-NC115. The thin bed of dark-black shale, in the southwest of the study area (*e.g.* B2-NC115), represents a condensed section corresponding to a maximum flooding surface. This defines the boundary between the transgressive systems tract beneath and the highstand systems tract above. The maximum flooding surface overlies a deeper water shale environment, and can be easily recognized in the most oil wells within B-Field, without core control (**Fig. 6.4**).

The maximum flooding surface lies at the point of maximum gamma-ray response and can be traced laterally into a basinward setting where sandstone is separated by radioactive shale in the southwest El-Sharara Field. It correlates very well between A8, B2 and H4-NC115 wells, because the gamma-ray signature of the maximum flooding surface has a more distinctive peak and forms a good marker horizon.

3) ***Marine Flooding Surface (FS):*** This is a surface separating younger from older strata across which there is evidence of abrupt increase in water depth. This deepening is commonly accompanied by minor submarine erosion or non-deposition, with a minor hiatus indicated (Van Wagoner *et al.*, 1990). A maximum flooding surface can be recognized from a sudden significant change in log value (abrupt increase in gamma-ray value). The marine flooding surface indicates a change in lithology, such as shale resting sharply on sandstone. This surface typically terminates coarsening-upward trends.

In the study area, the contact between the Lower and/or Middle Mamuniyat Formation is followed by a transgressive marine shale, that represents a parasequence, bounded at the top by a marine flooding surface. It can be easily correlated in B-Field, in the southwest of the study area (*e.g.* B2-NC115).

6.6 Electrosequence analysis of the Mamuniyat Formation

An electrosequence is an interval defined on wireline logs, through which there are consistent or consistently changing log responses and characteristics, sufficiently distinctive to separate it from other electrosequences (Rider, 1996). The main objective of an electrosequence analysis of the Mamuniyat Formation, is to extract from the logs as much geological information as possible, by identifying vertically continuous, depositional, stratigraphic and eventually sequence stratigraphic units. The electrosequence analysis uses all the available logs, and covers the entire well, not just sandbodies and reservoirs.

In the Mamuniyat Formation, shapes on the gamma-ray log can be interpreted as grain-size trends and by sedimentological association as facies successions. A decrease in gamma-ray values will indicate an increase in grain-size (Upper and Lower Members of the Mamuniyat Formation), and small grain-size will correspond to higher gamma-ray values (Middle member of Mamuniyat Formation). The sedimentological implication of this relationship leads to a direct correlation between facies and log shape, not just for the bell shape and funnel shape as described above, but for a whole variety of shapes.

The stratigraphical succession of the Mamuniyat Formation may be divided into parasequences, which together form systems tracts, deposited during relative sea-level rise and fall. Transgressive, highstand and lowstand systems tract are recognized in this succession and have been discussed in the Sequence Stratigraphy chapter. In this section a first attempt will be made to identify these systems tracts from wireline log trends.

1) ***Progradation:*** This is basinward migration of facies belt or facies belts within a depositional system (Van Wagoner *et al.*, 1988). A seaward advance of a shoreline results from the nearshore deposition of sediments. It can also recognized from an upward decrease in gamma-ray values resulting in an upward increase in grain-size (*i.e.* increase in sand/shale ratio). Progradation represents the funnel trends in the Mamuniyat Formation (**Figs. 6.3, 6.4 and 6.5**). The vertical pattern of upward coarsening and thickening reflects the progradational succession.

2) ***Retrogradation:*** This is the landward migration or a facies belt of facies belts within a depositional system (Van Wagoner *et al.*, 1988). It is indicated by fining-upward stacking patterns, which imply upward deepening (upward increase in gamma-ray values). In the study area the retrogradational successions occur within the Middle Mamuniyat Formation, particularly in the B-Field (*e.g.* B2-NC115) (**Fig. 6.4**). In this well the retrogradational successions show the fining-upward facies trend (vertical stacking patterns) from sandstone to shale.

3) ***Aggradation:*** This is accumulation of a facies or group of facies within a depositional system, with no significant lateral migration of the facies belts towards either the land or basin (Van Wagoner *et al.*, 1988). It is assumed to occur when accommodation space increases. In the study area the aggradation is marked by a somewhat subtle change in the relative proportion of shallow marine shelf siliciclastic of the Lower Mamuniyat Formation to the marginal marine shale/clastic parasequences of the Middle Mamuniyat Formation. Furthermore, the Middle Mamuniyat Formation is characterized by a thicker section of the black shale and thinner clastics than those in the underlying member of the Lower Mamuniyat Formation. This contact between Lower and Middle members of the Mamuniyat Formation appears to represent a change from largely progradational to aggradational parasequence sets.

6.6.1 Transgressive systems tract

The transgressive systems tract in the Upper Ordovician includes the Lower and Middle Mamuniyat deposits of sequence 1, throughout B2-NC115. The top of the transgressive systems tracts is defined by the most fine-grained interval, coinciding with the highest shale content part of the section (Middle Mamuniyat Formation, B2-NC115). This horizon represents a maximum flooding surface (MFS). The sandy base of this systems tract is represented by the Lower member of the Mamuniyat Formation and is recognized in A8 and H4-NC115.

The high gamma-ray reading and high resistivities displayed by the Middle Mamuniyat deposits, probably reflect a high content of radioactive shale as demonstrated in the B-Field. This suggests that the clastic source area had moved progressively further away (A and H-Fields), allowing radioactive shale to accumulate on the sea floor from suspension, with less dilution from terrestrial siliciclastic sediment. The radioactive shale of the Middle Mamuniyat succession thus represents continued transgression. The most radioactive shale interval is interpreted as a condensed section including the maximum flooding surface (MFS).

All the radioactive shale of the Mamuniyat succession in the B-Field wells are characterized by increasing resistivity and gamma-ray values, and decreasing sonic velocities. This indicates an upward decrease in grain-size and an increase in radioactive shale. The serrate shape of gamma-ray log patterns in parasequences is due to contrasting grain-size in response to stratification and cross-bedding.

Parasequences represent the shoreline progradation setting. The vertical pattern of upward-coarsening and thickening reflects progradational deposits. The marked facies change in the Lower and Middle Mamuniyat deposits may largely reflect an abrupt decrease in energy levels due to a major increase in water depth, but may be partly a result of a sudden cessation of sand supply from nearby source areas in the SW (Ghat/Tikiumit Arch) as a result of complete drowning of these local highs.

6.6.2 Highstand systems tract

A coarsening-upward interval above the MFS is interpreted as the prograding wedge of a highstand systems tract within the three type wells A8, B2 and H4-NC115. The HST consists predominantly of medium- to coarse-grained sandstone and subordinate dark shale, throughout the uppermost part of the Middle Mamuniyat Formation within the B-Field. The sandstone of the HST in B-Field is characterized by wavy-hummocky cross-stratification and small-scale cross-bedded sandstone in core particularly in type well B2-NC115.

Both the wavy-hummocky cross-stratified and small-scale cross-bedded sandstone are the product of deposition on the shoreface (discussed in Chapter Two). The HST in type well B2-NC115 is represented by coarse-grained sandstone, which may also have resulted from submarine or subaerial erosion of the shoreface due to a fall in relative sea-level (Fello and Turner, 2001b).

In A and H-Fields, the HST is characterized by an upward decrease in resistivity and gamma-ray values and increasing sonic velocity reflecting a coarsening-upward trend and an upward decrease in shale content, suggesting deposition during retrogradation. The sequence boundary (SB) forming the top of the highstand systems tract is placed at the most coarse-grained part of the coarsening-upward interval, representing maximum progradation of the offshore wedge in type wells A8 and H4-NC115.

The HST in A, B and H-Fields, is bounded at the top by a subaerial erosion surface, not evident on the wireline logs. The only possible evidence is an irregular shape followed by a funnel shape, which reflects a gradual upward decrease in gamma-ray value (**Figs. 6.1 and 6.9**). The irregular shape corresponds to the fine material (sandstone with subordinate shale) and may represent deeper water (*e.g.* in type well B2-NC115).

6.6.3 Lowstand systems tract

Depositional conditions of the Mamuniyat Formation changed greatly throughout the fluvial period within the upper Mamuniyat Formation (M1) in the B-Field. The coarsening-upward interval (from distal to proximal) above the sequence boundary (SB) throughout the Upper Mamuniyat Formation is interpreted as the progradation of a lowstand systems tract (*e.g.* B2-NC115). The LST is represented by downstream portion of the fluvial system, the abrupt vertical juxtaposition of coarse-grained fluvial deposits on marine or marginal marine strata throughout A and H-Fields may record the presence of a sequence boundary.

The lowstand systems tract in the fluvial record may represent a period of renewed alluvial plain aggradation associated with the initial period of slow relative sea-level rise following base-level fall (Emery and Myers, 1996). High sediment supply rates from the source area will result in thicker fluvial deposits (Van Wagoner *et al.*, 1990). The Mamuniyat Formation shows a coarsening-upward trend, seaward progradation and basinward-thinning clastic wedge to the northeast accompanied by a change from fluvial to marginal marine and neritic marine environments. Significant thickness variation probably reflects a strong tectonic control on sedimentation (Thomas, 1995).

The LST in the Upper Mamuniyat Formation (M1) is characterized by a gradual upward decrease in the gamma-ray value related to a gradual increase in grain-size indicative of a decrease in clay content. It is represented by an abrupt top and coarsening-upward grain-size trend (Funnel shape) probably produced by prograding systems.

Laterally the Mamuniyat Formation shows changes in grain-size, lithology, sedimentary structures, and channel and gravel bar morphology. These changes are fundamentally linked to the gradient decrease in passing outward from the source terrain, with concomitant decrease in stream capacity and competence (Vos, 1977). Although the sedimentary properties change continuously away from the basin edge, the depositional setting of the Mamuniyat Formation can be divided into a fluvial-marginal marine and shelf environments (discussed in Chapter Two).

6.7 Sequence stratigraphy and relative sea-level curves

6.7.1 Introduction

Sequence stratigraphy aims to use the vertical and lateral variations in sedimentary successions to divide the strata into cycles, which are thought to be controlled by relative sea-level changes. One of the first pieces of work involving the application of wireline logs to sequence stratigraphy was that of Van Wagoner *et al.* (1990). Since then, a number of other studies have been published on the subject (Vail and Wornardt, 1990; Armentrout *et al.*, 1993).

Rider (1996) in his latest edition of "The geological interpretation of well logs" has included a chapter on sequence stratigraphy, in which he states "The use of wireline logs as a tool in sequence stratigraphy has so far been seriously underdeveloped". Trends seen on the wireline logs are therefore important because they indicate patterns of progradation, retrogradation and aggradation, which in turn can be related to sea-level changes (see section 6.7.2).

The interpretation of log trends in terms of relative sea-level change is very important for wireline sequence stratigraphic interpretation. For example, a sequence boundary (*i.e.* an unconformity or its correlative conformity which bounds genetically related successions of strata) forms during the maximum rate of relative sea-level fall (Ahmadi, 1997). In particular, the long-term trend seen on the gamma-ray logs are correlated with the relative sea-level curve constructed in this study which is based on the sequence stratigraphic interpretation of the Upper Ordovician "Ashgillian" of the Mamuniyat Formation, in the El-Sharara Field (Fello and Herzog, 1996). This study will show that the interpretation of the gamma ray log alone can be inaccurate, and the maximum flooding surface (MFS) should not be picked on the basis of gamma-ray or radioactive shale peaks alone, but that it is better to look at the trends (*e.g.* B2-NC115). The issue of whether trends seen on the gamma-ray logs can be related to rise and falls in relative sea-level will also be addressed (**Fig. 6.10**).

6.7.2 Relative sea-level curves of the Mamuniyat Formation

Relative sea-level is measured between the sea-surface and a local moving datum, such as basement or a surface within the sediment pile (Posamentier *et al.*, 1988). A comparison of the relative sea-level curves for the Upper Ordovician produced in this section with that of Haq *et al.* (1987 and 1988) is shown in **Figure 6.10**. Comparison of the relative sea-level curve for the Mamuniyat Formation in type well B2-NC115, with the wireline logs demonstrates that the gamma-ray log trends do not exactly reflect the relative sea-level curve.

Throughout the Middle member of the Mamuniyat Formation, a sharp gamma-ray (GR) spike is seen near the top of this member interpreted to be a Maximum Flooding Surface (MFS) above which the first fine-grained sands of the Mamuniyat Formation are generally observed. In places the boundary between these two members (Upper and Middle) appears sharp and can be related to a fall in relative sea-level.

The regressive-transgressive cycle seen on the relative sea-level curve in the Mamuniyat Formation is also depicted on the gamma-ray log in type well B2-NC115, which also shows a funnel trend followed by a bell trend, which is interpreted as a prograding and retrograding cycle. The gamma-ray log for the lowermost part of the Mamuniyat Formation shows an irregular trend through about three quarters of the Lower member of the Mamuniyat Formation, followed by a funnel trend.

These shapes consist of shale with an upward increase in sandstone. This is interpreted to represent the coarsening-upward progradational part of the upper member of the Mamuniyat Formation, in response to sea-level rise followed by a fall. The middle member of the Mamuniyat succession in type well B2-NC115, and lower member of the Mamuniyat succession in type wells A8 and H4-NC115, mostly show funnel or cylindrical shapes, but may be serrated, and the nature of the contacts are gradational or abrupt according to the gamma-ray signatures.

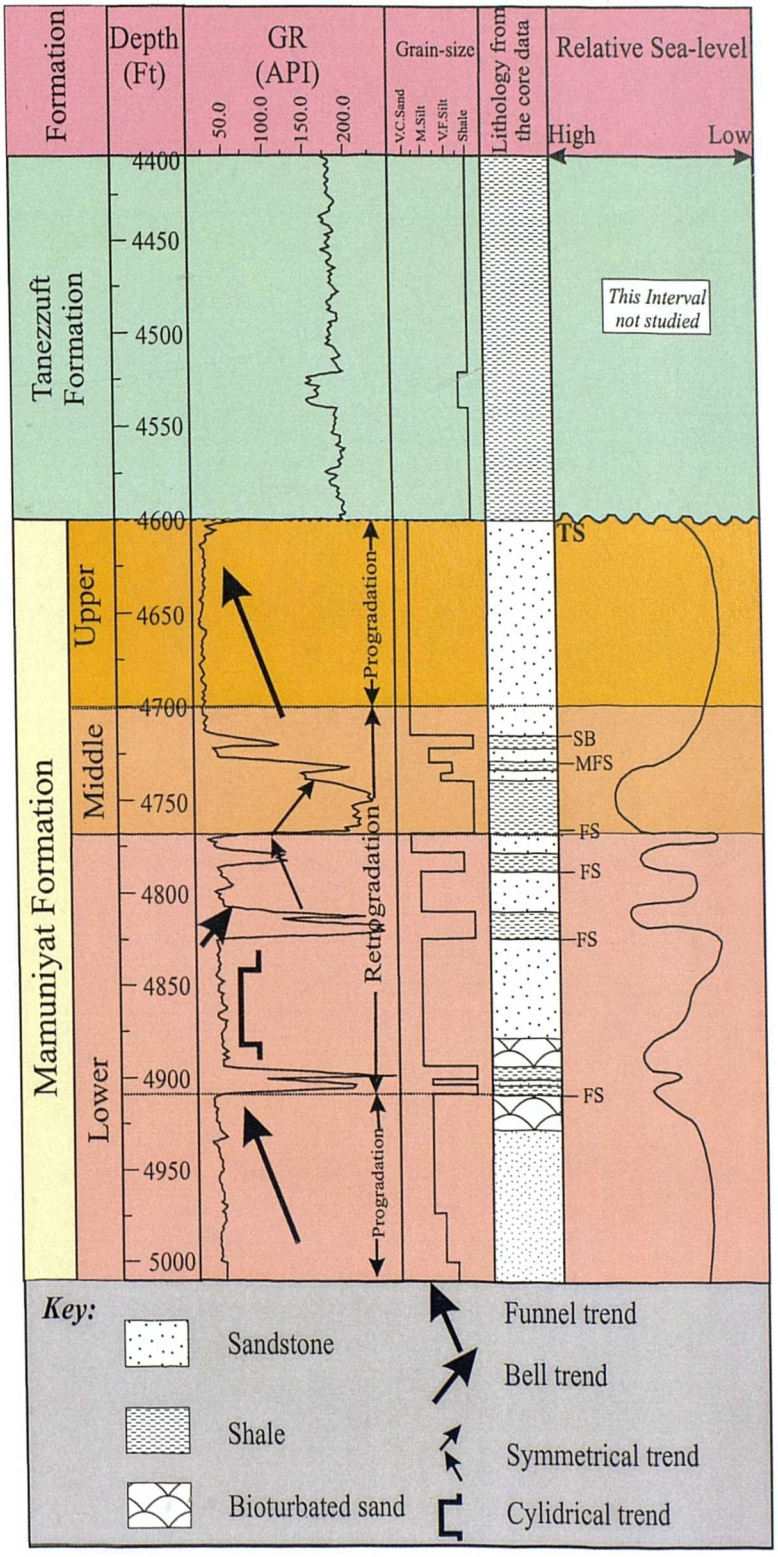

Fig. 6.10 Relative sea-level curve based on the sequence stratigraphic interpretation of the Upper Ordovician, Mamuniyat Formation, based on grain-size and gamma-ray trends of type well B2-NC115.

6.8 Summary

Analysis of wireline log trends based on the gamma-ray log can be interpreted in terms of grain-size trends. A decrease in gamma-ray values indicates an increase in grain-size (Upper and Lower Members of the Mamuniyat Formation) and an increase in gamma-ray values indicates a decrease in grain-size (Middle Member of Mamuniyat Formation). The sedimentological implication of this relationship leads to a direct correlation between facies and log shape, not just for the bell shape and funnel shape, but for a whole variety of log shapes.

CHAPTER 7

DEPOSITIONAL MODEL

DEPOSITIONAL MODEL

7.1 Sedimentological evolution of the Mamuniyat Formation in the Murzuq, Kufra and Ghadames Basins

7.1.1 Introduction

Libya is situated on the Mediterranean foreland of the Africa shield. Marine strata of Palaeozoic, Mesozoic, and Cenozoic ages abound in northern Libya, but continental rocks of Palaeozoic and Mesozoic ages predominate in southern Libya. Marine incursions in Ordovician, Silurian, Devonian, Carboniferous, Late Cretaceous and Early Tertiary times reached far into the country from the north, some crossing the southern border. The geology of the southern Palaeozoic basins of Libya is particularly important within the general palaeogeographic evolution of North Africa (Conant and Goudarzi, 1967).

The main focus of this section is concerned with the regional geological setting, the structural framework and stratigraphic development of the Palaeozoic succession of the Murzuq, Kufra and Ghadames Basins and their southerly extensions into adjacent countries (**Fig. 7.1**). The Murzuq and Kufra Basins cover large areas in the SW and SE of Libya extending cross the border into adjacent countries. The Ghadames basin covers the northwestern part of Libya whereas the Murzuq basin extends across much of its southwestern part. The southerly extension of this basin into northern Niger constitutes the Djado basin whilst the southerly extension of the Kufra basin in southeastern Libya becomes the Erdis basin into northern Chad. The distinction of Murzuq from Djado and Kufra from Erdis is primarily one of geology crossing a present-day political boundary.

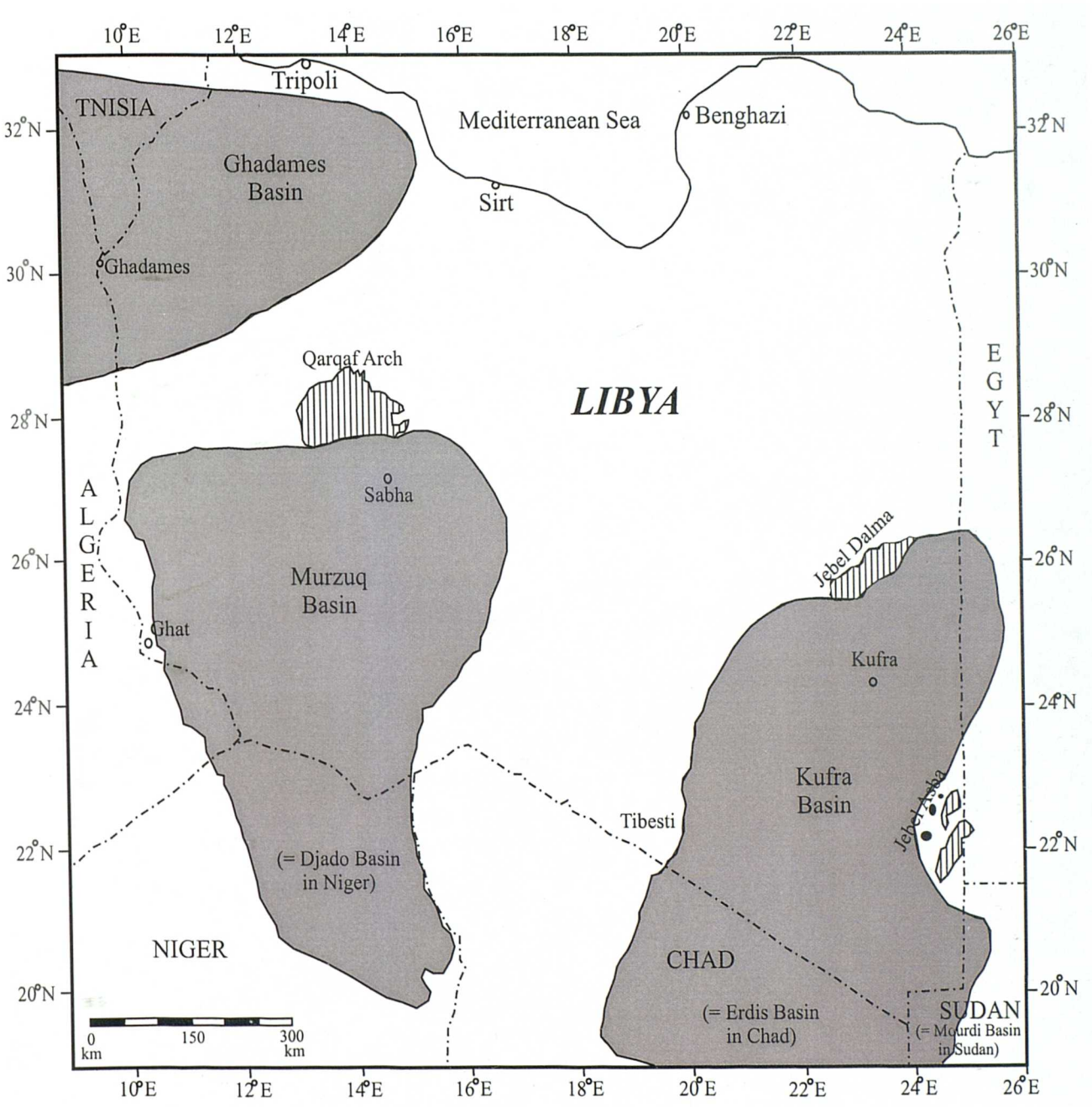

Fig. 7.1 Sketch map to show the location and regional setting of the Murzuq, Kufra and Ghadames Basins of Libya.

The Palaeozoic succession in the Murzuq, Kufra and Ghadames Basins record an interplay between continental influences associated with the African cratonic areas to the south, and marine influences which periodically extended southwards from the region now occupied by the Mediterranean Sea (Turner, 1980, 1991; Clark-Lowes, 1985). In this section only the Upper Ordovician (Ashgillian) part of the Mamuniyat succession in these basins **seen at outcrop** will be considered in detail.

7.1.2 Murzuq Basin

7.1.2.1 Introduction

The Murzuq Basin, SW Libya, covers an area of some 350,000 km^2, and has a roughly triangular shape, narrowing towards the south from Libya into Niger (**Fig. 7.1**). Cambro-Ordovician Mamuniyat reservoir rocks are exposed in several areas adjacent to Concession area NC115:

1) On the southeast flank of the Murzuq Basin, some 400 km away from NC115; and
2) The Ghat/Tikiumit and Qarqaf Arches on the western and northern flank of the Murzuq Basin, some 150 km and 200 km respectively, away from NC115 Concession.

This study focuses principally on outcrops of the Melaz Shuqran and Mamuniyat Formations, in Ghat/Tikiumit and western Qarqaf areas, although both Jebal Bin Ghanimah and Dor El-Gussa, on the eastern margin of the basin, are briefly reviewed (**Figs. 7.2 and 7.6**).

7.1.2.2 Melaz Shuqran Formation

This is predominantly a shale-rich unit up to 70 m thick (**Fig. 7.2**). The Melaz Shuqran Formation comprises 6 argillaceous lithofacies assigned to four facies associations (**Table 7.1**). At the most fundamental level the facies are differentiated into glacially-influenced and non-glacial facies. The former is chiefly identified by the presence of dropstones within argillaceous siltstones, interpreted as rain-out diamictites (Benn and Evans, 1998) and/or ice margin density underflows.

Non-glacial sediments are, in marked contrast, represented by heterolithic silty mudstones containing wave or current rippled sand lenses. It has been suggested that the Melaz Shuqran represents the highest relative sea-level attained during deposition of the Upper Ordovician (Klitzsch, 1981). On the Qarqaf Arch, the Melez Shuqran Shale Formation (Middle Ordovician) is locally cut out by the Mamuniyat Formation (Upper Ordovician). Similarly the Tanezzuft Shale Formation (Lower Silurian) cross-cuts both of these to unconformably overly the Hasawnah (Cambro-Ordovician) (Collomb, 1962).

7.1.2.3 Lower Mamuniyat Formation

This is the most aerially extensive part of the Mamuniyat Formation, being present over most of the studied areas (**Fig. 7.2**). It is largely synonymous, in the Tikiumit area, with the Tashgart Formation of Protic (1985) and Grubic *et al.* (1991), although elsewhere it is included within the Mamuniyat Formation (Parizek *et al.*, 1984; Radulovic, 1985). It is a predominantly fine-grained, sand prone succession with a maximum thickness of at least 100 m.

Principal features of the three outcrops facies associations (SF, SS and WS) (**Table 7.1**), include a distinctive, thick hummocky cross-stratification unit about 23 m thick, which can be correlated across much of the SE part of the Qarqaf study area, where it often forms the top of the Lower Mamuniyat Formation. This unit clearly has a sheet-like to wedge-shaped geometry, apparently thinning towards the south. Also shown are occurrences of facies association WS.

These outcrops at the base of the Lower Mamuniyat may have an elongate geometry with an erosional upper boundary. These represent deposition in a variety of mainly storm-influenced shallow marine environments, although locally, deposition appears to have occurred in sandflats and braidplains (McDougall and Martin, 1998).

7.1.2.4 Middle Mamuniyat Formation

This is a new stratigraphic subdivision in Upper Ordovician stratigraphy (McDougall and Martin, 1998). It principally occurs in the Qarqaf area and is the most varied unit in terms of facies characteristics. It is generally fine-grained, about 100 m thick, and often characterised by large-scale, syndepositional deformation features such as slumps, load balls, slides and growth faults. The Middle Mamuniyat sediments can be divided into 18 lithofacies organized into a total of 7 facies associations mostly deposited in a linked complex of unstable delta front (mouth bar, distributary channels), slope and shelf environments. Deposition also occurred, locally, in destructive delta front (foreshore/shoreface) and delta-braid plain environments (McDougall and Martin, 1998).

An unconformity, separating Middle and Lower Mamuniyat is clearly visible at outcrop (**Fig. 7.2**). Above the unconformity, there are largely scree-covered slope deposits with slumps and slides. Thin wave rippled and planar laminated layers are locally deformed. The Middle Mamuniyat is divided into silty slope (facies association SL) and wave-influenced mouth bar deposits (facies association WB) (**Table 7.1**). (McDougall and Martin, 1998).

Formation	*Facies Association*
Tanezzuft	TZb (Transgressivė sandstones) TZb (Slope deposits) TZw (Storm-dominated shelf deposits) TZs (Outer shelf deposits)
Upper Mamuniyat	BR (Braided stream deposits) BRB (Bedrock-confined braided stream deposits) BC (Basal conglomerate) EC (Ephemeral channel/interchannel deposits) CL (Clinoform deposits) CG (Gilbert delta facies)
Middle Mamuniyat	CS (Condensed sequence deposits) MSH (Muddy shelf deposits) SL (Slope) WB (Wave-influenced mouth bar) DF (Delta front) DP (Delta plain deposits) FS (Foreshore to shoreface deposits)
Lower Mamuniyat	SF (Storm-dominated sand-rich shelf) SS (Sandy shelf deposits) WS (Wave-dominated shelf/shoreface deposits) SN (Slumped sandflat sandstones) AP (Alluvial plain deposits)
Melaz Shuqran	GS (Glacially-influenced shelf deposits) SD (Non-glacial shelf deposits) GM (Subaqueous ice margin deposits) TL (Transgressive lag deposits)

Table. 7.1 Outcrop-based facies scheme for the Melaz Shuqran, Mamuniyat and Tanezzuft Formations in the Ghat/Tikiumit, Qarqaf and Dor El-Gussa Areas of the Murzuq Basin (After McDougall and Martin, 1998).

7.1.2.5 Upper Mamuniyat Formation

The Upper Mamuniyat Formation is present in all the studied areas although it is most extensive in the Ghat and southern Tikiumit (**Fig. 7.2**). In these areas the Upper Mamuniyat thickness may exceed 100 m, although elsewhere, such as the SW Qarqaf area, the average thickness is 20 m. McDougall and Martin (1998) note the well-bedded character typical of the former in the Qarqaf and Ghat/Tikiumit Arch. Also shown is the steep, irregular erosive base of the bedrock-confined braided stream facies deposits (**Table 7.1**), and large-scale trough cross-bedding. Common mud chips are also observed in the basal part of the facies unit.

The Upper Mamuniyat succession is divided into 13 lithofacies assigned to 6 facies associations mainly deposited in braid stream plain deposits, sandflat and bedrock-confined valley Locally the Upper Mamuniyat Formation also comprises discrete bodies of inclined sediment interpreted as braid-delta clinoforms and Gilbert deltas (McDougall and Martin, 1998).

7.1.2.6 Mamuniyat / Tanezzuft Formations

Chaotic sedimentation along the base of the Mamuniyat Formation is seen in the widespread slumped horizons and coarse, matrix-supported conglomerates. Near Ghat the basal conglomerate contains boulders up to 2 m in diameter. The Mamuniyat Formation is followed by the Tanezzuft Formation everywhere in the Ghat/Tikiumit Area and in the westernmost Qarqaf (**Fig. 7.2**). More to the east the Silurian sediments have been removed and the Devonian rests unconformably on Mamuniyat Formation. Erosional events at the onset of Tanezzuft Formation sedimentation generated the important buried hill traps of the NC115 oilfields (Herzog, 1997).

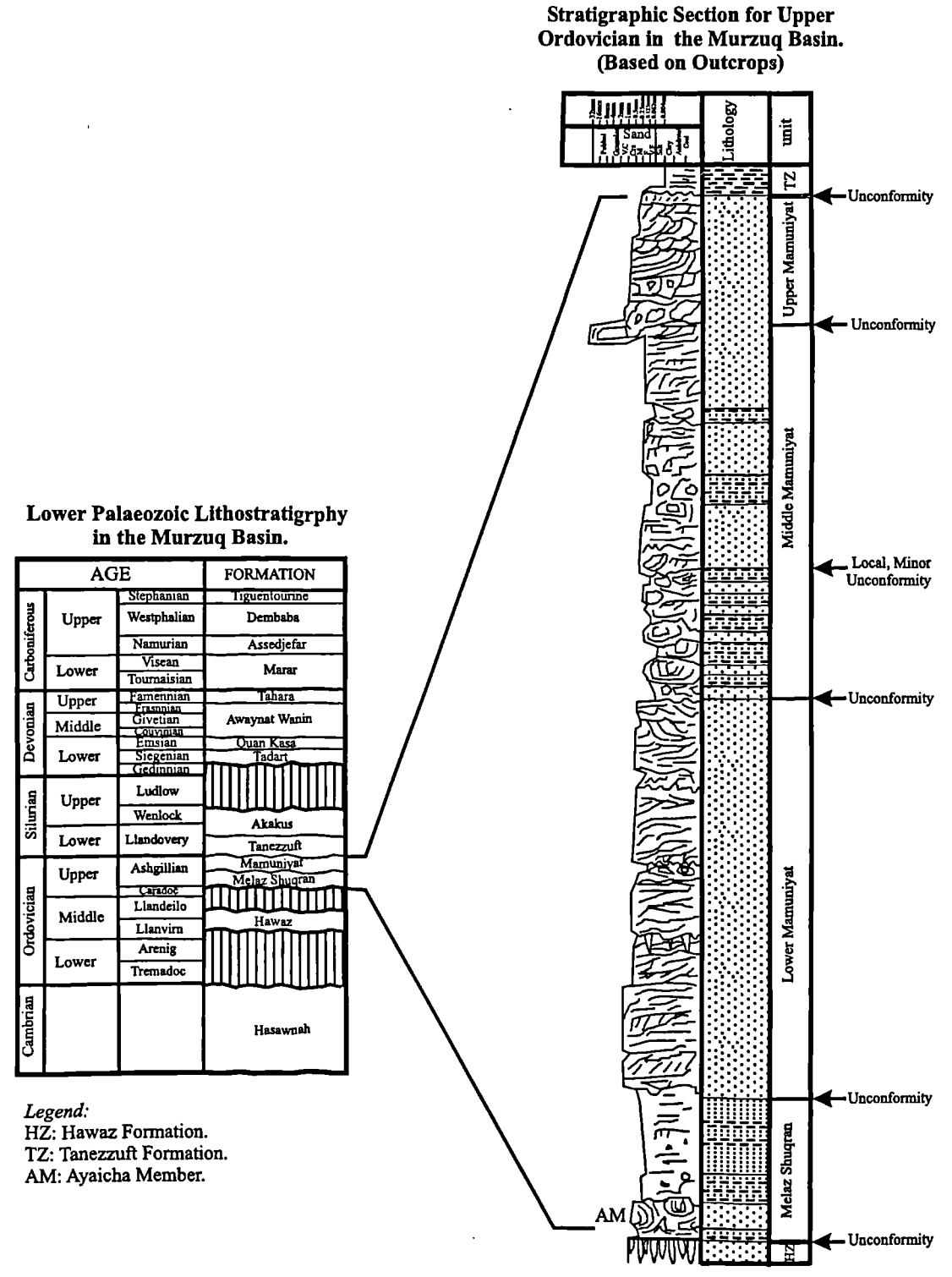

Fig. 7.2 Sedimentological summary of Upper Ordovician (Ashgillian) outcrops in the Murzuq Basin, SW Libya (After McDougall and Martin, 1998).

The Mamuniyat Formation is widespread, with thicknesses in the range 20-170 m; a regional thickening towards the Qarqaf high is noted (Pierobon, 1991). Its top part is normally in transitional contact with transgressive Silurian shales, but an unconformable upper boundary (marked by a hematite-rich layer) was reported by Klitzsch (1966). The regional thickening of the Tanezzuft Formation occurs towards the outcrop belt in the SW Murzuq Basin, where it reaches 475 m; in the subsurface it ranges from 45 m to 320 m, and the basal Tanezzuft Formation shows a gradational basal section of interbedded shales and medium- to coarse-grained sandstone, derived from reworking of the Cambro-Ordovician substratum under wave and tide action (Klitzsch, 1965, 1969).

7.1.3 Kufra Basin

7.1.3.1 Introduction

The Kufra Basin occupies a large part of SE Libya (**Fig. 7.1**). It extends into NE Chad (Erdis Basin) with further extensions into NW Sudan (Mourdi Basin) and SW Egypt. The basin has an area in excess of 400,000 Km^2 and forms an elongate NNE-SSW trending depression. The Kufra Basin is separated from the Murzuq Basin to the west by the Tibesti/Sirt Arch and from the Sirt Basin to the north by the Calanscio Arch. Its eastern limb forms the western edge of the Arabo-Nubian Shield to the east (Selley, 1997). The geological history of the Kufra Basin is very similar to the smaller Murzuq Basin in SW Libya, which recently presented Libya with its largest oil discovery for over a decade (Luning *et al.*, 1999).

Most of the hydrocarbon play elements know from the Murzuq Basin are also known to be present in the Kufra Basin: generally thick, porous Cambro-Ordovician sandstones which provide excellent potential reservoirs (**Fig. 7.3**). The Kufra Basin is bounded by four basement-high structures, namely the Tibesti Massif (including Jebal Nugay and Jebal Dohone) in the west, Jebal Aweinat Massif (including Jebal Asba) in the east, the Ennedi and Borkon mountains in the south and the Calanscio Arch (Jebal Dalma) in the north (Bellini and Massa, 1980; Turner, 1980).

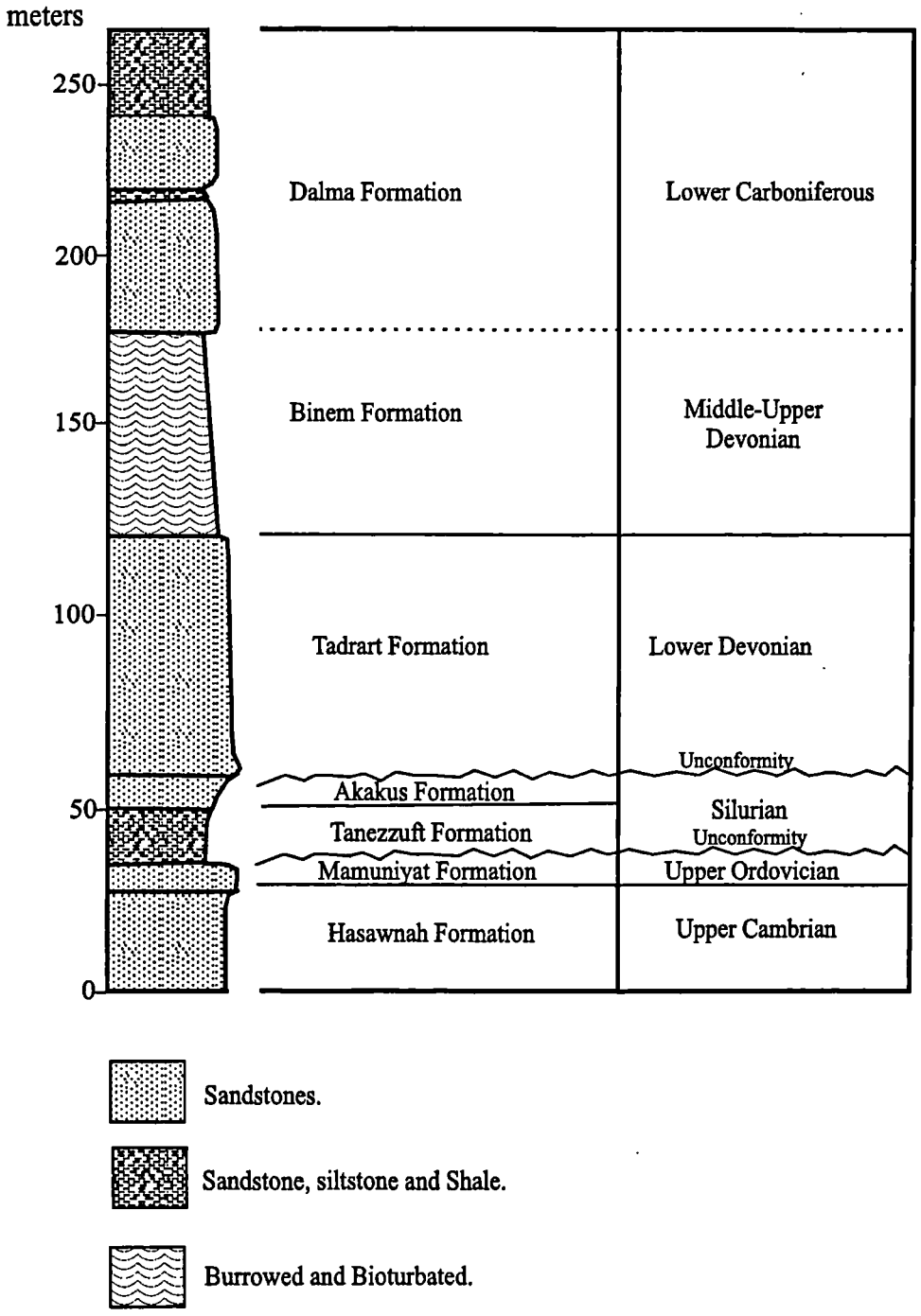

Fig. 7.3 Stratigraphic section of the Palaeozoic succession in the SE Kufra Basin (After Turner, 1980).

7.1.3.2 Sedimentological framework

The sedimentary succession in the Kufra Basin can be subdivided into eight major stratigraphic units, namely the Infra-Cambrian (Upper Neoproterozic to Lowermost Cambrian), Undifferentiated Cambro-Ordovician (=Qarqaf Group, consisting of Hasawnah, Melaz Shuqran and Mamuniyat Formations), Lower Silurian Tanezzuft Formation, Lower and Upper Silurian Akakus Formation, Lower Devonian Tadrart Formation, Middle and Upper Devonian Binem Formation, Carboniferous Dalma Formation and the Post-Hercynian Nubian Formation (Bellini *et al.*, 1991).

A detailed sedimentological field study of the Palaeozoic succession at the eastern margin of the Kufra Basin (**Fig. 7.4**) "Jebal Asba, Jebal Arkun" was carried out by Turner in the mid 1970s (Turner, 1980, 1991). However, the sedimentary rocks of the Cambrian and Ordovician age (Hasawnah and Mamuniyat Formations) remain undifferentiated in the Kufra Basin, because biostratigraphically relevant fossils are absent.

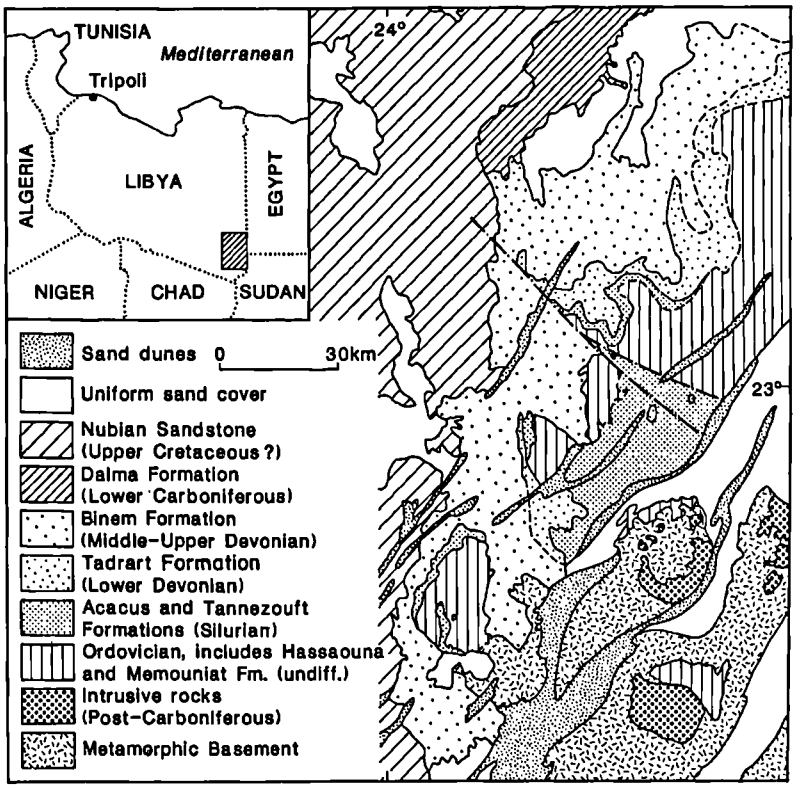

Fig. 7.4 Geological map of the eastern margin of the Kufra Basin (After Turner, 1980).

During Cambro-Ordovician times, the Kufra Basin area was dominated by braided fluvial to shallow marine sandy facies with few shaley marine intercalations (Turner, 1980, 1991; Bellini *et al.*, 1991). Such facies also prevailed in the Kufra area during later Ordovician times when major glaciation affected large parts of North Africa.

7.1.3.3 Sedimentary facies

The Palaeozoic succession at Jabal Asba, in the south-eastern part of Kufra Basin, consists of a 250 m thick sequence of clastic sediments. The sequence can be subdivided into marine shelf, shoreface and delta plain facies (Turner, 1991). The facies of the Mamuniyat outcrop in the Kufra Basin, is shoreface, gradationally overlying marine shelf deposits in a laterally persistent, coarsening-upward sequence up to 15 m thick, comprising sandstone with occasional interbeds of siltstones and silty-shale **(Fig. 7.5).**

The shoreface sands and overlying delta plain facies were not contemporaneous with one another, and it is uncertain as to whether the shoreface was attached to a delta, a strand plain or the seaward side of a barrier beach. The characteristics of these shoreface sands suggest that they may form part of a beach sequence deposited along a coastline of moderate wave energy. The shoreface sands form a coarsening-upward sequence typical of prograding shoreline models, which are normally overlain by other elements of the beach environment (foreshore, backshore and dunes).

However, the possible presence of a transgression from the north-northwest along the contact of the Mamuniyat (upper shoreface) and overlying Tanezzuft (marine shelf) Formations is consistent with the results of Pierobon (1991) in the Murzuq Basin, SW Libya, where transgressive-regressive events have been correlated with the sea-level curves of Vail *et al.* (1977) (Turner, 1991).

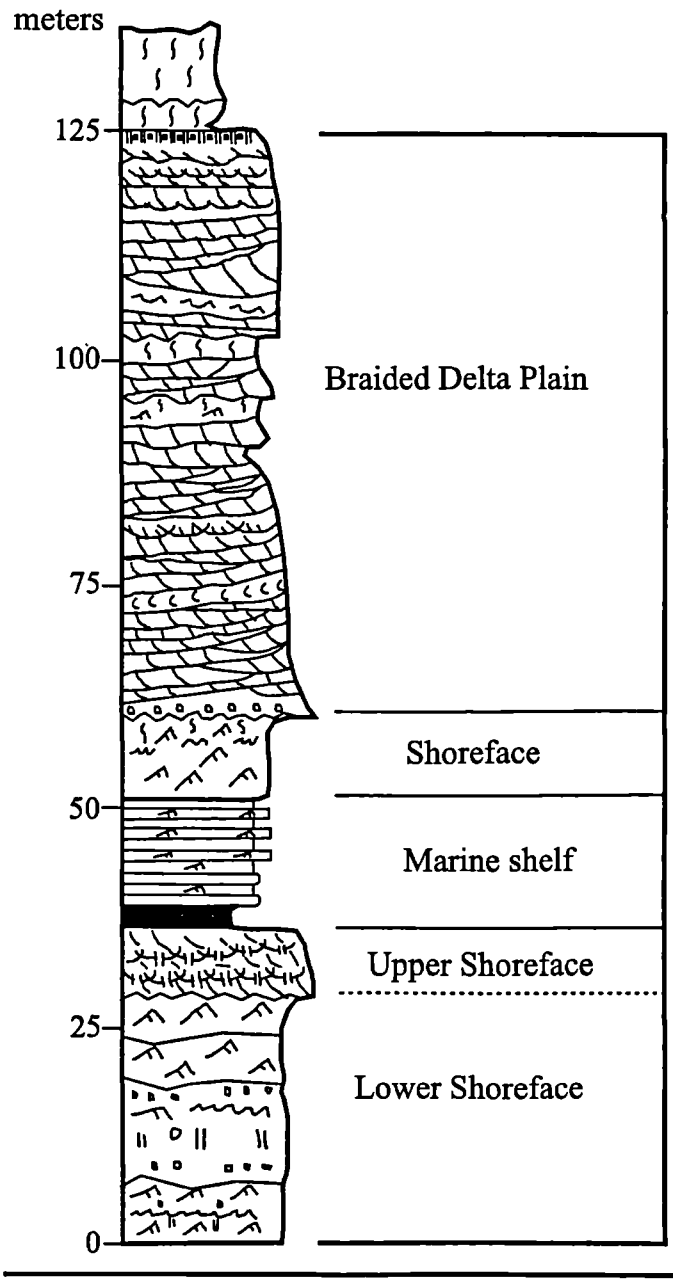

Fig. 7.5 Measured section through the Palaeozoic succession at Jabal Asba, Kufra Basin, showing the Silurian marine shelf deposits and the underlying Ordovician shoreface sands. The boundary between them may define transgressive events (After Turner, 1980).

7.1.4 Ghadames Basin

7.1.4.1 Introduction

The Ghadames Basin is a large intra-cratonic basin, covering parts of Algeria, Tunisia and Libya, and extending over 350,000 Km^2 (**Fig. 7.1**). The basin contains up to 6000 m of Palaeozoic and Mesozoic sediments. It is bounded to the north by the Dahar-Naffussah High, to the south by the Qarqaf Arch (Libya) and the Hoggar Shield, and in the west it is bounded by the Amguid-Elbiod Arch (Echikh, 1998).

The eastern boundary is not well defined, being overlapped by the western flank of the younger Sirt Basin (Boote *et al.*, 1998). The Ghadames Basin is not well known (outcrop areas and subsurface strata), and the basin stratigraphy has only now been established by Bellini and Massa (1980). The Ghadames Basin was affected by the Caledonian Orogeny, and in the south the Qarqaf Arch separates it from the Murzuq Basin. The northern part of the basin was uplifted during Hercynian folding, followed by subsidence during the Early Mesozoic.

The Ghadames Basin is mainly filled by Palaeozoic sediment overlain by a relatively thin Mesozoic-Tertiary cover. Most of the Palaeozoic sediments consist of sandstones deposited in continental, transitional and marine environments. Palaeozoic sediments are thickest in the centre of the basin but thin gradually toward the southern margin of the basin which flanks the Qarqaf Arch (Hammuda, 1980).

7.1.4.2 Sedimentology

Sedimentological studies of the Ghadames Basin are few, particularly Cambro-Ordovician outcrop studies, compared with the Murzuq and Kufra Basins. The formations of the Cambro-Ordovician within the Ghadames Basin, were defined in 1959 by Massa and Collomb (1960) in the southern part of the Basin (Jabal Fazzan area). These definitions have been published in the International Stratigraphic Lexicon (1960).

The Qarqaf Group is composed of 4 main lithostratigraphic Formations that have not been dated. Due to considerable lateral facies change correlation proved to be impracticable. As a general rule, the facies change from south to north (from a predominantly sandstone facies of "Fazzan type" to a sandstone of "Tripolitanian type") (Collomb, 1962).

In the Ghadames Basin, the various units of the Cambro-Ordovician form a rather thin sedimentary section, which has been deposited on a shelf several tens of thousands of square kilometres in area. Based upon the sections measured in Jabal Fazzan, formations of the same age outcropping in southern Libya can be identified (Mennig and Vittimberga, 1962). The Mamuniyat "Ashgillian" sandstones have considerable extent in North Africa (Beuf *et al.*, 1971). They show large glacial retreat preceding the Silurian marine transgression (Collomb, 1962; Klitzsch, 1981). The average thickness of the Mamuniyat outcrop, Upper Ordovician "Ashgillian" in the Ghadames Basin is ≈ 150 m (Havlicek and Massa, 1973).

The Mamuniyat Formation outcrops over a very large area in the Fazzan, Murzuq and Kufra Basins. It unconformably overlies, with a break in sedimentation, the Middle Ordovician or the Cambrian (Massa and Collomb, 1960; Collomb, 1962). In the Ghadames Basin, the available data on the Mamuniyat Formation, suggests a similar facies distribution pattern to that established in Algeria, passing from sandy periglacial deposits in the south, close to the Qarqaf uplift, to a marine shaly sequence in the central and northern parts of the basin (Echikh, 1998).

7.2 Comparison between Mamuniyat outcrops of the Murzuq, Kufra and Ghadames Basins

The Murzuq, Kufra and Ghadames Basins represent intracratonic basins of Libya and North Africa. They are sedimentary basins of prevailing marine facies, affected by recurrent continental influences which are more frequent in the Kufra basin. The lowermost Palaeozoic succession in the Murzuq, Kufra and Ghadames Basins in-fill topography eroded into a variety of metasedimentary rocks (Bellini and Massa, 1980; Pierobon, 1991).

The Upper Ordovician sequence of the Murzuq, Kufra and Ghadames Basins contains laterally discontinuous conglomeratic sandstones, pebbly and sandy mudstones, and mudstones (Mamuniyat and Melaz Shuqran Formations). In different areas, these are interpreted as fluvial or fluvial-glacial (Biju-Duval, 1974) to fluvial-marine with dropstones (Pierobon, 1991), and as glacial tills (Klitzsch, 1981) or periglacial deposits (Collomb, 1962; Beuf *et al.*, 1971). Either regional relative base level fell so much, that all these erosion products were transported beyond existing outcrops and wells, or the erosion products are represented in part by some of the heterogeneous and contorted Ashgillian sediments of the Mamuniyat Formation, which are usually interpreted as periglacial and glacial deposits (Bellini and Massa 1980; Pierobon, 1991).

Regionally, Mamuniyat outcrops seem to be present throughout the whole of the Murzuq Basin, SW Libya, except for eastern areas where data from outcrops (eastern Qarqaf, Dur Al-Gussah) indicate its absence. Overall, this formation is relatively simple and monotonous and characterized by rapid thickness variations range between 50 and 150 m, which makes it very prominent and easy to recognize throughout the area. In fact the Mamuniyat outcrops represent the second glacial-marine cycle of the Palaeozoic in the Murzuq Basin; a periglacial depositional setting is interpreted based on ecological grounds (Havlicek and Massa, 1973), sediment texture (diagenetic kaolinite) and structure (water-escape structures indication of perma-frost?) (Pierobon, 1991).

In the Kufra Basin the Upper Ordovician Mamuniyat outcrops are represented by approximately 150 m, of erosively-based, medium to coarse-grained reddish-brown sandstone containing low angle festooned trough cross-bedding. During the Mamuniyat there was a renewal of sedimentation in a continental environment with deposition of fine conglomerates, and sands with marked cross-bedding, which filled incised channels after ice withdraw. Between the end of this glacial epoch and before the deposition of the Mamuniyat Formation, a brief marine ingression (probably shallow water and lagoons) laid down silt and sandstone with frequent *Arthrophycus* (Bellini and Massa, 1980).

Mamuniyat outcrops of the Ghadames Basin have been identified throughout a large part of NW Libya, and the entire thickness is 150 m. It is characterized by quartzic sandstone of the second glacial-marine cycle (Massa and Collomb, 1960). Furthermore, the distribution of the Mamuniyat outcrop in Ghadames Basin is poorly known comparing with Mamuniyat outcrops within the Murzuq and Kufra Basins. In the Ghadames Basin, the Upper Ordovician Mamuniyat Formation unconformably overlies the Middle Ordovician or the Cambrian (Collomb, 1962).

7.3 Depositional model of the Mamuniyat Formation NC115 Concession, NW flank of the Murzuq Basin

The sedimentological and stratigraphical characteristics of the Upper Ordovician (Ashgillian) Mamuniyat Formation, have been described on a bed by bed basis throughout A, B and H-Fields within the main part of the NC115 Concession area (discussed in Chapters Two and Five). Three main representative facies associations including ten facies profiles of the Mamuniyat Formation (Upper, Middle and Lower Members), compiled from these 12 exploration and development oil wells across the concession area, have been distinguished based on sedimentary structures, geometric relationships and biogenic features (Fello and Turner, 2001a) (**Table 2.3**).

Throughout A, B and H-Fields, the repetition of similar facies suggests a recurring pattern of similar depositional processes and environments. This is attributed to coastline interaction with a braided alluvial plain, which fed in sediment from the Ghat/Tikiumit Arch to the southwest of the study area (**Fig. 7.6**).

The streams were probably short, high gradient types with a high bed load/suspension load ratio lying in close proximity to drainage divides. The depositional history of the Mamuniyat Formation can be related to activity of the fluvial systems followed by marine transgressive events (Fello and Turner, 2001b). During active fluvial input the depositional environments prograded seaward, either due to a switch in the depositional loci or increase in regional tectonism. The sediments of the Mamuniyat Formation in NC115, show the following characteristics:

1) Tabular and trough cross-bedding are a prominent feature of the sandstone;
2) Fining-upward sequence of siltstone were observed in the sandstone;
3) Mud rocks are rare and generally thin;
4) The fine- to medium-grained sandstones in the Lower Member of the Mamuniyat Formation record a shallowing of the depositional environment and may represent channel-fill sediments;
5) The burrowed horizons may reflect the activity of terrestrial burrows or alternatively the stream may have impinged on a marine shoreline with the burrowed sand recording marine incursion into the distal ends of the channels enabling marine organisms to inhabit temporarily the fluvial system (Turner, 1980); and
6) The Upper Ordovician of the Mamuniyat Formation illustrates a typical seaward progradation and basinward-thinning of a clastic wedge to the northeast and shows changes from fluvio-continental to marginal marine and marine-neritic environments. Significant thickness variations reflect strong tectonic control on sedimentation (Thomas, 1995).

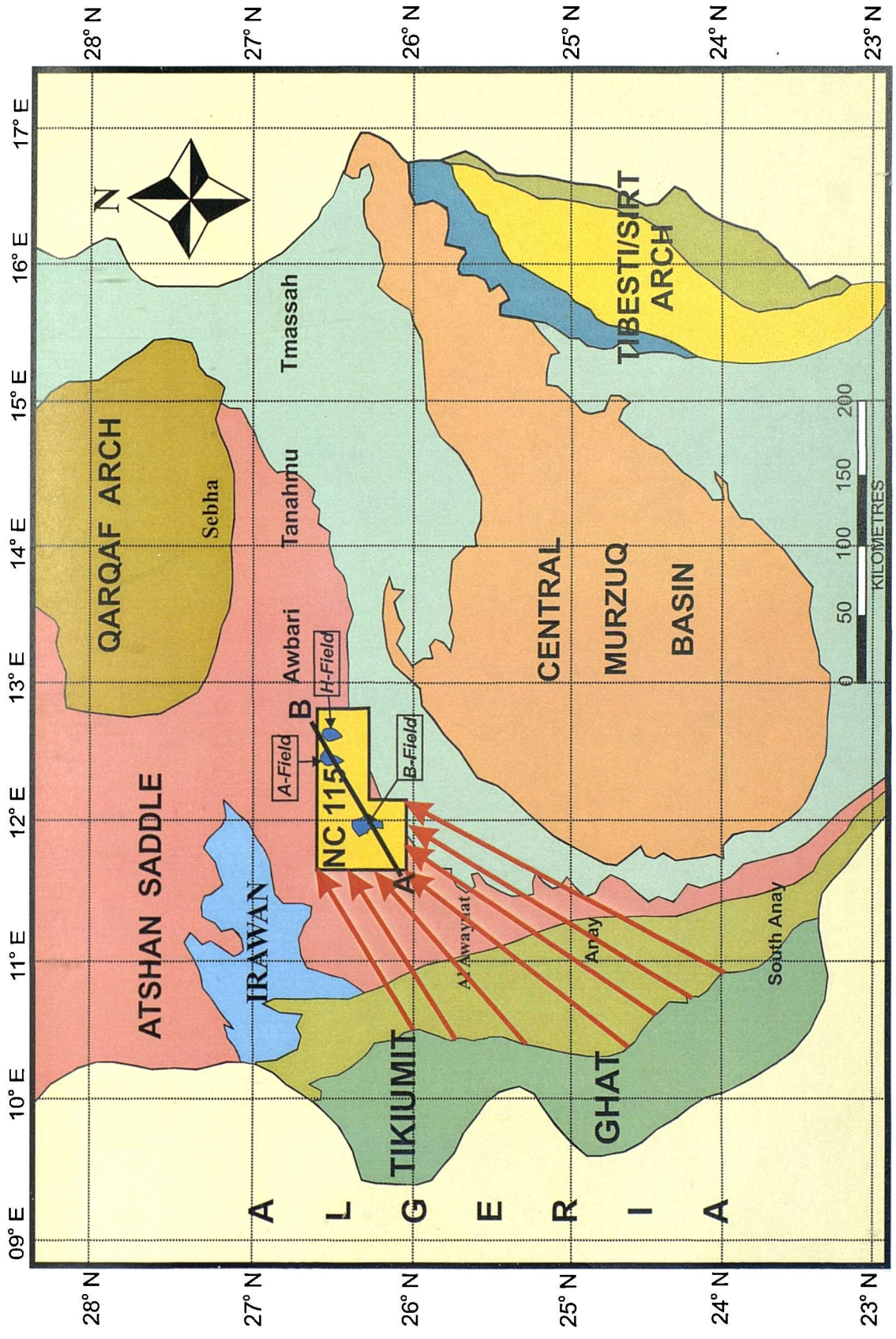

Fig. 7.6 Geological map of SW Libya showing the Ghat/Tikiumit Arch source area to the SW of NC115 Concession.

The geometry of the Mamuniyat deposits and their sedimentary structures, together with regional facies trends all suggest that the Mamuniyat reservoir sandstones were derived from a nearby, tectonically active, granitic basement source terrain, which was most probably the uplifted Ghat/Tikiumit Arch to the SW of NC115 Concession (Fello and Turner, 2001a).

Furthermore, the Mamuniyat sandstones are thickest in the southwest (B-Field) and fine towards the northeast (A and H-Fields) of the study area. This change, concomitant with a decrease in thickness of the sandstones, provides evidence of the palaeocurrent trend and their more distal location relative to the source area. The relation between palaeocurrent patterns and depositional environments is illustrated in **Figure 7.7**.

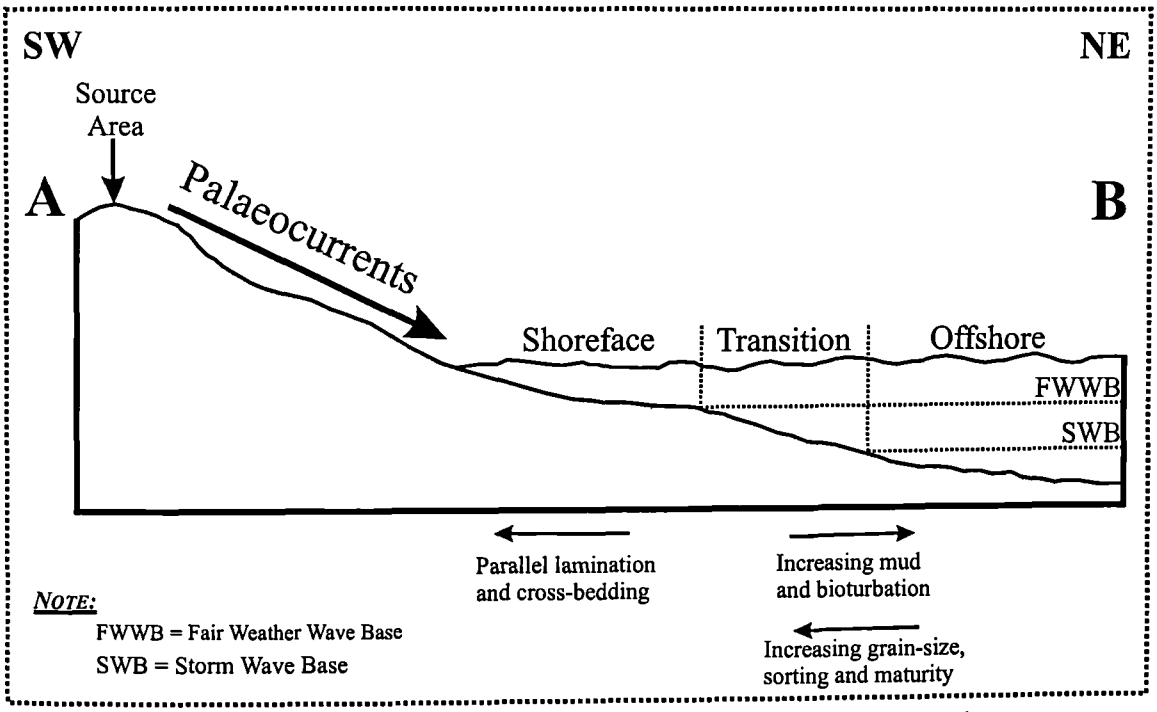

Fig. 7.7 Schematic cross-section along A-B in figure 7.6 showing changes in facies associations, textures and sedimentary structures in NC115 Concession, NW flank of the Murzuq Basin, SW Libya.

7.4 Sedimentological model of the Mamuniyat Formation

Facies analysis and modelling suggest that the Mamuniyat Formation was deposited by perennial, high energy, low sinuosity braided streams in which vertical channel aggradation and rapid channel shifting were important depositional processes (Vos, 1977; Turner, 1983). The rivers drained an extensive alluvial plain, which may have been built on to the (proximal and distal) slopes of an alluvial fan complex to the southwestern part of the NC115 Concession (**Fig. 7.8**).

Throughout deposition of the Mamuniyat Formation, coarsening-upward sequences were produced by shifts in the depositional system. Shifting is a function of slope and sediment input, which is in turn controlled by gradient changes providing that climate and run-off are constant (Blatt, Middleton and Murray, 1972).

In view of the thickness of the Mamuniyat sandstones, the lateral extent and stacking of coarsening-upward sequences and the abrupt vertical change from braid plain to marginal marine and shallow marine environments, tectonism was the major control on sedimentation (Fello and Turner, 2001b). Sediment composition and grain-size parameters, together with regional facies patterns all suggest that the Mamuniyat sandstones were derived from a nearby, tectonically active, granitic basement source terrain, identified here as the Ghat/Tikiumit Arch some 150 km to the SW of NC115 Concession, and that the braided streams moved to the NE.

The depositional model for the Upper Ordovician (Ashgillian) Mamuniyat Formation is represented as a series of three interrelated facies associations as shown in **Figure 7.8**. The interpretation of the facies and facies association of the Mamuniyat sandstones is consistent with a braided alluvial plain and shallow marine depositional model. Repetition of fluvial and marine facies is attributed to interaction of the fluvial and a marine water environment across a NW-SE oriented coastline, subjected to frequent storms (Fello and Turner, 2001a).

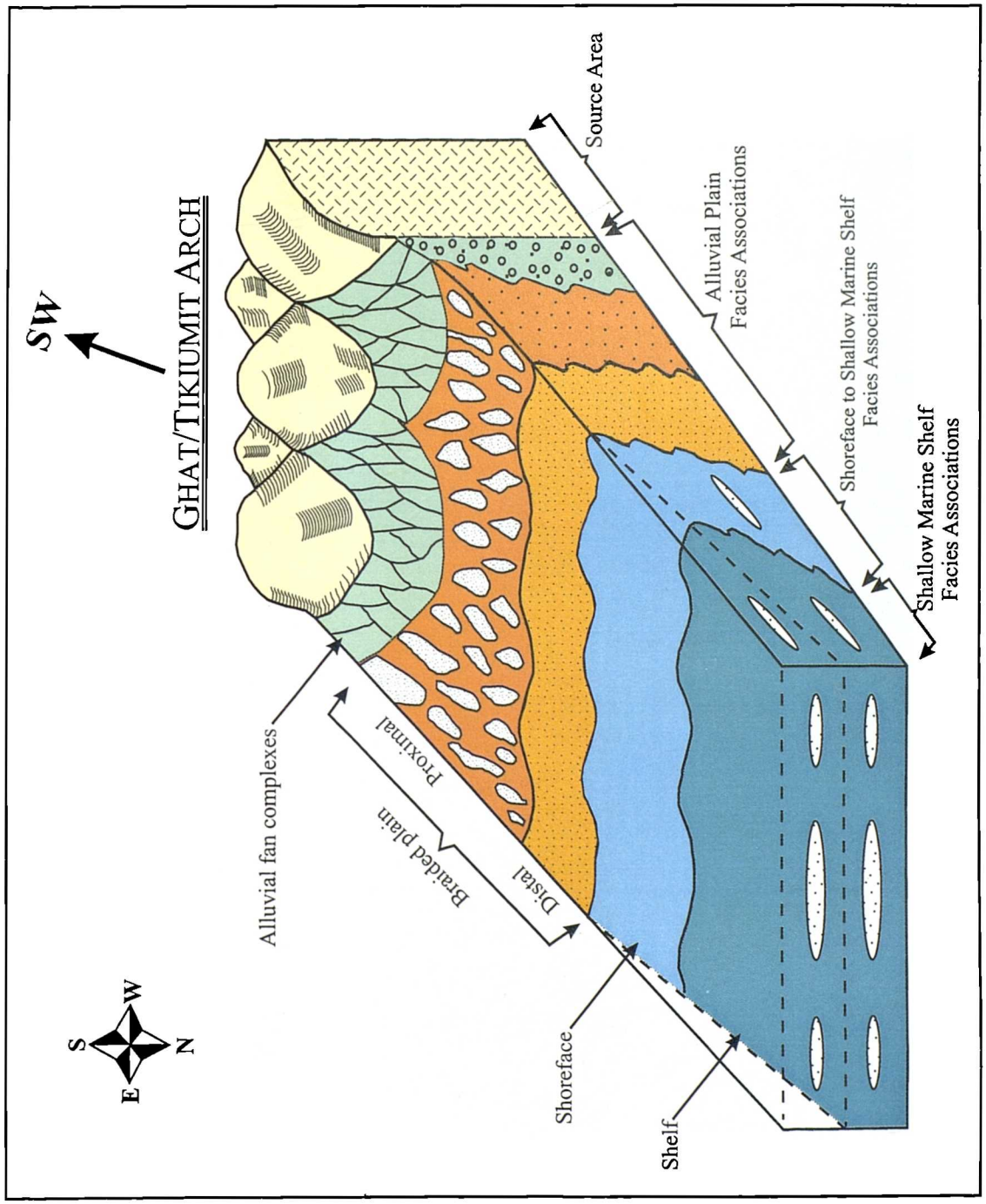

Fig.7.8 Schematic depositional model of the Mamuniytat Formation in NC115 Concession.

The abundance of fluvial cross-beds in the Upper Mamuniyat Formation is attributed to regional tectonism (Turner, 1980). In the study area, sediments eroded from the rising mountain chain (*e.g.* Ghat/Tikiumit Arch) were deposited along the basin margin as alluvial fan complexes (**Fig. 7.8**). The presence of braided systems feeding the shoreline and dominance of fines suggests that the climate was most probably humid (discussed in Chapter Three) (**Fig. 3.8**). Periodic, possibly fault controlled uplift, and base level changes, led to basinward progradation of the braided fluvial systems followed by marine transgressive events from the NE, across a marginally-influenced shallow marine shelf (Fello and Turner, 2001a). In summary the depositional model for the Mamuniyat Formation, in NC115 Concession, is as follows:

1) The abrupt vertical facies and facies associations changes of the Mamuniyat sequence from braided fluvial stream sandstones that pass basinwards, to the northeast, into marginal marine and shallow water marine shelf sediments dominated by sandstone, tectonism was probably the major control on sedimentation. Without this control the depositional system will migrate sourceward (onlap) and build fining-upward sequence as gradients and sediment input decline (Turner, 1983);

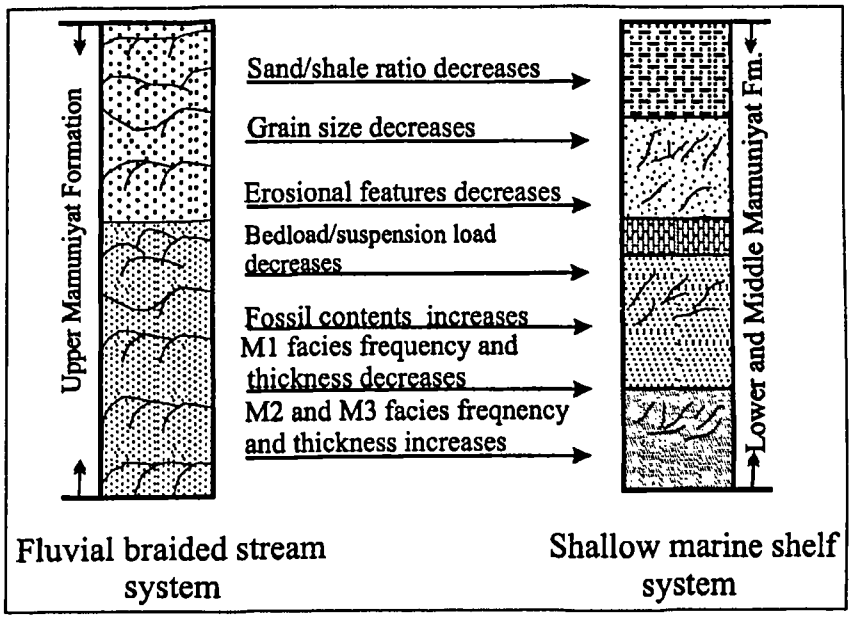

Fig. 7.9 General characteristics of the fluvial and shallow marine facies within the Mamuniyat Formation, NC115 Concession.

2) The Mamuniyat sediments are related to a northeasterly prograding, coarse-grained, braided fluvial marginal marine system (B-Field), and a fine- to medium-grained, shallow marine shelf system (A and H-Fields) **(Fig. 7.9)**; and

3) The fining-upward sequences of siltstone within the coarse grained sandstones were probably produced by shifts in the depositional system.

7.5 Upper Ordovician glaciation and possible effects

In the study area the distribution of the Mamuniyat reservoir rocks in the subsurface has been subdivided into three members. The Lower member comprises locally developed fine- to medium grained sandstones that were deposited in a shallow-marine environment. It is that sedimentation was a possible response to glacial melting and isostatic crustal uplift, since the underling Melaz Shuqran Formation is capped by a subglacial erosion surface (Bellini and Massa, 1980) and contains tillites and striated basal channels. These are absent in the Lower Mamuniyat member. The Middle member is characterized by offshore siltstone overlain by nearshore wavy and hummocky cross-stratified sandstone. The Upper member consists of coarse to very-coarse grained sandstones that were deposited by a braided stream system draining an alluvial plain, dipping towards the NE.

During Ordovician times, the northern borders of the Sahara belonged to a large marine platform located at high latitudes. Consequently, any sizeable local or global large sea-level variation had dramatic repercussions on these fairly shallow environments (Beuf *et al.*, 1971). No true glacial-material has been preserved in the Mamuniyat Formation within NC115 Concession, because either the fall in sea-level, induced by glacio-eustatic conditions, resulted in an emergence of land or post-glacial uplift of part of the Ghat/Tikiumit Arch to the SW of the study area resulted in erosion (Fello and Turner, 2001b). Tectonically induced uplift due to fault reactivation is less likely, because there is no evidence within the Murzuq Basin of tectonism at this time. This is consistent with most other Palaeozoic basins in Libya (Pierobon, 1991).

Although direct evidence for glaciation is seen in most of the Palaeozoic basins in Libya, it is absent on the northwest flank of the Murzuq Basin in NC115 Concession. This may be due to the fact that the ice was sourced from the southwest, and the study area was protected from direct glacial influences by the topography of the Ghat/Tikiumit Arch. Possible indirect indications of glacially influenced sedimentation include: persistent high sediment flux during deposition of the Lower Mamuniyat Formation, cyclic patterns of sedimentation, a high energy discharge fluvial channel in the Upper Mamuniyat Formation and sequence stratigraphic indications of rapid relative sea-level fluctuations. These features could be related to glacial advances and retreats, glacioeustatic sea-level changes and glacial ice isostatic effects.

7.6 Summary

Regional log correlations and core description of the Mamuniyat Formation have identified ten facies, based on their lithological, sedimentological and palaeontological characteristics. These facies have been grouped into three different facies associations. Based on facies and facies association analysis of the Mamuniyat Formation in the SW part of the study area (B-Field) the Mamuniyat is interpreted to have been deposited on a braided alluvial plain and shallow-marine shelf (A and H-Fields). It shows a coarsening-upward trend as a result of seaward progradation and basinward-thinning to the northeast accompanied by a change from braided fluvial systems and marginal marine to shallow-water marine shelf environments. Significant thickness variations reflect the strong tectonic control on sedimentation. Laterally the Mamuniyat Formation also shows systematic changes in grain-size, lithology and sedimentary structures. These changes are fundamentally linked to the gradient decrease in passing outward from the source terrain, with concomitant decrease in stream capacity and competence. Although the sedimentary properties change continuously away from the basin edge, the depositional setting of the Mamuniyat Formation can be divided into an upper braidplain (proximal), a lower braidplain (distal) and a shallow-marine shelf and nearshore marine environment. Although deposition may have been strongly influenced by the late Ordovician glaciation, there is no direct evidence for glacial condition within the study area.

CHAPTER 8

CONCLUSIONS

CONCLUSIONS

8.1 Introduction

The Murzuq Basin forms one of a series of Palaeozoic intracratonic sag basins on the Saharan Platform. The structural fabric, imparted during the late Proterozoic Pan-African orogenic event, has played an important role in controlling the subsequent structural and stratigraphic evolution of the basin. The basin covers an area of some 350,000 km^2, is sub circular in shape and clearly visible on satellite photographs of SW Libya. Repsol NC115 Concession, which lies on the northwestern flank of the Murzuq Basin, some 1,330 km southwest of Tripoli, covers an area of 25,850 km^2 (Selley, 1997).

The main focus of this study is the Upper Ordovician (Ashgillian) Mamuniyat Formation, which is the primary reservoir target in three oilfields: A, B and H within Repsol Concession area NC115 (**Fig. 1.4**). Early Palaeozoic tectonism effectively controlled the distribution of the Upper Ordovician hydrocarbon reservoirs with the main source and seal being the Lower Silurian Tanezzuft shale (Hot Shale), which onlaps early-formed fault blocks. A problem with the Mamuniyat Formation is the location of the sediment provenance, and the relationship and controls on sediment flux and depositional systems, due to inadequate subsurface and outcrop data.

This chapter summarises the research presented in chapters 1-7, and represents the results of an NC115 Concession-wide study, which includes data from three oilfields and a number of exploration wells in the El-Sharara Field. This study investigates the petrology, textural, sedimentology and sequence stratigraphy of the Mamuniyat reservoir interval drilled by Repsol Oil Operations. The Mamuniyat reservoir comprises quartzitic and conglomeratic sandstone deposited in braided fluvial and marginal marine to shallow marine shelf environments throughout Ashgillian times (Fello and Turner, 2001a).

8.2 Discussion

Previous work on the lowermost Palaeozoic succession in this area, carried out by Klitzsch (1981) and Pierobon (1991), recorded over 170 m of sandstone in the Mamuniyat Formation. In the study area, the thickness of the Mamuniyat reservoir sandstones between A, B and H-Fields is laterally very variable. This is attributed to tectonic activity, source area uplift, base level change, variable sediment flux and accommodation space. The Mamuniyat Formation shows an increase in marine influence toward the northeast. It is dominated by a proximal-distal braided plain in the southwest giving way to fluvial and marginal marine to marine shelf deposits in the northeast. Poor correlation within the Mamuniyat Formation is a function of the complex stratigraphy in response to a series of rapid changes in sea-level and corresponding drainage incision. Palaeocurrent was from the SW, probably from the uplifted Ghat/Tikiumit Arch to the southwest the concession area (Fello and Turner, 2001b).

The Mamuniyat Formation in NC115 Concession is an extremely sand-rich deposit, which can be tentatively subdivided into three facies associations. Each facies association has a distinctive character based on its component sedimentary facies. When the sedimentological character of each facies association is considered relative to adjacent facies association and viewed in the wider context of the geographical and climatological conditions prevailing during Upper Ordovician times, it is possible to explain the changing character of the Mamuniyat Formation as it evolved through time.

Petrographic study of the samples from the three oilfields throughout the Mamuniyat Formation shows that the sandstones in the Upper and Lower Members on the northwestern flank of the Murzuq Basin have good reservoir quality and are potential hydrocarbon reservoirs. Good reservoir quality is present in most wells of the study area due to early quartz cementation, which in turn preserved intergranular volume, and the diagenetic dissolution processes that have enhanced porosity. Microporous authigenic clays are also present in many samples but bitumen envelopes and kaolinite clay booklets occlude microporosity in some samples.

The petrography and diagenesis of the Mamuniyat Formation defines two groups in terms of feldspar and clay content. The A-Field can be assigned to the first group in that feldspar grains are completely absent. A second group containing traces of feldspar is present in a few samples from the B-Field particularly B3 and B8-NC115. Feldspars are only present in the H-Field, in well H5-NC115 (**Table 3.3**).

8.3 Results of Study

This study of the Mamuniyat sandstone shows that:

- The Mamuniyat Formation can be subdivided into Upper, Middle and Lower Members, based on textural properties, sedimentological characteristics and sequence stratigraphic analysis (gamma-ray profile);
- In general, the Upper Ordovician Mamuniyat reservoir is described as predominantly massive sandstones with irregular intercalations of siltstone. The sandstones are fine- to coarse-grained, with weak to strong fracturing. The fractures are mainly vertical or slightly inclined;
- The detrital mineral components are monocrystalline quartz with subordinate polycrystalline quartz, rock fragments, heavy minerals, kaolinite and extremely rare feldspar;
- The average total porosity of the Mamuniyat Formation for A, B and H-Fields is 18.02% based on thin section analysis. No permeability analysis of these samples has been carried out, and permeability data are not currently available;
- The Mamuniyat Formation is a regressive sequence composed of a massive, cross-bedded sandstone unit, with occasional high percentages of kaolinite matrix, which locally degrades reservoir porosity from good to very poor. There is a good correlation between kaolinite clay and feldspar, in that kaolinite clay is more abundant where feldspar is rare to absent. This suggests that the clays are derived from the breakdown of the feldspar, and that the feldspar content of the sandstones was originally higher;

- Compositional data indicates that the sandstones in the three oilfields were derived from a similar parent rock, but with differences in modal composition, textural attributes and porosity between the Lower, Middle and Upper Members of the Mamuniyat, which is attributed to temporal variations in source area uplift, base level change, sediment flux and accommodation space;
- The reservoir quality of the Mamuniyat Formation is good- to very good, particularly in the Upper Member and upper part of the Lower Member;
- Petrographic data shows that the Mamuniyat sandstones can be classified mainly as sublitharenites, with some quartz arenites and litharenites;
- Laterally, the Mamuniyat Formation within A, B and H-Fields shows changes in grain-size, lithology, and sedimentary structures. These changes are fundamentally linked to the gradient decrease and decrease in stream capacity and competence;
- Facies analysis of the Mamuniyat Formation is consistent with a braided alluvial plain and shallow marine depositional model. Repetition of fluvial and marine facies is attributed to interaction of the fluvial and marine environments across a NW-SE coastline with episodes of progradation interspersed with transgression;
- The Mamuniyat Formation shows (coarsening-upward trend), seaward progradational and basinward-thinning (clastic wedge) to the northeast accompanied by a change from fluvio-continental to marginal marine and marine-neritic environments. Significant thickness variations reflect strong tectonic control on sedimentation;
- The sedimentary properties change continuously away from the basin edge, enabling the depositional setting of the Mamuniyat Formation to be divided into an upper braid plain (proximal), a lower braid plain (distal), a nearshore environment and shallow marine shelf;

- The Mamuniyat sandstones were derived from a nearby tectonically active granitic basement source terrain, which was most probably the uplifted Ghat/Tikiumit Arch, which is only 150 km to the southwest of the Concession area NC115;
- The NC115 Concession is unlike other Palaeozoic basins in Libya, and there is no direct evidence of glacial influence on deposition during the Ordovician time;
- In the Mamuniyat Formation, trace fossils previously thought to provide evidence of marine conditions, have been shown to be present in fluvial deposits, and the straight-burrow variety of *Cruziana* has been tentatively identified as being characteristic of non-marine and restricted marine environments;
- Diagenetic cement is mainly in the form of quartz overgrowths, local calcite and clay matrix, all of which have reduced the porosity except in, the coarser-grained Upper Member of the Mamuniyat Formation;
- Saddle dolomite occurs as a pore-fill, mainly within secondary intergranular pores, or less commonly it replaces detrital feldspar and quartz within the Lower Mamuniyat sandstone reservoir. It occurs within the oil zone, particularly within Lower Mamuniyat Member (*e.g.* H5-NC115) at depth 1501 m (4922.75 ft), suggesting that it formed before the introduction of hydrocarbons;
- The Upper Ordovician deposits of the Mamuniyat sequence can be subdivided into transgressive, highstand and lowstand systems tracts; and
- The sequence stratigraphy of the Mamuniyat Formation throughout El-Sharara Field, shows the Lower Mamuniyat within both A, B and H-Fields, is easier to correlate using wireline logs than the Upper and Middle Members of the Mamuniyat Formation, which only occur in the B-Field.

8.4 Recommendations for future work

The author has attempted to build an integrated geological model of the Mamuniyat Formation by using textural and petrology analysis, facies analysis and sequence stratigraphy with a review to supporting the exploitation and exploration work in NC115 Concession, and in other concessions located in the northwestern flank of the Murzuq Basin. The results of this research suggests that more work needs to be done in future along the following lines:

- More detailed study of the biostratigraphic and palaeontology database in order to improve the regional biostratigraphy and correlation for the entire Palaeozoic, particularly during Upper Ordovician time. This may help to more precisely distinguish between fluvial and shallow marine elements of the Mamuniyat Formation;
- Extend the work lower down in the succession to include the Upper Ordovician (Caradocian) Melaz Shuqran and Middle Ordovician (Llandeilian/Llanvirnian) Hawaz Formations, and try to established more precisely the age relationship with the Upper Ordovician (Ashgillian) Mamuniyat Formation;
- Establish a detailed correlation between the El-Sharara Field and nearby outcrops of the Mamuniyat sandstone. Such a comparison would be very useful in order to understand and distinguish the geology of the El-Sharara Field sediments and to make predictions about any economic prospects in adjacent areas around NC115 Concession;
- More detailed study of sedimentary petrology, including heavy mineral analysis to try and establish whether the Ghat/Tikiumit Arch was exposed or covered during Upper Ordovician times. This may also help to determine whether the source area was tectonically active at this time, and whether the sediments were recycled or not;

- Extend the work outside the boundary of NC115 towards the southwest and northeast to try and establish sequence stratigraphic and lithofacies relationships (proximal, distal and marine facies equivalents);
- Permeability studies are required to confidently delineate Mamuniyat reservoir permeability fairways for oil exploration, especially throughout Upper and Lower Mamuniyat sandstones within A, B and H-Fields;
- Further detailed study of the finer-grained heterolithic claystone facies (Radioactive shale) throughout the Middle Member of the Mamuniyat Formation within B-Field could be useful in order to refine environmental interpretation. This may also yield more palaeontological evidence of the age of the sediments;
- More detailed study of the clay minerals and geochemical analysis is needed to define the nature of sediment processes operating at this time;
- The author has recommended on the basis of this study that additional wells should be drilled in a more proximal location close to Ghat/Tikiumit Arch (*i.e.* to the SW B-Field). This will be provide additional details on the depositional environments and sequence stratigraphy of the Mamuniyat Formation in more proximal locations where similar and possibly better reservoir sandstones to that in B-Field are likely to occur; and
- Combined well log correlation and seismic interpretation (particularly 3D) along regional key lines in the El-Sharara Field, could help to establish a more complete picture of the succession in the study area and the northwestern flank of the Murzuq Basin.

REFERENCES

REFERENCES

ADAMS, A. E., MACKENZIE, W. S. AND GUILFORD, C., 1984. Atlas of sedimentary socks under the microscope. William Clowes (Beccles) Ltd. London, 104 pp.

ADAMSON, K. R., 1999. Evolution of the Murzuq Basin, Southwest Libya and surrounding region during the Devonian. Ph.D. Thesis, University of Wales, Aberystwyth, UK, 231 pp.

ADAMSON, K., GLOVER, T., FITCHES, B., WHITTINGTON, R. AND CRAIG, J., 1997. Controls on sequence development in Lower Devonian sedimentary rocks of the intracratonic Murzuq Basin, Southwest Libya. BSRG, 36th annual meeting University of Liverpool (20th – 22nd December 1997).

AHMADI, Z. M., 1997. Sequence stratigraphy using wireline logs from the Upper Jurassic of England. Ph.D. Thesis, University of Durham, UK, 351 pp.

AINSWORTH, R. B. AND CROWLEY, S. F., 1994. Wave-dominated nearshore sedimentation and "forced" regression: Post-abandonment Facies, Great Limestone Claystone, Stainmore, UK. *Geological Society of London,* Vol. **151**, P. 681-695.

ALLEN, J. R. L. AND BANKS, N. L., 1972. An interpretation and analysis of recumbent-folded deformed cross bedding. *Sedimentology*, Vol. **19**, P. 257-283.

ALLEN, J. R. L. AND NARAYAN, J., 1964. Cross-stratified units, some with silt band, in the Folkestone Beds (Lower Greensand) of Southeast England. *Geology Mijnb,* Vol. **43**, P. 451-461.

ALLEN, J. R. L., 1962. Petrology, origin and deposition of the highest Lower Old Red Sandstone of Shropshire, England. *Journal of Sedimentary Petrology*, Vol. **32**, P. 657-697.

ALLEN, J. R. L., 1965. Late Quaternary Niger delta and adjacent area: Sedimentary environments and lithofacies. *American Association of Petroleum Geologists Bulletin*, Vol. **49**, P. 547-600.

ALLEN, J. R. L., 1970. Studies in fluvatiatile sedimentation: a comparison of fining-upwards cyclothems, with special reference to coarse-member composition and interpretation. *Journal of sedimentary petrology*, Vol. **40**, P. 298-323.

ALLEN, J. R. L., 1984. Gravel over passing on hump back bars supplied with mixed sediment: examples from the Lower Old Red Sandstone, Southern Britain. *Sedimentology*, Vol. **30**, P. 285-294.

ALLEN, J. R. L., 1986. Earthquake magnitude-frequency, epicentral distance, and soft-sediment deformation in sedimentary basin. *Sedimentary Geology*, Vol. **46**, P. 67-75.

ANDERTON, R., 1976. Tidal-Shelf Sedimentation: an example from the Scottish Dalradian. *Sedimentology*, Vol. **23**, P. 429-458.

ARMENTROUT, J. M., MALECEL, S. J., FEARN, L. B., SHEPARD, C. E., NAYLOR, P. H., MILES, A. W., DESMARAIS, R. J. AND DUNAY, R. E., 1993. Log-motif analysis of Palaeocene depositional systems tracts, Central and Northern North Sea: defined by sequence stratigraphic analysis. *In*: Parker, J. R (Ed.). Petroleum Geology of Northwest Europe: proceedings of the 4th Conference. *Geological Society of London,* P. 45-57.

ARNOTT, D. AND SOUTHARD, J., 1990. Exploratory flow-duct experiments on combined-flow bed configurations and some implications for interpreting storm-event stratification. *Journal of Sedimentary Petrology*, Vol. **60**, P. 211-219.

BANERJEE, S., 1980. Stratigraphic Lexicon of Libya. *Id. Res. Cent. Bull*, **13**, 300 pp.

BANKS, N. L., 1973. Tide dominated offshore sedimentation, Lower Cambrian, North Norway. *Sedimentology*, Vol. **20**, P. 213-228.

BARTEK, L., VAIL, P. R., ANDERSON, J. B. AND EMMET, P. A., 1990. The effect of Cenozoic ice sheet fluctuation in Antarctica on the stratigraphic signature of the Neogene. *Journal of Geophysical Research* (in press).

BASAN, P. B., 1978. Trace Fossil Concepts. *Society Economic Palaeontology Mineralogy,* short course Notes, No. **5**, 181 pp.

BASU, A., YOUNG, S. W., SUTTNER, L. J., JAMES, W. C. AND MACK, G. H., 1975. Re-evaluation of the use of undulatory extinction and polycrystallinity in detrital quartz for provenance interpretation. *Journal of Sedimentary Petrology*, Vol. **45**, P. 873-882.

BAUERLE, G., BORNEMANN, O., MAUTHE, F. AND MICHALZIK, D., 2000. Origin of Stylolites in Upper Permian Zechstein Anhydrite (Gorleben salt dome, Germany). *Journal of Sedimentary Research,* Vol. **70**, P. 726-737.

BEALES, F. W., 1971. Cementation by white sparry dolomite. *In*: Bricker, O. P (Ed.). Carbonate Cements: Baltimore, The Johns Hopkins Uni. Press, P. 330-338.

BELLINI, E. AND MASSA, D., 1980. A stratigraphic contribution to the Palaeozoic of southern basins of Libya. *In*: Salem M. J. and Busrewil M. T (Eds.). The Geology of Libya. Academic press, London, Vol. **I**, P. 3-56.

BELLINI, E., GIORI, I., ASHURI, O. AND BENELLI, F., 1991. Geology of Al Kufrah Basin, Libya. *In*: Salem, M. J., Sbeta A. M., and Bakbak, M. R (Eds.). The geology of Libya, Academic Press, London, Vol. **VI**, P. 2155-2185.

BENN, D. I. AND EVANS, D. J. A., 1998. Glaciers and glaciation, Arnold, A member of the Hodder Heading Group, London, 1st edition, 734 pp.

BENNACEF, A., BEUF, S., BIJU-DUVAL, B., DECHARPAL, O., GARIEL, O. AND ROGNON, P., 1971. Example of cratonic sedimentation: Lower palaeozoic of Algerian Sharara. *Bulletin American Association Petroleum Geology*, Vol. **55**, P. 2225-2245.

BERNER, R. A., 1964. Iron sulfides formed from aqueous solution at low temperatures and atmospheric pressure. *Geology,* Vol. **72**, P. 293-306.

BEUF, S., BIJU-DUVAL, B., DE CHARPAL, O., ROGNON, P., GARIEL, O. AND BENNACEF, A., 1971. Les gres du Palaeozoique inferieur au shahara. *Sci. Tech. Petrole*, Paris, No. **18**, 464 pp.

BIJU-DUVAL, B., 1974. Examples de depots fluvial-glaciaires dans l'Ordovician superieur et le precambrian superieus de Sahara Central. *Bulletin du Centre de Recherches de pa.* Vol. **8**, P. 209-226

BLATT, H. AND CHRISTIE, J. M., 1963. Undulatory extinction in quartz of igneous and metamorphic rocks and its significance in provenance studies of sedimentary rocks. *Journal of Sedimentary Petrology*, Vol. **33**, P. 559-579.

BLATT, H. H., 1979. Diagenetic Process in Sandstone. *In*: Scholle P. A. and Schluger P. R (Eds.) Aspects of diagenesis. *Society of Economic Palaeontologists and Mineralogists Special Publication,* No. **26**, P. 141–157.

BLATT, H. H., 1982. Sedimentary Petrology. W. H. Freeman and Company, San Francisco, 564 pp.

BLATT, H., 1967. Original character of clastic quartz. *Journal of Sedimentary Petrology,* Vol. **37**, P. 401-424.

BLATT, H., MIDDLETON, G. AND MURRAY, R., 1972. Origin of Sedimentary Rocks. Prentice-Hall, New Jersey, 1st edition, 634 pp.

BLATT, H., MIDDLETON, G. AND MURRAY, R., 1980. Origin of sedimentary rocks. Englewood Cliffs, New Jersey: Prentice-Hall, 2nd edition, 782 pp.

BOGGS, S. JR., 1995. Principles of Sedimentology and Stratigraphy. Merrill, Columbus, Ohio, – Hall, Upper Sander River, New Jersey, 2nd edition, 774 pp.

BOOTE, D. R. D. CLARK-LOWES, D. D. AND TRAUT, M. W., 1998. Palaeozoic petroleum systems of North Africa. *In*: MACCREGOR, D. S. MOODY, R. T. J. AND CLARK-LOWES, D. D (Eds.). Petroleum Geology of North Africa. *Geological Society Special Publication,* No. **132**. P.7-68.

BORGHI, P. AND CHIESA, C., 1940. Cenni geologicie paleontologici sul palaeozoic dell'Egghidi Uan Caza nel deserto di Taita (Fazzan Occidentale*). Ann. Mus. Libico Stor. Nat.,* **2**, P. 123-137.

BOSE, P. K., CHAUDHURI, A. K. AND SETH, A., 1988. Facies flow and bed form patterns across a storm-dominated inner continental shelf: Proterozoic Kaimur Formation, Rajasthan, India. *Sedimentary Geology*, Vol. **59**, P. 275-293.

BOURGEOIS, J., 1980. A transgressive shelf sequence exhibiting hummocky cross-stratification: the cape sebastian sandstone (Upper Cretaceous), Southwestern Oregon. *Journal of Sedimentary Petrology*, Vol. **50**, P. 681-702.

BRACACCIA, V., CARCANO, C. AND DERERA, K., 1991. Sedimentology of the Silurian-Devonian series in the southeastern part of Ghadames Basin. *In*: Salem, M. J. and Belaid, M. N (Eds.). The Geology of Libya. Academic press, London, Vol. **V**, P. 1727-1744.

BRENCHLEY, P. J., 1985. Storm influenced sandstone beds. *Modern Geological,* Vol. **9**, P. 369-396.

BRENCHLEY, P. J., NEWALL, G. AND STANISTREET, I. G., 1979. A storm surge origin for sandstone beds in an epicontinental platform sequence, Ordovician, Norway. *Sedimentary Geology*, Vol. **22**, P. 185-217.

BRIDGE, J. S. AND LEEDER, M. R., 1979. A simulation model of alluvial stratigraphy. *Sedimentology*, Vol. **26**, P. 617-644.

BRIDGE, J. S., 1981. Hydraulic interpretation of grain-size distribution using a physical model for bedload transport. *Journal of Sedimentary Petrology*, Vol. **51**, P. 1109-1124.

BROWN, L. F. AND FISHER, W. L., 1977. Seismic-stratigraphic interpretation of depositional systems: examples from Brazil rift and pull-apart basin. *In*: Payton, C. E (Ed.). Seismic stratigraphy-applications to hydrocarbon exploration. *American Association of Petroleum Geologists, Memoir* **26**, P. 213-248.

BUCHHEIM, H. P., BRAND, L. R. AND GOODWIN, H. T., 2000. Lacustrine to fluvial floodplain deposition in the Eocene Bridge Formation. *Palaeogeography, Palaeoclimatology, Palaeoecology.* Vol. **162**, P. 191-209.

BURLEY, S. D. AND KANTOROWICZ, J. D., 1986. Thin section and SEM textual criteria for the recognition of cement-dissolution porosity in sandstone. *Sedimentology*, Vol. **33**, P. 587-603.

BUROLLET, P. F., 1960. Lexique Stratigraphique international, 4, Libya, Conger's shoreline International Commission de stratigraphic, Recherché, Scientifique Paris, 62 pp.

BYERS, C. W. AND DOTT. R. J. JR., 1981. SEPM Research conference on modern shelf and ancient cratonic sedimentation-the orthoquartzite-carbonate suit revisited. *Journal of Sedimentary Petrology*, Vol. **51**, P. 329-347.

CADIGAN, R. A., 1961. Geological interpretation of grain-size distribution measurements of Colorado Plateau Sedimentary rocks. *Geology,* Vol. **69**, P. 121-144.

CAMPBELL, C. V., 1967. Laminae, lamina set, bed and bed-set. *Sedimentology,* Vol. **8**, P. 7-26.

CANT, D. J. AND WALKER, R. G., 1976. Development of a braided-fluvial facies model for the Devonian Battery point sandstone, Quebec. *Canadian Journal of Earth Sciences*, Vol. **13**, P. 102-119.

CANT, D. J., 1984. Subsurface facies analysis. *In*: Walker, R. G (Ed.). Facies models. *Geological Association of Canada*, P. 297-310.

CANT, D. J., 1992. Subsurface facies analysis. *In*: Walker, R. G (Ed.). Facies models, response to sea-level change. *Geological Association of Canada*, P. 27-45.

CARVER, R. E., 1971. Procedures in Sedimentary Petrology. Wiley – Interscience. A division of John Wiley and Sons, Inc. London, Sydney, Toronto, P. 95-105.

CASTLE, J. W., 1998. Regional sedimentology and stratal surface of a lower Silurian clastic wedge in the Appalachian Foreland Basin. *Journal of Sedimentary Research*, Vol. **68**, P. 1201-1211.

CASTRO, J. C., DELL FAVERA, J. C. AND EL-JADI, M., 1991. Tempestite facies, Murzuq Basin, Great Socialist People's Libya Arab Jamahiriya. Their recognition and stratigraphic implication. *In*: Salem, M. J. and Belaid, M. N (Eds.). The Geology of Libya. Academic press, London, Vol. **V**, P.1757-1765.

CASTRO, J. C., DELLA FAVERA, J. C. AND EL-JADI, M., 1985. Palaeozoic sedimentation facies, Murzuq Basin. Socialist Peoples Libya Arab Jamahiriya. Internal report. Braspetro-petrobras, Rio de Janeiro, 117 pp.

CEPEK, P., 1980. The sedimentology and facies development of the Hasawnah Formation in Libya. *In*: Salem, M. J., and Busrewil, M. T (Eds.). The geology of Libya, Academic Press, London, Vol. **II**, P. 375-382.

CHAYES, F., 1956. Petrographic modal analysis. An elementary statistical appraisal - John Wiley and sons Inc. New York.

CHEEL, R. J. AND LECKIE, D. A., 1992. Coarse-grained storm beds of the Upper Cretaceous Chungo Member (Wapiabi Formation), Southern Alberta, Canada. *Journal of Sedimentary Petrology*, Vol. **62**, P. 933-945.

CLARK, F. W., 1924. The data of geochemistry, *Geological Survey Bulletin*, 5th edition, P. 770-841.

CLARK-LOWES, D. D., 1985. Aspects of Palaeozoic cratonic sedimentation in southwest Libya and Saudi Arabia Vol. **1**, Libya. Ph.D. Thesis, London University, 171 pp.

COLEMAN, J. M. AND GAGLIANO, S. M., 1964. Cyclic sedimentation in the Mississippi River deltaic plain. *Gulf Coast Association of Geological Societies Transactions,* Vol. **14**, P. 67-80.

COLLINSON, J. D., 1970. Deep channels, massive beds and turbidity current genesis in the central Pennine Basin. Proc. Yorksh. *Geological Society of London,* Vol. **37**, P. 495-519.

COLLOMB, G. R., 1962. Etude geologique de jebel Fezzan et de sabordure palaeozoique. Notes Mem. C. F. P., **1**, 36 pp.

COLLOMB, G. R. AND HELLER, C., 1958. Etude geologique de la Bordure Occidentale du Bassin de Mourzouk. Unpublished Report Campagnie Petrole Total, Libya, 30 pp.

COLLOMB, G. R., BLEGIERS, A. DE., FAUCHOUX, E. AND MENNIG, J. J., 1960. Etude du Devono-Carboniferous du Massif du Djebel Fezzan. Unpublished Report Campagnie Petrole Total, Libya, 88 pp.

COLLOMB, G. R., FACHOUX, E. AND MENNING, J. J., 1961. Etude Stratigraphique du Palaeozoic des Regions serde les-Ghat. Unpublished Report Campagnie Petrole Total, Libya, 134 pp.

CONANT, L. C. AND GOUDARZI, G. H., 1964. Geological map of Libya scale 1:2000.000 2nd edition, 1977- Industrial Research Centre. Tripoli – Libya.

CONANT, L. C. AND GOUDARZI, G. H., 1967. Stratigraphic and tectonic framework of Libya. *American Association of Petroleum Geologists Bullet.* Vol. **51**, P. 719-730.

COTTER, E. AND GRAHAM, J. R., 1991. Coastal plain sedimentation in late Devonian of southern Ireland; hummocky cross-stratification in fluvial deposits?. *Sedimentary Geology,* Vol. **72**, P. 201-224.

CRAIG, E. J., LINK, P. K., HUGHES, D. D. AND ARCANGELLI, V., 1958. Geology of the NW Fazzan, Libya, Unpublished Report. Esso standard Libya, Inc., **23**, 101 pp.

CRIMES, T. P., 1970. The significance of trace fossils in sedimentology, stratigraphy and Palaeoecology with examples from Lower Palaeozoic strata. *In*: T. P. Crimes and J. C. Harper (Eds.). Trace Fossils. *Geology*, Vol. **3**, P. 101-126.

DALLONI, M., 1948. Materiaux pour l'etude du Sahara oriental: region entre la Libya, le Tibesti et al Kaouar (Niger). Geol. Et prehist. Mission sci.du Fazzan (1944-1945). *Inst. Reach. Sahara Univ.*, **6**, 119 pp.

DAPPLES, E. C., 1975. Laws of distribution applied to sand-size. *In*: Whitten, E. H. Timothy (Ed.). Quantitative studies in the geological sciences. *Geological Society American Bulletin,* Vol. **142**, P. 37-61.

DE RAAF, J. F. M., BOERSMA, J. R. AND VAN GELDER, A., 1977. Wave generated structures and sequences from a shallow marine succession. Lower Carboniferous, county cork, Ireland. *Sedimentology*, Vol. **24**, P. 451-483.

DE RAAF, J. F. M., READING, H. G. AND WALKER, R. G., 1965. Cyclic sedimentation in Lower Westphalia of north Devon, England. *Sedimentology*, Vol. **4**, P. 1-52.

DESIO, A., 1936a. Prime notizie sulla presenza del Silurico fossilifero nel Fazzan. *Boll. Soc. Geol. Ital.,* **55**, 118 pp.

DESIO, A., 1939-1953. Annuli del. Museo Libico distoria Natural. Vol. **1**, 431 pp, 1939; Vol. **2**, 366 pp, 1940; Vol. **3**, 280 pp, 1942; Tripoli, Vol. **4**, 1953, Rome.

DICKINSON, W. R., BEARD, L. S., BRAKENRIDGE, G. R., ERJAVEC, J. L., FERGUSON, R. C., INMAY, K. F., KNEPP, R. A., LINDBERGH, F. A. AND RYBERG, P. T., 1983. Provenance of North America Phanerozoic sandstones in relation to tectonic setting. *Geological Society American Bulletin*, Vol. **94**, P. 222-235.

DOE, T. W. AND DOTT, R. H. JR., 1980. Genetic significance of deformed cross bedding – with examples from the Navajo and Weber sandstone of Utah. *Journal of Sedimentary Petrology*, Vol. **50**, P. 793-812.

DOTT, R. H. JR. AND BOURGEOIS, J., 1982. Hummocky stratification: Signification of its variable bedding sequence; *Geological Society of American Bulletin*, Vol. **93**, P. 663-680.

DOYLE, L. J., CARDER, K. L. AND STEWARD, R. G., 1983. The hydraulic equivalence of mica. *Journal of Sedimentary Petrology*, Vol. **32**, P. 643-648.

DOYLE, L. J., CLEAR, W. J. AND PILKEY, O. H., 1968. Mica its use in determining shelf-depositional regimes. *Marine Geology,* Vol. **6**, P. 381-389.

DUKE, W. L., 1990. Geostropic circulation or shallow marine turbidity current? The dilemma of paleoflow patterns in storm-influenced prograding shoreline system. *Journal of Sedimentary Petrology*, Vol. **60**, P. 870-883.

DUKE, W. L., 1985. Hummocky cross-stratification tropical hurricanes and winter storms. *Sedimentology,* Vol. **32**, P. 167-194.

DUNOYER, DE, SEGONZAC, G., 1968. The birth and development of the concept of diagenesis. *Earth Science*, No. **4**, P. 153-201.

DUNSMORE, H. E., 1973. Diagenetic processes of lead zinc emplacement in carbonate: Trans. Inst. Min. Metallurgy (B) **82**: (Edinburgh Petroleum Development Services L.T.D, user-manual), P. 168-1173.

DUVAL, B. C. C. AND VAIL, P. R., 1992. Types and hierarchy of stratigraphy cycles. Abstract for conference on sequence stratigraphy of European Basin. CNRS-IFP, Dijon, France (18^{th} - 20^{th} May 1992), P. 44-45.

ECHIKH, K., 1998. Geology and hydrocarbon occurrences in the Ghadames Basin, Algeria, Tunisia, Libya. *In*: Macgregor, D. S., Moody, R. T. J. and Clark-Lowes, D. D (Eds.). Petroleum Geology of North Africa. *Geological Society London Special Publication,* No. **132**, P. 109-129.

EDWARDS, C. W., 1991. The Buchan Field, Blocks 20/5a and 21/1a, UK North Sea. *In*: Abbott's, I.L (Ed.) United Kingdom Oil and Gas Fields, 25 yeas Commemorative Volume. *Geological Society of London Memoir,* **14**, P. 253-259.

EKDALE, A., BROMLEY, R. G., AND PEMBERTON, S. G., 1984. The use of trace fossils in sedimentology and stratigraphy, *Society of Economic Palaeontologists and Mineralogists*, Short Course, Notes, **15**.

EL HAWAT, A. S. AND BEZAN, A., 1998. Early palaeozoic events stratigraphy of western Libya: Glacio-eustatic and tectonic signatures and their impact on hydrocarbon exploration. *In*: The geological conference of Exploration in Murzuq Basin.

EL-HINNAWI, E. E., 1966. Methods in chemical and mineral microscopy, 222 pp.

ELLIOTT, T., 1986. Siliciclastic shorelines. *In*: H. G. Reading (Ed.). Sedimentary environments and facies, Blackwell Scientific Publication, Oxford, 2^{nd} edition, P. 155-188.

EMERY, D. AND MYERS, K. J., 1996. Sequence stratigraphy. Blackwell Science, 297 pp.

ERIKSSON, K. A., 1978. Alluvial and destructive beach facies from the Archaon Moodies Group, Barberton Mountain Land, South Africa and Swaziland. *In*: Miall, A. D (Ed.). Fluvial Sedimentology. *Canadian Society of Petroleum Geology, Memoir* **5**, P. 287-311.

EUGSTER, H. P., 1970. Chemistry and origin of the brines of Lake Magadi, Kenya. *Mineralogists Society of American Special Paper,* **3**, P. 213-235.

FEKIRINE, B. AND ABDALLAH, H., 1998. Palaeozoic lithofacies correlatives and sequence stratigraphy of the Saharan Platform, Algerian. *In*: Macgregor, D. S., Moody, R. T. J. and Clark-Lowes, D. D (Eds.). Petroleum Geology of North Africa. *Geological Society Special Publication,* No. **132**, P. 97-108.

FELLO, N. M. AND HERZOG, U. 1996. Final formation tops of the Murzuq Basin, southwestern Libya, from Kelly Bushing (KB), Repsol Oil Operations, Exploration Department, 20 pp (*Unpublished*).

FELLO, N. M. AND TURNER, B. R., 2001a. Provenance analysis, tectonism and shifting depositional system in the NW part of the Murzuq Basin, Libya: implication for hydrocarbon prospectivity. 21st International Association Sedimentology (IAS) meeting of Sedimentology, Abstr., Davos, Switzerland (3rd – 5th September 2001).

FELLO, N. M. AND TURNER, B. R., 2001b. Depositional environments and hydrocarbon significance of the Mamuniyat Formation in the NW Murzuq Basin, SW Libya. 40th BSRG Annual Meeting of Sedimentary Research, Abstract, University of Plymouth, England (16th - 19th December 2001).

FELLO, N. M., 1996. Final well report, Geological section, A28-NC115, A-Field, Repsol Oil Operations, Exploration Department, 22 pp (*Unpublished*).

FIGUEIREDO, A. G. J., SANDERS, J. E. AND SWIFT, D. J. P., 1982. Storm graded layers on inner continental shelves: examples from South Brazil and Atlantic Coast of the Central United States. *Sedimentary Geology*, Vol. **31**, P. 171-190.

FINNEY, S. C., AND BERRY, W. B. N., 1997. New perspectives on graptolite distribution and their use as indicators of platform margin dynamics. *Geology*, Vol. **25**, P. 919-922.

FISCHER, A. G., 1982. Long-term climatic oscillations recorded in stratigraphy. *In*: Berger, W. H. and Crowell, J. C (Eds.). Climate in earth history. Studies in geophysics. National Academy Press. Washington, P. 25-57.

FOLK, R. L., 1977. Peculiar forms of diagenetic carbonate from hypersaline and cave deposits, ancient to recent. Newsletter West Texas, *Geological Society*, No.**11**.

FOLK, R. L. AND WARD, W. C., 1957. Brazos River Bar: A study in the Significance of Grain-size parameters. *Journal of Sedimentary Petrology*, Vol. **27**, P. 3-26.

FOLK, R. L., 1951. A comparison chart for visual percentage estimation. *Journal of Sedimentary Petrology*, Vol. **21**, P. 32-33.

FREULON, J. M., 1953. Sur la presence de gigantostraces dans les gres a Harlania du Tadrart (Sahara Central). *C. R. Soc. Geol. Fr.*, **11-12**, P. 216-218.

FREULON, J. M., 1964. Etude geologique des series primaries du Sahara Central (Tassili N'Ajjer et Fazzan). *Publ. Centre nation. Reach. SCI., Seri geol.*, No. **3**, 186 pp.

FREY, R. W., AND PEMBERTON, S. G., 1984. Trace fossil facies models. *In*: R. G. Walker (Ed.). Facies models, *Geosciences Canada Reprint Ser.* **1**, 2nd edition, P. 189-207.

FRIEDMAN, G. M. AND SANDERS, J. E., 1978. Principles of Sedimentology. John Wiley and Sons. New York, P. 58-80.

FRIEDMAN, G. M., 1958. Determination of sieve-size distribution from thin-section data for sedimentary petrology studies. *Journal Geology,* Vol. **66**, P. 394-416.

FRIEDMAN, G. M., 1962. On sorting, sorting coefficients, and the lognormality of the grain-size distribution of sandstone. *Journal Geology,* Vol. **70**, P. 737-753.

FURON, R., 1955. Histoire de la geologie de la France d'Outre-Mer. Mem. Mus. Nat. Hist. Nat., new series, Paris, 218 pp.

FURST, M. AND KLITZSCH, E., 1963. Late Caledonian Palaeogeography of the Murzuq Basin. Revue Inst. Fr. Petrole, **18**, P. 158-170.

GADOW, S. AND REINECK, H. E., 1969. A Blandiger sand transport bei sturmfluten. Senckenberg. Marit **1**, P. 63-78.

GALLOWAY, W. E. AND HOBDAY, D. K., 1983. Terrigenous clastic depositional system. Springer-Verlag, New York, 423 pp.

GALLOWAY, W. E., 1989. Genetic stratigraphic sequence in basin analysis: architecture and genesis of flooding surface bounded depositional units. *Bulletin of the Geological Society of America,* Vol. **73**, P. 125-142.

GARRELS, R. M. AND MACKENZIE, F. T., 1971. Evolution of sedimentary rocks. New York: W. W. Norton and Co, 397 pp.

GEOLOGY FIELD TRIP., 1996. The first geological field trip has been organised by Repsol Oil Operations "Exploration Department", covered the classic areas around Ghat/Tikiumit Arch and the Qarqaf Arch (24th November to 08th December 1996).

GHOSH, S. K., 1991. Palaeoenvironmental analysis of the late Proterozoic Nagthat Formation, NV Kumaun Lesser Himalaya, India. *Sedimentary Geology*, Vol. **71**, P. 35-45.

GILLIGAN, A., 1920. The Petrography of the Millstone Grit of Yorkshire. *Geological Society London Quaternary Journal*, Vol. **75**, P. 251-294.

GOLDRING, R. AND BRIDGES, P. 1973. Sublittoral sheet sandstones. *Journal of Sedimentary Petrology*, Vol. **43**, P. 736-747.

GRAHAM, J. R., 1975. Deposits of a near-coastal fluvial plain the Toe Head Formation (Upper Devonian) of Southwest cork. *Sedimentary Geology,* Vol. **14**, P. 45-61.

GREENWOOD, B. AND SHERMAN, D. J., 1986. Hummocky cross-stratification in the surf zone: flow parameters and bedding genesis. *Sedimentology*, Vol. **33**, P. 33-45.

GRESSLY, A., 1838. Observation geologiques sur le Jura Soleurois. Neue Denkschr, allg. Schweiz, Ges. Nturw. Vol. **2**, P. 1-112.

GRIFFITHS, J. C., 1953. Estimation of error in grain-size analysis. *Journal of Sedimentary Petrology*, Vol. **23**, P. 75-84.

GRIFFITHS, J. M., 1961. Measurement of the properties of sediments. *Geology,* Vol. **69**, P. 487-498.

GRUBIC, A., DIMITRIJEVIC, M., GALECIC, M., JAKOVLJEVIC, Z., KOMARNICKI, S., PROTIC, D., RADULOVIC, P. AND RONCEVIC, G., 1991. Stratigraphy of western Fezzan, SW Libya. *In*: Salem, M. J. and Belaid, M. N (Eds.). The geology of Libya, Academic Press, London, New York, Vol. **IV**, P. 1529-1565.

HADLEY, D. F., 1992. Sedimentology and facies of the Mamuniyat Formation of SW Libya. Lasmo internal report *(Unpublished).*

HALLAM, A., 1977. Secular changes in marine inundation of USSR and North America through the Phanerozoic. Nature **269**, P. 769-772.

HAMBLIN, A. P. AND WALKER, R. G., 1979. Storm-dominated shallow marine deposits; he ferine-kootenay (Jurassic) transition, southern Rocky Mountains; *Canadian Journal of Earth Sciences*, Vol. **16**, P. 1673-1690.

HAMMUDA, O. S., 1980. Geological factors controlling fluid and anomalous freshwater occurrence in the Tadrat sandstone, Al Hamadah Al Hamra area, Ghadames basin. *In*: Salem, M. J. and Busrewil, M. T (Eds.). The geology of Libya. Academic Press. London, Vol. **II**, P. 501-507.

HAQ, B. U., HARDENBOL, J. AND VAIL, P. R., 1987. Chronology of fluctuating sea-levels since the Triassic. *Science*, **235**, P. 1153-1165.

HAQ, B. U., HARDENBOL, J. AND VAIL, P. R., 1988. Mesozoic and Cenozoic chronostratigraphy and cycles of sea-level change. *In*: C. K. Wilgus, B. S. Hastings, C. G. St Kendall, H. W. Posamentier, C. A. Ross and J. C. Van Wagoner (Eds.). Sea-level changes: An Integrated Approach. Special Publication, *Society of Economic Palaeontologists and Mineralogists, Tulsa.* **42**, P. 40-45.

HARMS, J. C., SOUTHARD, J. B., SPEARING, D. D. R. AND WALKER, R. B., 1982. Structures and sequences in clastic rocks. Short course *Society. Economic. Palaeontology. Mineralogy,* No. **9**.

HARMS, J. C., SOUTHARD, J. B., SPEARING, D. R. AND WALKER, R. G., 1975. Depositional environments as interpreted from primary sedimentary structures and stratification sequence. *Society of Economic Palaeontologists and Mineralogists.* Short Course **2**, 161 pp.

HAVLICEK, V. AND MASSA, D., 1973. Brachiopodes de l'ordovician superieur de Libya occidental: Implications Stratigraphiques Regionales. *Geobios*, **6(4)**, P. 267-290.

HAYCOCK, C. A., MASON, T. R. AND WATKEYS, M. K., 1997. Early Triassic Palaeoenvironment in the eastern Karoo Foreland Basin. South Africa. *Journal of African Earth Sciences*, Vol. **24**, P. 79-94.

HEALD, M. T. AND LARESE, R. E., 1973. The significance of solution of feldspar in porosity development. *Journal of Sedimentary Petrology,* Vol. **43**, P. 458-460.

HEIN, F. J., ROBB, G. A., WOLBERG, A. C. AND LONGSTAFFE, F. J., 1991. Facies descriptions and associations in ancient reworked (? transgressive) shelf sandstones: Cambrian and Cretaceous example. *Sedimentary*, Vol. **38**, P. 405-431.

HERZOG, U., 1997. Technical Report for the Geological Field Trip to Ghat/Tikiumit Arch, and Qarqaf Arch, Repsol Oil Operations: Guidebook, 27 pp (*Unpublished*).

HOBDAY, D. K. AND HORNE, J. C., 1977. Tidally influenced barrel island and estuarine sedimentation in the upper Carboniferous of Southern West Virginia. *Sedimentary Geology*, Vol. **18**, P. 97-122.

HOBDAY, D. K. AND READING, H. G., 1972. Fair weather versus storm processes in shallow marine sand bar sequences in the late Precambrian of Finnmark, North Norway. *Journal of Sedimentary Petrology*, Vol. **42**, P. 318-324.

HOWARD, J. D. AND REINECK, R. E., 1981. Depositional facies of high-energy beach-to-offshore sequence: comparison with low energy sequence; *American Association of Petroleum Geologist Bull*etin, Vol. **65**, P. 807-830.

HUBERT, J. F. AND HYDE, M. G., 1983. Sheet flow deposits of graded beds and mudstones on an alluvial sandflat-playa system: Upper Triassic Blomidon red bed, St. Mary's Bay, Nova Scotia. *Sedimentology,* Vol. **29**, P. 457-474.

HUNTER, R. E., 1967. The petrography of some Illinois Pleistocene and Recent sands. *Sedimentary Geology*, Vol. **1**, P. 57-75.

INMAN, D. L., 1952. Measures for describing the size distribution of sediment. *Journal of Sedimentary Petrology*, Vol. **22**, P. 125-145.

JAGO, C. F., 1980. Contemporary accumulation of marine sand in a macrotidal estuary, Southwest Wales. *Sedimentary Geology*, Vol. **26**, P. 21-49.

JAMIESON, T. F., 1860. On the drift and rolled gravel of the north of Scotland. *Geological Society London, Quaternary Journal*, Vol. **16**, P. 347-371.

JANSA, L., 1972. Depositional history of the coal bearing Upper Jurassic-Lower Cretaceous Kootenay Formation, southern Rocky Mountains. *Canada Geological Society of America Bulletin,* Vol. **83**, P. 3199-3222.

JERVEY, M. T., 1988. Quantitative geological Modelling of siliciclastic rock sequences and their seismic expressions. *In*: C. K. Wilgus, B. S. Hastings, C. G. St Kendall, H. W. Posamentier, C. A. Ross and J. C. Van Wagoner (Eds.). Sea-level changes: An Integrated Approach. Special Publication, *Society of Economic Palaeontologists and Mineralogists, Tulsa*, **42**. P. 47-69.

JOHNSON, H. D., 1977. Shallow marine sandbars sequence: an example from the late Precambrian of North Norway. *Sedimentology*, Vol. **24**, P. 245-270.

JOHNSON, H. D., 1978. Shallow siliciclastic seas. *In*: Reading, H. G (Ed.). Sedimentary environment and facies. Blackwell Scientific Publications, Oxford, P. 207-258.

JONES, B. G. AND RUST, B. R., 1983. Massive sandstone facies in the Hawkesbury sandstone, A Triassic fluvial deposit near Sydney, Australia. *Journal of Sedimentary Petrology*, Vol. **53**, P. 131-161.

KIMBERLEY, M. M., 1978. Palaeoenvironmental Classification of Iron Formation. *Economic Geology,* Vol. **73**, P. 215-229.

KLEIN, G. DE V., 1970. Depositional and dispersal dynamics of intertidal sand bars. *Journal of Sedimentary Petrology*, Vol. **40**, P. 1095-1127.

KLEIN, G. DE, VRIES., 1963. Analysis and review of sandstone classification in the North American geological literatures. *Geological Society American Bulletin,* Vol. **74**, P. 555-576.

KLITZSCH, E., 1965. Ein Profil aus dem Typusgebiet gotlandischer und devonischer Schichten der Zentral Sahara (Western Murzuk Becken, Libyen). *Erdol. Kohle*, **18**, P. 605-607.

KLITZSCH, E., 1966. Comments on the geology of the central parts of southern Libya and northern Chad. *In*: J. J. Williams (Ed.). South central Libya and Northern Chad. Petrol. Explore. Soc. Libya, 8th Annu. Field Conf., P. 1-17.

KLITZSCH, E., 1969. Stratigraphic section from the type areas of Silurian and Devonian strata at Western Murzuq Basin, Libya. *In*: J. J. Williams (Ed.). Geology Archaeology and Prehistory of the southwestern Fezzan, Libya. Petrol. Explore. Soc. Libya, 8th Annu. Field Conf., P. 83-101.

KLITZSCH, E., 1981. Lower Palaeozoic rocks of Libya, Egypt and Sudan. *In*: Holland C. H (Ed.). Lower Palaeozoic of Middle East; eastern and southern Africa and Antarctica, **III**, P. 131-163,

KLITZSCH, E., 1995. Libyan/Libya. *In*: Kulke, H. (Ed.). Regional Petroleum Geology of the World, Vol. **22**, P. 45-56.

KOMAR, P. D., 1985. The hydraulic interpretation of turbidites from their grain-size and sedimentary structures. *Sedimentology*, Vol. **32**, P. 395-407.

KREISA, R. D., 1981. Storm-generated sedimentary structures in subtidal marine facies with examples from the middle and upper Ordovician of southwestern Virginia. *Journal of Sedimentary Petrology*, Vol. **51**, P. 823-848.

KRUMBEIN, W. C., 1934. Size frequency distributions of sediments. *Journal of Sedimentary Petrology*, Vol. **4**, P. 65-77.

KRUMBEIN, W. C. AND PETTIJOHN, F. J., 1938. Manual of Sedimentary Petrography. D. Appleton-Century Company. New York, London, 549 pp.

KRUMBEIN, W. C. AND SLOSS, L. L., 1963. Stratigraphy and Sedimentation, W. H. freeman and Company San Francisco, 2nd edition, P. 93-147.

KRUMBEIN, W. C., 1935. Thin section mechanical analysis of indurated sediments. *Journal Geology*, Vol. **43**, P. 482-496.

KRUMBEIN, W. C., 1941. Measurement and geological significance of shape and roundness of sedimentary particles. *Journal of Sedimentary Petrology*, Vol. **11**, P. 64-72.

KRYNINE, P. D., 1940. Petrology and genesis of the Third Bradford sand: Penn. State College Mineral Industries Expt. *Sta. Bull.* **29**, 134 pp.

LANCASTER, N., 1986. Grain-size characteristics of liner dunes in the southwestern Kalahari. *Journal of Sedimentary Petrology*, Vol. **56**, P. 395-400.

LAPPARENT, A. F. AND LELUBRE, M., 1948. Interpretation stratigraphic des series continentales entre Ohanet et Bourharet. *C. R. Acad. Sci.* **227**, P. 1106-1108.

LEEDER, M. R., 1978. A quantitative stratigraphic model for alluvium with special reference to channel deposit density and interconnectedness. *In*: Miall, A. D (Ed.). Fluvial Sedimentology. *Canadian Society of Petroleum Geology, Memoir,* **5**. P. 587-596.

LEEDER, M. R., 1982. Sedimentology: Processes and Products, London, P. 35-43.

LEITH, C. K. AND MEAD, W. J., 1915. Metamorphic geology. New York, 337 pp.

LELUBRE, M., 1946. Sur le Palaeozoique du Fazzan. *C. R. Acad. Sci.*, **222**, P. 1403-1404.

LELUBRE, M., 1952. Apercu Sur la geologie du Fazzan. Travaux recents des collaborators. *Bull. Serv. Care. Geol. Al gerie,* **3**, P. 109-148.

LEOPOLD, L. B. AND WOLMAN, M. G., 1957. River channel patterns: braided, meandering and straight. Physiographic and hydraulic studies of river. US Geol. Surv. Prof. Pap. **282B**, P. 39-85.

LEVELL, B. K., 1980. A late Precambrian tidal shelf deposits, the Lower Sandfjord Formation, Finnmark, North Norway. *Sedimentology,* Vol. **27**, P. 539-557.

LEWIS, D. W., 1983. Practical Sedimentology. Hutchinson Ross Publishing Company. Stroudsburg, Pennsylvania, 58 pp.

LINDHOLM, R. C., 1979. Utilization of programmable calculators in sedimentology. *Journal of Sedimentary Petrology*, Vol. **49**, P. 615-620.

LIPPMANN, F., 1973. Sedimentary Carbonate Minerals. Springer-Verlag. New York. USA, 228 pp.

LOUCKS, R. G., BEBOUT, D. G. AND GALLOWAY, W. E., 1977. Relationship of porosity formation and preservation to sandstone consolidation history-Gulf Coast Lower Tertiary Frio Formation. *Gulf Coast Association Geological Science Translation*, No. **27**, P. 109-116.

LOWE, D. R., 1982. Sediment gravity flows: II. Depositional models with special reference to the deposits of high-density turbidity currents. *Journal of Sedimentary Petrology*, Vol. **52**, P. 279-297.

LOWE, D. R., 1988. Suspended-load fallout rate as an independent variable in the analysis of current structures. *Sedimentology*, Vol. **35**, P. 765-776.

LUNING, S., CRAIG, J., FITCHES, B., MAYOUF, J., BUSEREWIL, A., EL-DIED, M., GUMMUID, A., LOYDELL, D. AND MCLLROY, D., 1999. Re-evaluation of the petroleum potential of the Kufrah Basin (SE Libya, NE Chad): does the source rock barrier fall?. *Marine and Petroleum Geology,* Vol. **16**, P. 693-718.

MACDONALD, D. J. M., 1993. Controls on sedimentation and convergent plate margins. *In*: Frostick, L. E. and Steel, R. J (Eds.). Tectonic controls and signatures in sedimentary successions. *International Association of sedimentologists Special Publication*, No. **20**, P. 225-257.

MACHEL, H. G., 1987. Saddle dolomite as a by-product of chemical compaction and thermo-chemical sulphate reduction. *Geology*, Vol. **15**, P. 936-940.

MACKIE, W., 1896. The sand and sandstones of Eastern Moray. Edinburgh. *Geological Society Transport*, Vol. **7**, P. 148-172.

MASSA, D. AND COLLOMB, G. R., 1960. Observations nouveiles sure la regions d'Aouinet Ouenine et du Djebel Fezzan (Libya). Proc. 21st Int. Geol. Conger. **12**, P. 65-73.

MASSA, D. AND MOREAU-BENOIT, A., 1976. Essai de synthese stratigraphique et palynologique du systeme Devonien en Libya Occidentale. Rev. inst. Fr. Petrole, **31**, P. 287-333.

MCBRIDE, E. F. AND YEAKEL, L. S., 1963. Relationship between parting lineation and rock fabric. *Journal of Sedimentary Petrology*, Vol. **33**, P. 779-782.

MCDOUGALL, N. AND MARTIN, M., 1998. Facies models and sequence stratigraphy of upper Ordovician outcrops, Murzuq Basin, Libya. *In*: The geological conferences on Exploration in Murzuq Basin. September 20th – 22nd 1998, Sabha University.

MCMANUS, J., 1988. Grain-size determination and interpretation. *In*: M. E. Tucker (Ed.). *Techniques in Sedimentology,* Blackwall, Oxford, P. 63-85.

MENNING, J. J. AND VITTIMBERGA, P., 1962. Application des methods petrographic an l'etude du Palaeozoique Anacin du Fazzan, 64 pp.

MIALL, A. D., 1977. A review of braided river depositional environments. *Earth Science Review*, Vol. **13**, P. 1-62.

MIALL, A. D., 1978. Lithofacies types and vertical profile models in braided river deposition, *Canada Society of Petroleum Geology, Memoir,* Vol. **5**, P. 597-604.

MIALL, A. D., 1991. Stratigraphy sequence and their chronostratigraphic correlation. *Journal of Sedimentary Petrology*, Vol. **61**, P. 497-505.

MIALL, A. D., 1996. The geology of fluvial deposits. Sedimentary Facies, Basin Analysis and Petroleum Geology. Spring, 582 pp.

MIALL, A. D., 1997. The geology of stratigraphy sequences. Springier, 433 pp.

MIDDLETON, G. V., 1973. Johannes Walther's Law of the correlation of facies. *Geological Society of America Bulletin*, Vol. **84**, P. 979-988.

MIDDLETON, G. V., 1978. Facies. *In*: Fairbridge, R. W., and Bourgeois, J (Eds.). Encyclopedia of sedimentology. Stroudsburg, Pa., Dowden, Hutchinson and Ross, P. 323-325.

MILLEPIED, P., 1979. Palynological study of the Braspetro A1-NC58 onshore well, Libya. Total-CFT, Unpubl. Rept. No. **1808**, 6 pp.

MILLEPIED, P., 1984. Palynological study of the Braspetro C1-NC58 onshore well, Libya. Total-CFT, Unpubl. Rept. No. **3199**, 8 pp.

MILLIKEN, K. L., 1988. Loss of provenance information through subsurface diagenesis in Plio-Pleistocene sandstones, northern Gulf of Mexico. *Journal of Sedimentary Petrology*, Vol. **58**, P. 992-1002.

MITCHUM, R. M., 1977. Seismic stratigraphy and global changes of sea-level, part 1: glossary of terms used in seismic stratigraphy. *In*: Payton, C. E (Ed.). Seismic stratigraphy-applications to hydrocarbon exploration. *American Association of Petroleum Geologists, Memoir*, **26**, P. 205-212.

MITCHUM, R. M. JR., VAIL, P. R. AND THOMPSON, S., 1977. Seismic stratigraphy and global changes of sea-level, part 2: the depositional sequence as a basic unit for stratigraphic analysis. *In*: Payton, C. E. (Ed.). Seismic stratigraphic application to hydrocarbon exploration. *American Association of Petroleum Geologists, Memoir*, **26**, P. 53-62.

MITCHUM, R. M. AND VAN WAGONER, J. C., 1991. High frequency sequence and their stacking patterns: Sequence stratigraphic evidence of high frequency eustatic cycles. *Sedimentary Geology*, Vol. **170**, P. 135-144.

MITCHUM, R. M., JR. SANGREE, J. B., VAIL, P. R. AND WORNARDT, W. W., 1990. Sequence stratigraphy in Late Cenozoic expanded sections, Gulf of Mexico. *In*: J. M. Armentrout and B. F. Perkins (Eds.). Sequence stratigraphy as an Exploration Tool: Concepts and practices from the Gulf Coast. 11th Annual Research Conference, Gulf Coast Section, *Society of Economic Palaeontologists and Mineralogists*, P. 237-256.

MORTON, A. C., 1985. Heavy minerals in provenance studies. *In*: Zuffa, G. G (Ed.). Provenance of arenites. Dordrecht-Boston-Lancaster: D. Reidel Pub. Co.

MORTON, R. A., 1981. Formation of storm deposits by wind-forced currents in the Gulf of Mexico and North Sea. *In*: S. D. Nio, R. T. E. Shuttenhelm and Tj. C. E. Van Wearing (Eds.). Holocene marine sedimentation in the North Sea Basin, P. 385-396.

MUELLER, G., 1967. Methods in Sedimentary Petrology; Hafner publication Company, New York, 283 pp.

NELSON, C. H., 1982. Modern shallow water graded sand layers from storm surges, Bering Shelf: a mimic of Bouma sequence and turbidite systems. *Journal of Sedimentary Petrology*, Vol. **52**, P. 737-545.

NOTTVEDT, A. AND KREISA, R. D., 1987. Model for the combined-flow origin of hummocky cross-stratification. *Geology*, Vol. **15**, P. 357-361.

OKADA, H., 1966. Non-graywacke "turbidite" sandstones in the welsh geosyncline. *Sedimentology,* Vol. **7**, P. 211-232.

OKADA, H., 1971. Classification of sandstone: analysis and proposal. *Journal Geology,* Vol. **79**, P. 509-525.

OTTO, G. H., 1939. A modified logarithmic probability graph for the interpretation of mechanical analysis of sediments. *Journal of Sedimentary Petrology,* Vol. **9**, P. 62-76.

PAGE, H. G., 1955. Phi-millimeter conversion table. *Journal of Sedimentary Petrology*, Vol. **25**, P. 285-292.

PARIZEK, A., KLEN, L. AND ROHLICH., 1984. Geological map of Libya, 1:250000. Sheet: Idri (NG33-1). Explanatory Booklet. Ind. Res. Cent., Tripoli.

PARK, R. G., 1988. In Geological structures and moving plates. Glasgow and London: Blackie and Son Ltd., 337 pp.

PAYTON, C. E., 1977. Seismic stratigraphy-applications to hydrocarbon exploration: *American Association of Petroleum Geologist Memoir,* **26**, 516 pp.

PEDERSEN, G. K., 1985. Thin, fine-grained storm layers in a muddy shelf sequence: an example from lower Jurassic in the Stenlille 1 well, Denmark: *Journal of the Geological Society of London*, Vol. **142**, P. 357-374.

PEMBERTON, S. G., MACEACHERN, J. A. AND FREY, R. W., 1992. Trace fossil facies models: environmental and allostratigraphic significance. *In*: R. G. Walker and N. P. James (Eds.). Facies models: response to sea level change: *Geological Association of Canada*, St. Johns, Newfoundland, Canada, P. 47-72.

PESCE, E., 1969. Exploration of the Fazzan. *In:* W. H. Kanes (Ed.). Geology, Archaeology and Prehistory of southwestern Fezzan, Libya. Petroleum Exploration Soc. Tripoli-Libya, P. 53-65.

PETTIJOHN, F. J., 1949. Sedimentary Rocks, New York, 1st edition, 526 pp.

PETTIJOHN, F. J., 1957. Sedimentary Rocks. New York, 2nd edition, 718 pp.

PETTIJOHN, F. J., 1975. Sedimentary Rocks. New York, 3rd edition, 628 pp.

PETTIJOHN, F. J., POTTER, P. E. AND SIEVER, R., 1987. Sand and sandstones, Springer-Verlag, 2nd edition, 553 pp.

PHILIPPI, G. T., 1965. On the depth, time and mechanism of petroleum generation: Geochim. Cosmochim. Acta, Vol. **29**, P. 1021-1049.

PHLLIPS, J., 1836. Illustrations of the geology of Yorkshire. Part 2. The Mountain Limestone district. Murray, London.

PIEROBON, E. S. T., 1991. Contribution to the stratigraphy of the Murzuq Basin, SW Libya. *In*: Salem, M. J. and Belaid, M. N (Eds.). The geology of Libya, Academic Press London, Vol. **V**, P. 1767-1784.

PITMAN, W. C., 1978. Relationship between ecstasy and stratigraphic sequence of passive margins. *Bulletin of the Geological Society of America,* Vol. **89**, P.1389-1403.

PITTMAN, E. D., 1979. Recent advance in sandstone diagenesis. *Annual Review Earth Palaeontology Science* No. **7**, P. 39-62.

PLUMLEY, W. J., 1948. Black hills terrace gravel: A study in sediment transport. *Journal Geology,* Vol. **48**, P. 526-577.

POLDERVAART, ARIE., 1956. Zircon in rocks, 2 Igneous rocks. *American Journal Science,* No. **254**, P. 521-554.

POMAR, L., 1991. Reef geometries, erosion surfaces and high frequency sea-level changes upper Miocene Reef complex, Mallorca, Spain. *Sedimentology,* Vol. **38**, P. 243-269.

POSAMENTIER, H. W. AND ALLEN, G. P., 1993. Siliciclastic sequence stratigraphic patterns in foreland ramp-type basins. *Geology,* Vol. **21**, P. 455-458.

POSAMENTIER, H. W. AND VAIL, P. R., 1988. Eustatic controls on clastic deposition I – sequence and systems tract models. *In*: C. K. Wilgus, B. S. Hastings, C. G. St Kendall, H. W. Posamentier, C. A. Ross and J. C. Van Wagoner (Eds.). Sea-level changes: An Integrated Approach. Special Publication, *Society of Economic Palaeontologists and Mineralogists, Tulsa,* **42**, P. 109-124.

POSAMENTIER, H. W., AND JAMES, D. P., 1993. An overview of sequence stratigraphic concepts: uses and abuses. *In*: Posamentier, H. W. Summerhayes, C. P. Haq, B. U., and Allen, G. P (Eds.). Sequence stratigraphy and facies associations. *Special Publications. International Association of Sedimentologists.* Blackwell Scientific Publications, Oxford, Vol. **18**, P. 3-18.

POSAMENTIER, H. W., JERVEY, M. T. AND VAIL, P. R., 1988. Eustatic controls on clastic deposition II – conceptual framework. *In*: C. K. Wilgus, B. S. Hastings, C. G. St Kendall, H. W. Posamentier, C. A. Ross and J. C. Van Wagoner (Eds.). Sea-level changes: An Integrated Approach. Special Publication, *Society of Economic Palaeontologists and Mineralogists, Tulsa,* **42**, P. 125-154.

POTTER, P. E. AND PRYOR, W. A., 1961. Dispersal centers at Palaeozoic and later clastics of the upper Mississippi valley and adjacent areas. *Geological Society American Bulletin,* Vol. **72**, P. 1195-1250.

POWERS, M. C., 1953. A new roundness scale for sedimentary particles. *Journal of Sedimentary Petrology*, Vol. **23**, P. 117-119.

PROTIC, D., 1985. Geological map of Libya, 1:250000. Sheet: Tikiumit (NG32-37). Explanatory Booklet. Ind. Res. Cent., Tripoli.

RADKE, B. M. AND MATHIS, R. L., 1980. On the information and occurrence of saddle dolomite. *Journal of Sedimentary Petrology*, Vol. **50**, P. 1149-1168.

RADULOVIC, P., 1985. Geological map of Libya; 1:250 000. Sheet: Wadi Tanezzuft. Explanatory Booklet. Ind. Res. Cent., Tripoli-Libya.

READING, H. G. 1996. *In*: Reading, H. G (Ed.). Sedimentary Environments: Processes, Facies and Stratigraphy, Blackwells Science, 3rd edition, P. 18-35.

READING, H. G., 1978. Sedimentary environments and facies. Oxford, Blackwell Science, 557 pp.

READING, H. G., 1986. Facies. *In*: Reading, H. G (Ed.). Sedimentary environments and facies. Blackwell Scientific Publication, Oxford, 2nd edition, P. 4-19.

REINECK, H. E. AND SINGH, I. B., 1972. Genesis of laminated sand graded rhythmites in storm-sand layers of shelf mud. *Sedimentology*, Vol. **18**, P. 123-128.

REINECK, H. E. AND SINGH, I. B., 1973. Depositional sedimentary environments-with Reference to Terrigenous Clastic, 439 pp.

REINECK, H. E. AND WUNDERLICH, F., 1968. Classification and origin of flaser and lenticular bedding. *Sedimentology*, Vol. **11**, P. 99-104.

REVELLE, R. AND EMERY, K. O., 1951. Barite concretions from the ocean floor: *Geological Society of American Bulletin*, Vol. **62**, P. 707-724.

RICHARD, A. AND DAVIS, JR., 1983. Depositional System. A genetic Approach to Sedimentary Geology, 669 pp.

RIDER, M. H., 1990. Gamma-ray log shape used as facies indicator: critical analysis of an oversimplified methodology. *In*: Hurst, A., Lovell, M. A. and Morton, A. C (Eds.). Geological Application of Wireline Logs. *Geological Society Special Publication,* No. **48**, P. 27-37.

RIDER, M. H., 1996. The geological interpretation of well logs, 2nd edition, 280 pp.

RODRIGUES, R., LOBOZIAK, S., DE MELO, J. H. G. AND ALVES, D. B., 1995. Geochemical characterization and miospore biochrostratigraph of the Frasnian anoxic events in the Parnaiba Basin, northeast Brazil, *Bulletin des centres de Recherches Exploration-Production Elf-Aquitaine*, Vol. **19**, P. 319-327.

ROSENFELD, J. L., 1950. Determination of all principle indices of refraction on difficult oriented minerals by direct measurement. *American Mineralogist,* **35**, P. 902-905.

RUBIN, D. M., 1987. Cross-bedding, Bedforms, and Paleocurrents. *Society Economic Palaeontology Mineralogy,* Concept in Geology, **1**, Tulsa, 187 pp.

RUSSELL, R. D. AND TAYLOR, R. E., 1937. Roundness and shape of Mississippi River sands. *Journal Geology*, Vol. **45**, P. 225-267.

RUST, B. R., 1978. Depositional model for braided alluvium. *In*: Miall, A. D (Ed.). Fluvial Sedimentology. *Canadian Society Petroleum Geologists Memoir,* Calgary, Albert, No. **5**, P. 605-626.

SANDERSON, I. D., 1984. Recognition and Significance of Inherited Quartz Overgrowths in quartz arenites. *Journal of Sedimentary Petrology*, Vol. **54**, P. 475-486.

SAUNDERSON, H. C. AND LOCKETT, F. P. J., 1983. Flume experiments on bedforms and structures at the dune-plane bed transition. *In*: Collinson, J. D. and Lewin, J (Eds.). Modern and Ancient fluvial systems. *International Association Special Publication,* **6**, P. 49-58.

SCHMIDT, VICTOR. AND MCDONALD, D. A., 1979. The role of secondary porosity in the course of sandstone diagenesis. *In*: Scholle, Peter, A. and Schluger, Paul, R (Eds.). Aspects of diagenesis. *Society Economic Palaeontology Mineral Special Publication,* No. **26**, P. 175-207.

SCHNEIDEROHN, P., 1954. Eine vergleichende studies ubr Methadone zur quantitativen Bestimmung Von Abrundung und form an sandkornern (im Hinblick auf die Verwendbarkeit an Dunnschliffen). Heidelb. Beitr. Miner. Petrogr. **4**, P. 172-191.

SCHOLLE, P. A., 1979. A colour illustrated guide to constituents, textures, cements and porosities of sandstones and associated rocks. *American Association of Petroleum Geologist Memoir*, **28**, 201 pp.

SEILACHER, A., 1967. Bathymetry of trace fossils. *Marine Geology,* Vol. **5**, P. 413-428.

SELLEY, R. C., 1985. Ancient sedimentary environments, Chapman and Hall Inc. London, 3rd edition, 317 pp.

SELLEY, R. C., 1976. An Introduction to Sedimentology, Academic Press Inc. London, 2nd edition, 408 pp.

SELLEY, R. C., 1988. Applied Sedimentology. London: A cadmic Press, 446 pp.

SELLEY, R. C., 1996. Ancient Sedimentary Environments and their subsurface diagnosis, Chapman and Hall, London, 4th edition, 300 pp.

SELLEY, R. C., 1997. Sedimentary Basin of the world. African Basins. Elsevier Science, B. V. Amsterdam-Lausanne-New York-Oxford-Shannon-Tokyo, P. 17-26.

SERRA, O. AND SULPICE, L., 1975. Sedimentological analysis of sand-shale series from well logs. The Society of Professional Well Log Analysis, 16th Annual Logging Symposium, Paper **W**, P. 1-23.

SHANLEY, K. W. AND MCCABE, P. J., 1991. Predicting facies architecture through sequence stratigraphic-An example from the Kaiparowits Plateau, Utah. *Geology,* Vol. **19**, P.742-745.

SHIKI, T., 1959. Studies on sandstone in the Maizuru zone, Southwest Japan. Pt. I. Importance of some relations between mineral composition and grain-size. Mem. Coll. Sci. Univ. Kyoto. Ser. B, **29**, P. 291-324.

SIMONS, D. B., RICHARDSON, E. V. AND NORDIN, C. F. JR., 1965. Sedimentary structures generated by flow in alluvial channels. *In*: Middleton, G. V (Ed.). Primary sedimentary structures and their hydrodynamic interpretation, Special Publication, *Society of Economic Palaeontologists and Mineralogists, Tulsa*, **12**, P. 34-52.

SIPPEL, R. F., 1968. Sandstone petrology, evidence from luminescence petrography. *Journal of Sedimentary Petrology*, Vol. **38**, P. 530-554.

SLOSS, S. A., KRUMBEIN, W. C. AND DAPPLES, E. C., 1949. Integrated facies analysis. *In*: Scott, D. F. and Glass, J. D (Ed.). Sedimentary facies geological history. *Geological Society of America, Memoir*, **39**, P. 91-124.

SMITH, N. D., 1970. The braided stream depositional environment: Comparison of the Platte River with some Silurian clastic rocks, North Central Appalachians. *Bulletin of the Geological Society of America,* Vol. **81**, P.2993-3014.

SNEED, E. D. AND FOLK, R. L., 1958. Pebbles in the Lower Colorado River, Taxes, and a study in particle morphogenesis. *Journal Geology*, Vol. **66**, P. 114-150.

SPENCER, D. W., 1963. The interpretation of grain-size distribution curves of clastic sediments. *Journal of Sedimentary Petrology*, Vol. **33**, P. 180-190.

STOW, D. A. V. AND JOHANSSON, M., 2000. Deep-water massive sands: nature, origin and hydrocarbon implications. *Marine and Petroleum Geology,* Vol. **17**, P. 145-174.

SUTTNER, L. J., BASU, A. AND MACK, G. H., 1981. Climate and the Origin of Quartz arenite. *Journal of Sedimentary Petrology*, Vol. **51**, P. 1235-1246.

SURLYK, F. AND NOE-NYGAAD., 1991. Sand bank and dune facies architecture of a wide intracratonic seaway: late Jurassic-early Cretaceous Raukev Formation, Jameson Land, East Greenland. *In*: A. D. Miall, and N. Tyler (Eds.). The Three-dimensional Facies Architecture of Terrigenous clastic sediments, and its Implication for Hydrocarbon Discovery and Recovery, P. 261-276.

SWIFT, D. J. P., 1969. Inner shelf sedimentation: process and products *In*: D. J. Stanley (Ed.). The New Concept of Continental margin sedimentation: Application to the Geological Record, Washington, P. 4-46.

SWIFT, D. J. P., PHILLIPS, S. AND THORNE, J. A., 1991. Sedimentation on continental margins IV: lithofacies and depositional systems *In*: Swift, D. J. P., Oertel, G. F., Tillman, R. W. and Thorne, J. A (Eds.). Shelf sand and sandstone bodies: Geometry facies and sequence stratigraphy. *International Association of sedimentologists Special Publication*, No. **14**, P. 89-152.

TALBOT, M. R. AND ALLEN, P. A., 1996. Lakes. *In*: Reading, H. G (Ed.). Sedimentary environments: Processes, facies and stratigraphy, Blackwell Scientific Publications, Oxford, 3rd edition, P. 83-124.

TANKARD, A. J. AND HOBDAY, D. K., 1977. Tide-dominated back-barrier sedimentation, early Ordovician Cape Basin, Cape Peninsula, South Africa. *Sedimentary Geology*, Vol. **18**, P. 135-159.

TANNER, W. F., 1959. The important of modes in cross-bedding data. *Journal of Sedimentary Petrology*, Vol. **29**, P. 221-226.

TAYLOR, J. M., 1950. Pore space reduction in sandstone. *American Association of Petroleum Geologist Bulletin,* Vol. **34**, P. 701-716.

TEICHERT, C., 1958. Concepts of facies. *American Association of Petroleum Geologist Bul*letin, Vol. **42**, P. 2718-2744.

TEKNICA CANADA REPORT, 1996. The geology and hydrocarbon potential of the Murzuq Basin, Libya. Client Report for NOC Tripoli. Teknica, Calgary.

THOMAS, D., 1995. Geology, Murzuq oil development could boost S. W. Libya prospects. *Oil and Gas Journal*, March 6, P. 41-46.

TIEJE, A. J., 1921. Suggestions as to the description and naming of sedimentary rocks. *Journal Geology,* Vol. **29**, P. 650-666.

TISSOT, B., CALIFET-DEBYSER, Y., DEROO, G., AND OUDIN, J. L., 1971. Origin and evolution of hydrocarbons in Early Toarcian shales, Paris Basin, France: *American Association of Petroleum Geologists Bulletin,* Vol. **55**, P. 2177-2193.

TODD, S. P., 1996. Process deduction from fluvial sedimentary structures. *In*: Carling, P. A., and Dawson, M. R (Eds.). Advance in fluvial dynamics and stratigraphy. P, 299-350.

TOMITA, T., 1954. Geologic significance of the colour of granite zircon and the discovery of the Pre-Cambrian in Japan. Kyushu Univ. Mem. Fac. Sci., Ser. D. *Geology*, Vol. **4**, P. 135-161.

TSCHERMAK, G., 1884. Lehrbuch der Mineralogy: Vienna, Alfred Holder, 589 pp.

TUCKER, M. E., 1982. Sedimentary Petrology. An introduction to the origin of sedimentary rocks, Blackwells Scientific, Oxford, 1st edition, 252 pp.

TUCKER, M. E., 1991. Sedimentary Petrology. An introduction to the origin of sedimentary rocks, Blackwells Scientific, Oxford, 2nd edition, 260 pp.

TUNBRIDGE, I. P., 1981. Sandy high-energy floods sediments-some criteria for their recognition, with an example from the Devonian of SW England. *Sedimentary Geology*, Vol. **28**, P. 79-95.

TURNER, B. R., 1980. Palaeozoic Sedimentology of the southeastern part of Al Kufrah basin, Libya: a modal for oil exploration. *In*: Salam M. J. and Busrewil M. T (Eds.). The Geology of Libya, Academic press, London, Vol. **II**, P. 351-374.

TURNER, B. R., 1983. Braidplain deposition of the Upper Triassic Molteno Formation in the main Karoo Gondwana Basin, South Africa. *Sedimentology,* Vol. **30**, P. 77-89.

TURNER, B. R., 1991. Palaeozoic delta sedimentation in southeastern part of Al-Kufrah Basin, Libya. *In*: Salam, M. J. and Belaid, M. N (Eds.). The Geology of Libya, Elsevier, Vol. **V**, P. 1713-1726.

TURNER, B. R., 1998. Field guide to the Palaeozoic rocks of the southeastern part of the Kufra Basin, Libya. Field Report, 27 pp (*Unpublished*).

TURNER, B. R. AND MONRO, M., 1987. Channel formation and migration by massive-flow processes in the Lower Carboniferous fluviatile fell Sandstone Group, northeast England. *Sedimentology*, Vol. **34**, P. 1107-1122.

TURNER, B. R., BENZAGOUTA, M. S., AND LEE, M., 1991. Saddle dolomite in the Buchan Oilfield, Central North Sea: diagenetic factors in relation to reservoir quality, 8 pp (*Unpublished*).

UDDEN, J. A., 1914. Mechanical composition of clastic sediments. *Geological Society American Bulletin,* Vol. **25**, P. 655-744.

UESUGUI, N., 1984. Palynological study of well E1-NC58 Murzuq Basin. Int. Rept Cenpes-Petrobras, onshore well, Libya, 7 pp.

VAIL, P. R. AND WORNARDT, W. W., 1990. Well Log-seismic sequence stratigraphy: an integrated tool for the 90's, GCSSEPM Foundation Eleventh Annual Research Conference, P. 379-388.

VAIL, P. R., 1987. Sequence stratigraphic workbook. Fundamental of sequence stratigraphy. *American Association of Petroleum Geologists,* Annual Short Course Notes, Tulsa.

VAIL, P. R., AUDEMART, F., BOWMAN, S. A., EISNER, P. N. AND PEREZ-CRUZ, G., 1991. The stratigraphic signatures of tectonics, eustasy and sedimentation-an overview. *In*: G. Einsele, W. Ricken and A. Seilacher (Eds.). Cyclic stratigraphy. Springer-Verlag, NewYork, P. 617-659.

VAIL, P. R., BUBB, J. N., HATLELID, W. G., MITCHUM, R. M., SANGREE, J. B., THOMPSON III, S., TODD, R. G. AND WIDMER, J. M., 1977. Seismic stratigraphy and global changes in sea-level, part 1-11. *In*: Payton, C. E (Ed.). Seismic stratigraphy-applications to hydrocarbon exploration. *American Association of Petroleum Geologists, Memoir,* **26**, P. 49-212.

VAIL, P. R., HARDENBOL, J. AND TODD, R. G., 1984. Jurassic unconformities, chronostratigraphy and sea-level changes from seismic stratigraphy and biostratigraphy. *In*: Schlee, J. S (Ed.). Interregional unconformities and hydrocarbon exploration. *American Association of Petroleum Geologists, Tulsa, Memoir,* **33**, P. 129-144.

VAN HOUTEN, F. B. AND KARASEK, R. M., 1981. Sedimentology framework of late Devonian Oolithic iron formation, Shatti Valley, West Central Libya. *Journal of Sedimentary Petrology*, Vol. **51**, P. 415-427.

VAN HOUTEN, F. B., 1981. The odyssey of molasse. *In*: A. D. Miall (Ed.). Sedimentation and Tectonic in alluvial basins: *Geological Association of Canada Special Paper,* **23**, P. 35-48.

VAN WAGONER, J. C., MITCHUM, R. M., JR., CAMPION, K. M. AND RAHMANIAN, V. D., 1990. Siliciclastic sequence stratigraphy in well logs, core and outcrop: Concepts for High Resolution Correlation of Time and Facies. *American Association of Petroleum Geologist* Methods in Exploration Tulsa, Series No. **7**, 55 pp.

VAN WAGONER, J. C., POSAMENTIER, H. W., MITCHUM, R. M., VAIL, P. R., SARG, J. F., LOUTIT, T. S. AND HARDENBOL, J., 1988. An overview of the fundamentals of sequence stratigraphy and key definitions. *In*: C. K. Wilgus, B. S. Hastings, C. G. St C. Kendall, H. W. Posamentier, C. A. Ross and J. C. Van Wagoner (Eds.). Sea-level changes: An Integrated Approach. Van Wagoner. Special Publication, *Society of Economic Palaeontology and Mineralogists, Tulsa,* **42**, P. 39-45.

VASSOYEVICH, N. B., *et al.*, 1970. Principal phase of oil formation: *International Geological Review*, Vol. **12**, P. 1276-1296.

VISHER, G. S., 1969. Grain-size distribution and depositional processes. *Journal of Sedimentary Petrology*, Vol. **39**, P. 1074–1106.

VISHER, G. S., 1972. Physical characteristics of fluvial deposits. *In*: Rigby, J. K (Ed.). Recognition of Ancient Environments. Special Publication *Society Economic Palaeontologists Mineralogists,* **16**, P. 84-97.

VOLL, G., 1960. New work on petrofabrics. *Liverpool and Manchester Geology Journal*, Vol. **3**, P. 503-567.

VOS, R. G., 1981a. Sedimentology of an Ordovician Fan Delta Complex, Western Libya. *Sedimentary Geology,* Vol. **29**, P. 153–170.

VOS, R. G., 1981b. Deltaic Sedimentation in the Devonian of Western Libya. *Sedimentary Geology,* Vol. **29**, P. 67–88.

VOS, R. G., 1977. Sedimentology of an upper Palaeozoic River, wave and Tide influenced Delta system in southern Morocco. *Journal of Sedimentary Petrology*, Vol. **47**, P. 1242-1260.

WADELL, H., 1935. Volume, shape and roundness of quartz particles. *Journal Geology,* Vol. **43**, P. 250-280.

WADMAN, D. H., LAMPRECHT, D. E. AND MROSOVSKY, I., 1979. Joint geologic/ engineering analysis of the sadlerochit reservoir, Prudhoe Bay Field. *Journal Petroleum Technology,* Vol. **31**, P. 933-940.

WALKER, R. G. AND PLINT, A. G., 1992. Wave and storm dominated shallow marine systems. *In*: R. G. Walker and N. P. James (Eds.). Facies Models: Response to sea-level change, P. 219-238.

WALKER, R. G., 1984. Shelf and shallow marine sands. *In*: R. G. Walker (Ed.). Facies Models, Geoscince Can., Repr. Ser., **1**, 2nd edition, P. 141-170.

WALTHER, JOHANNES., 1894. Einleitung in die Geologie als historische Winssenschaft. Jena, Fischer, 24 pp.

WANLESS, H. R. AND SHEPARD, F. P., 1936. Sea-level and climatic changes related to late Palaeozoic cycles. *Bulletin Geological Society of America,* Vol. **47**, P.1177-1206.

WELLER, J. M., 1930. Cyclical sedimentation of the Pennsylvanian period and its significance. *Journal of Geology,* Vol. **38**, P. 97-135.

WENTWORTH, C. K., 1933. Fundamental limits to the sizes of clastic grains. *Science,* No. **77**, P. 633-634.

WHITBREAD, T. AND KELLING, G., 1982. Marar Formation of western Libya evolution of an early Carboniferous delta system. *American Association of Petroleum Geologist Bulletin,* Vol. **66**, P. 1091-1107.

WIGNALL, P. B. AND MYERS, K. J., 1988. Interpreting benthic oxygen levels in mudrocks: Anew approach. *Geology,* Vol. **16**, P. 452-455.

WILGUS, C. K., HASTINGS, B. S., KENDALL, C. G. ST. C., POSAMENTIER, H. W., ROSS, C. A. AND VAN WAGONER, J. C., 1988. Sea-level changes: An Integrated Approach. Special Publication, *Society of Economic Palaeontologists and Mineralogists, Tulsa,* **42**. 407 pp.

WILLIAMS, P. F. AND RUST, B. R., 1969. The Sedimentology of a braided river. *Journal of Sedimentary Petrology*, Vol. **39**, P. 649-679.

WINKELMOLEN, A. M. AND VEENSTRA, H. J., 1974. Size and shape sorting in a Dutch tidal inlet. *Sedimentology*, Vol. **21**, P. 107-126.

ZIMMERLE, WINFRED., 1976. Petrographische Beschreibung und Deutung der erbohrten Schichten. *Geol. Jahrbuch*, Vol. **427**, P. 91-305.

* * *